

Early predictive model for COVID-19 mortality and ventilator support: reducing risks for patients



Anshu SS Kotia^a | Jaya Gupta^b | Vinod Singh K.^c

^aJaipur National University, Jaipur, India, Associate Professor, Department of Anaesthesia.

^bSanskriti University, Mathura, Uttar Pradesh, India, Assistant Professor, Department of Ayurveda.

^cTeerthanker Mahaveer University, Moradabad, Uttar Pradesh, India, Professor, Department of Medicine.

Abstract The COVID-19 virus, which is caused by the Severe Acute Respiratory Syndrome Coronavirus 2 (SARS-CoV-2), has the potential to generate a wide range of symptoms, including mild respiratory symptoms, severe respiratory distress, and even death. Prediction models cannot replace clinical judgment and patient assessment. Instead of depending solely on the estimates provided by models, healthcare providers should use them as decision-support tools to help them make the best possible choices. As part of this investigation, we construct a prediction model that we refer to as the Hybrid Spider Monkey Optimized eXtreme Gradient Boosting (HSMO-XGB). Patients who were part of the COVID-19 trial were hospitalized in King Abdul-Aziz Medical City in Riyadh for the purpose of this study. The dataset includes the patient's personal data, the outcomes of any tests performed in laboratories, and any chest X-ray (CXR) outcomes. The first step in preprocessing is called normalization, and the second step is called feature extraction using linear discriminate analysis (LDA). The reasonable expectation model for HSMO-XGB that is presently being shown will work on the administration of clinics by helping doctors in the early recognizable proof of Coronavirus patients who are in danger of death or need respiratory support. The model that has been provided can be utilized, in particular, as a tool that can assist physicians in predicting patients who are at risk and that can assist hospitals in effectively managing and organizing their resources.

Keywords: COVID-19, chest X-ray, LDA, HSMO-XGB, ventilatory support

1. Introduction

Predictive models for COVID-19 mortality have been developed and kept up to date ever since the start of the epidemic. It's essential to remember that these models are prone to change when fresh data becomes available since they were developed using the data and hypotheses that were accessible from the point in time (Alaa et al 2020). Any prediction model's accuracy is influenced by the caliber of the data it uses and the underlying assumptions it is built upon. Considering this, I could give you an example of a COVID-19 mortality early prediction model that was commonly used in the earliest phases of the epidemic. The "Case Fatality Rate" (CFR), which estimates the percentage of confirmed COVID-19 patients that have died, is one such model. Despite not taking into consideration undiagnosed cases or the whole population, this statistic gives an assessment of the disease's severity (Gershengorn et al 2021). To simulate the transmission of the virus and calculate the possible number of infections and fatalities, other prediction models are used, such as the "Susceptible-Exposed-Infectious-Removed" (SEIR) model. These models take into account a variety of variables, including healthcare availability, infection rates, transmission patterns, and population demographics. But it's important to note that when new information becomes available and the situation changes, these models need to be updated often (Maghbooli et al 2020). Get the most recent and precise COVID-19 mortality prediction models, it is crucial to visit reliable sources such government health organizations, academic institutions, and epidemiological specialists. Based on recent advancements and research, these sources may provide you the most up-to-date knowledge and perceptions (Kassirian et al 2020). Significant respiratory sickness brought on by COVID-19 may need ventilator assistance in certain individuals. The term "ventilator support" describes the use of artificial ventilation or other methods to supplement or take the place of the body's natural breathing mechanism (Arvind et al 2021). Patients with COVID-19 whose respiratory symptoms are severe and whose illness is progressing often need ventilator assistance. When given supportive treatment, such as rest, water, and monitoring, many virus-infected people recover from their mild to severe symptoms. Nevertheless, if the system for breathing is seriously damaged, more dangerous conditions such as acute respiratory distress syndrome (ARDS) and respiratory failure may arise (Lu et al 2020).

In these circumstances, ventilator assistance is essential for maintaining normal breathing and supplying oxygenation. When a COVID-19 patient is critically sick, mechanical ventilation may assist provide oxygen to the lungs and eliminate carbon dioxide from the body, easing their respiratory distress. Based on the patient's health and the medical team's



evaluation, several ventilation techniques, such as positive pressure ventilation, may be used (Goyal et al 2021). It's important to highlight that the choice to begin ventilator support is decided by medical specialists based on evaluations of each individual patient, taking into consideration elements like saturation with oxygen levels, breathing rate, results from imaging, and other clinical indications. When choosing a course of therapy for COVID-19 patients who need ventilator support, the availability of intensive care unit (ICU) resources and ventilators is particularly important (Barbosa et al 2023). It's essential to note that a number of variables, including age, underlying medical problems, and access to treatment, might affect the fatality rate of COVID-19. Ventilators assistance is a crucial procedure that may greatly increase the odds of life for patients who are critically sick, but it does not ensure success. The overall death rates related to COVID-19 are continuously updated as new information becomes available and as medical procedures and methods of treatment advance (Núñez et al 2021).

Early prediction models for COVID-19 mortality and the requirement for ventilator support have been devised to help medical facilities and states anticipate the possible impact of the global epidemic and allocate assets effectively. These models are designed to pinpoint risk-raising variables and provide suggestions for lowering mortality and the need for ventilator assistance (Bonadia et al 2020). Age and current health issues Age and pre-existing conditions including cardiovascular disease, diabetes, obesity, and respiratory diseases increase the risk of COVID-19-related severe illness and death. Early theories highlighted the need of locating and safeguarding these vulnerable people (Wollenstein-Betech et al 2020). Early-stage prediction models for hospital capacity have emphasized the need of providing enough hospital capacity, including ICU beds, ventilators, and medical staff. The need for ventilator support may be met and death rates can be lowered by maintaining enough resources (Twe et al 2022). Early detection and action: Prompt detection of severe cases and early action may enhance results. It is possible to take prompt action, such as providing oxygen treatment and ventilator support, if necessary, by identifying those who are more likely to have severe sickness and carefully monitoring their health (Calligaro et al 2020). The chance of a fatal COVID-19 infection and severe sickness may be significantly decreased with vaccination. In order to safeguard vulnerable people and lessen the overall strain on healthcare systems, early prediction models have underlined the significance of vaccination efforts (Dayan et al 2021). To examine reliable sources including government health organizations, research institutes, and expert consensus statements from epidemiologists and healthcare specialists in order to acquire the most current and accurate prediction models and recommendations. These resources may provide precise recommendations that are adapted to the present level of awareness and comprehension of COVID-19 (Carrasco-Sánchez et al 2021).

The COVID-19 patients that had CXR in the ED between March 1 and March 13, 2020, are prospectively included. Accumulation on the CXR and ground-glass transparency (GGOs) was each assessed independently by two assessors. Two different scoring methods were used. The reliability between observers was assessed using weighted Cohen's kappa or the intraclass correlation coefficient (ICC). By using logistic or Poisson regression analysis, indicators of mortality and respiratory assistance were found (Balbi et al 2021). The study analyzes a database of blood samples from 485 infected individuals in the Wuhan region of China to identify important prognostic markers of disease mortality. The decision-making procedure described in the article may be used to quickly identify high-risk patients, provide them priority treatment, and perhaps reduce the mortality rate (Yan et al 2020). Sub analysis of a hypothetical, global database of critically ill COVID-19 patients. Patients were subcategorized into high-flow oxygen therapy (HFNC), noninvasive ventilation with positive pressure (NIV), and early IMV in accordance with the breathing assistance technique employed on the day of admission to the ICU. To establish comparability across groups, propensity score matching was used (Wendel Garcia et al 2021). The goal of the research is to summarize P-SILI etiology and the role of passive oxygen therapy in COVID-19 pneumonia. Debates are had on the esophagus volume swings, breathing structure, vascular dysfunction, elastomeric properties, homogenization of the lungs, and effort while breathing (Battaglini et al 2021). The goal of the study was to determine whether there was a connection between blood sodium levels while a patient was hospitalized and significant clinical outcomes like mortality, the requirement for advanced respiratory support, and acute kidney damage (AKI), in addition to whether serum sodium could be used to gauge a state of inflammation in COVID-19 (Tzoulis et al 2021). The decision models for a random forest method, Least Absolute Shrinkage and Selection Operator (LASSO), and reverse selection were combined to provide a projected risk score. Death, the need for or tracheal intubation, and the necessity for minimally invasive breathing were all considered severe outcomes. The research comprised 610 individuals in all, 313 of whom had a catastrophic result (Ageno et al 2021). In the research, they included successive hospitalized with PCR-confirmed COVID-19 who received treatment to Newcastle upon Tyne Hospitals and University College London Hospitals in the UK during the first wave of community-acquired infection. The demographics, research results, and medical condition were documented from the day of hospitalization until death throughout a maximum monitoring period of 28 days (Manson et al 2020).

2. Materials and Methods

The study's primary goals were to identify patients who might benefit from ventilator assistance and to forecast patient death. For patients with COVID-19 who were hospitalized, the first instance indicated death, whereas cases 2 and 3 indicated ventilator support. The whole feature collection was used to perform three sets of experiments for each case, and the EAI

feature importance approach was used to choose a selected group of characteristics for each trial. In the third trial, instances 2 and 3 only used CXR features, whereas case 1 was completed using the co mortality component. Figure 1 depicts the flow of the overall methodology.

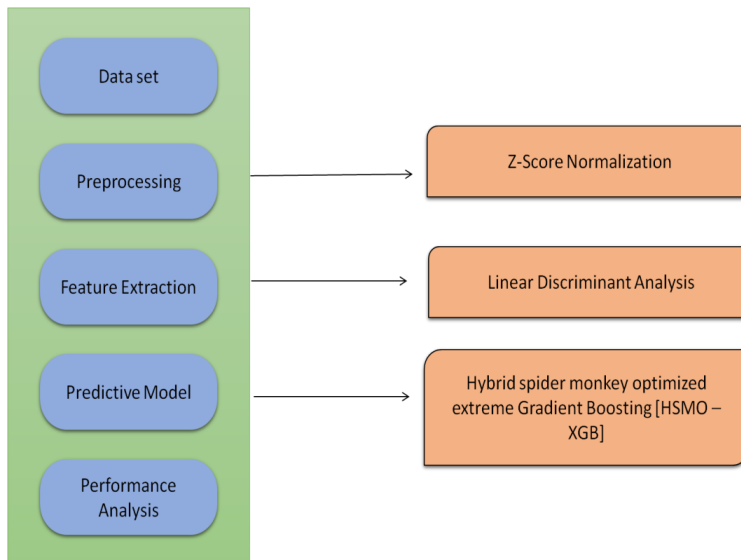


Figure 1 Flow of the proposed methodology.

2.1. Dataset

The study examined retrospectively data from individuals who had COVID-19 and got hospitalized in the Kingdom of Saudi Arabia (KSA). Data from clinical and laboratory testing, as well as CXR findings, are included in the collection along with information on 5739 patients. Additionally, the dataset includes two objective attributes: ventilator support and patient outcome. The eligibility requirements for the patient sample used in this analysis are the same as those used to compile the mortality and ventilator support datasets. The data set contains details on the demographics, testing results from “complete blood counts”, “mean corpuscular hemoglobin concentration”, “mean corpuscular hemoglobin”, “mean corpuscular volume”, “mean platelet volume”, “red blood cells”, “platelet count, red cell distribution width”, “white blood cells”, radiological results, and co-morbidity. The only numerical qualities are age and all CBC characteristics; all other variables are qualitative. Figure 1 depicts the 12 zones in which the CXRs are marked. The junction (C), upper (A), and lower zones (B) are the first divisions of the CXR. Then, twelve more zones are created from these zones, to represent the locations where a radiologist assigns seriousness ratings. There are three potential values (0–2) for the zone characteristics that represent the degree of ground glass opacity (GGO). GGO is not present when the value is zero. In all, there are 2 class characteristics and 35 predictors in the dataset. Additionally, the age feature was separated using equal-width binning for the dataset’s an exploratory examination. The dataset’s lowest and highest patient ages respectively were 19 and 107.



Figure 2 Zone segmentation and annotation for chest X-rays.

2.2. Preprocessing using Z-score normalization

Z-score normalization, usually referred to as standardization, is a method frequently used in predictive modeling to standardize numerical data. By dividing by the standard deviation and removing the mean from the data, it turns the data into a distribution with a mean of zero and a standard deviation of one. This normalization approach may be used to verify that the characteristics in a COVID-19 mortality prediction model are on a comparable scale.

Obtain the information you want for your prediction model, including the target variable (COVID-19 mortality) and any pertinent characteristics (such as age, co morbidities, vital signs, etc.).

Data should be normalized for each characteristic before being divided by the standard deviation and the mean. The z-score normalization formula (1) is as follows:

$$Z = (x - \mu)/\sigma \quad (1)$$

Where:

The normalized value (z-score) is called z.

X is the feature's initial value.

μ is the feature's mean.

σ is the feature's standard deviation.

Use this formula to convert each feature in your dataset into its corresponding z-score for each data point.

The values obtained after normalizing the features using z-score normalization may be used as inputs for your COVID-19 mortality prediction model. Make careful to normalize any additional data that you wish to use for predictions using the same mean and standard deviation figures that you acquired from your training data. It is simpler for the model to learn from the data when the scale discrepancies between the features are removed via Z-score normalization. Additionally, it avoids the learning process from being dominated by characteristics with greater sizes. To the characteristics, not the target variable, normalization should be done. The COVID-19 mortality goal variable should be left normalized and in its original state. It is important to remember that there are several normalizing methods available, such as min-max scaling, which scales the data within a certain range. Your dataset's unique needs and features, as well as the selected predictive modeling technique, will influence the normalization approach you choose.

2.3. Feature extraction using Linear discriminate analysis

A statistical technique known as linear discriminate analysis (LDA) is often used to resolve issues involving pattern recognition. LDA was first used for face recognition. Fisher's Linear Discriminate is the name of this approach. To extract crucial information from data and minimize data dimensionality, LDA is becoming increasingly often utilized. To divide the data into two or more object classes or groups, this approach essentially seeks for linear combinations of properties that represent the primary characteristics. The distribution of fresh data will be more diffused after it has undergone LDA processing, which will ultimately improve recognition success. Following that, both linear and non-linear classification techniques may be used to reprocess the new data combination that was produced. The primary properties of the Caesar dataset are determined using LDA in this study, and the researcher also attempts to decrease the dimensions from the available data if at all feasible. This is done in the hopes that the outcomes of the dimensional reduction would be correctly categorized using SVM. The LDA algorithm is shown below. To better understand them; let's first create the covariance matrix in class SW and the interclass covariance matrix SB, each of which is shown by the following for formula (2).

$$T_x = \sum_{j=1}^d \sum_{w_l \in W_j} (w_l - \mu_j)(w_l - \mu_j)^S; \quad (2)$$

$$T_x = \sum_{j=1}^d M_j (w_l - \mu_j)(w_l - \mu_j)^S; \quad (3)$$

Where X_k denotes data in the k-position, C is the whole class, N_i denotes the quantity of data in the class, μ denotes the average across all data, and μ_j denotes the average data in class i .

A matrix of covariance across classes is then maximized in order to reduce the covariance matrix inside the class. The eigenvector may then be found, allowing us to maximize the ratio of (4):

$$\frac{\det(UT_A U^S)}{\det(UT_X U^S)} \quad (4)$$

$$T_A = \lambda T_X U \quad (5)$$

$$\text{cov} = T_A (T_X)^{-1} \quad (6)$$

The eigenvector utilized is c^{-1} since the LDA technique covered in this study is the LDA method with two classes. The biggest eigenvalue of the covariance matrix may be used to determine the eigenvector value.

Once the eigenvector is known, the LDA feature may be calculated by doing the following formula:

$$E_w = \sum_{j=1}^l (w_j - \mu)^T \times U \quad (7)$$

2.3. Predictive model using hybrid spider monkey optimized extreme gradient boosting (HSMO-XGB)

2.3.1. Spider Monkey Optimization

A more modern optimization technique based on swarm intelligence is the hybrid spider monkey optimization (SMO) algorithm. Distances calculated according to between possible solutions serve as the foundation for the update equations. The technique has been used widely to resolve challenging optimization issues. A fuzzy rule foundation was designed and optimized using SMO. The SMO method optimizes the amplitudes of each element and the positions of each element in the extended sparse sub array to minimize the side lobe levels of the whole array while adhering to a number of real-world limitations. Built SM-Rule Miner to do rule extraction on diabetic data. The array factor of a linear antennas array was additionally synthesized using the SMO, as well as an E-shaped antenna patches that has been perfectly designed for use in wireless networks.

2.3.2. Extreme gradient boosting

The Extreme Gradient Boosting (XGBoost) technique is a regression tree with decision-tree-like decision-making capabilities. It supports both classification and regression. This approach is a scalable and effective variation of the gradient boosting machine (GBM), which has been extensively used in computer vision, data mining, and other areas. Recently, XGBoost has primarily advanced in two areas as a sort of gradient boosting machine: speeding up the tree building and suggesting a new distributed technique for tree searching. The heart of XGBoost is optimizing the value of the goal function. Considering the dataset $D = \{(x_i, y_i)\}$ represents the x_i tumor's gene expression profile and the related y_i binary label (early stage or late stage) is used to identify the tumor. Equation is the optimization objective function for the XGBoost model with K decision trees.

$$z_j = \sum_{l=1}^L e_l(w_j), e_l \in E \quad (8)$$

Where each f_k represents a separate tree with leaf scores and F is the space of the regression tree. In formula (9), the loss function is shown.

$$K(e_k) = \sum k(z_j^*, z_j) + \sum \Omega e_k \quad (9)$$

Differentiable loss function l in the first term assesses the discrepancy between the output \hat{y}_i that was anticipated and the actual output y_i .

$$\hat{z}_j^{(s)} = \hat{z}_j^{(s-1)} + e_s(w_j) \quad (10)$$

$$\Omega(e) = \gamma S + \frac{1}{2} \|x\|^2 \quad (11)$$

W is the score on each leaf, and T is the total number of leaf nodes. Therefore, we might conclude that

$$S(e_s) \approx \sum_{i=1}^S [(\sum_{j \in J_i} h_j) x_i + \frac{1}{2} (\sum_{j \in J_i} g_j + \lambda) x_i^2] + \gamma \quad (12)$$

Where g_i and h_i are the loss function's first-order and second-order gradient statistics, respectively.

2.4. Assessment measures

A comparison of “accuracy, sensitivity, specificity, Youden index, and area under the curve” (AUC) was used to assess the proposed model's efficacy. The effectiveness of the categorization algorithms may be examined using a variety of assessment metrics. Some of these metrics, including accuracy, precision, and recall, are significantly impacted by class distribution. Consequently, the uneven class distribution, including recall, accuracy, and precision. The imbalanced class issue thus employs metrics like balanced accuracy, AUC, and Youden index. Sensitivity (SN), which is generated using the formula below, is used to reflect the model's genuine positive rate.

$$SN = \frac{\text{sum(positive class samples in the dataset)}}{\text{sum(correctly predicted positive class)}} \quad (13)$$



The following formula is used to compute specificity, which stands for the real negative rate:

$$SP = \frac{\text{sum}(\text{negative class samples in the dataset})}{\text{sum}(\text{correctly predicted Negative class samples})} \tag{14}$$

Equations (13) and (14) demonstrate that the following metrics are unaffected by class distribution

The mean of the sensitivity and specificity is the same for balanced accuracy:

$$\text{Balanced Accuracy} = \frac{SP + SN}{2} \tag{15}$$

One of the metrics used to assess how well the diagnostic test works is the Youden index (YI). It rates the diagnostic test's capacity for discrimination. The following equation is used to calculate it:

$$\text{Youden Index} = SN + SP - 1 \tag{16}$$

The YI values range from 0 to 1. A result that is closer to one demonstrates the test's relevance, while a score that is lower indicates insufficient diagnostic ability.

AUC is used to confirm the model's ability to discriminate further. AUC values range from 0 to 1, and like the Youden index, values closer to 0 indicate poor performance while values closer to 1 indicate significant effectiveness of the model.

3. Results

In this section, the results for all three situations that indicate that COVID-19 patients will die and need ventilator assistance are discussed. Additionally, the dataset is unbalanced, which is why data-sampling strategies like SMOTE with oversampling and SMOTE with under sampling were used. A cross-validation with process was used to split the data among all trials, with k set to a value of 10. After that, training and validation sets were created from the training parts. The validation set was used throughout the parameter tweaking procedure. Figure 3 depicts the results of the experimentation using the recommended model for Case 1 in order to establish when the patient would be either deceased. Similar responsiveness is accomplished utilizing the full-and chose highlight sets with the underlying data set without the utilization of any information testing methods. After SMOTE under sampling, the whole feature set and dataset produced the results with the maximum sensitivity. However, the entire feature set with oversampling and SMOTE produced the best results for other metrics like specificity, balanced accuracy, the Youden index, and AUC.

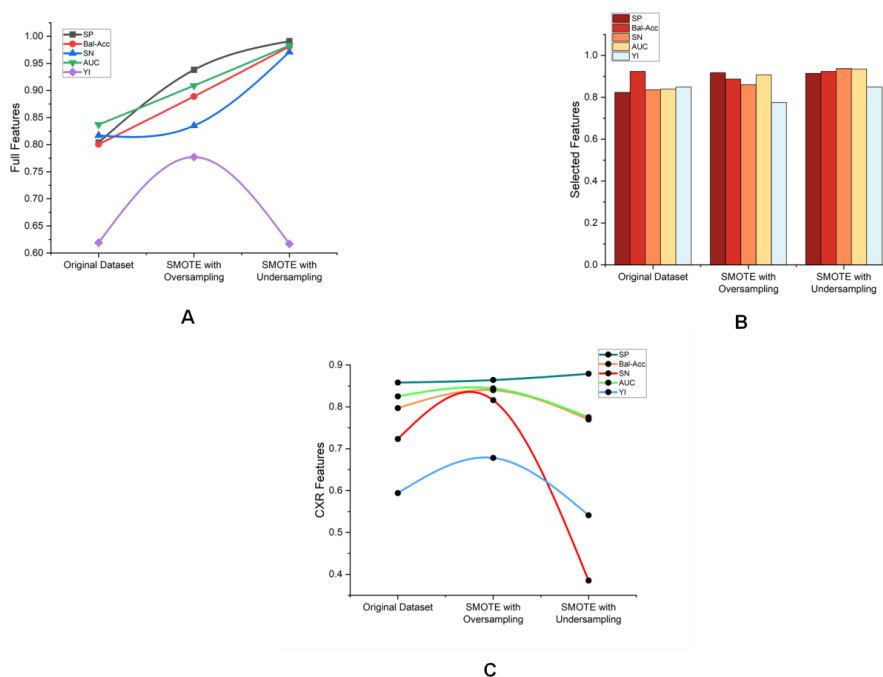


Figure 3 The outcome of the suggested mortality prediction model.

A comparable AUC for SMOTE surpassing was achieved using the whole feature set as well as the original dataset with the specified features. Using specific characteristics and SMOTE oversampling, the best overall AUC was found.



However, utilizing the co morbidity variables and the original dataset, the maximum AUC attained in the suggested research was 0.875, and the balanced accuracy was 0.904. We discovered that utilizing co morbidity features, a comparable AUC was obtained after oversampling the sample. Additionally, studies were carried out to determine whether patients need ventilator assistance. The tests were at first done for the numerous classes, i.e., to lay out when patients required a “mechanical ventilator”, a “painless ventilator”, utilizing each quality, chose highlights, and CXR highlights. The use of CXR facial appearance was made possible by the author’s discovery that CXR traits could be used to forecast whether COVID-19 patients would need ventilator assistance during a foundation experiment. The effectiveness of the suggested DL model employing various feature sets is shown in Figure 4.

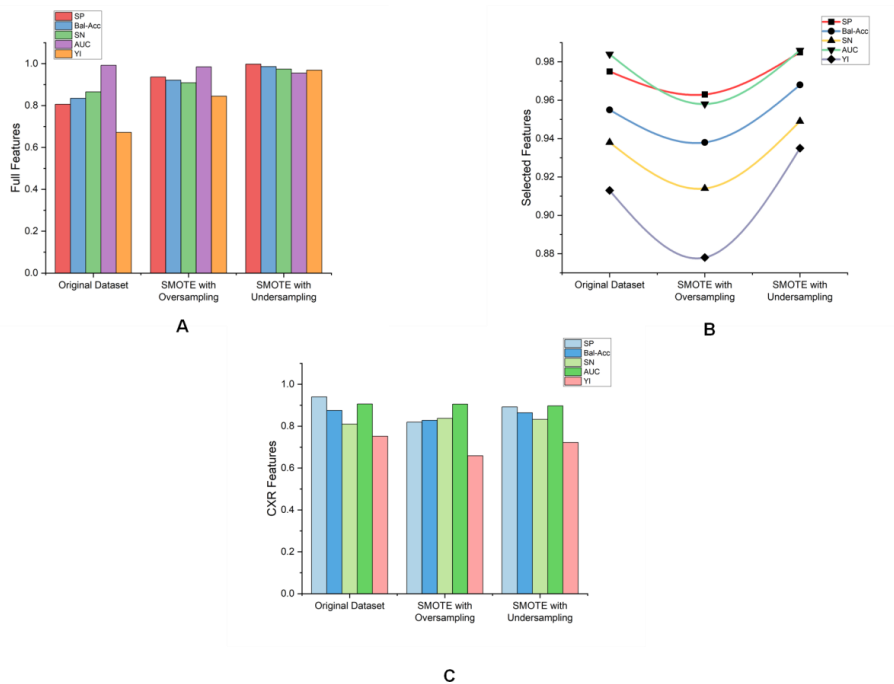


Figure 4 The outcome of the suggested ventilator-support prediction model (Multiclass).

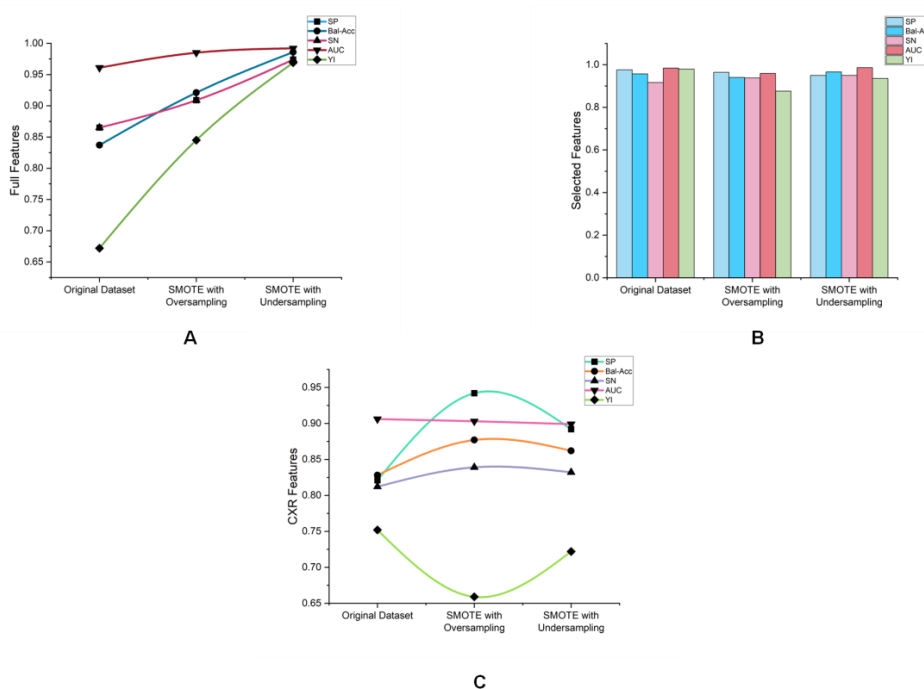


Figure 5 Results of the ventilator-support prediction model suggested.



The test results are listed in the table. Similar to scenario 1, the model in this instance performed best when all features were enabled. It shows the importance of each characteristic in determining whether individuals need ventilator assistance. SMOTE with the under-sampling dataset set, however, produced the best outcomes in this instance for all assessment metrics. Both the full-feature set and the chosen feature set produced a comparable AUC for the mortality prediction (case 1) task. However, the model AUC utilizing complete and chosen characteristics in this instance differed significantly. In addition, we discovered that the oversampling method outperformed the original and under sampled datasets in terms of performance with CXR features. To determine which patients would need ventilation, trials for the binary class were carried out. Figure 5 uses the test set to display the outcome of the suggested model. Similar to example 2, the best results were also obtained for a single class using full features and under sampled data. The model's performance was marginally enhanced after switching from a multiclass to a binary class. However, there were substantial differences between the results of the full-feature dataset and the other datasets, such as the original and over- and under-sampling. They discovered that XGB and the dataset with a low sample size produced the best results for determining whether the patient would require ventilator support. With an AUC of 0.904 and balanced accuracy of 0.875, the proposed research outperformed a foundational study when applied to the initial dataset. All findings show that the suggested model is significant in each of the three scenarios.

4. Discussion

It is essential to develop an electronic model that is able to identify patients who are at risk for mortality and provide assistance for ventilators due to the severe clinical signs of Coronavirus and, occasionally, its rapid breakdown in moderate-stage patients. Additionally, a model that can provide healthcare practitioners a trustworthy explanation must be made available. As a result, to predict mortality and ventilator support in the planned research, the DL model was combined with the EAI (Vila-Corcoles et al 2021). Multiple studies have examined the use of laboratory results, signs and symptoms, data on demographics, and radiological results to make predictions. As a result, the suggested research made use of demographic, clinical, co morbidities, and CXR zone characteristics. Age and gender were shown to be important elements among the demographic characteristics. To predict mortality and ventilator support, however, radiomics characteristics and two demographic factors (age and gender) were utilized. Experienced radiologists who gave the radiomic ratings discovered that radiomic characteristics significantly improved the efficiency of the algorithms. Included pharmaceutical data and discovered that individuals on medication for pneumonia and respiratory disorders were more likely to use a ventilator. On the other hand, it was discovered that several of the patients who had received a COVID-19-negative diagnosis through RT-PCR test had pneumonia upon CXR examination. Similar to this, several of the patients' CXR results showed no significant indications, but the RT-PCR test anticipated that they would be positive. But they discovered that CXR properties can only be utilized for prediction if additional variables, such SpO₂, PaO₂, and certain other clinical factors, are also present. On the other hand, use demographic, co morbidity, and symptom data to forecast death (Wendel Garcia et al 2021). Despite this, the research produced important findings; however, they were missing certain important CXR and lab test data from the dataset. Additionally, three co morbidities (heart issues, diabetes, and hypertension) were looked at as critical aspects. However, it was shown that although several lab tests were a significant factor in predicting death, the top attributes to do so were shortness of breath and further oxygen treatment. Even so, the present research has shown notable findings, although there is always opportunity for advancement. The dataset used for the research came from a single center and nation (Karthikeyan et al 2021). Several clinical parameters that have been found to be crucial are also absent from the dataset, including CPR, D-dimer, heartbeat, SpO₂, and PaO₂. To further confirm the effectiveness of the model, it must be examined using the multicenter dataset while also taking into consideration other elements that have been shown to be pertinent in earlier studies.

5. Conclusions

This study examined whether Coronavirus patients required ventilator support and whether the DL model could predict mortality. The dataset contains information on the demographics, test outcomes, co-morbidities, and CXR of the COVID-19 patients. To solve the issue of data imbalance, both under- and over-sampling were done using the SMOTE data-sampling method. The EAI feature significance method was used to choose the features. Utilizing the hybrid spider monkey optimized, the extreme gradient boosting was optimized. For the purpose of predicting mortality and ventilator support, many sets of experiments were conducted utilizing CXR results and complete features, chosen features, and co morbidity characteristics alone. The suggested model may be used, in particular, as a tool to help clinicians forecast patients who are at risk and to help hospitals manage and organize their resources efficiently. On the other hand, this research may be expanded to look at performance utilizing the multicenter and multicounty dataset. It's also necessary to take into account several of the key test investigation outcomes and COVID-19 immunizations.

References

- Ageno W, Cogliati C, Perego M, Girelli D, Crisafulli E, Pizzolo F (2021) List of contributors Lucia Maria Caiano Federica Magni Elisabetta Tombolini Chiara Aloise Francesca Maria Casanova Benedetta Peroni Andrea Ricci Stefania Scarlini Ivan Silvestri Matteo Morandi Sara Pezzato Francesca Stefani Virginia Trevisan, Clinical risk scores for the early prediction of severe outcomes in patients hospitalized for COVID-19 Internal and emergency medicine 16:989-996.
- Alaa A, Qian Z, Rashbass J, Bengler J, van der Schaar M (2020) Retrospective cohort study of admission timing and mortality following COVID-19 infection in England BMJ open 10:e042712.
- Arvind V, Kim JS, Cho BH, Geng E, Cho SK (2021) Development of a machine learning algorithm to predict intubation among hospitalized patients with COVID-19 Journal of critical care 62:25-30. DOI: 10.1016/j.jcrc.2020.10.033
- Balbi M, Caroli A, Corsi A, Milanese G, Surace A, Di Marco F, Sironi S (2021) Chest X-ray for predicting mortality and the need for ventilatory support in COVID-19 patients presenting to the emergency department European radiology 31:1999-2012. DOI: 10.1007/s00330-020-07270-1
- Barbosa HC, Martins MAP, Jesus JCD, Meira KC, Passaglia LG, Sacioto MF, Marcolino MS (2023) Myocardial Injury and Prognosis in Hospitalized COVID-19 Patients in Brazil Results From The Brazilian COVID-19 Registry. Arquivos Brasileiros de Cardiologia 120. DOI: 10.36660/abc.20220151
- Battaglini D, Robba C, Ball L, Silva PL, Cruz FF, Pelosi P, Rocco PR (2021) Noninvasive respiratory support and patient self-inflicted lung injury in COVID-19: a narrative review British Journal of Anaesthesia 127:353-364. DOI: 10.1016/j.bja.2021.05.024
- Bonadia N, Carnicelli A, Piano A, Buonsenso D, Gilardi E, Kadhim C, Franceschi F (2020) Lung ultrasound findings are associated with mortality and need for intensive care admission in COVID-19 patients evaluated in the emergency department. Ultrasound in medicine & biology 46:2927-2937. DOI: 10.1016/j.ultrasmedbio.2020.07.005
- Calligaro GL, Lalla U, Audley G, Gina P, Miller MG, Mendelson M, Koegelenberg CF (2020) The utility of high-flow nasal oxygen for severe COVID-19 pneumonia in a resource-constrained setting: A multi-centre prospective observational study. Eclinicalmedicine 28:100570. DOI: 10.1016/j.eclim.2020.100570
- Carrasco-Sánchez FJ, López-Carmona MD, Martínez-Marcos FJ, Pérez-Belmonte LM, Hidalgo-Jiménez A, Buonaiuto V, SEMI-COVID-19 Network (2021) Admission hyperglycaemia as a predictor of mortality in patients hospitalized with COVID-19 regardless of diabetes status: data from the Spanish SEMI-COVID-19 Registry. Annals of medicine 53:103-116. DOI: 10.1080/07853890.2020.1836566.
- Dayan I, Roth HR, Zhong A, Harouni A, Gentili A, Abidin AZ, Li Q (2021) Federated learning for predicting clinical outcomes in patients with COVID-19 Nature medicine 27:1735-1743.
- Gershengorn HB, HuY, Chen JT, Hsieh SJ, Dong J, Gong MN, Chan CW (2021) The impact of high-flow nasal cannula use on patient mortality and the availability of mechanical ventilators in COVID-19. Annals of the American Thoracic Society, 18(4), 623-631. <http://orcid.org/0000-0002-7360-2489>
- Goyal D, Inada-Kim M, Mansab F, Iqbal A, McKinstry B, Naasan AP, Burke D (2021) Improving the early identification of COVID-19 pneumonia a narrative review BMJ Open Respiratory Research 8:e000911.
- Karthikeyan A, Garg A, Vinod PK, Priyakumar UD (2021) Machine learning based clinical decision support system for early COVID-19 mortality prediction. Frontiers in public health 9:626697. DOI: 10.3389/fpubh.2021.626697
- Lu J, Hu S, Fan R, Liu Z, Yin X, Wang Q, Hou J (2020) ACP risk grade a simple mortality index for patients with confirmed or suspected severe acute respiratory syndrome coronavirus 2 disease (COVID-19) during the early stage of outbreak in Wuhan, China. MedRxiv 2020:02. DOI: 10.1101/2020.02.20.20025510
- Maghbooli Z, Sahraian M A, Ebrahimi M, Pazoki M, Kafan S, Tabriz HM, Holick MF (2020) Vitamin D sufficiency, a serum 25-hydroxyvitamin D at least 30 ng/mL reduced risk for adverse clinical outcomes in patients with COVID-19 infection. PloS one 15:e0239799. DOI: 10.1371/journal.pone.0239799
- Manson JJ, Crooks C, Naja M, Ledlie A, Goulden B, Liddle T, Tattersall RS (2020) COVID-19-associated hyperinflammation and escalation of patient care: a retrospective longitudinal cohort study The Lancet Rheumatology 2:e594-e602. DOI: 10.1016/j.fsr.2020.07.002
- Núñez I, Priego-Ranero Á. A, García-González HB, Jiménez-Franco B, Bonilla-Hernández R, Domínguez-Cherit G, Valdés-Ferrer SI (2021) Common hematological values predict unfavorable outcomes in hospitalized COVID-19 patients. Clinical Immunology 225:108682. DOI: 10.1016/j.clim.2021.108682
- Twe CW, Khoo DKY, Law KB, Nordin A, Sathasivan S, Lim KC, Chidambaram SK (2022) The role of procalcitonin in predicting risk of mechanical ventilation and mortality among moderate to severe COVID-19 patients. BMC Infectious Diseases 22:1-13.
- Tzoulis P, Waung JA, Bagkeris E, Hussein Z, Biddanda A, Cousins J, Baldeweg SE (2021) Dysnatremia is a predictor for morbidity and mortality in hospitalized patients with COVID-19. The Journal of Clinical Endocrinology & Metabolism 106:1637-1648. DOI: 10.1210/clinem/dgab107
- Vila-Corcoles A, Satue-Gracia E, Vila-Rovira A, de Diego-Cabanes C, Forcadell-Peris MJ, Ochoa-Gondar O (2021) Development of a predictive prognostic rule for early assessment of COVID-19 patients in primary care settings. Atención Primaria 53:102118. DOI: 10.1016/j.aprim.2021.102118
- Wendel Garcia PD, Aguirre-Bermeo H, Buehler PK, Alfaro-Farias M, Yuen B, David S, Roche-Campo F (2021) Implications of early respiratory support strategies on disease progression in critical COVID-19: a matched subanalysis of the prospective RISC-19-ICU cohort. Critical care 25:1-12.
- Wollenstein-Betech S, Cassandras CG, Paschalidis IC (2020) Personalized predictive models for symptomatic COVID-19 patients using basic preconditions: hospitalizations, mortality, the need for an ICU or ventilator. International Journal of Medical Informatics 142:104258. DOI: 10.1016/j.ijmedinf.2020.104258
- Yan L, Zhang HT, Goncalve J, Xiao Y, Wang M, Guo Y, Yuan Y (2020) An interpretable mortality prediction model for COVID-19 patients. Nature machine intelligence 2:283-288.

Hybrid neural network for non-image-based knee osteoarthritis prediction



Abhishek Rathore^a | Rakesh Ashokrao Bhongade^b | Man Mohan Sharma^c

^aJaipur National University, Jaipur, India, Assistant Professor, Department of Orthopedics.

^bSanskriti University, Mathura, Uttar Pradesh, India, Professor, Department of Ayurveda.

^cTeerthanker Mahaveer University, Moradabad, Uttar Pradesh, India, Professor, Department of Orthopaedics.

Abstract Osteoarthritis (OA) of the knee is a common degenerative joint condition that adversely affects millions of people worldwide. Early detection and forecasting risks of knee OA can help with prompt interventions and individualized treatment plans to slow the disease's progression. 2 million patients' worth of Taiwanese data was sampled (2001–2015). 1,068,464 comprised control subjects, while 132,594 patients had Knee Osteoarthritis. Over the course of a three-year period, we sequentially used diagnoses, medication, age, and sex to build a feature matrix. In this study, we developed a risk prediction model using a hybrid strategy (CNN-FFNN) that combines a convolutional neural network (CNN) and a feed-forward neural network (FFNN). The performance of the hybrid approach is also evaluated using a variety of performance indicators. Age and sex were excluded from the list of significant disease variables, and drugs like antacids, cough relievers, and stimulants demonstrated discriminative efficacy. The proposed methodology may help medical personnel identify people who are most at risk of getting knee OA, allowing for preventative measures and individualized treatment regimens to lessen the impact of this crippling ailment.

Keywords: osteoarthritis, knee joint, risks, early detection, hybrid strategy

1. Introduction

The pathologic changes in the osteochondral unit, composed of subchondral bones, the meniscus, and cartilage, are the hallmarks of knee osteoarthritis, a degenerative condition (Saravi et al 2022). It is the cause of about 85% of osteoarthritis's burden. Knee Osteoarthritis is more common in older people in Taiwan than in any other country, affecting about 37% of people over 50. In contrast, in the US, Knee Osteoarthritis has been observed in 13% of girls and 10% of men 60 years of age or older, adults 65 years of age, and adults (Sebro et al 2022). Age is among the main aetiologies for Knee Osteoarthritis, and it may be linked to cumulative access to much different etiology, which can cause structural changes in the joints. Additional pathogenic signs of Knee Osteoarthritis include the presence of women, obesity, and injuries (Shah et al 2021). According to earlier research, high-impact sports, heavy lifting, and repetitive kneeling are all linked to Knee Osteoarthritis.

Additionally, genetic factors may contribute to roughly 40–80% of the risk of Knee Osteoarthritis, which is more than the risk for hand and hip osteoarthritis (Ciliberti et al 2022). Even long-term use of oral N-acetylcysteine (NAC) medication delivery is linked to an increased risk of Knee Osteoarthritis. Although it remains difficult, forecasting the risk of Knee Osteoarthritis could be done by using artificial intelligence. Recent studies have demonstrated the enormous potential of deep learning (DL) and extensive clinical information to provide personalized healthcare through risk prediction to boost the effectiveness and efficiency of prevention. Managing large-scale data, such as photographs and sizable EMR, uses DL development of conventional statistics methods (Sukerkar et al 2022).

The CNN, a sort of DL technique, can examine generic tasks with extreme variability exhibited in the visual data; significant computing tasks, such as object recognition, the categorization, and the segmentation of images, can be carried out using the DL architecture CNN, which is very frequently used. The building blocks that makeup CNN are similar to filters, which can use convolution to separate the pertinent features from the sequential incoming data. CNN was also able to effectively pinpoint a target and its placement of other elements in a picture by capturing the spatial properties of the image (Clark et al 2020). The alternative DL approach uses a Feed Forward Neural Network (FFNN) with triple levels: concealed, output, and input. Incredibly interconnected neural networks called Feed Forward Neural Networks (FFNNs) has the ability to process input in simultaneously and comprehend format. The learning of complex non-uniform input-output correlations is made possible by FFNNs. Furthermore, most prior relevant studies only employed image-based information to identify the risk of Knee Osteoarthritis, not cohorts of EMR or time sequence. DL has been applied to chronic disorders like cancer and



cardiovascular disease, relying on nonimage EMRs rather than using photos to train it for Knee Osteoarthritis risk prediction (He et al 2022).

Wang et al (2021) suggested a novel learning method that divides the information into two sets in real-time based on their reliability. Additionally, to assist CNN in learning appropriately from the two sets, we build a hybrid loss function. We focus on typical samples using the suggested method, and we manage the effects of cases with low confidence. The five-class task and the early-stage OA task are both the subject of experiments. Wassan et al (2021) proposed scoping assessment of publications utilizing DL methods to forecast major aging-associated diseases, including related to age macular degeneration, cardiovascular and breathing disorders, arthritis, Alzheimer's disease, and lifestyle factors related to disease development. DL publications on typical aging-related concerns released between the beginning of 2017 and Aug 2021 are searched using Google Scholar, IEEE, and PubMed. These publications were examined, reviewed, and the conclusions were compiled. Akgun et al (2021) summarize current radiopharmaceuticals and how they treat various diseases.

Additionally, theranostics is outlined. In conclusion, researchers in this field may find this review helpful. In this article, they provide a Dempster-Shafer theory (DST)-based multi-modal data fusion paradigm that is evidence-aware. There are three branches in the backbone models: an image branch, a non-image branch, and a fusion branch. The extracted characteristics are inputted into an evidence network for each unit, which generates an evidence score for each chapter that is intended to indicate the accuracy of the result from the existing branch. Alexopoulos et al (2022) examined how MRI and patient data affect the estimation of the incidence of knee OA. Using a series of 600 individuals from the Osteoarthritis Initiative, intermediate-weighted turbo spin-echo (IW-TSE) was used to predict the occurrence of knee OA within 25 months. A U-Net model was built and utilized to part bones on a dual-echo stable state (DESS) sequence to identify an area of interest from the IWTSE series that contained the knee joint.

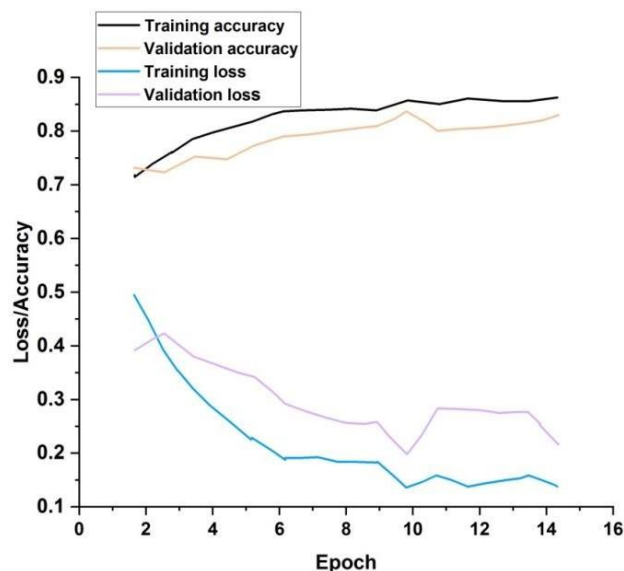


Figure 1 The proposed KOA model's learning curve.

Tolpadi et al (2020) described a DL pathway to indicate TKR with an AUC of 0.834 0.036 using MRI pictures, clinical data, and demographic data. For patients without OA, the pipeline most impressively means TKR with AUC 0.943 0.057. To discover TKR imaging biomarkers, we also create occlusion images for case-control pairings in test data and evaluate the model's utilization of different locations in each Farajzadeh et al (2023) aimed a deep residue neural network called IJES-OA Net is provided to autonomously assess the seriousness of knee osteoarthritis using radiographs. This is accomplished by calibrating it so that it is concentrated on the distance between the borders of the bones within the knee joint. The IJES-OA Net achieves high average accuracy and average precision while possessing less complexity compared to other approaches, according to experimental results using the datasets. The objective of this work was to develop a machine-learning model based on images for identifying TKA loosening. Lau et al (2022) explained a model for image-based machine learning was created using ImageNet, the Xception model, and a dataset of X-ray images from TKA patients. Then, a new method was developed for creating the medical-information-based neural network model with a random forest classifier, which was based on a dataset of TKA patient clinical parameters. Additionally, the TensorFlow DL framework and Python were used to pre-train the Xception Model on the ImageNet database to forecast loosening.

The following sections make up the remainder of the paper. The method is described in Part 2. The data analysis is in Part 3. The conclusions are covered in Part 4.

2. Materials and Methods

2.1. Dataset

The National Health Insurance Research and Development (NHIRD) of Taiwan, which keeps track of all diagnostic findings, prescriptions, and treatments from approximately 100% of Taiwanese citizens, is one of the most extensive databases for the administration of medical treatment on the planet from which we gathered our data. The National Health Insurance Reimbursement Database (NHIRD) includes information on insurance reimbursement claims, demographic data, Diagnostic and therapeutic ICD-9-CM codes, and prescriptions for drugs with the WHO-ATC codes. From January 1, 2001, to December 31, 2015, we looked at two million data samples. The patient's informed consent was unnecessary for this study's approval by the Taipei Medical University Academic Review Board because all data had been de-identified and anonymized.

2.2. Research the people and terminology

Aged 26 or older, with details on gender, age, and at minimum three years of documentation, we identified the Taiwan person database who had at least a single admittance claim between 2001 and 2015, and sufferers who had a bed confinement level code were removed from the study or Before the index date, complete repair of the knee were acceptable treatments for behind cruciate ligament injuries. The initial day when Knee Osteoarthritis was diagnosed is the index date for the Knee Osteoarthritis group. The ICD-9-CM codes, Knee Osteoarthritis localized, or Knee Osteoarthritis unspecified, were used to validate the Knee Osteoarthritis group. The mastery cohort baseline date is the final day the data was accessible. To forecast the likelihood of a Knee Osteoarthritis incidence one year later, we analyzed patients' EMRs from the previous three years.

2.3. Development of Prediction Systems

To build the feature, we took into account the patient's highest age, gender, ICD9-CM diagnosis code, WHO-ATC drug policy, and the overall amount of medical checkups discovered throughout the three-year term of monitoring. Additional V-codes were also employed, totaling 1098 ICD-9-CM policy divided into seventeen organ structures (001-999). In this investigation, the ICD-9-CM policy's first three digits were used. The cohort data included 1029 different diagnostic categories. There are 830 different drug categories contained in the WHO-ATC code, and 695 of those are recommended, according to the group data. The majority of the prescriptions were covered by the initial 5 characters.

2.4. Hybrid CNN and FFNN

It is possible to forecast the likelihood of developing knee osteoarthritis using convolutional neural networks (CNNs) and feedforward neural networks (FFNNs).

Although CNNs are frequently employed for image identification tasks, they can also be used to analyze medical pictures like X-rays or MRI scans of the knees. Convolutional and pooling layers in CNNs are intended to automatically learn and extract significant features from the input images. Then, for jobs requiring classification or regression, these features are supplied into layers that are fully coupled. A CNN could examine knee photos in the context of osteoarthritis prediction and discover patterns that point to the development or risk factors of the condition.

The input, hidden, and output layers are present in the neural network design of FFNNs, on the other hand. A feedforward connection pattern is created when every neuron in a layer is coupled to every neuron in the layer above it. For tabular data, where each input sample is represented by a collection of features, FFNNs are appropriate. The input elements for predicting knee osteoarthritis may include biomarkers, medical history, lifestyle factors, and demographic data. To provide an accurate forecast, the FFNN would learn the correlations between these traits and the likelihood of developing knee osteoarthritis.

Hybrid architecture can benefit from the CNN's ability to extract pertinent features from complex data and the FFNN's capability for learning nonlinear relationships and making predictions by fusing the strengths of both CNNs and FFNNs.

A CNN is frequently used as a feature extractor, and the recovered features are then fed into an FFNN for additional processing and decision-making. The FFNN layers can then learn to classify or regress based on these extracted characteristics. The CNN layers can remove high-level visual features from photos or other grid-like input.

Depending on the task, a hybrid CNN and FFNN may have a different architecture and design. It might entail changing the number of layers, the CNN's filter size, the FFNN's layer count, and the activation functions applied.

To tackle the prediction of the risk label for knee osteoarthritis, we approached it as the issue of bi-categorization and developed a supervising CNN and FFNN training model. An image-like matrix was created from the EMR input for each patient. We also provided information on the time dimension. The codes for diagnoses and drugs are listed on the input matrix's vertical axis. Each cell in the diagram represents the patient's visit history. The horizontal axis comprises 3 years, and Each visit consists of a diagnostic policy for each week split by 7 and a pharmaceutical code for each week divided by 28. The convolution phases, median pooling, maximal pooling, leak rectified linear unit (ReLU), and flattening make up the EMR matrices data input to network design employing CNN. The FFNN architecture receives the patient's maximum age and sex

values, which are merged to determine the categorization result. All patient data were divided into two groups: 85% for training and 15% for testing, followed by 70% for learning and 30% for internal validity in the training set.

3. Results

The Knee Osteoarthritis group had 83,111 females and 49,483 males, with a mean age and standard deviation of 64.20 and 12.49 years, respectively (Table 1). With 545,902 females and 522,562 men, the mean age of the non-knee osteoarthritis control group was 51.0015.79 years. The average number of medical checkups per sufferer per year in the groups with knee osteoarthritis and those without it was 38.50 and 21.90, respectively. In the Knee Osteoarthritis group and the non-Knee Osteoarthritis mastery group, the yearly average number of diagnoses per patient was 34.60, while it was 21.90 in the non-Knee Osteoarthritis group. In the Knee Osteoarthritis and mastery groups, the average number of prescriptions per sufferer per year was 30.54, while 62.11 were seen in the Knee Osteoarthritis group. If we multiply the number of medications by the number of prescription days each patient receives each year, in the Knee Osteoarthritis cohort and the mastery cohort, we discover, respectively, 694.81 and 298 drugs per sufferers. In the mastery cohort and Knee Osteoarthritis cohort, there were similarly 1.90 and 0.82 drugs per patient per day, respectively. Based on the Knee Osteoarthritis model's learning curve employing diagnoses and pharmaceutical characteristics (Figure 2), the validate and learning losing line demonstrates that It has been shown that the Knee Osteoarthritis technique is less prone to excessive matching. A minor gap formed between the plots of learning loss and verification failure, which both decreased to a center of stabilization. The learning losses and verification losses plots, as well as the plots of learning accuracy and efficacy of verification, which rise until they reach a point of equilibrium and have little gaps within them, demonstrate that the training and validation datasets were representative. With ICD-9-CM codes as its only input attributes, the Knee Osteoarthritis model achieved an AUROC of 0.94 at its optimum levels of 0.34 (Table 2). The Knee Osteoarthritis, on the other hand, showed an AUROC 0.79 with the optimal level set at 0.05 when only pharmaceutical (WHO-ATC code) input features were used. The Knee Osteoarthritis demonstrated an AUROC, Particularity, recall (positive predictive value), and precision (positive predictive value) of 0.96, 0.88, 0.92, and 0.8, respectively, at the best threshold of 0.15 while using both WHO-ATC medicines and ICD-9-CM diagnostics as input features (Figure 2). The total risk probability score, which ranged from zero (non-Knee Osteoarthritis) to one (Knee Osteoarthritis), allowed us to find the best balance between the true positive ratio and the false positive ratio. By severing some links between nodes inside layers, we used the TensorFlow optimization toolbox to improve the Knee Osteoarthritis model (Figure 3). After optimization, the model's size was drastically reduced from its initial (442 MB) by up to 33% (147 MB). The AUROC between the initial and optimized models was discovered to be very similar.

Table 1 Population of the collected Data.

Characteristics	Mastery cohort (n=1,068,464)	KOA Group (n=132,594)
Race/Ethnicity	All Asian	All Asian
	Age, year	
Average	51	66
Max	113	106
Min	27	26
M ±SD	51.01 (±15.78)	64.21 (±12.48)
	Sex, n (%)	
Men	523,563 (48.92)	48,482 (37.33)
Women	546,903 (51.08)	85,113 (62.68)
	median sufferers yearly accumulation, n/ sufferers /year	
(WHO-ATC) Pharmaceutical values	31.55	63.12
Counting pharmaceuticals (WHO-ATC) days prescribed	297.62	695.82
Diagnosis (ICD-9-CM) values	23.92	35.61
Medical checkup values	22.91	39.51

Table 2 The effectiveness of KOA with various input characteristics.

Input Features	Diagnoses and medications	Diagnoses only	Medications only
AUROC	0.96	0.95	0.78
Recall	0.88	0.84	0.64
specficity	0.92	0.92	0.82
Precision	0.80	0.77	0.62



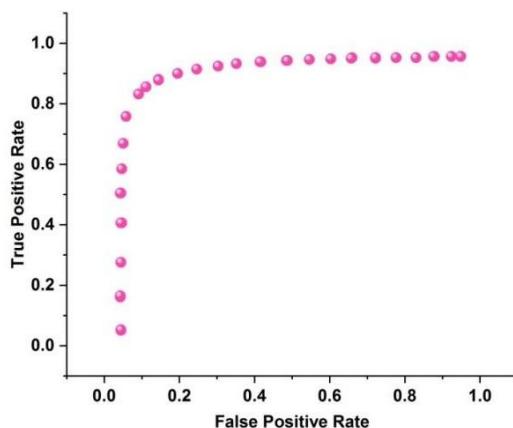


Figure 2 True and False Positive Ratios (Before optimization).

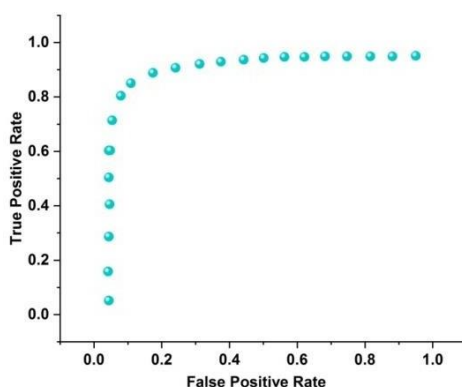


Figure 3 True and False Positive Ratios (After optimization).

Table 3 Example of sufferers Information for the KOA Model Assessment.

ID Patient	A	B	C	D	E	F
Gender	Men	Women	Women	Men	Women	Women
Age	59	64	60	54	38	46
Results	0.17	0.638	0.941	0.138	0.013	0.125
	3					
Labelling	KOA	KOA	KOA	NonKOA	NonKOA	NonKOA
Days prescribed for medications in total throughout a three-year period	85	159	1356	26	31	308
Medication intake overall over three years (n)	8	7	25	8	9	21
In three years, all diagnoses (n)	4	7	13	5	6	13
All medical check-up every three years (n)	6	11	31	4	12	34

Chronic comorbidities, acute respiratory infections, esophageal, stomach, and duodenal disorders, and a greater illness occurrence in the eyes and adnexa were distinguishing factors for Knee Osteoarthritis prediction. While antacids, cough suppressants, and the most popular were expectorants discriminating characteristics. To compare the performance of the theory, three sufferers from the mastery cohort for people without knee osteoarthritis and those who do were chosen at random according to the comparison of features, especially the abundance of characteristics over three trips (Table 3). According to this investigation, the Knee Osteoarthritis model's optimum threshold was computed at 0.152, with the highest non-Knee Osteoarthritis score coming in at 0.137 and the least Knee Osteoarthritis score coming in at 0.172. These individuals shared a similar number of characteristics, such as diagnoses and drugs, as non Knee Osteoarthritis sufferers, but their scores differed noticeably.

4. Conclusions

Knee Osteoarthritis was created to focus on vulnerable sufferers of Knee Osteoarthritis and give them a precision preventative program. It achieved great sensitivity and specificity and could have a one-year forecast of the chance of having knee osteoarthritis. Before performing an imaging or biomechanical retrieval screening procedure, based on longitudinal



medical records, Knee Osteoarthritis can assist doctors in identifying patients who have a greater chance of getting Knee Osteoarthritis in the future. There are a few restrictions on this study. The results of MRI or other imaging tests, laboratory findings, physique mass index, exposure (such as occupational exposure), genetic markers, and details on the kinds, pathologic features, and grading of Knee Osteoarthritis were not included in the NHIRD. As a result, distinct Knee Osteoarthritis predictions were not possible. Because it has non-image characteristics, this model can still be used in an overall population anywhere in the universe. To improve the efficiency and detailed tagging result, additional research using picture factors under the same concept will be required.

Ethical considerations

Not applicable.

Declaration of interest

The authors declare no conflicts of interest.

Funding

This research did not receive any financial support.

Reference

- Akgun E, Ozgenc E, Gundogdu E (2021) Therapeutic Applications of Radiopharmaceuticals: An Overview. *FABAD Journal of Pharmaceutical Sciences* 46:93-104.
- Alexopoulos A, Hirvasniemi J, Tümer N (2022) Early detection of knee osteoarthritis using DL on knee magnetic resonance images. *arXiv preprint arXiv:2209.01192*.
- Clark IM, Davidson RK, Cassidy A, MacGregor AJ (2020) The Potential for Dietary Factors to Prevent or Treat OA. *Osteoarthritis and Cartilage* 28:S16-S17.
- Farajzadeh N, Sadeghzadeh N, Hashemzadeh M (2023) IJES-OA Net: A residual neural network to classify knee osteoarthritis from radiographic images based on the edges of the intra-joint spaces. *Medical Engineering & Physics* 113:103957.
- He K, Gan C, Li Z, Rekik I, Yin Z, Ji W, Gao Y, Wang Q, Zhang J, Shen D (2022) Transformers in medical image analysis: A review. *Intelligent Medicine*.
- Lau LCM, Chui ECS, Man GCW, Xin Y, Ho KKW, Mak KKK, Ong MTY, Law SW, Cheung WH, Yung PSH (2022) A novel image-based machine learning model with superior accuracy and predictability for knee arthroplasty loosening detection and clinical decision making. *Journal of Orthopaedic Translation* 36:177-183.
- Liu X, Wang J, Zhou SK, Engstrom C, Chandra SS (2023) Evidence-aware multi-modal data fusion and its application to total knee replacement prediction. *arXiv preprint arXiv:2303.13810*.
- Saravi B, Hassel F, Ülkümen S, Zink A, Shavlokhova V, Couillard-Despres S, Boeker M, Obid P, Lang GM (2022) Artificial intelligence-driven prediction modeling and decision making in spine surgery using hybrid machine learning models. *Journal of Personalized Medicine* 12:509.
- Sebro R, De la Garza-Ramos C (2022) Statistically based nomograms for the minimal needle length required to achieve intra-articular fluoroscopic-guided injections of the shoulder, hip, and knee. *PM&R*.
- Shah A, Lepkowsky E, Duke A, Moriarty M, Riordan H, Khan F (2021) Treatment Approach for Knee Osteoarthritis with Ipsilateral Femoral Cartilage Tumor: A Case Series. *Orthopedic Research and Reviews* 89-93.
- Sukerkar PA, Doyle Z (2022) Imaging of Osteoarthritis of the Knee. *Radiologic Clinics* 60:605-616.
- Tolpadi AA, Lee JJ, Padoia V, Majumdar S (2020) DL predicts total knee replacement from magnetic resonance images. *Scientific reports* 10:6371.
- Wang Y, Bi Z, Xie Y, Wu T, Zeng X, Chen S, Zhou D (2021) Learning From Highly Confident Samples for Automatic Knee Osteoarthritis Severity Assessment: Data From the Osteoarthritis Initiative. *IEEE Journal of Biomedical and Health Informatics* 26:1239-1250.
- Wassan JT, Zheng H, Wang H (2021) Role of DL in Predicting Aging-Related Diseases: A Scoping Review. *Cells* 10:2924.

Enhancing sepsis detection with nature-inspired optimization integrated neural network



Jigar Manilal Haria^a | Deepak Mewara^b | Anupama Nanasaheb Tarekar^c

^aTeerthanker Mahaveer University, Moradabad, Uttar Pradesh, India, Professor, Department of Medicine.

^bJaipur National University, Jaipur, India, Assistant Professor, Department of Gen Surgery.

^cSanskriti University, Mathura, Uttar Pradesh, India, Professor, Department of Ayurveda.

Abstract Sepsis, a disorder that can be fatal that is brought on by a dysregulated immunological reaction to an infection, keeps presenting complex problems for early detection and treatment. In this article, they suggest a novel (MBSO-LSTM) method for improving sepsis diagnosis that combines long short-term memory (LSTM) networks and modified bird swarm optimization (MBSO). The biases and weights of the network known as LSTM are optimized using the MBSO algorithm, which was developed in response to research on the social behavior of bird flocks. MBSO enables faster and more successful learning of the LSTM model, resulting in increased sepsis detection performance by emulating the self-organizing behavior of bird swarms. Our work uses a sizable collection of medical records from individuals who have probable sepsis, including demographic information, laboratory findings, and vital signs. The LSTM network in the suggested framework recognizes the time-dependent relationships and patterns present in the data by using these characteristics as inputs. They contrast our method's effectiveness with other cutting-edge sepsis detection strategies, such as conventional approaches. The outcomes show that concerning sensitivity, specificity, accuracy, and area under the receiver operating characteristic curve (AUC-ROC), our proposed system performs better than alternative methods.

Keywords: sepsis, medical records, detection, MBSO-LSTM.

1. Introduction

Sepsis is a typical systemic response to infection that, according to Owen et al (2021), frequently has life-threatening consequences for hospitalised patients. One of the primary causes of death for patients in intensive care units is sepsis in particular. In the USA, severe sepsis was diagnosed in roughly 750,000 individuals in 1995, and around one-third of these diagnoses resulted in mortality (Naruei et al 2023)—costs associated with sepsis treatment range between 15.4 to 20 billion USD annually. As sepsis worsens, it leads to organ failure and a significant rise in mortality. Therefore, it's critical to identify sepsis as soon as possible and stop it from worsening (Parashar et al 2022).

A great deal of recent research has focused on patients who are experiencing sepsis and uses lab results, biomedical information, and electronic health records to determine status shifts as sepsis developments to acute pneumonia or septic tremor, which is challenging to forecast and thereby prevent catastrophic impairment and death via extended treatment, or examine the mortality rate of sepsis patients. (Chong et al 2021). In the past, researchers have concentrated on using the Systemic Proinflammatory Reaction Syndrome (SIRS) criteria or excessive heart rate variation in a preventive strategy to anticipate and identify sepsis early on by analyzing complaints both earlier and later than the intended occurrences. Though, there is little data-based modeling research utilizing regression models or machine learning techniques for sepsis early detection (Sabzalian et al 2023).

Sepsis detection could be much improved by combining neural networks and optimization techniques inspired by nature. This method enhances the precision, productivity, and flexibility of sepsis detection systems by combining the feature identification powers of neural systems with the optimization capability of nature-inspired algorithms (Aslan et al 2021).

Kandati and Gadekallu (2023) suggested algorithm distributes the combined evaluation value of the framework developed on the system. On the COVID-19 dataset for inflammatory chest disease as well as the chest X-ray (pneumonia) dataset, they created a three-layer CNN and a two-layer CNN. Predictions for the abdomen ulcer caused by the COVID-19 infections dataset had an accuracy rate of 96.15%, and forecasts for the X-ray of the chest (pneumonia) dataset had an accuracy rate of 96.55%; the modeling results demonstrated that the recommended approach performed better than other methods.

Swain et al (2023) effectiveness of the suggested algorithm for diagnosing COVID-19 disease was thoroughly verified through statistical measurements, F1 score, and matrix of consternation, particularity, and sensitivity parameters. For detecting COVID-19 using noisy cough data set across GFCC feature parameters, the sensitivity and specificity of the DHO-

ANN approach were determined to be 0.90 and 0.91, respectively. Additionally, it was clear that the suggested algorithm using GFCC outperformed other methods in identifying the COVID-19 disease from the hectic gathered cough dataset, COUGHVID.

Singh et al (2021) suggested a strategy for detecting COVID-19 infection using CXR pictures. The CXR images were then classified using a variety of classifiers utilizing the chosen attributes. Thanks to its excellent precision and accuracy, the proposed pipeline can be used to create smartphone applications that help doctors identify COVID-19 early.

Goel et al (2021) proposed a dual-stage Deep learning (DL) architecture for COVID-19 diagnosis utilizing CXR. The "feature obtaining and classification" stages comprise the proposed DL architecture. The DL network layers are optimized using the "Multi-Objective Grasshopper Optimization Algorithm (MOGA)," hence the moniker "Multi-COVID-Net" for these networks. This algorithm automatically categorizes the photos of tuberculosis patients, non-COVID-19, and COVID-19. The Multi-COVID-Net has been tested using publicly accessible datasets, and the findings show that it performs better than other cutting-edge techniques.

Selvakumar and Balasundaram (2023) described an automated method in which the pictures being used are taken from reliable sources, feature-enhanced using improved contrast, and then segmented using Fuzzy C Means (FCM) that have been optimized. Deviation-based Updated Dingo Optimizer (D-UDOX) optimizes parameters. The Optimized Recurrent Neural Network (WO-RNN) classification algorithm is given its weighted features. Additionally, ResNet-150 is used to extract complex characteristics from a fragmented image. The recommended model's outcome is superior to recent efforts, achieving 96% accuracy and 93% F1 score.

El-Rashidy et al (2022) proposed a theoretical framework comprising two layers. The first is a sepsis prediction deep learning classification model. This neural network combining collective models determines which patients will have sepsis. Data from the first six hours following an individual's arrival to the ICU are obtained for patients who had been predicted to be diagnosed with sepsis, and this information is utilized for further enhancement of the model.

The suggested method by Alani (2021) was used with extraordinarily high accuracy—over 98%. Investigations also showed a false-positive rate of 1.9% and a false-negative rate of less than 0.02%. This research presents a deep neural network-based detection approach for the website of things monitoring and reconnaissance techniques.

Hallawa et al (2019) recommend a context for developing CPNs and evolving their topology, arc weights, locations, changes, and kinetics. With scant experimental data, this makes it easier to simulate complicated biological systems, such as the signaling route that is activated in sepsis. They created a system with a genotype-to-phenotype relationship based on the CPN consequences matrix of and a function of fitness that takes into account both the behavioral traits of the growing CPN and its resultant foundational diversity. Our framework was influenced by NEAT, which is utilized in computerized neural networks (ANNs). In ten different situations with various intricacy structures, they tested our system. The worst-case scenario yields an NMSE in the learning phase of less than 2% and an MSE in the verification phase of 13%.

Lauritsen et al (2020) develop an efficient intelligence framework for early detection and differentiation of COVID-19 intensity from the viewpoint of coagulation indices. The brainstorming optimizing algorithm (EBSO), an improved new stochastic optimizer, and an advanced artificial intelligence (AI) method known as EBSO-SVM are combined to form the framework.

Our study aimed to identify sepsis early enough to minimize organ damage, prevent patient deaths, and promote disease recovery through proactive sepsis management. In this work, they suggest a broad methodology that is driven.

The rest of this paper is arranged as follows: Part 2-Literature Review, part 3- methods, Part 4- Results, and Part 5- a conclusion with limitations and future scope.

2. Materials and Methods

2.1. Data set

The Multipara-meter Artificial Intelligence Tracking in Critical Care (MIMIC-II, version 3) database was used for this research because it is a freely available clinical file that contains data on nearly 500,000 Patients who received admission to the intensive care unit at the Boston Beth Israel Metropolitan Healthcare Centre during 2001 and 2012. This database's components include free-text health information, treatment orders, laboratory test results, individual health indicators, hospital records, knowledge of hydration, and hospital records. Data transformation and other anonymization processes were also completed. For research objectives, patient-identifying numbers were de-identified and given new IDs.

Arguments concerning the applicability of the recently suggested criteria are still being had, even though a new Sepsis-3 criterion for sepsis occurrence was created in 2016. Studies that used the MIMIC database and focused on the 1991 SIRS are currently being conducted. The current research suggests a universal methodology that, without additional feature extraction steps, when learning feature extraction and generates predictions in a network of deep neural networks. As shown in Table 1, the following requirements had to be met for our study to be included.

Table 1 Patient Inclusion Data.

Criteria	Patients Included
1.	Patients brought to an ICU who were older than 18 years old.
2.	Patients who met the requirements for SIRS throughout the first four hours after being admitted to the hospital
3.	Patients who completed the requirements for SIRS within the first hour of their initial ICU admission

2.2. Sepsis

The body's overpowering reaction to infection results in sepsis, a potentially fatal medical illness. The diffuse inflammatory response that it exhibits can cause organ failure and malfunction. Severe sepsis, which can develop quickly and become life-threatening, can result in septic shock, a painful health condition.

The appearance of a viral infection and an inflammatory response to it are the main diagnostic criteria for sepsis. The SIRS (Systemic Inflammatory Response Syndrome) requirements, which are the most frequently applied standards, comprise the following:

1. Body temperature: a fever (A person's body temperature above 39 °C) or hypothermia (body temperature less than 36°C).
2. Rhythm of the heart: Faster-than-normal heartbeat (more than 90 beats per minute).
3. Breathing rate: Hyperventilation or increased respiratory rate (over 20 breaths per minute; PaCO2 < 32 mmHg).
4. The number of white blood cells: a high white blood cell count (above 12,000 cells/mm3), leukopenia (below 4,000 cells/mm3), or a high percentage of immature (band) forms.

2.3. Data pre-processing min-max normalization

The MIMIC II database contains around 460 variables measured as signals from the body. In the current study, two types of data, essential, a brief overview data, and the features extracted and used in the Insight mission (shown in Table 2), were taken from these factors and used for model construction. The following two paragraphs give a more in-depth explanation of each.

Table 2 Pre-processing of the Data Min-Max Normalisation.

Parameter	Description
Systolic Blood Pressure	Pressure in the arteries when the heart beats.
Pulse Pressure	Diastolic and systolic blood pressure variations.
Heart Rate	Number of heart beats per minute.
Body Temperature	A measure of the body's internal heat.
Respiration Rate	Number of breaths per minute.
White Blood Cell Count	Number of white blood cells in a sample of blood.
pH	Measure of acidity or alkalinity in a solution.
Blood Oxygen Saturation	Percentage of oxygen n-saturated haemoglobin in the blood.
Age	Number of years since birth.

2.4. Reference elements for the five hours

In their work, they employed the methods described in the snippet you gave for the extraction of features and categorization. The steps they took are broken down as follows:

2.4.1. Feature Extraction

- Several assessments were made after hospitalization (N hours).
- The mean value (Mi) associated with every measured value (i) was determined for 5 hours from the moment of measurement TN-5 to TN.
- The disparity between the standard deviation of the average at time TN and the mean value at time TN-5 was used to define the change in all measurements (Di).
- Because age was seen as non-variable, it was not included in the change calculation.
- Thus, for the eight measurements (age excluded), there were nine medians (Mi) and eight change numbers (Di).

2.4.2. Classification

- The alteration in the value (Di) was given a label: positive (+1), negligible (0), or negative (-1) to categorize every measurement (i) as increasing, roughly constant, or declining.
- Thresholds set at the mean of the percentages of Di were used to calculate the categorization, denoted as (Di).



- When considering the eight measures (aside from age), the median values that served as thresholds were taken from the overall regular patient group.

2.4.3. Correlation Calculation

- For pairs of measurements (i and j), the correlation indicator (D_{ij}) was calculated to assess the trend: positive (+1), negligible (0), or negative (-1).
- Associations between the three children of observations were also computed similarly.
- The statistical analysis for the association did not account for age.

2.5. Regarding the data used in the study

- The study for the sepsis case group concentrated on information from three hours before the target hour.
- If the point of infection was far from the desired hour, no data points were used.
- The whole-time window block, except the final three hours (the wash-out period), was utilized for educational input for the control group.
- Each episode was treated independently in the study, which split the information into Training (80%), and test (20%) sets.
- Randomly selected data entries were taken from a 5-hour rolling time window.
- It was excluded if data from another ICU fell within the segment's target of five straight hours.
- Data from the sepsis case group was randomly picked to match the comparator group's sample size to equalize the information between the control and sepsis case groups.

It's critical to remember that the details given are an overview of the technique outlined in the work. It is advised to consult the original book for complete understanding and additional information.

2.6. Modified Bird Swarm Optimization (MBSO)

A novel bio-inspired optimization technique called the bird's swarm algorithm has been suggested. The interplay between swarm behaviour and swarm interaction is simplified in BSA. The algorithm mimics the three fundamental behaviours of birds: foraging, watching, and flying order to solve the optimization problem using this swarm intelligence. The algorithm can be condensed into five idealized rules, briefly outlined.

Step (1) Birds randomly decide whether to forage or to be watchful.

Step (2) Birds record and update the best positions of individuals and swarms as they seek food, sharing this knowledge with the entire multitude.

Step (3): Meanwhile, birds are alert; they try reaching the middle of the swarm to protect themselves from predator assaults.

Step (4) Birds migrate to other places to forage regularly. The producer has the highest food reserve, and the scrounger has the smallest. Others are chosen at random to be producers or scroungers.

Step (5) Creators look for food, and scavengers follow them and look for food randomly.

In the initial bird swarm method, each bird searches for food based on its own experience and knowledge of the swarms.

A closer look at foraging behaviours also revealed parallels to avian night-time behaviour, suggesting that birds continue to require differentiating between creators and scroungers. Before each foraging trip, the birds are graded based on how much food they have stored. While scavengers follow producers to get food, certain birds search for food as producers. Some birds would be producers if their reserves were more significant, whereas birds with smaller accounts would-be scroungers. Producers' variety of activities is expanding due to their substantial food reserves in the flock.

Each producer is in charge of several scroungers. They also consider the possibility that scroungers could abandon their producers and join different manufacturers or scroungers.

Moreover, Table 1 shows the cross-border analysis procedure when a component in the initial BSO algorithm crosses a barrier. The higher and lower boundaries are then used to replace this element equally.

In this study, BSO replaces the original boundary processing method with the region-analyzing process, which increases the algorithm's capacity for random searching and keeps it from stepping into the optimal local solution too soon.

2.8. Long short-term memory (LSTM)

LSTMs are widely employed in several disciplines, particularly time series analysis, machine translation, speech recognition, and natural language processing. They are exceptionally well suited for activities requiring long-term memory and complicated temporal interactions because they are excellent at catching and remembering long-term dependencies in sequences.

The memory cell of LSTMs, which can either remember or forget information over time, represents the technology's central innovation. There are three main parts to a memory cell:

1. Input Gate: Select the data that should be saved in a memory cell given the present input and the last hidden state.

Input: Previous hidden states s_{u-1} , input at time u y_u

$$\text{Calculation: } j_u = \sigma(v_j[s_{u-1}, y_u] + c_j) \tag{1}$$

2. Forget gate: Determines which information from the memory cell should be discarded.

Input: Previous hidden states s_{u-1} , input at time u y_u

$$\text{Calculation: } g_u = \sigma(v_g[s_{u-1}, y_u] + c_g) \tag{2}$$

3. Output gate: Determines which values from the memory cell should be output as the hidden state.

Input: Previous hidden states s_{u-1} , input at time u y_u

$$\text{Calculation: } p_u = \sigma(v_p[s_{u-1}, y_u] + c_p) \tag{3}$$

$j_u \rightarrow$ Signifies an input gate.

$g_u \rightarrow$ Signifies forget gate.

$p_u \rightarrow$ Illustrates the output gate.

$\sigma \rightarrow$ Signifies sigmoid function.

$v_y \rightarrow$ Weight for the relevant gate (x) neuron.

$s_{u-1} \rightarrow$ Output from the previous lstm block (at the timestamp t-1).

$y_u \rightarrow$ Input at the current time stamp.

$c_y \rightarrow$ Biases for the respective gates (x).

In the above equations:

The sigmoid activation function, represented by σ , compresses the range of values between 0 and 1.

The hyperbolic tangent activation function, or \tanh , compresses the range of values between -1 and 1.

$[s_{u-1}, y_u]$ combines the current input y_u and the previous hidden state s_{u-1} .

The weight matrices are $v_g, v_j, v_d,$ and $v_p,$ and the bias matrices are $v_g, c_j, v_d,$ and $v_p.$ The training procedure is when these characteristics are learned.

The forget gate determines which information from the initial state of the cell C_{t-1} must be ignored.

The input gate chooses which new data should be retained in the state of a cell $d_u.$

The initial cell state is combined with the new data in the update cell state stage.

Which information should be output as the signal from the gate influences the concealed state s_u ? These equations allow an LSTM cell to selectively retain and forget data over time, enabling it to recognize long-term dependencies in sequential data.

3. Results

In this part, we assess the effectiveness of the proposed approach for sepsis detection using Python. The existing methods MGP-RNN and LSTM-RNN are compared in the proposed way. The parameter includes Accuracy, Sensitivity, Specificity, and AUC are classified.

Regarding data analysis or forecasts, accuracy measures correctness or precision about a standard or expected value. Figure 1 shows the accuracy comparison for existing MGP-RNN and LSTM-RNN is 89.3 and 92.71, and our proposed approach MBSO-LSTM has 96.2. It demonstrates that our suggested method is more precise than the current approaches.



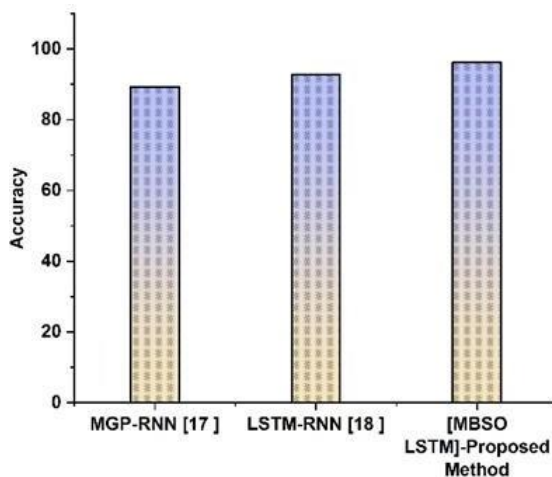


Figure 1 Accuracy.

Sensitivity is the degree of exactness or accuracy in a task or evaluation. It measures the level of accuracy and specificity of the obtained results. Figure 2 depicts a Sensitivity comparison of the existing and proposed approaches. The current guidelines, MGP-RNN and LSTM-RNN, have 0.835 and 0.865, and our proposed method MBSO-LSTM has 0.927. It indicates that our proposed technique has more precision.

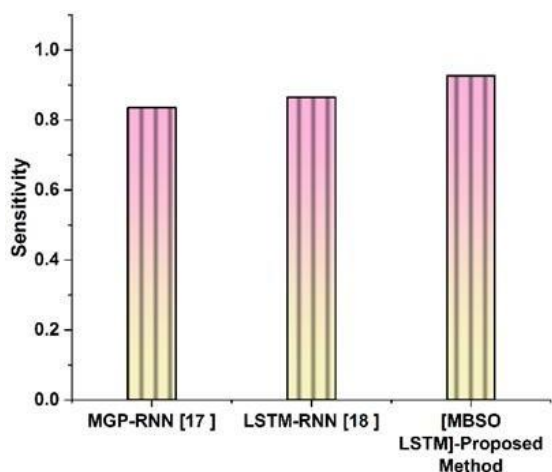


Figure 2 Sensitivity.

Specificity measures accuracy or the capacity to locate specific data or instances in a dataset or memory. It measures how effective retrieval is at a given task. This provides the percentage used in the calculation of Specificity as Figure 3 displays the performance of Specificity for MGP-RNN, LSTM-RNN in 0.957, 0.962 compared with the proposed approach MBSO-LSTM in 0.991.

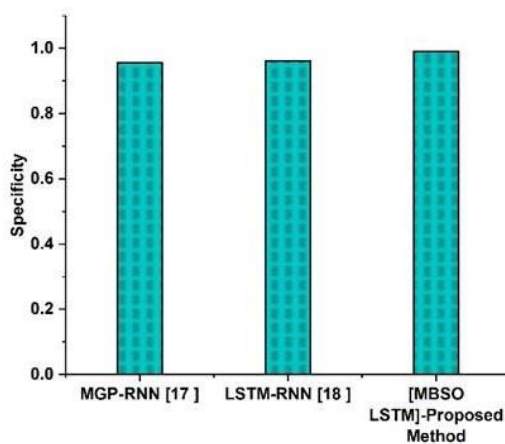


Figure 3 Specificity.



The mean percentage of AUC and Sensitivity is the AUC. The AUC comparison for existing and proposed approaches is shown in Figure 4. The existing systems, MGP-RNN and LSTM-RNN, have values of 0.889, 0.929, and the proposed technique, MBSO-LSTM, has a value of 0.948.

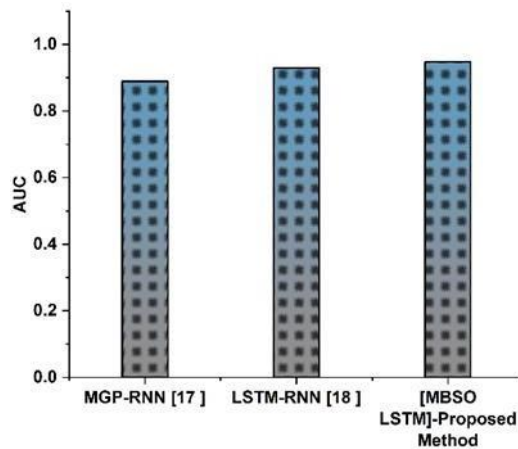


Figure 4 AUC.

5. Conclusions

The MBSO-LSDM methods for enhancing sepsis detection. This methodology improves the accuracy and efficiency of sepsis detection models by optimizing the BSO parameters and architecture using Modified Bird Swarm Optimization (MBSO). The result has the potential to enable early detection and prediction of sepsis, leading to improved patient outcomes and reduced mortality rates. The Values of performance metrics for our proposed method were obtained in terms of accuracy (96.2%), sensitivity (0.927%), specificity (0.991%), and AUC (0.948%). Moreover, this approach can be extended to other medical diagnostic tasks beyond sepsis detection, offering a flexible framework for the early detection and diagnosis of various diseases. Further research and validation in real-world healthcare settings are necessary to fully realize the potential impact of this approach on improving patient care.

Ethical considerations

Not applicable.

Declaration of interest

The authors declare no conflicts of interest.

Funding

This research did not receive any financial support.

Reference

Alani MM (2021) Detection of reconnaissance attacks on IoT devices using deep neural networks. In *Advances in Nature-Inspired Cyber Security and Resilience* 9-27. Cham: Springer International Publishing.

Aslan MF, Unlersen MF, Sabanci K, Durdu A (2021) CNN-based transfer learning–BiLSTM network: A novel approach for COVID-19 infection detection. *Applied Soft Computing* 98:106912.

Chong HY, Yap HJ, Tan SC, Yap KS, Wong SY (2021) Advances of metaheuristic algorithms in Training neural networks for industrial applications. *Soft Computing* 25:11209-11233.

El-Rashidy N, Abuhmed T, Alarabi L, El-Bakry HM, Abdelrazek S, Ali F, El-Sappagh S (2022) Sepsis prediction in intensive care unit based on genetic feature optimization and stacked deep ensemble learning. *Neural Computing and Applications* 1-30.

Goel T, Murugan R, Mirjalili S, Chakrabartty DK (2022) Multi-COVID-Net: Multi-objective optimized network for COVID-19 diagnosis from chest X-ray images. *Applied Soft Computing* 115:108250.

Hallawa A, Zechendorf E, Song Y, Schmeink A, Peine A, Marin L, Ascheid G, Dartmann G (2019) On the Use of Evolutionary Computation for In-Silico Medicine: Modelling Sepsis via Evolving Continuous Petri Nets. In *Applications of Evolutionary Computation: 22nd International Conference, EvoApplications 2019, Held as Part of EvoStar 2019, Leipzig, Germany, April 24–26, 2019, Proceedings* 254-269. Cham: Springer International Publishing.

Kandati DR, Gadekallu TR (2023) Federated Learning Approach for Early Detection of Chest Lesion Caused by COVID-19 Infection Using Particle Swarm Optimization. *Electronics* 12:710.

Lauritsen SM, Kalør ME, Kongsgaard EL, Lauritsen KM, Jørgensen MJ, Lange J, Thiesson B (2020) Early detection of sepsis utilizing deep learning on electronic health record event sequences. *Artificial Intelligence in Medicine* 104:101820.



- Naruei I, Keynia F (2022) Wild horse optimizer: A new meta-heuristic algorithm for solving engineering optimization problems. *Engineering with computers* 38:3025-3056.
- Owen AM, Fults JB, Patil NK, Hernandez A, Bohannon JK (2021) TLR agonists as mediators of trained immunity: mechanistic insight and immunotherapeutic potential to combat infection. *Frontiers in immunology* 11:622614.
- Parashar V, Kashyap R, Rizwan A, Karras DA, Altamirano GC, Dixit E, Ahmadi F (2022) Aggregation-based dynamic channel bonding to maximize the performance of wireless local area networks (WLAN). *Wireless Communications and Mobile Computing* 2022.
- Sabzalian MH, Kharajinezhadian F, Tajally A, Reihanisarsari R, Alkhazaleh HA, Bokov D (2023) New bidirectional recurrent neural network optimized by improved Ebola search optimization algorithm for lung cancer diagnosis. *Biomedical Signal Processing and Control* 84:104965.
- Selvakumar A, Balasundaram A (2023) Automated Mango Leaf Infection Classification using weighted and Deep Features with Optimized Recurrent Neural Network Concept. *The Imaging Science Journal* 1-19.
- Singh AK, Kumar A, Mahmud M, Kaiser MS, Kishore A (2021) COVID-19 infection detection from chest X-ray images using hybrid social group optimization and support vector classifier. *Cognitive Computation* 1-13.
- Swain BK, Khan MZ, Chowdhary CL, Alsaeedi A (2023) SRC: Superior Robustness of COVID-19 Detection from Noisy Cough Data Using GFCC.

Enhancing diagnostic accuracy for unidentified primary tumors with remora-optimized novel machine learning approach



Ashok Kumar Singh^a | Pradeep Kumar^b | Samir Sapkota^c

^aTeerthanker Mahaveer University, Moradabad, Uttar Pradesh, India, Associate Professor, Department of General Surgery.

^bJaipur National University, Jaipur, India, Assistant Professor, Department of Gen Medicine.

^cSanskriti University, Mathura, Uttar Pradesh, India, Assistant Professor, Department of Ayurveda.

Abstract Unidentified originating Tumors (UPT) are a kind of cancer where the originating location of the disease is still unclear, despite cancer cells throughout the body. In other words, even when malignant cells are present, medical professionals are unable to pinpoint the precise organ or tissue where the disease first started. The medical industry offers a big opportunity for Machine Learning (ML) to contribute significantly to illness prediction. One of the primary health challenges that each country faces is the tumor or cancer. In this study, we create a Remora Optimized Gated Recurrent Neural Network (RO-GRNN) to predict UPTs. The proposed approach consists of three stages: pre-processing, classification, and optimization. At first, we classified the UPT using the datasets given in the UCI ML library. The acquired Magnetic Resonance Imaging (MRI)/ Computed Tomography (CT) images will therefore have noise, lowering the efficiency with which classification may be accomplished. Pre-processing techniques like filtering and contrast augmentation could be used to eliminate unwanted noise from the offered images. The Gated Recurrent Neural Network (GRNN) and the Remora Optimization Algorithm (ROA) were both used in the development of the suggested classifier. Multiple optimization procedures, including basic and parametric optimization, take advantage of the ROA inside the GRNN. The proposed approach is employed in Origin Pro, and F1-Measure, recall, precision, and accuracy are some of the performance matrices that are used to evaluate effectiveness. The suggested approach is contrasted with the current ANN, SVM, and LSTM approaches. This research revealed that the proposed method has a 98% accuracy rate for UPT prediction.

Keywords: machine learning, UPT, RO-GRNN, prediction

1. Introduction

Clinical oncology faces major difficulties because of Unidentified Primary Tumors (UPTs). These tumors create diagnostic challenges that impede prompt and efficient treatment choices because they lack a distinct origin. Finding the main location is essential for picking the best treatments, determining the prognosis, and directing patient care. However, since UPTs are so varied and the available diagnostic techniques are so limited in many situations, proper diagnosis is still difficult to achieve (Herruer et al 2020). Despite thorough clinical evaluation, UPT is defined as the accepted metastatic involvement of an organ without a clear primary location. A proper diagnostic strategy produces positive outcomes in these individuals. UPT is regarded as a diagnostic and therapeutic challenge. In 10–30% of individuals with advanced disease, Brain Metastases (BM) is common and has fatal consequences. Brain metastasis often occurs at the end of a patient's clinical course (Mohamed and Kamel 2021). The accessibility of such information for patients with BM-UPTS is still unknown; however, several papers claimed that the identification rate of original tumors among individuals with extracranial metastases as the initial presentation was 40%.

Despite its crucial clinical implications, metastasis is poorly understood. For instance, it has been reported that metastases may arise from one, many, or clones of the original tumor's cells, but it is uncertain if these patterns are common across various tumor types. It is also unknown how treatment will affect these patterns and when metastatic seeding will occur (Lin et al 2019). Since metastases are often collected after treatment, with such data, it is hard to distinguish between the factors that cause metastasis and those that are related to treatment because several recent studies have classified genomically unrelated metastatic tumors without the matched primary tumor. However, because of the challenges in collecting matched original tumors and metastases, assessments have been significantly more constrained. There hasn't been enough research on monoclonal vs. polyclonal planting, when systemic dispersion occurs, or how therapy affects different types of cancer (Hunter et al 2018). As a result, the necessity of diagnostic testing for UPT patients' therapeutic care



increased. The main tumor location, tumor size, local-regional metastases, and metastatic sites may all be identified by PET/CT with more accuracy than with contrast-enhanced CT or MRI alone. This makes it easier to choose a treatment that is more suitable and site-specific and to follow up in a way that increases overall survival and improves therapeutic outcomes. Precision head and neck radiation treatment requires laborious tumor target contouring, and radiation oncologists' approaches to this task vary greatly.

The survival of individuals with head and neck cancer is significantly harmed by contouring errors (Reinert et al 2020). With the increased utilization of proton beam radiotherapy and intensity-modulated radiation therapies, the initial contouring of the Gross Tumor Volume (GTV) has extended dramatically since it is now necessary to imagine data sets that use many modalities or multiple parameters. After an extensive examination of the tumor on diagnostic imaging, the GTV is calculated using the set of CT or MRI information for treatment planning in the traditional way of tumor segmentation (Bakshayeshkaram et al 2018). Nasopharyngeal carcinoma (NPC) is medically unique from other head and neck malignancies and extraordinarily sensitive to radiation treatment; as a result, radiation therapy is used to treat most of these tumors. The preferred radiation therapy approach for NPC nowadays is intensity-modulated radiation treatments. Because of the following aspects, the NPC may reach nearby cerebral networks and the skull base; GTV contouring for NPC is very labor-intensive and error-prone, but during an MRI, small signal changes often show the extent of participation (Hu et al (2020). To prevent unwanted radiation treatment toxicities, the delineation of the GTV must be precise due to its closeness to the important brain and other organs. Accordingly, the radiation oncologist's knowledge is essential to designing radiation therapy for NPC. If accessible, deep learning automation of GTV contouring might be a useful situation. The need to increase the diagnostic efficacy of UPTs has gained more attention in recent years. Developing genetic profiling methods, imaging modalities and computational analysis provides potential new perspectives for improving our comprehension of these puzzling cancers (Fatima et al 2020).

According to the Israel et al (2020), the major uses for these nanoparticles include MRI, magnetic targeting, gene transfer, magnetic hyperthermia for the treatment of tumors, and macrophage polarization for the manipulation of the immune system in the fight against cancer. Because it is more sensitive than MRI, Magnetic Particle Imaging (MPI) has received a lot of interest recently. The most frequent and dangerous primary brain tumors in children and adults exhibit genomic and transcriptional variability. Gonzalez Castro et al (2023) investigated the recognition of the intra-tumoral heterogeneity of primary brain tumors has improved due to the use of these methods to investigate them. They have also learned new information about how these tumors use developmental programs and micro-environmental signaling to promote tumor growth and invasion.

Due to their outstanding performance in image identification tasks, Deep Learning (DL) algorithms are receiving much attention. Medical image properties may be quantitatively evaluated automatically using DL models, leading to improved diagnostic accuracy and more efficiency. According to the Zhou et al (2020), it is feasible to predict clinically undetectable axillary lymph node metastases in individuals with initial breast cancer using US images. Clinically, ultrasound images and biopsies are the best monitoring method for Asian women. Building a model for automated identification, segmentation, and categorization of breast lesions using ultrasound images was the goal of the study (Chiao et al (2019). A method for identifying lesions and differentiating benign from malignant ones was created based on DL and uses mask areas with Convolutional Neural Networks (CNNs). A brain tumor diagnosis approach combining fuzzy logic with edge recognition and the U-NET CNN method of classification was suggested in (Maqsood et al (2021).

The proposed tumor segmentation method uses fuzzy logic image enhancement, edge detection, and classification. Dual-Tree Complex Wavelet Transform (DTCWT) is used at various scale ranges to identify the edge in the input images after contrast improvement, and edge recognition using fuzzier logic has been performed on the original images. The location, shape, and size of a specific form of brain tumor known as a glioma might vary. High-Grade Glioma (HGG) is a more hazardous malignancy than Low-Grade Glioma (LGG). MRI helps assess gliomas in clinical settings because it gives crucial information about the locations of the tumors.

To segment and identify brain tumors, Sharif et al (2020) proposed an active DL-based feature selection technique. The first stage is improving the contrast, which is then given to SbDL for building a saliency map, which is then converted into a binarized form by using straightforward thresholding. Timely and precise identification of a brain tumor is crucial for therapy. Using MRI images, Cinar and Yildirim (2020) aimed to identify a brain tumor. The diagnosing method uses CNN models, one of the deep learning networks. The basis is the Resnet50 architecture, one of the CNN models. The Resnet50 model's last five layers were deleted, and eight new layers were created in their place. In this research, we use an ML technique called the Remora Optimized Gated Recurrent Neural Network (RO-GRNN) to improve the diagnosis accuracy for UPT.

2. Materials and Methods

This section intends to create the Remora Optimized Gated Recurrent Neural Network (RO-GRNN) for primary tumor prediction. Pre-processing, classification, and optimization are the three stages of the suggested methodology. Figure 1 depicts the whole design of the proposed approach.

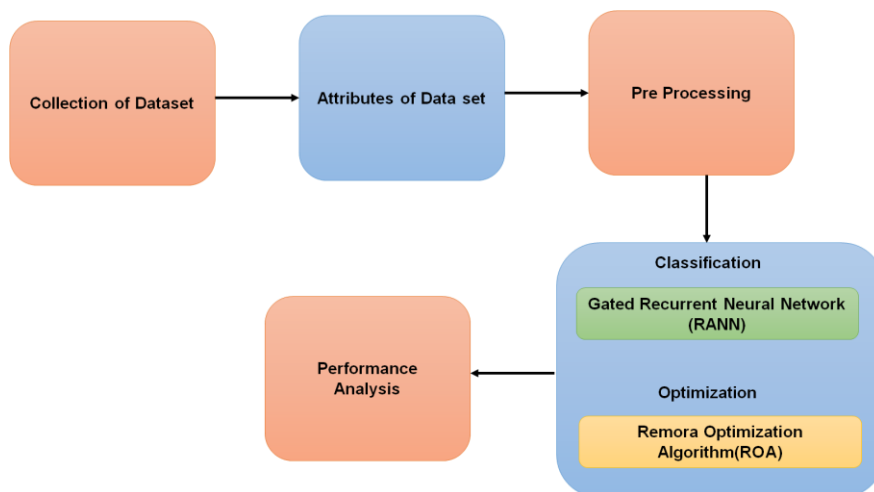


Figure 1 The architecture of the proposed approach.

2.1. Dataset

The initial step in system processing is data gathering. In this study, the UCI ML primary tumor dataset was used to assess the performance metrics of the two suggested methods. The collection contains 339 instances, 18 characteristics, and one class attribute. The overall number of main tumor classifications is 22. While the "goal" field indicates whether or not the patient has a primary-stage tumor, the other attributes demonstrate the sources of primary tumors. Table 1 describes the key feature qualities. Attributes of a dataset are qualities that are used by systems. In this study, data were preprocessed before the analytical step. One of them is the handling of missing values. As part of this work, we must change a few classed data sets using dummy value meanings that represent 0 and 1. For reliable findings, you need a balanced collection of data. By equalizing both target classes via data balancing, we have increased the validity of the validation.

Table 1 An explanation of the dataset's characteristics.

S. No.	Attribute	Description of the Parameters
1	Age	Demographic data related to patient's age (<30, 30-59, >=60) in years
2	Sex	Demographic data related to the Gender of the patient Male-1, Female-0
3	degree-of-differ	Multivariate data of 3 degrees well, fairly, poorly
4	histologic-type	Multivariate data of 3 types type1: epidermoid, type 2: adeno, type 3: anaplastic
5	Brain	Yes-1(tumor detected), No-0(not detected)
6	Lung	Yes-1(tumor detected), No-0(not detected)
7	Bone	Yes-1(tumor detected), No-0(not detected)
8	Liver	Yes-1(tumor detected), No-0(not detected)
9	Skin	Yes-1(tumor detected), No-0(not detected)
10	Neck	Yes-1(tumor detected), No-0(not detected)
11	bone-marrow	Yes-1(tumor detected), No-0(not detected)
12	abdominal	Yes-1(tumor detected), No-0(not detected)
13	axillar	Yes-1(tumor detected), No-0(not detected)
14	mediastinum	Yes-1(tumor detected), No-0(not detected)
15	Pleura	Yes-1(tumor detected), No-0(not detected)
16	supraclavicular	Yes-1(tumor detected), No-0(not detected)
17	peritoneum	Yes-1(tumor detected), No-0(not detected)

2.2. Pre-Processing

Preprocessing MRI/CT images include several processes to increase the information required for analysis, enhance image quality, and reduce noise.

Inspect the images to make sure the images are focused appropriately and that the anatomical alignment is constant across all slices. To guarantee constant voxel dimensions, scaling may also be used. Utilize noise reduction methods to



eliminate random noise and raise the signal-to-noise ratio. Many techniques use wavelet demising or spatial filtering, such as Gaussian or median filtering.

The acquired MRI/CT tumor images include undesired sounds, which should lessen the anticipated technique's ability to function well. The filter reduces the amount of noise in the images. The image has noise in the last few surrounding pixels, and by previously using the average value to alter the pixel quality, pixel worth may range from 0 s to 255 s. The adaptive histogram equalization approach helps to improve contrast after the image has been cleaned of noise. The formulation of the equalization procedure is as follows:

$$CONTRAST(J, I) = RANK * MAX_{intensity(j,i)} \text{ ie., initially rank} = 0 + 1 \quad (1)$$

The leading position of the final row across the preceding column it is possible to create the graph in the first position of each line, which contains the new beginning row. The interval, which it continuously identifies as the imaging gray stage, also changes the dispersion of two close gray levels in the current histogram and raises the complexities of the MRI/CT pictures.

2.3. Remora Optimized Gated Recurrent Neural Network (RO-GRNN)

2.3.1. Gated Recurrent Neural Network (GRNN)

We utilize a GRNN framework with Gated Recurrent Units (GRUs) in this study. Recurrent neural networks (RNNs), also known as GRNNs, are a feature of the design of neural networks. Gating mechanisms are included in GRNNs to regulate the flow of information through the network, in contrast to conventional RNNs, which only have one hidden state.

The presence of gating units, often implemented as a mix of sigmoid activation functions and element-wise multiplication operations, is the crucial component of GRNN. These gating components control the information flow between the network's input, hidden state, and output. GRNNs are designed to deal with the vanishing gradient issue that standard RNNs often run into during training. GRNNs may selectively keep and update data in the hidden state with the help of gating units, allowing them to detect long-term relationships in sequential data. The following are the GRU's update equations:

$$y_s = \sigma(X_y u_s + X_y g_{s-1} + a_y) \quad (2)$$

$$q_s = \sigma(X_y u_s + X_y g_{s-1} + a_y) \quad (3)$$

$$\tilde{g}_s = \text{tanh}(X_u u_s + X(q_s \odot g_{s-1} + a)) \quad (4)$$

$$g_s = (y_s \odot g_{s-1} + (1 - y_s) \odot \tilde{g}_s) \quad (5)$$

Where $\sigma(\cdot)$ stands for the elementwise multiplication, the activated sigmoid function tanh , and \odot the hyper-tangent activation function. Equations 2-5 are, respectively, the candidate hidden state, update gate, reset gate, and hidden state. $\{X_y, X_q, X\}$ are hidden weight matrices that accept input. $\{V_y, V_q, V\}$ are matrices from hidden to hidden. Bias vectors are $\{a_y, a_q, a\}$. The candidate hidden state \hat{g}_s is computed using the output of the hidden state g_s , and the reset gate q_s is updated using the update gate's result y_s .

One GRU layer makes up our regression model. An 83-point sensor reading series is provided as the input. To predict the tumor concentration, the final hidden state is run through a linear regressor. In this paper, several GRU models are evaluated using layer sizes of 50, 100, and 200 units.

2.3.2. Remora Optimization Algorithm (ROA)

The capacity of the remora to swim alongside whales or other marine creatures to preserve power and avoid predation is well known. The shipping industry often uses tropical waterways. However, like a virus, it also displaces into the host's water. The remora's primary supply of nourishment is other fish or invertebrates. It leaves the premises when it locates a region in the ocean with adequate food, ingests it, and then absorbs it back onto the host to continue its voyage to more sponsors and other marine locations. With the number of remora and different dimensions, the ROA algorithm is launched at the present location in the search space. Here is an example of the initial operations phase:

$$q_1 = (q_{j1}, q_{j2}, \dots, q_{jC}) \quad (6)$$

J is the number of remoras, and C is the remora's capacity specified.

This place is designated for the updating procedure with a comparable timeframe since the remora is linked to the swordfish. The formulation of this method is as follows:

$$q_j^{s+1} = q_{best}^s \left[\text{RAND}(0,1) * \frac{(q_{best}^s \text{ RAND})}{2} - q_{RAND}^s \right] \quad (7)$$

Where q_{RAND} is the random position, S is the greatest number of repetitions, while s is the present amount of repetitions being carried out. The elite select the historically wisest course of action, which continues the update process. The pseudocode of ROA is shown in Algorithm 1.

Algorithm 1: Pseudocode of ROA

Set the population and storage location for the random place at the beginning.
 Choose the ideal option that is also connected to optimum fitness.
 When $S > S_{max}$
 Determine each remora's health benefits parameter
 Check to see if any search agents go outside of the search area
 Update α, A, U
 For each remora listed by I
 If $G(J) = 0$ then
 The location of the linked whales is updated using Equation (7)
 Else if $G(J) = 1$ then
 The associated sailfishes' location is updated using Equation (5)
 End if
 Calculate (6) the one-step identity.
 Calculate the parameter $G(J)$ using Equations (7) and (8) to determine if a host change is necessary.
 Equation (12) may be used as the host feeding mode for remora if the host is left unchanged.
 End for
 End while

The experience of attack is considered while calculating the necessary change of host. The formulation of the experience attack is as follows:

$$q_{att} = q_J^S + (q_J^S - q_{pre}) * randn \quad (8)$$

Here, q_{att} is referred to as a tentative step, and q_{pre} is referred to as the position of the preceding generation.

The following is a description of the status of the formula change based on the standard WOA technique:

$$q_{J+1} = c * F^b * \cos(2\pi\alpha) + q_1 \quad (9)$$

$$\alpha = RAND(0,1) * (b - 1) + 1 \quad (10)$$

$$b = - [1 + \frac{2}{s}] \quad (11)$$

$$C = |q_{best} - q_J| \quad (12)$$

In a higher resolution time, the remora could represent a whale, and its locations would be reduced accordingly. In this case, e stands for the distance between the hunter and the prey while for the random number in the range $[1, 1]$. Furthermore, $[2, 1]$ appears as a random number.

This is an exploiting strategy. At this point, less solution space is available in the main location region. Following is a formulation for the crowd going on the little steps:

$$q_J^S = q_J^S + B \quad (13)$$

$$B = A * (q_J^S - d * q_{best}) \quad (14)$$

$$A = 2 * Y * RAND(0,1) - Y \quad (15)$$

$$Y = 2 * (1 - \frac{s}{Maximum\ iteration}) \quad (16)$$

Here, D represents the location of the remora, while B is a representation of minor motions that could be related to the host volumetric area.

According to the details that have been presented, it would seem that the ROA method is used to optimize the parameters for the GRNN classifier to increase the performance of the classifier when it comes to predicting UPT. During optimization, the GRNN classifier's parameters are evaluated using a fitness assessment to determine which ones should be changed.

3. Results

Performances of the proposed method are assessed using performance matrices, including accuracy, precision, recall, and F1-Measure for the suggested approach, which is implemented in Origin Pro. TP for True positive, TN for True negative, FP for False positive, and FN for False negative. The proposed strategy is evaluated by contrast with well-established methods like Artificial Neural Network (ANN) (Muhammad et al (2019), Support Vector Machine (SVM) (Manju et al (2021), and Long Short-Term Memory (LSTM) (Amin et al (2020), respectively, to ensure its validity.

3.1. Accuracy

Accuracy is a term used to describe how successfully a prediction model recognizes the presence or absence of a tumor in a given dataset when discussing tumor prediction. It is often reported as a percentage and is determined by dividing the total number of instances by the number of cases that were properly predicted (both true positives and true negatives). The accuracy comparison between the suggested technique and current methods is shown in Figure 2 and Table 2. The formula for accuracy is:

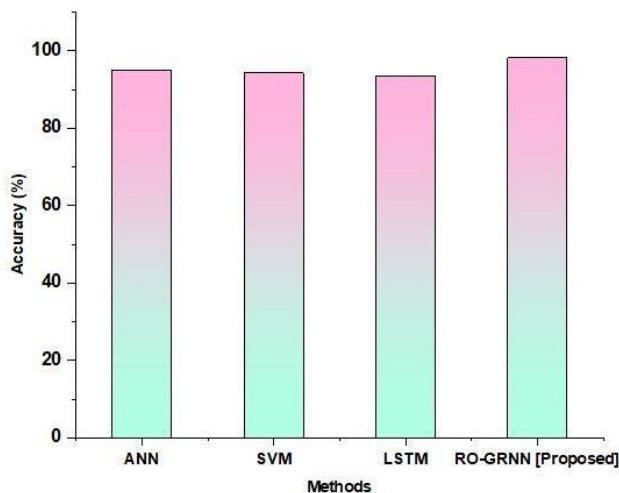


Figure 2 Accuracy evaluation of the proposed approach versus current methods.

Table 2 Accuracy Comparison.

Methods	Accuracy (%)
ANN	95
SVM	94.3
LSTM	93.6
RO-GRNN [Proposed]	98.2

$$Accuracy = \frac{TP+TN}{TP+FP+FN+TN} \tag{17}$$

3.2. Precision

Precision is a statistical parameter that assesses the accuracy of the optimistic predictions produced by a predictive model or algorithm in the setting of tumor prediction. Out of all occurrences anticipated as positive (including true positives and false positives), it measures the percentage of accurately predicted positive cases (true positives). The accuracy comparison between the suggested technique and current methods is shown in Figure 3 and Table 3. The formula for precision is:

Table 3 Precision Comparison.

	Precision (%)			
	ANN	SVM	LSTM	RO-GRNN [Proposed]
1	96.2	82.5	92	95
2	80	76	90	99
3	83	70	86	97
4	86	75	79	98
5	81	79	91	96

$$Precision = \frac{TP}{TP+FP} \tag{18}$$



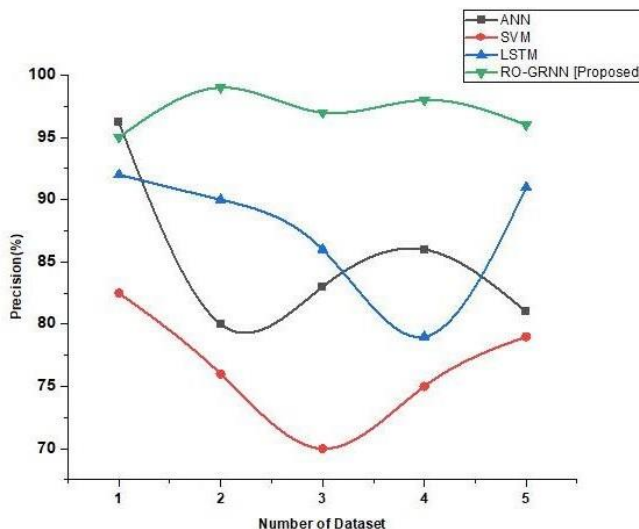


Figure 3 Precision evaluation of the proposed approach versus current methods.

3.3. Recall

The recall is a performance statistic that is often used in the field of tumor prediction to assess how accurate a model or algorithm is. Recall, sometimes referred to as sensitivity or the percentage of instances that the prediction model properly classified as positive (i.e., those in which a person develops a tumor), quantifies the proportion of real positive cases. It offers data on the model's accuracy in identifying those who are at tumor development risk. The recall comparison between the suggested technique and current methods is shown in Figure 4 and Table 4. The formula for the recall is:

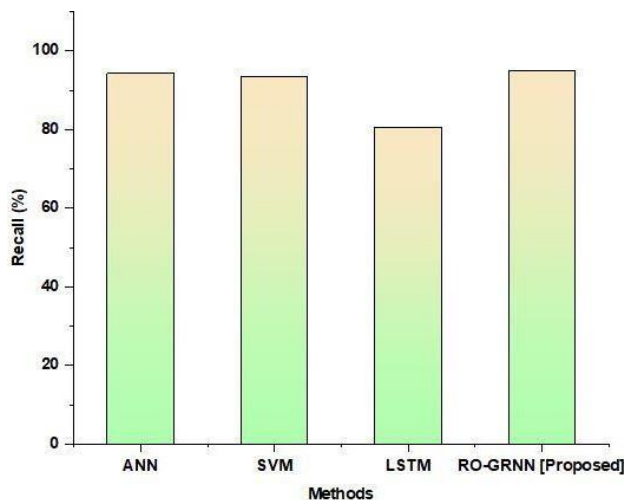


Figure 4 Recall evaluation of the proposed approach versus current methods.

Table 4 Recall Comparison

Methods	Recall (%)
ANN	94.3
SVM	93.6
LSTM	80.7
RO-GRNN [Proposed]	95

$$Recall = \frac{TP}{TP+FN} \quad (19)$$

3.4. F1-measure

The frequently used measurement for assessing the efficacy of a binary classification model is the F1 measure. It provides a fair assessment of the model's accuracy by combining recall and precision. The harmonic mean of accuracy and



memory, known as the F1 measure, yields a single score for precision and recall. The F1-measure comparison between the suggested technique and current methods is shown in Figure 5 and Table 5. The formula used to compute it is as follows:

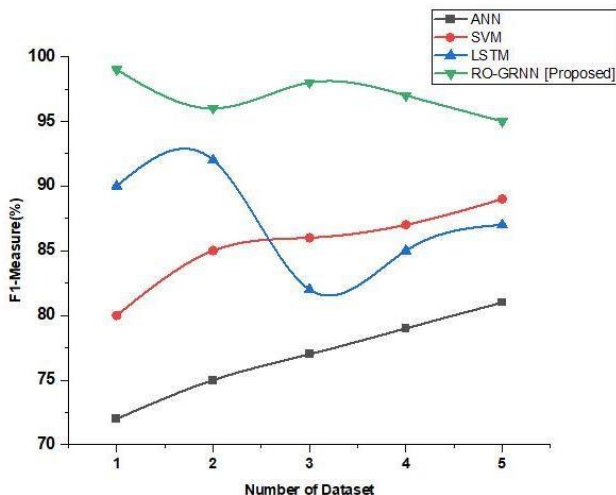


Figure 5 F1-measure evaluation of the proposed approach versus current methods.

Table 5 F1-measure Comparison.

F1-Measure (%)				
	ANN	SVM	LSTM	RO-GRNN [Proposed]
1	72	80	90	99
2	75	85	92	96
3	77	86	82	98
4	79	87	85	97
5	81	89	87	95

$$F1 - measure = 2 * \frac{Precision * Recall}{Precision + Recall} \tag{20}$$

According to the findings above, the suggested approach is 98% accurate. The ANN, SVM, and LSTM also obtained 95.1%, 94.3%, and 93.6%, respectively. The suggested method's precision score is 97%. The ANN, SVM, and LSTM also obtained 96.2%, 82.5%, and 87.6%, respectively. The suggested method's recall measurement is 95%. The ANN, SVM, and LSTM obtained 94.3%, 93.6%, and 80.7%, respectively. The suggested method's F1-measure is 94%. The ANN, SVM, and LSTM also obtained 92%, 87.4%, and 81.9%, respectively. These results demonstrate that RO-GRNN outperforms other presently available methods.

4. Conclusions

Early tumor detection is important for clinical care and cancer monitoring and is a prominent area of current study. It may enhance a patient's quality of life. The focus of this study, which used ML approaches, was on UPT prediction utilizing a variety of algorithms and a combination of numerous targeted characteristics. Depending on the dataset, a specific ML approach was used, and it was often found that binary classifiers were effective with no more than two categories, classifiers incorporating binary classifiers, called RO-GRNN, were more precise with more classes. It has been compared with traditional methods like ANN, SVM, and LSTM to verify the predicted methodology. The accuracy, precision, recall, and F-Measure of the suggested approach are 98.2%, 97%, 95%, and 94%, respectively. According to the study, the proposed approach produced effective results in terms of statistical measures. Future development and enhancement of the work may automate the detection of initial cancers. When working with big datasets, the suggested approach takes a long time. The development of primary tumor detection will be aided by considering a new, effective strategy to help overcome the disadvantages. This is a solid closing point that we would want to make: the settings of the learning algorithms weren't optimized to produce the best results with our data. Therefore, there is still an opportunity for improvement.

Ethical considerations

Not applicable.

Declaration of interest

The authors declare no conflicts of interest.



Funding

This research did not receive any financial support.

References

- Amin J, Sharif M, Raza M, Saba T, Sial R, Shad SA (2020) Brain tumor detection: a long short-term memory (LSTM)-based learning model. *Neural Computing and Applications* 32:15965-15973.
- Bakhshayeshkaram M, Tavakoli F, Hassanzad M, Seifi S, Jamaati HR (2018) Brain-Included 18F FDG PET/CT Acquisition Protocol: Cancer-Specified Clinical Impact of Newly-Diagnosed Brain Metastasis in Extra-Cerebral Cancer Patients. *Novelty in Biomedicine*, 6(1):21-28.
- Chiao JY, Chen KY, Liao KYK, Hsieh PH, Zhang G, Huang TC (2019) Detection and classification the breast tumors using mask R-CNN on sonograms. *Medicine* 98.
- Fatima N, Zaman MU, Zaman A, Zaman U, Zaman S, Tahseen R (2020) Detection efficiency of 18F-fluorodeoxyglucose positron emission tomography/computed tomography for primary tumors in patients with carcinoma of unknown primary. *World journal of nuclear medicine* 19:47-51.
- Gonzalez Castro LN, Liu I, Filbin M (2023) Characterizing the biology of primary brain tumors and their microenvironment via single-cell profiling methods. *Neuro-oncology* 25:234-247.
- Herruer JM, Taylor SM, MacKay CA, Ubayasiri KM, Lammers D, Kuta V, Bullock MJ, Corsten MJ, Trites JR, Rigby MH (2020) Intraoperative primary tumor identification and margin assessment in head and neck unknown primary tumors. *Otolaryngology–Head and Neck Surgery* 162:313-318.
- Hu Z, Li Z, Ma Z, Curtis C (2020) Multi-cancer analysis of clonality and the timing of systemic spread in paired primary tumors and metastases. *Nature genetics* 52:701-708.
- Hunter KW, Amin R, Deasy S, Ha NH, Wakefield L (2018) Genetic insights into the morass of metastatic heterogeneity. *Nature Reviews Cancer* 18:211-223.
- Israel LL, Galstyan A, Holler E, Ljubimova JY (2020) Magnetic iron oxide nanoparticles for imaging, targeting and treatment of primary and metastatic tumors of the brain. *Journal of Controlled Release* 320:45-62.
- Lin L, Dou Q, Jin YM, Zhou GQ, Tang YQ, Chen WL, Su BA, Liu F, Tao CJ, Jiang N, Li JY (2019) Deep learning for automated contouring of primary tumor volumes by MRI for nasopharyngeal carcinoma. *Radiology* 291:677-686.
- Manju BR, Athira V, Rajendran A (2021) Efficient multi-level lung cancer prediction model using support vector machine classifier. In *IOP Conference Series: Materials Science and Engineering* 1012:012034.
- Maqsood, S., Damasevicius, R. and Shah, F.M., 2021. An efficient approach for detecting brain tumor using fuzzy logic and U-NET CNN classification. In *Computational Science and Its Applications–ICCSA 2021: 21st International Conference, Cagliari, Italy, September 13–16, 2021, Proceedings, Part V* 21:105-118. Springer International Publishing.
- Mohamed, D.M. and Kamel, H.A., 2021. Diagnostic efficiency of PET/CT in patients with cancer of unknown primary with brain metastasis as initial manifestation and its impact on overall survival. *Egyptian Journal of Radiology and Nuclear Medicine* 52:1-8.
- Muhammad W, Hart GR, Nartowt B, Farrell JJ, Johung K, Liang Y, Deng J (2019) Pancreatic cancer prediction through an artificial neural network. *Frontiers in Artificial Intelligence* 2:2.
- Reinert CP, Sekler J, la Fougère C, Pfannenber C, Gatidis S (2020) Impact of PET/CT on clinical management in patients with cancer of unknown primary—a PET/CT registry study. *European Radiology* 30:1325-1333.
- Sharif MI, Li JP, Khan MA, Saleem MA (2020) Active deep neural network features selection for segmentation and recognition of brain tumors using MRI images. *Pattern Recognition Letters* 129:181-189.
- Zhou LQ, Wu XL, Huang SY, Wu GG, Ye HR, Wei Q, Bao LY, Deng YB, Li XR, Cui XW, Dietrich CF (2020) Lymph node metastasis prediction from primary breast cancer US images using deep learning. *Radiology* 294:19-28.

Novel machine learning method in skin cancer diagnosis based on patient's metadata



Gajanand Ojha^a | Aishwary Awasthi^b | Vinita Gupta^c

^aJaipur National University, Jaipur, India, Professor, Department of Skin & VD.

^bSanskriti University, Mathura, Uttar Pradesh, India, Research Scholar, Department of Mechanical Engineering.

^cTeerthanker Mahaveer University, Moradabad, Uttar Pradesh, India, Professor, Department of Dermatology.

Abstract The skin's fundamental function in human body as a whole-body covering is crucial. Only if it is discovered while it is in its early stages can skin cancer be cured. Skin function plays a big part in the body's overall system and will be significantly impacted by even the slightest modification. The goal of this work was to develop an effective Machine Learning (ML) based technique for identification of skin cancer using patient information. To diagnose skin cancer with lesions image, this research introduces a novel Augmented May Fly optimized with K-Nearest Neighbors (AMFO-KNN) technique. Here, the AMFO approach is used to improve the classification efficiency of KNN. Utilizing the PAD-UFES-20 and Fitzpatrick17k datasets, the efficiency of suggested method is examined. The noisy data are removed from the raw data samples using Adaptive Median Filter (AMF). The properties are taken out of segmented data using Kernel Principal Component Analysis (KPCA). The performance metrics of research show that recommended methodology performs better than traditional approaches in terms of accuracy, precision, f1-score, and recall measures. The encouraging results demonstrate the effectiveness of suggested strategy and show that including the patient's information with lesions image may improve the performance of skin cancer diagnosis.

Keywords: SCD, metadata, patients, AMFO-KNN

1. Introduction

The challenge for dermatologists is produced from melanocyte cells, which provide a problem in the proper diagnosis of benign vs malignant lesions. Comparing malignant keratinocyte carcinoma to benign keratosis presents the same difficulties (Kousis et al 2022). Furthermore, it is difficult to distinguish between inflammatory non-neoplastic skin conditions such as dermatitis and eczema from malignant cutaneous lymphomas. The difference between benign dermal lesions (such as dermatofibroma and vascular lesions and malignant dermal lesions (like Kaposi sarcoma) is also not always easy to discern. The gold standard of diagnosis is based on biopsy and histological analysis since the visual inspection is prone to inaccuracies. The incidence of all skin-related malignancies will be divided into eight groups, which will account for 97% of the total (Malo et al 2022). Additionally, a link has been shown between the kind of lesion and the anatomical location on the body. The results prompted us to examine the effects of age, gender, and anatomical location being input into the automated model for skin cancer diagnosis (Kumar et al 2021).

Malignant lesions and benign moles often resemble one another rather closely, and both have tiny diameters that make it difficult to get good photographs with ordinary cameras (Zakhem et al 2021). For instance, because melanoma and nevus are both melanotic kinds, the categorization challenge between them is significantly greater. Additionally, the majority of patients only see their dermatologist on occasion, which results in a fatally late diagnosis (Omeroglu et al 2023). Therefore, it is necessary to provide a simple alternative for certain situations. Smartphones are the kind of digital technologies that are often the most accessible to people. With a smartphone's photography capabilities, dermatologists, general practitioners, and patients may be able to communicate naturally about changes in skin lesions that may be concerning. (Kawahara et al 2018).

The pigment-containing cells known as melanocytes often produce the malignant melanoma type of skin cancer. Melanoma accounts for around 75% of fatalities from skin cancer and is common in non-Hispanic white men and girls (Malik and Dixit 2022). The framework is based on identifying benign or cancerous tissue using images taken with a dermatoscopic instrument. Signal and image processing use a sort of neural network called a Convolutional Neural Network (CNN). The recommender system also uses convolutional neural networks. The reason CNN was selected for image processing was its great accuracy. Four standards are in use at CNN. The main layer serves as the input layer, where dermatologists enter all of the data have gathered. When it happens, the information is dense enough to be shifted to the category that corresponds to



the scenario, whether benign or malignant. The study proposes an autonomous method for detecting skin cancer that uses convolutional neural networks to categorise cancer photos as either malignant or benign melanoma (Wang et al 2021).

The word "cancer" initially emerged from the Greek word "karkinos," which also refers to a tumor and a crab. Cancer is a word that has been used in medicine since the 1600s to describe cells that are invasive or spreading and may impact other physiological regions. Cancer metastasis is uncontrolled cell growth that starts in one part of the body and spreads to other bodily regions. Malignant and benign cancer cells are the two kinds of cancer cells. To maximize the survival percentage of cancer patients, early, accurate diagnosis is necessary (Guergueb and Akhloufi 2022). Genetic mutations that affect cells' activity, particularly how technique grows and divides, cause the genetic condition that causes it. Additional modifications will take place when the tumor cells expand. In essence, cancer cells contain more genetic alterations, such as DNA mutations, than healthy ones. Few cancer cells can evade the immune system, although it often eliminates damaged or aberrant cells from the body. The immune system promotes the development and survival of the tumor (Das et al 2023). (Tajjour et al 2023) suggested the hybrid model is a network structure that manages both structured (patient information and other helpful elements from various color spaces linked to light, energy, darkness, etc.) and unstructured (images) data. The research shows the suggested hybrid model's superiority over the solo model with a 2% gain in accuracy and promising behavior when compared to ensemble approaches. Additional patient data will be used in the subsequent study to create a skin cancer screening tool. Pacheco and Krohling (2021) evaluated applying deep learning models to the issue of merging images and metadata elements for the classification of skin cancer. The suggested technique was contrasted in the research with two alternative ways to combine, one using features concatenation and the other the MetaNet. Results from two distinct skin lesion datasets demonstrate that strategy performs better than existing combination methods in six out of ten cases and improves classification for all evaluated models.

Qureshi and Roos (2022) suggested the method that enhances the model's capacity to deal with sparse and unbalanced input. Using a dataset of 33,126 dermoscopic images from 2056 patients, the study illustrates the advantages of the suggested method. The chosen method compares well across all assessment measures. (Ningrum et al 2021) indicated the capacity of deep convolutional neural networks (CNN) to forecast outcomes from both simple and complex imagery. However, its execution requires a sophisticated computing infrastructure, which is impractical in rural and low-resource healthcare settings. The combination of image and patient information has promise, but further research is needed. On several publically accessible datasets, image feature extraction and lesion classification were carried out. Bhimavarapu and Battineni (2022) suggested Support Vector Machine (SVM) and fuzzy together provided a classification accuracy and sensitivity and specificity of 100% and 99.75%, respectively. Dai et al (2019) presented an on-device inference App and presents a proof of concept using a dataset of skin cancer photos.

Combalia et al (2022) aimed to inform doctors and regulatory bodies about security and accurate real-world classification, the research simulates each diagnostic category that was contained in the training data as well as extra diagnoses not included in the training data were represented by images in the test datasets. Luu et al (2021) compared the performance of the algorithms in contrast to 18 dermatologists in a setting simulating their intended clinical use. The 32 tissue samples with Squamous Cell Carcinoma, Basal Cell Carcinoma, melanoma, and normal characteristics are used in the proposed approach, which feeds 669 data points corresponding to the 16 Mueller matrices components as predictors into a Random Forest (RF) classifier. Babu and peter (2021) suggested a reliable method for detecting skin cancer that uses the Support Vector Machine (SVM) features. The grayscale conversion and a median filter for pre-processing skin cancer photos from the International Skin Imaging Collaboration 2018 dataset. After that, the class distribution is balanced again using the image-resembling process. The preprocessed images are used to extract the features. Saba et al (2019) preferred a revolutionary automated system for recognizing and diagnosing skin lesions that are based on Deep Convolutional Neural Networks (DCNN). The following are some potential noteworthy contributions that a study on transformation based on skin cancer detection may emphasize:

- The performance of the machine learning algorithm used to diagnose skin cancer across a variety of skin lesion datasets was examined in a publication that provided an update on the subject.
- The technical difficulties of these algorithms are reviewed in the context of digital dermatology, along with chances to augment the present machine learning (ML) based image classification solutions so that physicians may utilize them to increase efficiency.

The remaining part of the study is organized into three sections: Section 2 offers recommendations for further research based on the findings and describes the research strategy and techniques used to collect and evaluate data. Before presenting the research results concisely and systematically, we go through the Discussion and results in section 3 and evaluate and describe them in light of the study aims or objectives. Section 4 provides an overview of the Study's main elements, as well as its relevance and contributions, potential repercussions for practice or policy, and potential future study areas.

2. Materials and Methods

2.1. Data Collection

The PAD-UFES-20, the International Skin Imaging Collaboration Dermoscopic Archive, and a portion of the Fitzpatrick17k images were the three datasets utilised to train and assess the proposed system. The International Skin Imaging Collaboration Dermoscopic Archive was published for the 2019 and 2020 melanoma detection challenges. International Skin Imaging Collaboration 2019 includes photos that fall under nine distinct diagnostic categories. According to (Ahmadi Mehr and Ameri 2022), International Skin Imaging Collaboration 2020 includes photos of distinctive benign and malignant skin lesions from over 2,000 individuals, and all images are dermoscopic, biopsy-proven, and labeled as malignant or benign. Histopathology was used to confirm all malignant diagnoses; benign diagnoses were either verified by expert consensus, long-term follow-up, or histopathology. The metadata in both International Skin Imaging Collaboration databases include details on the patient's gender, age, and anatomical location of the lesion on their bodies. The PAD-UFES-20 is made up of photographic samples of six distinct kinds of skin lesions, with each image indicating whether or not it has undergone a biopsy, which is the only way to confirm the presence of malignant lesions. Additional information included in this dataset includes the patient's gender, age, and anatomical location of the lesion. Figure 1 shows the image difference between Malignant, benign are all included in the Fitzpatrick17k's three-partition label for photographic images. Fitzpatrick17k did not, however, include any information. Our dataset, created from the three aforementioned databases, consists of 66735 clinical photos that reflect 16 distinct skin-disease situations. These images include 58031 dermoscopy images and 8704 photographs, respectively. To illustrate the differences between photographic and dermoscopic images for melanocytic lesions, one example image from the dataset is provided.

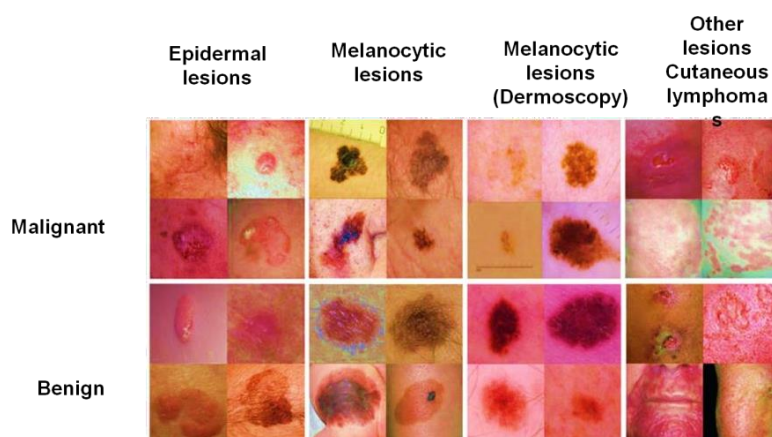


Figure 1 Photographic and dermoscopic images for melanocytic lesions to visualize the difference (Ahmadi Mehr and Ameri 2022).

2.2. Data pre-processing using Adaptive median filter (AMF)

A more sophisticated variation of the conventional median filter is the AMF technique. Through spatial processing, impulse noise is eliminated. The AMF classifies each pixel in the skin image with its neighboring pixels to determine whether there is noise or not. It is superior to other filters because it preserves the image's fine features and reduces non-impulse noise. It is also quite probable that it can adjust to impulsive noise. Similar to how the mean channel reduces disorder in a image, the median channel does the same. The median channel might be different for two descriptions, as in equation 1,

$$\text{med}(n_k) = \begin{cases} n_i + 1^a = 2i + 1(\text{ODD}) \\ \lfloor \frac{n_i+n_{i+1}}{2} \rfloor^a = 2i(\text{even}) \end{cases} \quad (1)$$

Here n_i is the i^{th} the biggest observed data and $n_1; n_2; n_3... n_i$ are the observed data. Consider a situation in which there are 7 samples total in the data collection 2, 3.5, 1, 3, 1.5, and 4 and the median filter yields an output of 2.5. The signal will remain intact if the pulse is $n + 1$ or longer; if not, it will be eliminated from the series. What distinguishes the median filter from other filters is its ability to suppress pulse noise while maintaining local characteristics. This method then sends the signal it produces to the feature extraction stage.

2.3. Feature extraction by using Kernel Principal Component Analysis (KPCA)

A basis transformation known as Principal Component Analysis (PCA) is used to diagonalize an approximation of the covariance matrix of the data in equation 2,

$$D = \frac{1}{k} \sum_{i=1}^k v_l v_l^S \quad (2)$$



Principal components are the new coordinates in the tile Eigenvector basis or the orthogonal projections onto the Eigenvectors. This setting is expanded upon in this study to a nonlinear setting of the following kind. If equation 3 were to first nonlinearly map the data into a feature space.

$$\Phi: Q^M \rightarrow E, v \rightarrow V \quad (3)$$

We'll demonstrate that, for certain values, we can still do PCA in E even if it has arbitrarily high dimensionality.

Assume that equation 4 maps data into feature space for the time being. For the covariance matrix, do PCA.

$$\bar{D} = \frac{1}{k} \sum_{i=1}^k \Phi(v)_1 \Phi(v)_1^s \quad (4)$$

Principal component analysis (KPCA) is a nonlinear variation that is often used in denoising and wavelet transform applications. When the manifold is linearly buried in the observation space, the conventional PCA method seeks to decrease dimensionality. The manifold is linearized using one of the two components of KPCA, the kernel method, to meet the needs of the PCA, the other component. KPCA automatically projects data into a pairwise-specific pairwise formula between the mapped data in the feature set using feature mapping. This pairwise formula is computed by the kernel. Finding a suitable kernel that takes the geometry of the input space into account and linearizes the surface in the feature space is challenging. A poor projection that does not meet these requirements would render KPCA's nonlinear dimensionality reduction useless.

2.4. Augmented May Fly optimized with K-Nearest Neighbors (AMFO-KNN)

The specific combination of Augmented May Fly optimized with k-nearest neighbors (KNN) in the field of skin cancer detection based on patients' information may not be widely accepted. When the two components (May Fly optimization and KNN) are combined, we may propose a concept where the May Fly optimization is included in the k-nearest neighbors method to improve the efficiency of cancer detection and attention optimization. The attention optimization within the integrating binary attention modules may be changed at different KNN levels as part of this integration. The effectiveness of the proposed approach would vary depending on the specific dataset, the nature of the skin cancer detection issue, and the computational resources available. May Fly and k-nearest neighbors may be combined to enhance attention optimization and the efficiency of intrusion detection systems. Based on these factors, we may investigate a potential idea: To establish the practicality and use of this precise combination in the context of skin cancer detection, more research and development would be necessary.

2.4.1. Augmented May Fly optimization

The insects' interactions with one another, especially during mating, served as the inspiration for the mayfly algorithm. Mayflies are presumptively regarded as adults as soon as the eggs hatch. Mayflies have a lifetime, but only the fittest often survive. There is a spot for each mayfly in the search region that relates to a solution to the issue. In the traditional Mayfly method and functions are used to create new variables that ultimately lead to the local optimum. The researchers combined MA with Levy flight to improve ability to find and provide the optimal solution. The Levy flight hypothesis says that, in contrast to stochastic random search, a Levy flight-based approach for system identification rapidly converges and does not need derivative knowledge. Levy flying significantly enhances local search avoidance and local trapping of the best solution. Figure 2 depicts the flowchart for the suggested AMFO approach.

The suggested mayfly optimization technique needs the following steps to work:

Step 1: There should be two groups of mayflies, one for each gender, representing the male and female populations.

Step 2: A mayfly's positional shift serves as the initiation of its velocity. A composite interplay between people and social flying experiences determines its course. Every mayfly tends to change its course to match its current personal best position (pbest). Additionally, it changes dependent on the best position attained by every other mayfly in the swarm up to that point (gbest). Equation 5's male mayfly population was initiated as,

$$O_{Hnj}(j = 1, 2, \dots, MH) \quad (5)$$

Step 3: Male mayfly swarms show that each mayfly's location varies based on its experiences and those of its neighbors. The mayfly's current location in the search space at the current time step is denoted by O_j^{s+1} , and its position is altered by adding the current velocity O_{Hnj}^{s+1} . Equation 6 is represented by the following notation:

$$O_{Hnj}^{s+1} = O_{Hnj}^s + O_j^{s+1} \quad (6)$$

Male mayflies are categorized as equation 7 when they are seen dancing nuptially a few meters above the water,

$$O_{Hjn}^0 W(O_{Hnnjm}, O_{Hnnbv}) \quad (7)$$

It may be assumed that these mayflies don't have very fast speeds since they are always moving. Equation 8 may be used to compute the speed of a male mayfly as shown below:

$$w_{ji}^{s+1} = h * w_{ji}^s + b_1 b^{-\beta q^2} (obest_{ji}^s - O_{Hnj}^s) + b_2 b^{-\beta q^2} (obest_i^s - O_{Hnj}^s) \quad (8)$$

Additionally, $obest_i$ represents the best location the mayfly has ever been. The personal best position at the next time step equation 9 was computed as stated below based on the minimization issues under consideration,

$$obest_i = \begin{cases} O_{Hnj}^{s+1}, & \text{if } e(O_{Hnj}^{s+1}) < e(obest_i) \\ \text{is kept the same, otherwise} \end{cases} \quad (9)$$

The female mayflies indicate in equation 10 that each mayfly's location changes according to its own experience. The equation for the world's best position, $gbest$ at time step, is given below,

$$gbest = \min\{e\{pbest_1, pbest_2, \dots, pbest_M, e\{cbest\}\}, \dots, e\{pbest_{MH}\}\} \quad (10)$$

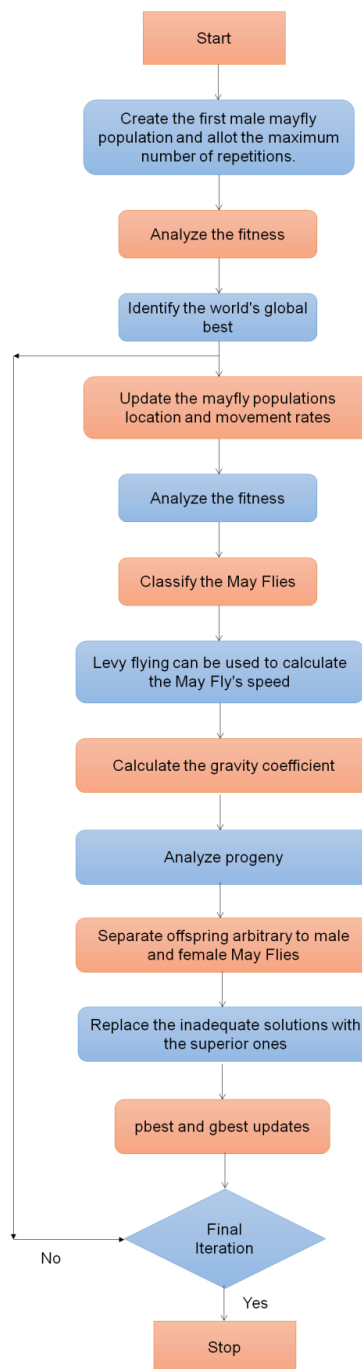


Figure 2 Flow chart of Augmented May Fly Optimization.



2.4.2. K-Nearest Neighbors

Using the KNN algorithm, skin cancer is detected. With the discovery of his method, skin cancer classification may be done while test samples and training samples are fed into databases. The closest diameter to the preparation casing is used to classify samples. The classification of the sample is then completed by its portion. By capturing the k nearby position and announcing the indication of the mainstream, the KNN classifier broadens this recommendation. It is distinct to choose k values. Choosing the value of k is often done during cross-validation, and larger values of k may help to mitigate the effects of noise levels in the pixels rate within the training data set. Here, one of the many solutions available for this issue is to choose a portion of the training data such that classification by 1-NN rules may be done utilizing values from several subsets. Using the K-Nearest Neighbors (KNN) technique, the geometrical feature extraction result values were categorized. The researchers manually entered the datasets into the same system and kept track of them. The diagnosis for each sample image in the collection was accurately labeled and sourced from the International Skin Imaging Collaboration repository.

3. Results

3.1. Evaluation of the performance of the AMFO-KNN model by comparing proposed and existing technique

Figures 3, 4, 5, and 6 show that the four-assessment metrics of prediction performance based on present and planned AMFO-KNN algorithms are especially clear in the macro recall metric. Although there are significant variances in F1-score, precision, accuracy, and recall, the results of predictions don't vary much.

3.1.1. Accuracy

An important parameter to evaluate the dependability and efficiency of the system is how reliably the skin cancer diagnosis employing *the AMFO-KNN* detects the skin cancer. It takes into account both accurately predicted positive and negative outcomes as well as accurately predicted positive and negative outcomes that were incorrect. As seen in equation 11, detection with more accuracy may detect with more precision, resulting in fewer false positives and false negatives.

$$Accuracy = \frac{TP+TN}{TP+TN+FP+FN} \tag{11}$$

The accuracy of the suggested and existing approaches is shown in Figure 3. A percentage of the total is often used to represent the accuracy level. Both the existing procedure and the suggested one have the potential for inaccurate estimates. This danger is recognized by both systems. However, the suggested method AMFO-KNN has a 48% accuracy rate compared to 18% for SVM, 24% for DCNN, and 34% for RF. The proposed approach thus has the best accuracy rate. Table 1 displays the recommended method's accuracy.

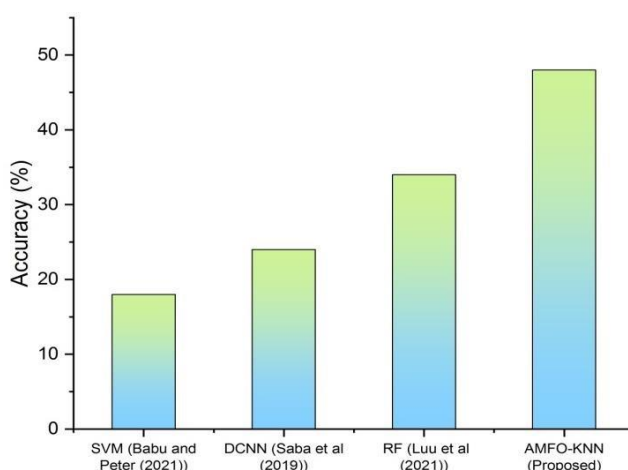


Figure 3 Comparison of accuracy.

Table 1 Numerical outcomes of the accuracy of a proposed and existing method.

Methods	Accuracy (%)
SVM (Babu and Peter 2021)	18
DCNN (Saba et al 2019)	24
RF (Luu et al 2021)	34
AMFO-KNN (Proposed)	48



3.1.2. Precision

The ability of a system to identify cases of skin cancer diagnosis is measured by precision, a performance metric. The proportion of correct diagnoses among all positive predictions given by the system, including both true positives and false positives, is the object of particular attention. A high accuracy value in equation 12 indicates that there are fewer false positives than false alerts, demonstrating that the system is effective in properly identifying true invasions while reducing false alarms. On the other side, a low accuracy score suggests that the system may produce a large percentage of false positives, which might cause unnecessary alerts and add to the workload.

$$\text{precision} = \frac{TP}{TP+FP} \tag{12}$$

The Precision of the suggested and existing approaches is shown in Figure 4. A percentage of the total is often used to represent the accuracy level. Both the existing procedure and the suggested one have the potential for inaccurate estimates. This danger is recognized by both systems. This danger is recognized by both systems. The suggested approach, AMFO-KNN, has a 45% Precision rate, compared to 20%, 26%, and 36% for SVM, DCNN, and RF, respectively. The proposed approach, therefore, has the greatest Precision rate. Table 2 displays the proposed method's Precision.

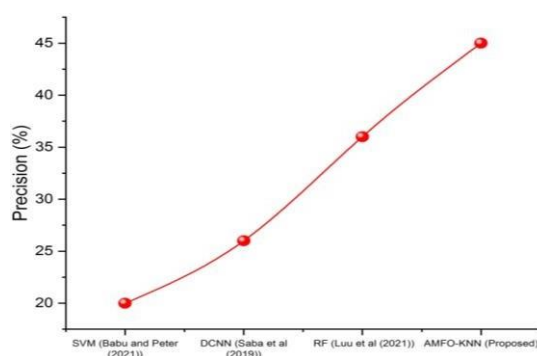


Figure 4 Comparison of precision.

Table 2 Numerical outcomes of precision of proposed and existing method.

Methods	Precision (%)
SVM (Babu and Peter 2021)	20
DCNN (Saba et al 2019)	26
RF (Luu et al 2021)	36
AMFO-KNN (Proposed)	45

3.1.3. Recall

The recall is a performance metric that evaluates how effectively a system can discriminate between skin cancer diagnoses, also known as sensitivity or true positive rate. Equation 13 shows that a system with a high recall value is likely to be effective in identifying the majority of cancer diagnoses with a low occurrence of false negatives. On the other side, a low recall value suggests that the system may have a large percentage of false negatives and may miss a significant amount of real invasions.

$$\text{Recall} = \frac{FN}{FN+TP} \tag{13}$$

The recollection of the recommended and existing strategies is shown in Figure 5. Recall percentages are often stated as a percentage of the whole sample. Both the existing procedure and the suggested one have the potential for inaccurate estimates. This danger is recognized by both systems. This danger is recognized by both systems. However, SVM, DCNN, and RF only obtain 15%, 23%, and 32% Recall rates, respectively, but the suggested approach, AMFO-KNN, has a 47% Recall rate. The proposed approach, therefore, has the greatest Precision rate. Table 3 displays the recall for the recommended strategy.

Table 3 Numerical Outcomes of Recall of Proposed and existing methods.

Methods	Recall (%)
SVM (Babu and Peter 2021)	15
DCNN (Saba et al 2019)	23
RF (Luu et al 2021)	32
AMFO-KNN (Proposed)	47



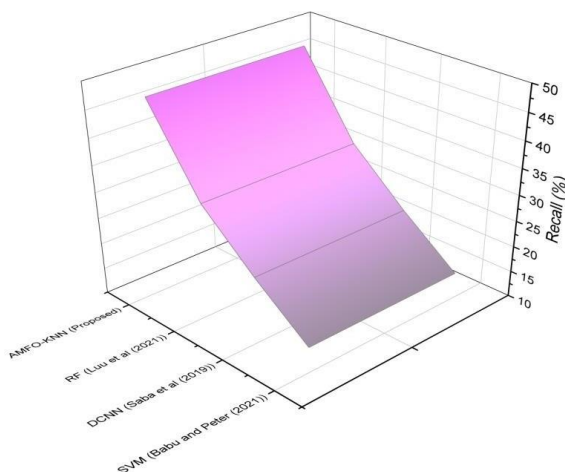


Figure 5 Comparison of recall.

3.1.4. F1-score

An achievement statistic called the F1 score combines recall and accuracy into a single factor. It provides a fair evaluation of the system's ability to correctly identify both positive and negative situations by accounting for both false positives and false negatives. Equation 14 is trade-off between minimizing false positives and false negatives is balanced by the F1-score, which provides a detailed evaluation of the system's performance.

$$F1 - score = \frac{(precision) \times (recall) \times 2}{precision + recall} \tag{14}$$

The F1-Score for the proposed and existing approaches is shown in Figure 6. The F1-Score levels are often reported as a percentage of the total. Both the existing procedure and the suggested one have the potential for inaccurate estimates. This danger is recognized by both systems. However, the suggested technique AMFO-KNN has a 49% F1-score rate compared to 23% for SVM, 28% for DCNN, and 36% for RF. The proposed approach, therefore, has the greatest Precision rate. Table 4 displays the F1-Score for the proposed strategy.

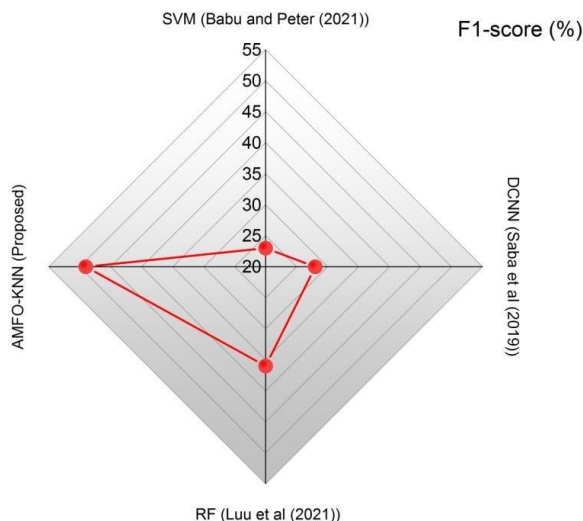


Figure 6 Comparison of F1-score.

Table 4 Numerical outcomes of proposed and existing method.

Methods	F1-score (%)
SVM (Babu and Peter 2021)	23
DCNN (Saba et al 2019)	28
RF (Luu et al 2021)	36
AMFO-KNN (Proposed)	49



4. Conclusions

A brand-new AMFO-KNN technique for classifying skin lesions in photos with integrated information was presented in this study. The findings show that by integrating the patient's information as the model's input data, the suggested strategy enhanced the performance of skin cancer detection. The suggested technique was successful in classifying four significant skin disorders and was 94.5% accurate in identifying benign from malignant lesions. Larger public datasets with metadata should be developed in this area going forward to support research community efforts and improve deep learning-based automated categorization of skin lesions. Future research is required to look at how augmentation techniques such as cutout regularization affect CNN performance. Early detection is crucial if this kind of skin cancer is to be treated completely. However, it won't be able to cure it if it gets aggressive and spreads to other body parts. Therefore, early detection of skin cancer may enhance a patient's prognosis and lower the danger of the illness transmitting to patients. Future uses of this study may include incorporating this model into automated diagnostic technologies to improve the diagnostic proficiency of clinical dermatologists and oncologists. To create an effective diagnostic system for skin cancer detection, this research presented a novel KNN approach. Further, we conclude that the accuracy of the classification stage of the KNN is improved by this model's usage of the Swish activation function and depth-wise separable convolutions. The Fitzpatrick17k skin cancer dataset was then used to apply the suggested KNN algorithm, and the outcomes were compared with various cutting-edge techniques. The suggested strategy performed the best among the others, according to the results, with 48% accuracy, 45% precision, 47% recall, and 49% F1-score. It seems that employing any of the implementations we developed using machine learning has a considerable increase in accuracy based on the findings obtained in the comparison of these techniques.

Ethical considerations

Not applicable.

Declaration of interest

The authors declare no conflicts of interest.

Funding

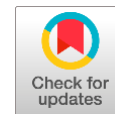
This research did not receive any financial support.

References

- Ahmadi Mehr R, Ameri A (2022) Skin Cancer Detection Based on Deep Learning. *Journal of Biomedical Physics and Engineering* 126:559-568. DOI: DOI: 10.31661/jbpe.v0i0.2207-1517
- Babu GNK, Peter VJ (2021). Skin cancer detection using support vector machine with histogram of oriented gradients features. *ICTACT Journal on Soft Computing* 11. DOI: DOI: 10.21917/ijsc.2021.0329
- Bhimavarapu U, Battineni G (2022, May). Skin Lesion Analysis for Melanoma Detection Using the Novel Deep Learning Model Fuzzy GC-SCNN. In *Healthcare* 10:962. DOI: DOI: 10.3390/healthcare10050962
- Combalia M, Codella N, Rotemberg V, Carrera C, Dusza S, Gutman D, Malvey J (2022) Validation of artificial intelligence prediction models for skin cancer diagnosis using dermoscopy images: the 2019 International Skin Imaging Collaboration Grand Challenge. *The Lancet Digital Health* 4:e330-e339. DOI: DOI: 10.1016/S2589-7500(22)00021-8
- Dai X, Spasić I, Meyer B, Chapman S, Andres F (2019) Machine learning on mobile: An on-device inference app for skin cancer detection. In 2019 fourth international conference on fog and mobile edge computing (FMEC), pp 301-305. IEEE. DOI: 10.1109/FMEC.2019.8795362
- Das D, Arya N, Saha S (2023) Efficient-Nets and Their Fuzzy Ensemble: An Approach for Skin Cancer Classification. In *Neural Information Processing: 29th International Conference, ICONIP 2022, Virtual Event, November 22–26, 2022, Proceedings, Part VII*, pp 151-162. Singapore: Springer Nature Singapore. DOI: DOI: 10.1007/978-981-99-1648-1_13
- Guergueb T, Akhloufi MA (2022) Multi-Scale Deep Ensemble Learning for Melanoma Skin Cancer Detection. In 2022 IEEE 23rd International Conference on Information Reuse and Integration for Data Science (IRI), pp. 256-261. IEEE. DOI: DOI: 10.1109/IRI54793.2022.00063
- Kawahara J, Daneshvar S, Argenziano G, Hamarneh G (2018) Seven-point checklist and skin lesion classification using multitask multimodal neural nets. *IEEE Journal of biomedical and health informatics* 23:538-546. DOI: DOI: 10.1109/JBHI.2018.2824327
- Kousis I, Perikos I, Hatzilygeroudis I, Virvou M (2022) Deep learning methods for accurate skin cancer recognition and mobile application. *Electronics* 11:1294. DOI: DOI: 10.3390/electronics11091294
- Kumar Y, Gupta S, Singla R, Hu YC (2021) A systematic review of artificial intelligence techniques in cancer prediction and diagnosis. *Archives of Computational Methods in Engineering* 1-28. DOI: DOI: 10.1007/s11831-021-09648-w
- Luu NT, Le TH, Phan QH, Pham TTH (2021) Characterization of Mueller matrix elements for classifying human skin cancer utilizing random forest algorithm. *Journal of Biomedical Optics* 26:075001-075001. DOI: DOI: 10.1117/1.JBO.26.7.075001
- Malik S, Dixit VV (2022) Skin cancer detection: state of art methods and challenges. In *ICCCE 2021: Proceedings of the 4th International Conference on Communications and Cyber Physical Engineering*, pp 729-736. Singapore: Springer Nature Singapore. DOI: DOI: 10.1007/978-981-16-7985-8_76
- Malo DC, Rahman MM, Mahbub J, Khan MM (2022) Skin Cancer Detection using Convolutional Neural Network. In 2022 IEEE 12th Annual Computing and Communication Workshop and Conference (CCWC), pp 0169-0176. IEEE. DOI: DOI: 10.1109/CCWC54503.2022.972075

- Ningrum DNA, Yuan SP, Kung WM, Wu CC, Tzeng IS, Huang CY, Wang YC (2021) Deep learning classifier with patient's metadata of dermoscopic images in malignant melanoma detection. *Journal of Multidisciplinary Healthcare* 877-885. DOI: DOI: 10.2147/JMDH.S306284
- Omeroglu AN, Mohammed HM, Oral EA, Aydin S (2023) A novel soft attention-based multi-modal deep learning framework for multi-label skin lesion classification. *Engineering Applications of Artificial Intelligence* 120:105897. DOI: DOI: 10.1016/j.engappai.2023.10589
- Pacheco AG, Krohling RA (2021) An attention-based mechanism to combine images and metadata in deep learning models applied to skin cancer classification. *IEEE journal of biomedical and health informatics* 25:3554-3563. DOI: DOI: 10.1109/JBHI.2021.3062002
- Qureshi AS, Roos T (2022) Transfer learning with ensembles of deep neural networks for skin cancer detection in imbalanced data sets. *Neural Processing Letters* 1-19. DOI: DOI: 10.1007/s11063-022-11049-4
- Saba T, Khan MA, Rehman A, Marie-Sainte SL (2019) Region extraction and classification of skin cancer: A heterogeneous framework of deep CNN features fusion and reduction. *Journal of medical systems* 43:289. DOI: DOI: 10.1007/s10916-019-1413-3
- Tajjour S, Garg S, Chandel SS, Sharma D (2023). A novel hybrid artificial neural network technique for the early skin cancer diagnosis using color space conversions of original images. *International Journal of Imaging Systems and Technology* 33:276-286. DOI: DOI: 10.1002/ima.22784
- Wang Y, Louie DC, Cai J, Tchvialeva L, Lui H, Wang ZJ, Lee TK (2021) Deep learning enhances polarization speckle for in vivo skin cancer detection. *Optics & Laser Technology* 140:107006. DOI: DOI: 10.1016/j.optlastec.2021.107006
- Zakhem GA, Fakhoury JW, Motosko CC, Ho RS (2021) Characterizing the role of dermatologists in developing artificial intelligence for assessment of skin cancer. *Journal of the American Academy of Dermatology* 85:1544-1556. DOI: DOI: 10.1016/j.jaad.2020.01.028

Bio-inspired swarm-intelligent with machine learning framework for prediction and classification of lung cancer



Naveen Kumar Singh^a | Rahul Gupta^b | Satyaapir Sahu^c

^aTeerthanker Mahaveer University, Moradabad, Uttar Pradesh, India, Professor, Department of General Surgery.

^bJaipur National University, Jaipur, India, Assistant Professor, Department of Resp Medicine.

^cSanskriti University, Mathura, Uttar Pradesh, India, Assistant Professor, Department of Ayurveda.

Abstract Early detection of lung cancer nodules, which is often dependent on a tomography scan filmic examination, greatly increases the probability of survival. Earlier tumor detection reduces lung cancer mortality by increasing the likelihood of successful therapy. Traditionally, radiologists have analyzed medical pictures for signs of lung cancer using a laborious and inaccurate systematic approach. The confidentiality and integrity of medical data have become a serious challenge for healthcare applications as a result of the tremendous improvement in the transmission of medical data in the healthcare sector. This research makes use of computational intelligence methods. In this research, a brand-new Enhanced vortex search algorithm optimized Support Vector Machine (EVSAO-SVM) is developed for detection and classification. Preprocessing using the Gaussian Filter, segmentation with Otsu thresholding, feature extraction with local binary patterns (LPB), and classification and prediction with the EVSAO-SVM are the processes that are simulated. Regarding performance criteria including accuracy, sensitivity, specificity, and F1-measure, this study indicates the suggested framework's superiority over the traditional approaches. The results of the tests conducted demonstrate that the suggested model can reach up to 95.42 percent sensitivity, 96.24 percent accuracy, 98.92 percent specificity, and 94.26 percent F1 measure.

Keywords: lung cancer, Gaussian filter, Otsu thresholding, LPB, EVSAO-SVM

1. Introduction

A malignant growth that develops in the lungs' cells is called lung cancer. One of the most prevalent and deadly cancers in the world, it is generally brought on by prolonged exposure to tobacco smoke, environmental causes, or a genetic predisposition (ALZubi et al 2019). Adenocarcinoma, squamous cell carcinoma, and giant cell carcinoma are other subtypes of NSCLC. The characteristics, methods of treatment, and prognoses of the many lung cancer types and subtypes vary (Chen et al 2021). Early lung cancer symptoms may not be apparent, which might delay diagnosis until it is too late. Long-lasting coughs, chest discomfort, shortness of breath, exhaustion, unintentional weight loss, and recurring respiratory infections are among the symptoms of lung cancer that are often seen. Imaging examinations like X-rays, computed tomography (CT) scans, or magnetic resonance imaging (MRI) are among the diagnostic methods for lung cancer. To confirm the diagnosis and identify the kind of malignancy, tissue samples taken by bronchoscopy, needle aspiration, or surgical procedures are required (Radhika et al 2019). The patient's general health, cancer stage, and kind are only a few of the variables that affect how lung cancer is treated. Aside from surgery, treatment options also include radiation, chemotherapy, targeted therapy, and immunotherapy.

Chemotherapy employs medications to eradicate cancer cells across the body, while targeted treatment and immunotherapy focus on certain molecular markers or strengthen the body's defenses against cancer (Hyun et al 2019). Compared to many other malignancies, lung cancer has a relatively poor overall survival rate. For lung cancer, the five-year survival rate varies from roughly 10–20% for SCLC to 25–40% for early-stage NSCLC. But improvements in treatment choices, early detection methods, and campaigns to stop smoking have led to a modest increase in survival rates (Bonavita et al 2020). The majority of instances of lung cancer are significantly correlated with cigarette use. Avoiding or quitting smoking is the most efficient approach to stopping lung cancer from developing. Adopting a healthy lifestyle, quitting smoking, and limiting exposure to environmental toxins may all help lessen the risk of lung cancer (Lai et al 2020). The high incidence of lung cancer highlights the need for early detection, effective treatment options, and preventative measures. Research is still concentrated on developing targeted medications, advancing screening procedures, and comprehending the genetic and molecular elements of lung cancer to significantly enhance patients (Ibrahim et al 2021). X-rays of the chest or CT scans are

two common imaging techniques used in diagnosis, along with tissue biopsies to look for cancer cells. The stage of lung cancer is established after a diagnosis to help with treatment choices (Haragan et al 2019). Therapy is to eliminate or reduce the tumor, kill cancer cells, and stop or control the disease's spread (He et al 2020). It also affects the hue they show up on CT scans. The difficulty of characterizing them is exacerbated by these factors. The remaining segments are as follows: Part 2 covers the related works, Part 3 explains the proposed method, Part 4 evaluates the results, and Part 5 provides a conclusion.

Computing-based methods of intelligence are used in this investigation. Consequently, this research proposes a unique Hybrid model for detection and data transfer. The suggested approach has two stages: first, various image processing techniques are employed to identify cancer in MATLAB, and then, data is sent to authorized individuals through the IoT cloud. Preprocessing, segmentation using Otsu thresholding and the swarm intelligence technique, feature extraction using a local binary pattern, and classification using an SVM are all part of the simulated workflow. Through a variety of performance criteria including training time, this study proves that the swarm intelligent framework is superior to traditional algorithms (Venkatesh and Bojj 2020). Classifying lung illness, heart rhythm, brain activity, forest cover, and other medical images, among other uses, is only one example. The ability of deep learning models to efficiently choose features is crucial for all of these uses. Iterative window-based feature processing is often used by these models to assess various feature combinations. This means attempting to account for an infinite number of feature combinations to properly categorize a limited set of characteristics. The models cease iterating when the error rate between the current iteration and the one before it becomes too large to ignore (Baviskar et al 2021). Mandave demonstrated how these methods are often used to diagnose illnesses including cancer, anemia, Alzheimer's, renal disease, and skin disease by resolving issues like feature selection, classification, optimization, and picture segmentation. The current state of bio-inspired algorithms for diagnosing dementia is also discussed. A bio-inspired approach was shown to be significant in this study's diagnosis of dementia. They use an evolutionary machine learning strategy in this chapter to concurrently tune the parameters of SVM and conduct feature weighting to solve common diagnostic issues. The salp swarm method, a novel, and strong metaheuristic, is paired with SVM to accomplish this. When compared to alternative SVM-based frameworks using highly recognized algorithms like the genetic algorithm (GA) and the particle swarm optimization, the SVM method demonstrates several advantages (Al-Zoubi et al 2020).

Most cancer datasets include features measuring different levels of gene expression, but they often have fewer samples overall, therefore it is important to first remove duplicate features so that prediction algorithms can converge more quickly. These characteristics (genes) allow us to diagnose cancer, choose an effective treatment plan, and find methodological differences. The next step is to use Deep Learning (DL) to categorize the genes into groups that are associated with certain cancer types (Joshi et al 2023). Han et al (2021) concluded that combining the strengths of several swarm intelligence (SI) -based feature selection methods yield a superior feature subset compared to using the algorithms alone. The chosen characteristics were improved via the dynamic recursive feature removal framework after being voted. Priyadarshini and Kanimozhi (2020) proposed using a mean-based GA to select optimal subsets from the raw dataset based on the mean value of the features, and then we use an SVM classifier to evaluate the subset's accuracy, thereby reducing the computational cost and size of the model. Results comparing the suggested technique to the ant colony optimization (ACO) algorithm demonstrate the proposed method's superior accuracy. Pal et al (2022) proposed an attention Net to connect the encoder and decoder layers with a new intermediate layer. Since micro-calcifications all seem the same to the naked eye and segmenting breast pictures is a difficult procedure, radiologists have tried and failed to do it manually. As a result, automated techniques for early-stage identification of the illness are required to aid radiologists in making accurate diagnoses and subsequent treatment choices for their patients. SI plays a crucial role in illness classification and prediction by helping to get the best possible answer with little training. The effectiveness of SI in disease prediction modeling for breast cancer is reviewed and analyzed by (Kumar et al 2020). Hariprasath et al (2021) exploit the challenge of breast cancer detection to demonstrate the efficacy of several NIC-based methods. Separate and combined methods for diagnosis are also briefly discussed in this section. In the end, the experimental findings and additional statistical evaluations are presented. The goal of this chapter is to help the upcoming researcher in the field draw motivation from the established canon of works and develop a novel, cutting-edge strategy for improving upon existing methods.

2. Material and Methods

Images from CT scans of the lungs are sent into a system with pre-processing, segmentation, feature extraction, and classification steps.

The input picture is first process using a Gaussian filter to remove noise. Segmentation of the images is followed by the extraction of characteristics from the identified tumor, including average intensity, perimeter, area, and eccentricity. The tumor is binarized to determine whether or not it is malignant. If a malignant tumor is found, its stage may be determined as well.

2.1. The IQ-OTH lung cancer dataset

Three months of data were collected in the fall of 2019 on lung cancer cases at the Iraq-Oncology Teaching Hospital (IQ-OTH). It consists of computed tomography (CT) images from both patients with various stages of lung cancer and healthy controls. Oncologists and radiologists from these institutions annotated IQ-OTH slides. As can be seen in Figure 1, the collection includes a thousand hundred and ninety pictures representing CT scan slices from 110 patients. Normal, benign, and malignant describe the three categories into which these situations fall. Forty have cancerous diagnoses, fifteen are benign, and the remaining fifty-five are considered to be typical. Initially, the CT scans were gathered in DICOM format. Siemens's SOMATOM is the name of the scanner being utilized. Breathe hold at full inspiration and a CT protocol including one hundred and twenty kV, one mm slices, three hundred fifty- thousand two hundred HU windows, and fifty-six and hundred HU centers were employed for readings. Before any examination, all photos were scrubbed of all identifying information. The institutional review boards of the hospitals involved in the research decided to forgo obtaining written permission from the patients. There are several "slices" in each scan. There might be anywhere from eighty to two hundred of these slices, and each one is a picture of a human chest seen from a different perspective. There is a wide range of ages, sexes, levels of education, regions of residency, and socioeconomic positions among the hundred and ten cases.

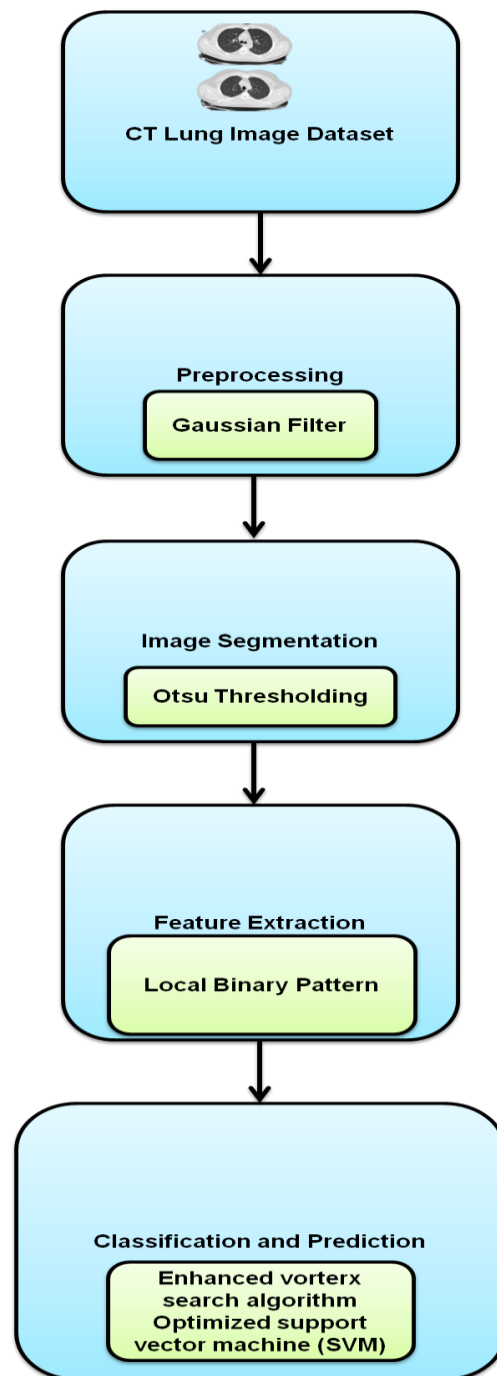


Figure 1 Flow Diagram of this research.

2.2. Gaussian Filter

Image smoothing is the initial step in this pre-processing stage for images. On the input picture, the Gaussian filter is used for smoothing. Noise may be eliminated quite well with Gaussian smoothing. The image's high-frequency components are eliminated with Gaussian. Smoothing eliminates noise and produces a more precise intensity surface. Equation (1) contains the numerical formula for the Gaussian filter.

$$H(w, z) = \frac{1}{2\pi\sigma^2} f \frac{-(w^2+z^2)}{2\sigma^2} \quad (1)$$

Where w represents the horizontal distance from the center, z is the vertical distance and represents the standard deviation of a Gaussian distribution.

2.3. Segmentation

Segmentation typically divides the image's pixels into regions that correspond to the image's subjects. For most computer vision systems, this is the starting point. Pixel intensities are often used by segmentation algorithms. Setting a threshold parameter is required for all algorithms. Better segmentation occurs when the threshold is set correctly. Given the concentration measurements, a threshold is determined. In this study, the Otsu thresholding methods are applied to get the best possible threshold worth.

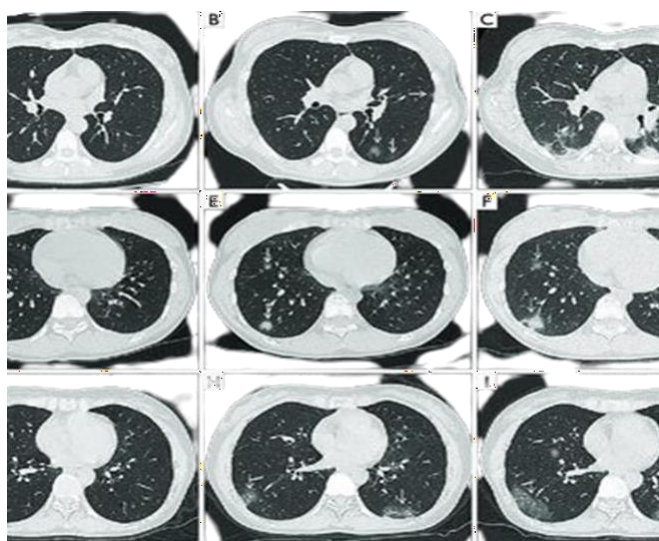


Figure 2 CT lung cancer images (Kareem et al 2021).

2.3.1. Otsu Thresholding

It is predicated on the principle of finding an entrance that minimizes the subjective discrepancy in the class, which is equivalent to finding a threshold that maximizes the variation across classes. Grayscale bimodal histograms are processed directly. There is no need to describe the structure of any additional entities or ensure regional consistency. It uses standard numerical values that may be adjusted regionally.

2.4. Feature extraction by LBP

The LBP approach has been utilised in several contexts. This operator describes textures by using symbols representing differences between centers and neighboring pixels. By thresholding the pixels around the central pixel with the threshold pixel, a binary cypher of each pixel may be obtained. If the value of the neighboring pixel is greater than or equal to the threshold value, then 1 is assigned to that location. At first, a histogram is built to analyze the frequency values of binary patterns. Characteristics of the image's texture stand in for the probability that a binary pattern is present. The following is the LBP equation (2).

$$LBP(n_d, m_d) = \sum_l^{K-1} 2^l e(hl - h(n_d, m_d)) \quad (2)$$

Where $f(x)$ is a purpose whose result is 0 if $h < 0$ and 1 if $h \geq 0$; where $g(n_d, m_d)$ is the gray value of the center and adjacent pixels. The center pixel (n_d, m_d) is the LBP value.

2.5. Enhanced vortex search algorithm optimized Support Vector Machine Methodology

2.5.1. Initial guess solution

A vortex pattern may be used to describe the VSO algorithm's operation. Figure 3 depicts a 2-dimensional nested loop model of the VSO.

2.5.2. Candidate solutions

In Equation (3), r represents the random number used to produce the neighbor solutions around the center:

$$q(\zeta \setminus \mu, v) = \frac{1}{\sqrt{(2\pi)^e |\mu|}} \exp \left[-\frac{1}{2} \frac{(\zeta - \mu)^u (\zeta - \mu)}{v} \right] \quad (3)$$

To determine the value of, we use equation (4). The literature provides further in-depth details.

$$v = T^2 \cdot [I]_{e \times e} \quad (4)$$

Where T^2 is the distribution's variance and I is the $d \times d$ identity matrix. Using Eq. (5), we can get the standard deviation at time zero (T_0):

$$T_0 (= p_0) = \frac{\max(\text{upper_lim}) - \min(\text{lower_lim})}{2} \quad (5)$$

Where T_0 is the starting radius (P_0), which is set to a high amount to ensure that the SS is completely covered.

2.5.3. Substitution of the current solution

During the selection process, $C_0(X)$ is consulted to find a new center for the circle, and the optimal answer, ($i=0$), is chosen and stored in memory. As indicated in equation (6), before proceeding to the collection phase, the contender solutions must be contained inside the exploration limits.

$$\text{lower_lim}^e \leq T_f \leq \text{upper_lim}^e \quad (6)$$

Where $k = 1, 2, \dots, n$, and e is the number of dimensions. A new set of solutions $C_1(X)$ is generated around the new center by decreasing the effective radius (r_1) of the previous circle, which was assigned the learned best solution X in the previous iteration.

It's important to notice that as the radius becomes smaller in the next step, the region of the found national solutions improves. In the second stage, solutions $C_1(X)$ are picked at random and analyzed to see which one is the best; if it is better than the previous best solutions; it is designated as the new finest explanation and stored. Then, after the minimal function evaluation termination requirement is met, the designated middle of the third phrase is remembered as the best answer up to that point. Figure 3 is an illustrative case study of the search procedure. The resultant pattern takes on a vortex structure after the algorithmic rule is broken, with the optimal location being smack in the center of the smallest circle. The interpreter pattern for a 2-dimensional issue with upper and lower bounds between $[-10, 10]$ is also shown in Figure 4.

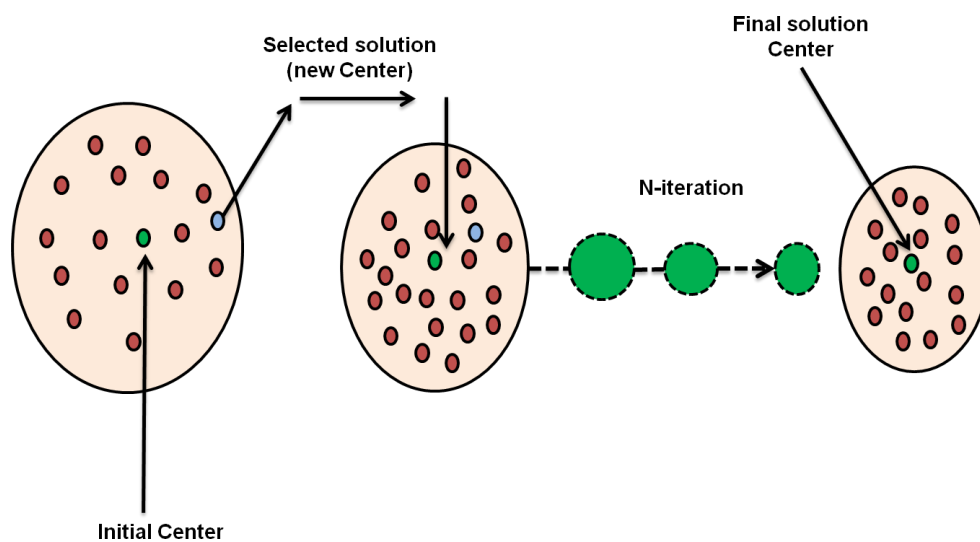


Figure 3 Two-dimensional nested-circle VSO model representing the active search process.

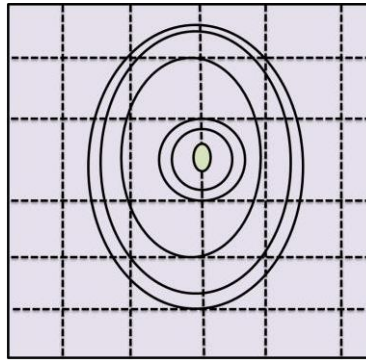


Figure 4 Search algorithms represented by a vortex-shaped VSO.

2.5.4. The radius step-down process

The strategy for performing this adjustment is particularly crucial to the performance of the VSO algorithm; the radius step-down procedure is an example of an understanding step size alteration approach that is also used in random search algorithms. This procedure has to be carried out to guarantee that it enables the algorithmic program to act exploratory in the first stages and exploitative in the latter ones. Proper tuning of the radius value throughout the search procedure is necessary to accomplish such a process. Flow charts are used to offer a full explanation of the VSO method (see Figure 5), and more information about this procedure can be found in the reference.

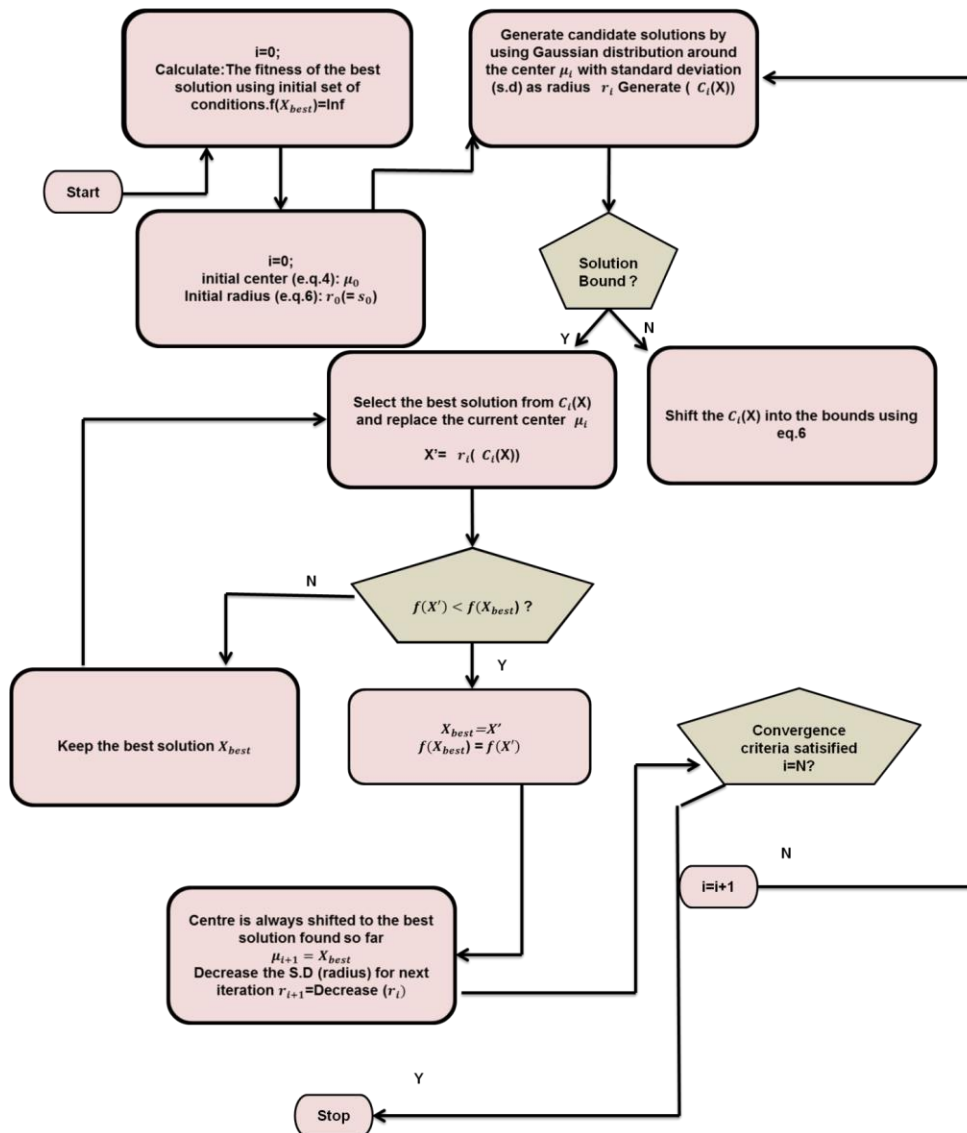


Figure 5 is a working flowchart for the VSO algorithm.

2.5.5. Support Vector Machine

SVM is the most effective classification machine learning algorithm. It can take action on sets if there are only two possible categories. Classification problems for multi-class datasets may be simplified to binary classification problems by splitting the sets into subsets. The partitioning problem is not as severe since fewer sets are required for training. The outcome is a simple SVM yes/no comparison. It functions by generating the optimal hyperplane that divides points into their respective categories. It represents a plane or set of planes in a huge or multidimensional space. Aircraft further from the nearest training data have higher classification results. A larger margin means less room for error. The primary goal of SVM is to estimate the gaps between groups. The following figure 6 illustrates these points:

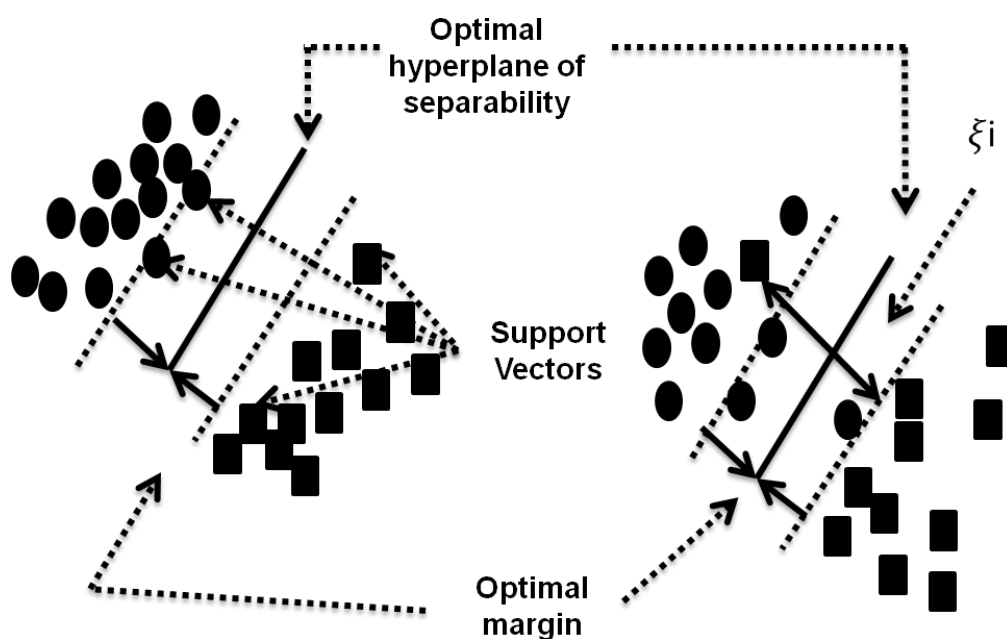


Figure 6 SVM Hyperplane.

Several approaches may be used to improve regression and classification. SVM has earned acclaim for its ability to find answers to issues both those with salient features and those without. Fast feature extraction from well-known sets and the generation of decision planes for splitting datasets are also part of this method. Results were obtained by constructing the line distant from the closest training data. The linear plane excels at dividing the world into two groups. For multi-class situations involving nonlinear planes, we use a variety of kernels from the toolbox.

SVMs may also be used to categorize cancer stages. When training a binary SVM classifier, it doesn't matter whether each document belongs to that category or not. A medical report may not contain information about a single operation. The toolbox features allow the SVMs to perform as expected. The system is taught by being exposed to a huge dataset of possible outcomes across a range of difficulties. After being applied to test data, it gives a score that may be used as a threshold to identify whether something of the same kind has changed. After training the code to enhance the quality of the data, we run the validation step to ensure that it is functioning correctly. The initial step is to divide the data into smaller chunks, each of which may be processed by the trained machine. To use the computer to distinguish between stages depending on the degree of tissue development, feature extraction is followed by training an SVM to integrate the features and get familiar with points of data. If data is cross-checked, it may be possible to understand a system's operation with less validation. Tolerable results are achieved, but when the number of features exceeds the number of samples, it becomes impractical to apply the essential functions promptly.

The difficulty of this approach ranges from doubles the number of features to three times the number of features, depending on the toolkit. Based on statistical theory, SVM is a one-of-a-kind process that utilizes sparse data and many attributes to get around the two-class classification problem and arrive at a judgment line. To divide non-linear data, functions may be used to create a copy of the data in a highly-featured space. All classification tasks on all datasets may have their accuracy and other metrics calculated using the aforementioned equations. The precision of a classifier refers to how well it reliably divides information. Accuracy in data classification is also represented by the value. The quality of the categorization is proportional to the amount of information utilised for training and testing. More aspects affect accuracy that includes kernel functions, box limits, etc.

3. Results and Discussion

The lung cancer detection process in this study begins in MATLAB and continues with the communication of the resulting characteristics to medical professionals. Algorithms were developed and implemented in this study using MATLAB on a 1.80 GHz Intel Core i5 PC with 8 GB of RAM. The results of this study show that the suggested framework is superior to the traditional algorithms in terms of many performance criteria. The results of the tests reveal that the suggested model's maximum sensitivity is 95.42%, accuracy is 96.24%, specificity is 98.19%, and F1- measure is 94.26%.

The percentage of samples for which the suggested approach accurately predicted results is used to assess how accurate the system. The accuracy is calculated using the equation (8).

$$\text{Accuracy} = \frac{TP+TN}{TP+TN+FP+FN} \quad (8)$$

Figure 7 displays comparable values for the accuracy metrics and makes it evident that the suggested technique can generate performance results that are better than those generated by the current research approaches. The suggested method's accuracy of 96% outperforms the results of the current ones, which include K-nearest neighbors (KNN) having a 88% accuracy rate, RF at 90%, AlexNet at 92%, and EVSAO-SVM at 98.27%. When classifying the data, the suggested technique outperformed existing techniques.

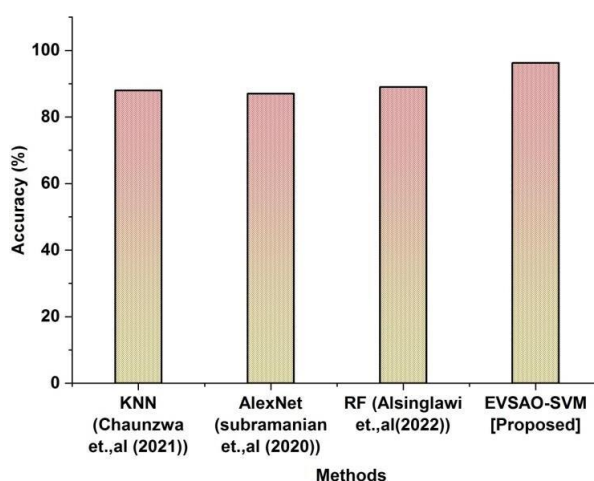


Figure 7 Results of accuracy.

The suggested model's sensitivity is its ability to recognize each important sample in a data collection. It is derived statistically by dividing the percentage of TPs by the total of TPs and FNs. The sensitivity is assessed using the equation (9).

$$\text{sensitivity} = \frac{TP}{TP+FN} \quad (9)$$

In Figure 8 Sensitivity-wise, KNN scores 82%, RF 85%, AlexNet 88%, and EVSAO-SVM 95.42%.

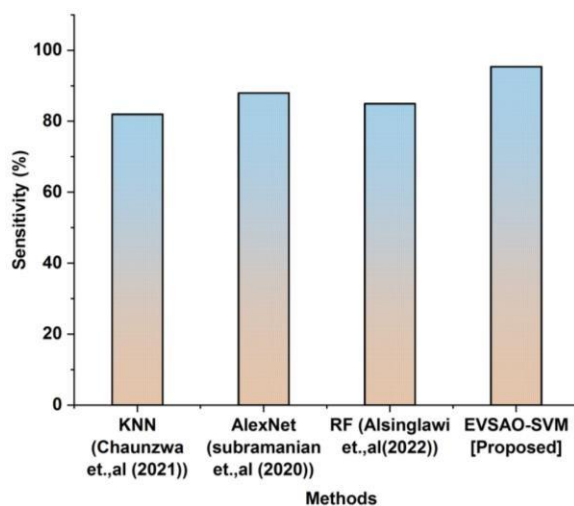


Figure 8 Results of sensitivity.

The harmonic mean of the proposed model is computed to merge "recall and precision" into a single component called the f1-measure. The f1-score is calculated using equation (10).

$$F1 - \text{measure} = \frac{(\text{precision}) \times (\text{recall}) \times 2}{\text{precision} + \text{recall}} \tag{10}$$

In Figure 9, EVSAO-SVM scored (94.26%) on the f1-score, followed by KNN (86%), RF (88%), and AlexNet (94.26%).

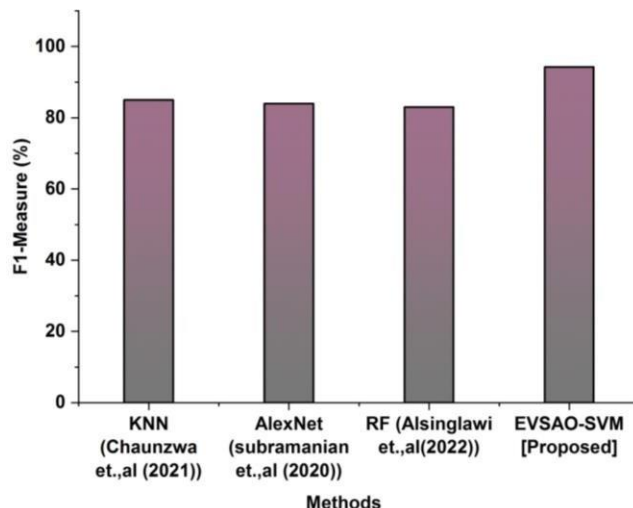


Figure 9 Results of f1-measure.

Specificity is the ability to assess the substance in the condition of elements that could be predicted to be present. The ratio between the value of TNs and the sum of TNs and FPs is a general understanding of specificity. The specificity is calculated using equation (11).

$$\text{specificity} = \frac{TN}{TN+FP} \tag{11}$$

In Figure 10, the Specificity for KNN is 88%, RF is 92%, AlexNet is 94%, and EVSAO-SVM 98.92%.

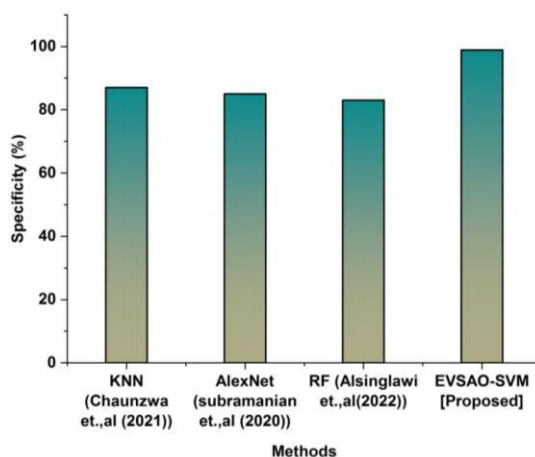


Figure 10 Results of specificity.

4. Conclusions

Lung cancer is a malignant tumor that develops in the cells of the lungs. It is one of the majority common and deadliest cancers in the globe, and its main causes include chronic tobacco use, environmental factors, or a genetic predisposition. Computational intelligence approaches are used in this investigation. This research proposes a unique EVSAO-SVM for detection and classification. The confidentiality and honesty of medical information have grown to be significant problems for healthcare applications as a consequence of the considerable development in the spread of medical information in the healthcare industry. The accuracy offered by the suggested method is superior, at 96.5 percent. Due to the



algorithm's local optima's tendency to converge, the accuracy and specificity parameters that may be used to interpret the findings are constrained. Shortly, these findings may also be more efficiently examined by utilizing deep learning methods and cutting-edge hardware processors.

Ethical considerations

Not applicable.

Declaration of interest

The authors declare no conflicts of interest.

Funding

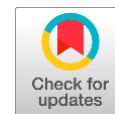
This research did not receive any financial support.

References

- Al-Zoubi AM, Heidari AA, Habib M, Faris H, Aljarah I, Hassonah MA (2020) Salp chain-based optimization of support vector machines and feature weighting for medical diagnostic information systems. *Evolutionary machine learning techniques: algorithms and applications* 11-34. <https://dx.doi.org/10.2139/ssrn.4363703>
- ALzubi JA, Bharathikannan B, Tanwar S, Manikandan R, Khanna A, Thaventhiran C (2019) Boosted neural network ensemble classification for lung cancer disease diagnosis. *Applied Soft Computing* 80:579-591. DOI: 10.1016/j.asoc.2019.04.031
- Baviskar V, Verma M, Chatterjee P (2021) Improving Classification Performance of Deep Learning Models Using Bio-Inspired Computing. In *2021 Thirteenth International Conference on Contemporary Computing (IC3-2021)*, pp 333-340. DOI: 10.1145/3474124.3474174
- Bonavita I, Rafael-Palou X, Ceresa M, Piella G, Ribas V, Ballester MAG (2020) Integration of convolutional neural networks for pulmonary nodule malignancy assessment in a lung cancer classification pipeline. *Computer methods and programs in biomedicine* 185:105172. DOI: 10.1016/j.cmpb.2019.105172
- Chaunzwa TL, Hosny A, Xu Y, Shafer A, Diao N, Lanuti M, Aerts HJ (2021) Deep learning classification of lung cancer histology using CT images. *Scientific reports* 11:1-12. DOI: 10.1038/s41598-021-84630-x
- Chen CL, Chen CC, Yu WH, Chen SH, Chang YC, Hsu TI, Chen CY (2021) An annotation-free whole-slide training approach to pathological classification of lung cancer types using deep learning. *Nature communications*, 12(1), 1193. DOI: 10.1038/s41467-021-21467-y
- Han Y, Huang L, Zhou F (2021) Zoo: Selecting transcriptomic and methylomic biomarkers by ensembling animal-inspired swarm intelligence feature selection algorithms. *Genes* 12:1814. DOI: 10.3390/genes12111814
- Haragan A, Field JK, Davies MP, Escriu C, Gruver A, Gosney JR (2019) Heterogeneity of PD-L1 expression in non-small cell lung cancer: Implications for specimen sampling in predicting treatment response. *Lung Cancer*, 134, 79-84. DOI: 10.1016/j.lungcan.2019.06.005
- Hariprasath K, Tamilselvi S, Saravana Kumar NM, Kaviyavarshini N, Balamurugan S (2021) Performance Analysis of Nature-Inspired Algorithms in Breast Cancer Diagnosis. *Nature-Inspired Algorithms Applications* 267-294. DOI: 10.1002/9781119681984.ch10
- He B, Dong D, She Y, Zhou C, Fang M, Zhu Y, Chen C (2020) Predicting response to immunotherapy in advanced non-small-cell lung cancer using tumor mutational burden radiomic biomarker. *Journal for immunotherapy of cancer* 8. DOI: 10.1136%2Fjito-2020-000550
- Hyun SH, Ahn MS, Koh YW, Lee SJ (2019) A machine-learning approach using PET-based radionics to predict the histological subtypes of lung cancer. *Clinical nuclear medicine* 44:956-960. DOI: 10.1097/RLU.0000000000002810
- Ibrahim DM, Elshennawy NM, Sarhan AM (2021) Deep-chest: Multi-classification deep learning model for diagnosing COVID-19, pneumonia, and lung cancer chest diseases. *Computers in biology and medicine* 132:104348. DOI: 10.1016/j.combiomed.2021.104348
- Joshi AA, Aziz RM (2023) Metaheuristic Model of Gene Selection for Deep Learning Early Prediction of Cancer Disease Using Gene Expression Data. DOI: 10.21203/rs.3.rs-2896430/v2
- Kareem HF, AL-Husieny MS, Mohsen FY, Khalil EA, Hassan ZS (2021) Evaluation of SVM performance in the detection of lung cancer in marked CT scan dataset. *Indonesian Journal of Electrical Engineering and Computer Science* 21:1731. DOI: 10.11591/ijeecs.v21.i3.pp1731-1738
- Kumar M, Khatri SK, Mohammadian M (2020) Review on breast cancer disease predictive modelling using swarm intelligence. In *2020 International Conference on Computational Performance Evaluation (ComPE)*, pp. 523-530. IEEE. DOI: 10.1109/ComPE49325.2020.9200117
- Lai YH, Chen WN, Hsu TC, Lin C, Tsao Y, Wu S (2020) Overall survival prediction of non-small cell lung cancer by integrating microarray and clinical data with deep learning. *Scientific reports* 10:4679. DOI: 10.1038/s41598-020-61588-w
- Mandave DD, Patil LV (2023) Bio-Inspired Computing Algorithms in Dementia Diagnosis—An Application-Oriented Review. Available at SSRN 4363703. <https://dx.doi.org/10.2139/ssrn.4363703>
- Pal D, Reddy PB, Roy S (2022) Attention UW-Net: A fully connected model for automatic segmentation and annotation of chest X-ray. *Computers in Biology and Medicine* 150:106083. DOI: 10.1016/j.combiomed.2022.106083
- Priyadarshini J, Kanimozhi C (2020) An Optimized Feature Selection Method for High Dimensional Data. *International Journal of Research in Engineering, Science and Management* 3:416-419.
- Radhika PR, Nair RA, Veena G (2019). A comparative study of lung cancer detection using machine learning algorithms. In *2019 IEEE International Conference on Electrical, Computer and Communication Technologies (ICECCT)*, pp 1-4. IEEE. DOI: 10.1109/ICECCT.2019.8869001
- Subramanian RR, Mourya RN, Reddy VPT, Reddy BN, Amara S (2020) Lung Cancer Prediction Using Deep Learning Framework. *International Journal of Control and Automation* 13:154-160.
- Venkatesh C, Bojja P (2020) Lung Cancer Detection using Bio-Inspired Algorithm in CT Scans and Secure Data Transmission through IoT Cloud. *International*



Data-driven approach for effective fatigue detection in drivers during driving events



Manoj Rameshachandra Vyas^a | Manish Tyagi^b | Rohit Kumar Sharma^c

^aSanskriti University, Mathura, Uttar Pradesh, India, Associate Professor, Department of Ayurveda.

^bTeerthanker Mahaveer University, Moradabad, Uttar Pradesh, India, Assistant Professor, Department of Psychiatry.

^cJaipur National University, Jaipur, India, Assistant Professor, Department of Gen Medicine.

Abstract: The effectiveness of transportation and the safety of the road depend heavily on drivers during driving events. The way people drive, and the likelihood of accidents or other occurrences may both be strongly impacted by their actions and behaviors. Promoting safe and sensible driving behaviors requires an understanding of the traits and variables that affect drivers during driving incidents. The rising number of traffic accidents highlights the critical necessity to rein in and lessen the prevalence of careless driving. One of the most common causes of these serious mistakes is drowsiness while driving. To combat this problem, algorithms have been created to identify signs of driver weariness and sound an alarm. The developed algorithms have a serious flaw in their accuracy, and it also takes too long to identify driver drowsiness before alerting them. Timeliness and precision are two of the most important factors in preventing traffic mishaps. Multiple datasets have been utilized to improve methods for identifying signs of exhaustion or drowsiness. These data were acquired either through video streaming records of the driver's behavior or from the driver's brain electroencephalogram (EEG) readings. In order to create a high-performance fatigue detection system, this research designs a novel firefly-integrated optimum cascaded convolutional neural network (FI-OCNN). The suggested approach offers the greatest detection accuracy among the existing classifiers, up to 98.75%. The studies further show that the recommended methods provide the greatest level of detecting precision with the quickest testing time (TT) compared to all other existing and successful tiredness detection techniques.

Keywords: electroencephalogram signals, video streaming, FDS, testing time

1. Introduction

As Fatigue may be regarded as one of the primary causes of engineering breakdown since frequent loading and unloading of materials results in much damage. As a result, throughout the years, many experiments have been carried out to ascertain how materials behave during fatigue. Mechanical devices' and structure elements' fatigue behavior often depends on the resilience of the material's inherent qualities, which should be taken into account while designing the parts. Three crucial variables stand out among the key variables that affect how materials behave as they get fatigued processing, which include residual stresses, geometric form, which regulates average nominal stress levels, and surface roughness, which influences the likelihood of fracture development (Nasiri and Khosravani 2022). Millions of people throughout the globe are impacted by the significant issue of driving tiredness. Accidents brought on by fatigue may have serious repercussions, including injury and death. Therefore, it is crucial to identify and address driver weariness in order to maintain road safety. In the past, detecting weariness has depended on subjective techniques like self-reporting or physical examination (Chitra and Shanthi 2022).

These approaches, instead, often lack objectivity and dependability. A data-driven technique has emerged as a possible remedy for efficient tiredness identification during driving events to get beyond these restrictions. To solve the issue of driver tiredness by creating a system to detect driver drowsiness, several initiatives are now under progress in the vehicle manufacturing industry (Zhang et al 2019). IoT elements and applications, including sensors, cloud servers, and smartphones, provide both centralized and decentralized data processing. To build a reliable and efficient fatigue detection system, three key strategies are being employed. These methods fall under the categories of behavioral-based, physical-based, and vehicle-based methods. The three main methods used by systems for tiredness detection. Start by utilizing image processing and computer vision to assess photographs and videos that were taken of the driver depending on their behavior. These crucial variables are determined by monitoring aspects including eye blindness, mouth opening and shutting, facial features, eye closure, head posture, and moving head (Zablocki et al 2022).



Then vehicle-based methods integrate a system for detecting driver weariness using devices and sensors into the wheels of the vehicle. This embedded device track measures such as Steering Wheel Velocity (SWV), Steering Wheel Angle (SWA), Steering Wheel Movements (SWM), hand location, hand absences, and lane departure to identify driver actions (Li et al 2019). Driving events may quickly turn into hazardous scenarios due to fatigue. Real-time monitoring of multiple metrics is made possible by the data-driven methodology, allowing for the early identification of the start of weariness. The data-driven approach may assist drivers in taking the required steps to minimize accidents caused by exhaustion by providing timely intervention tools, such as warnings or recommendations for rest breaks (Horberrry et al 2021). The use of efficient tiredness detection systems has the potential to significantly improve traffic safety and lower the number of accidents caused by weariness. These technologies enable drivers to take the required pauses, modify their behavior, or get the right amount of rest in order to reduce the hazards connected with being fatigued (Ansari et al 2021). Overall, efforts to improve driver safety and lower the risks of fatigue-related accidents on the road are being made in the area of detecting driver tiredness during driving events.

Sathesh et al (2022) included a way to tell whether a person is feeling sleepy before they start driving. This approach uses a system where the driver receives permission to drive. For the purpose of detecting tiredness in drivers, the system uses a two-level validation method. captcha processes utilizing audio playing or Python libraries processes using the GTTS library make up the first stage of the validation procedure. Anderson et al (2019) prospective on divers who tested positive for Patent foramen ovale (PFO) or an Atrial Septal Defect (ASD) and chose to either stop diving altogether or to have their PFO or ASD closed and resume driving. At enrolment and then on a yearly basis after that, the features, medical history, diving history, and DCS history of the divers were recorded. The outcome variables included the incidence rate of DCS, the frequency and quantity of diving activities, and unfavourable closure events. The development of passive brain-computer interfaces (BCIs) includes important steps such as estimating response times (RTs) and sleepiness states from brain signals. Before the advent of deep learning, it was difficult to reliably estimate RTs and sleepiness from electroencephalogram (EEG) information, which made neuro-engineering systems unreliable (Reddy and Behera 2022).

Hu and Lodewijks (2020) attempted to distinguish between physical and mental exhaustion in order to provide psychological insight into the current non-invasive assessments for driver and pilot fatigue. A study like this enhances research outcomes for a variety of investigators with interest in the creation of in-vehicle tiredness detection technologies. EEG is often regarded as an accurate indicator of exhaustion, sleepiness, and assessment of performance. The present research in this area, as well as its next directions, is briefly covered in this study. For EEG-based sleepiness research, power spectral density (PSD) based features are found to be the most often employed characteristics (Majumder et al 2019). Song et al (2022) suggested a wireless system for evaluating and detecting muscle tiredness in real time that can concurrently capture electromyography (EMG) data from many separate muscles and data from various image sensors. Different bodily muscles are equipped with a variety of wireless wearable EMG sensors. With a unique acquisition channel for each EMG sensor, Bluetooth low energy is used to send data.

Flores-Monroy et al (2021) presented a real-time driver sleepiness detection system that uses a specially built shallow convolutional neural network (SS-CNN) to extract the driver's facial area and incorporate it into the system. One of the leading causes of mortality worldwide is a traffic collision, which is often brought on by the driver's exhaustion and tendency to doze off behind the wheel. Pandey and Muppalaneni (2021) used machine learning and deep learning to the two distinct models using temporal and geographical features. Long short-term memory (LSTM) and computer vision methods are used in one model to extract temporal characteristics, while convolution neural networks (CNN) and LSTM are used in the other model to extract spatial features. Navastara et al (2020) suggested a method that might detect tiredness and warn sleepy drivers. The initial stage is to use a Funnel-structured cascade algorithm to identify the face. Then take off the facial landmark characteristics from the face to determine where the eyes are. Utilizing the Eyes Aspect Ratio (EAR) and a Uniform Local Binary Pattern (ULBP), the characteristics of the eyes are retrieved. Khan et al (2023) suggested an end-to-end non-intrusive automatic approach for tracking driver behavior that is tailored for logistical and public transportation applications. The system combines an embedded system, edge computing and cloud computing modules, and an application for mobile phones in an effort to provide a comprehensive, integrated solution for sleepiness detection, monitoring, and driver assessment.

2. Materials and Methods

In this section, we discuss the data-driven strategy for efficient driver tiredness identification during driving events, which comprises identifying driver indicators of weariness based on multiple data sources gathered during driving events. This technology aims to improve driving safety by detecting driver fatigue early and alerting drivers or authorized authorities to take appropriate action.

3.1. Cascaded Convolutional Neural Network

A cascaded convolutional neural network (CCNN) is a kind of deep learning architecture made up of many CNNs organized sequentially. Each CNN in the cascade processes the output of the prior CNN, resulting in a cascading effect. A cascaded CNN uses the hierarchical structure of CNNs to learn progressively and sophisticated characteristics from incoming data. Each succeeding network may concentrate on learning more high-level representations of the data by stacking numerous CNNs. Object identification and face recognition are just a few of the computer vision applications for which cascaded CNNs have been effectively used. These models can perform better and generalize more effectively than single CNN models by using many CNNs in a cascade.

Figure 1 displays the suggested CNN diagram utilized in our DD system. The input for our suggested model is made up of all EEG windows lasting 3.75 s. EEG signals go across one max-pooling layer and four convolutional layers, then a completely linked layer and seven batch-normalized layers. In order to achieve both dimensionality reduction and invariance, the pooling process selects the largest pooling strategy possible. In order to lower the possibility of over-fitting, dropout processing is also performed. During the mapping of high and low dimensions, the layer that is completely connected acts as a classifier across the whole structure of our network. The following is a breakdown of the many CNN layers that were employed in our DD system.

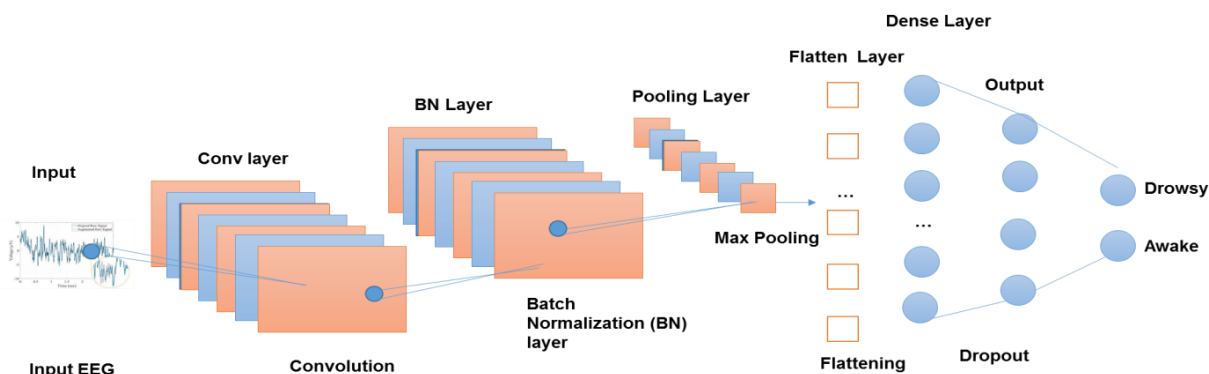


Figure 1 Cascaded convolutional neural network (CCNN) model presented in a diagram.

- Convolutional layers
The layers enable the application of filters and the extraction of features derived from the EEG signal input. The following equation explains the convolution process in equation (1).

$$Z_j = a_j + \sum_m U_{in} * U_m \tag{1}$$

Where * is the operation of convolution, Z_j displays the feature map, a_j is the bias term, U_{in} is the channel's sub-kernel U_m is the input signal.

- Batch Normalization layers
Two main issues, over-fitting and lengthy training periods are well-known in DL. To scale and hasten the learning procedure, the Batch Normalization (BN) layers are used. The preceding activating layer is therefore normalized in each BN stratum by dividing it by the standard deviation and removing the average batches from it.
- The dropout layers
Each dropout layer is thought of as a regularization strategy that enhances over-adjustment on neural networks and lowers the classification error rate. The value of dropout in the suggested model is equivalent to 0.2. 20% of the neurons have been deactivated to prevent over-fitting. In our model, we employed three dropout layers.
- Maximal Pooling 1D layer
By minimizing the dimensionality of every input layer and the number of characteristics that must be learned, each input layer is sub-sampled using the sample-based discretization max-pooling-1D blocks, lowering the cost of computation.
- Flatten layer
The model is flattened since the preceding phase produced a multidimensional data output that this neural network cannot read directly.
- Dense layers
The dense layer's job is to describe the connections between the neurons in the lower and middle levels. In our architecture, we have employed two completely linked layers. To get more accurate classification outcomes, we employed a hidden layer of 128 neurons in the initial dense of our model. The last neuron's value for the second dense is equal to 1. In this study, binary classification is used. Therefore, class "1" or class "0" may be indicated by a single neuron.

3.2. Firefly Optimum Algorithm



Firefly optimum algorithm (FOA) has been one of the optimization methods developed to handle difficult issues. In FOA, fireflies are created knowingly and spread at random locations around the issue's space. Each firefly then emits a signal of light for the other fireflies to see. In comparison to other fireflies, the firefly's light output is shown. It moves closer to the firefly's blazing brightness. To determine the light amplification, use equation 2.

$$\beta(dis) = \beta_0 \times f^{-\gamma dis^2} \quad (2)$$

Where β , dis , and γ indicate light absorbing, firefly separation, and light absorption coefficient, respectively. From equation 3, the separation among fireflies is estimated.

$$dis = \sqrt{\sum_{l=1}^c (z_{jl} - z_{il})^2} \quad (3)$$

Where dis represents the space among fireflies z_j and z_i . The fireflies' movements i is founded on the appeal of the firefly j , and it is computed from Equation 4

$$z_j = \bar{z} + \beta_0 \times f^{-\gamma dis^2} (z_{jl} - z_{il}) + \alpha (rand - \frac{1}{2}) \quad (4)$$

Where the firefly's present location is shown by the first term, the attraction is indicated by the second term, and the random function is indicated by the third term, which has a range of 0 to 1. In addition, the constraints, β_0 , γ represent the light absorption, the light captivation coefficient, and the randomizing parameter, respectively. The information is exchanged by fireflies by light. The firefly with the brightest glow circles the issue space's ideal resolution. Every firefly tries to go to the firefly that is the greatest in the issue area. Algorithm 1 contains firefly's algorithm. Figure 2 shows a diagrammatic depiction of a firefly.

Algorithm 1: Firefly algorithm

Input: N - the number of fireflies, J_i - the degree of brightness for the goal function, γ - light-absorbing capacity.

Output: Finest firefly in the ith iteration.

- 1: Set the firefly population to zero.
 - 2: Each firefly's vector values should be set.
 - 3: Calculate each firefly's unique light intensity.
 - 4: Beginning the iteration = 0;
 - 5: But (iteration < greatest amount of iterations) do
 - 6: for $j = 1$ to m do
 - 7: for $i = 1$ to m do
 - 8: if ($J_j < J_i$), then
 - 9: It's the firefly i the direction of J_j
 - 10: end if
 - 11: end for
 - 12: end for
 - 13: iteration++
 - 14: end while
 - 15: find the brightest firefly in the area of difficulty
-

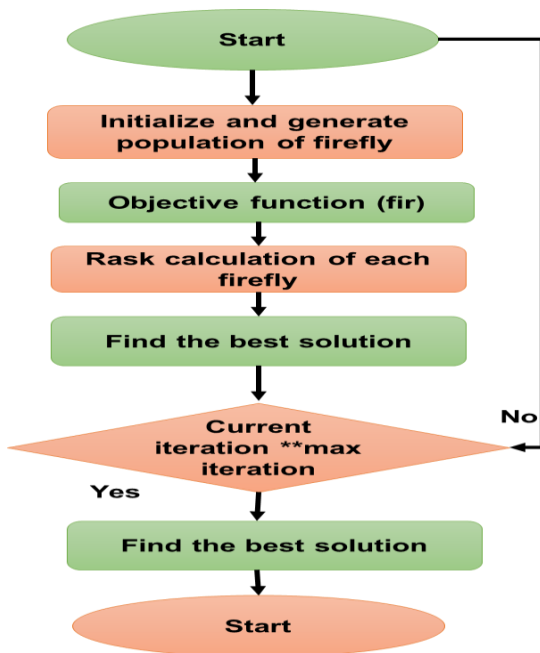


Figure 2 Flow diagram of firefly.

3. Results

This section addresses the efficient identification of driver weariness during actual driving situations. Convolutional Neural Networks (CNN), Recurrent Neural Networks (RNN) Artificial Neural Networks (ANN) are the current approaches that have been compared with the proposed method, and the parameters such as accuracy, F1 score, precision, specificity, and sensitivity.

3.1. Accuracy

Depending on the particular technology or approach employed for detection, the accuracy of detecting driver weariness during driving events might vary. The detection of driver weariness may be done in a number of ways, including physiological tests, behavioral signs, and monitoring devices installed in the car itself. These systems use a number of in-car sensors, such as steering angle sensors, accelerometers, and lane departure warning systems, to detect signs of fatigue.

$$Accuracy = \frac{TP+TN}{TP+TN+FP+FN} \tag{5}$$

Figure 3 and table 1 depict the accuracy of the proposed method. To analyze data and find trends related to tiredness, they often use algorithms. When compared, the proposed method is higher accuracy than the existing method. External elements, including illumination, road conditions, and the presence of distractions, may have an impact on how well tiredness detection systems work. As a result, although tiredness detection systems may be helpful in warning drivers of possible exhaustion, they are not perfect and should not be depended upon as the only method of accident prevention.

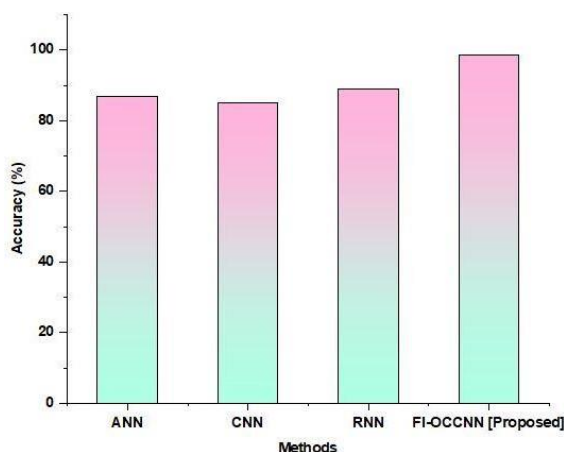


Figure 3 Accuracy of the proposed method.



Table 1 Comparison of accuracy.

Methods	Accuracy (%)
ANN	87
CNN	85
RNN	89
FI-OCCNN [Proposed]	98.75

3.2. Precision

Different methods, such as physiological tests, behavioral indicators, and monitoring systems based on moving vehicles, have varying degrees of accuracy. It is important to keep in mind that owing to differences in research techniques and the absence of standardized assessment procedures, specific numbers might be difficult to ascertain with accuracy.

$$Precision = \frac{TP}{TP+FP} \quad (6)$$

Figure 4 and table 2 demonstrate the suggested method's accuracy. Low false alarm rates and accurate identification of tiredness episodes are the goals of high-precision fatigue detection systems. It shows that the proposed method is higher than the existing one.

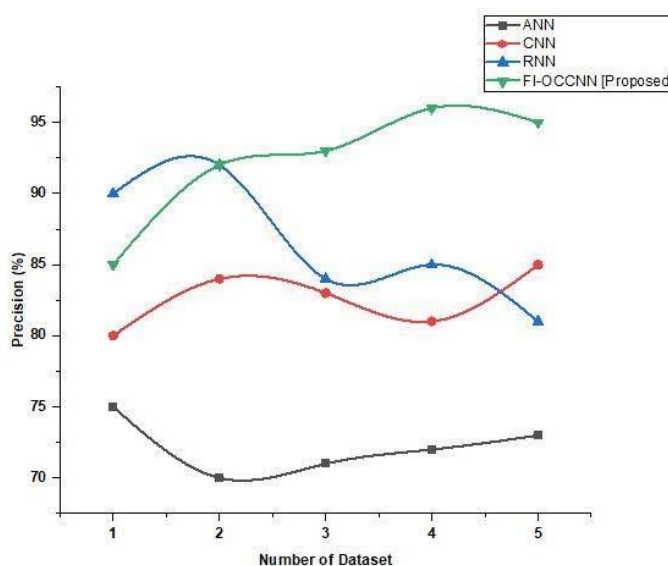


Figure 4 Precision of the proposed method.

Table 2 Result of the precision.

Number of Datasets	Precision (%)			
	ANN	CNN	RNN	FI-OCCNN [Proposed]
1	75	80	90	85
2	70	84	92	92
3	71	83	84	93
4	72	81	85	96
5	73	85	81	95

3.3. F1 Score

The harmonic mean of accuracy and recall is used to create the F1 score, which considers both true positives (cases of tiredness that were successfully recognized) and false positives (cases of fatigue that were wrongly identified) in the output of the system. According to studies, F1 scores for various ways of detecting tiredness ranged from around 0.6 to 0.9. These numbers point to a moderate to high degree of performance, with higher numbers indicating more reliable and accurate tiredness detection overall.

$$F1\ Score = \frac{2 \times Precision \times Recall}{Precision + Recall} \quad (7)$$



Figure 5 and table 3 demonstrate the F1 score of the proposed method. The quality of the data, the algorithms utilized, and the particular circumstances in which the system functions may all have an impact on the F1 score. Therefore, it is essential to test and verify tiredness detection systems in actual driving situations in order to precisely determine their efficacy. When compared, the proposed method is greater than the existing methods.

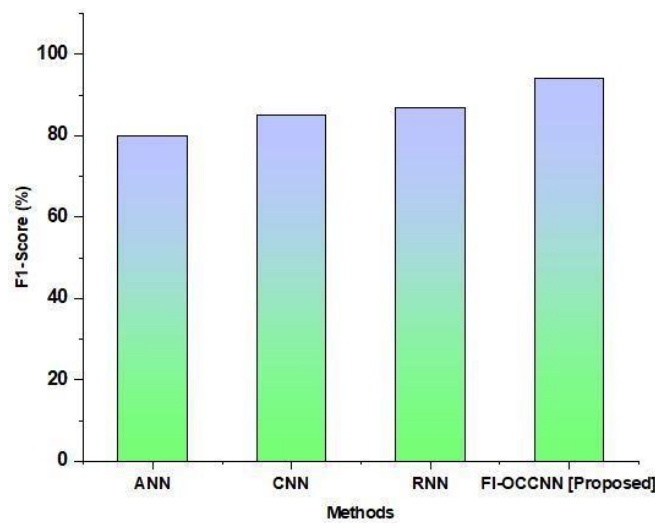


Figure 5 F1 score of the proposed method.

Table 3 Comparison of the F1 score.

Methods	F1-Score (%)
ANN	80
CNN	85
RNN	87
FI-OCNN [Proposed]	94

3.4. Sensitivity

The percentage of real tiredness occurrences that are accurately recognized by the system is measured by the sensitivity, sometimes referred to as recall or true positive rate, of fatigue detection in drivers during driving events. It demonstrates the system's capacity to detect instances of weariness. High sensitivity means that the system can accurately identify occurrences of exhaustion and reduce false negatives or instances of weariness that the system misses. Low sensitivity, on the other hand, raises the possibility that the system has a greater incidence of false negatives, which might result in the system missing real tiredness episodes. Figure 5 and table 4 demonstrate the sensitivity of the proposed method. It shows that the highest value than the existing one.

Table 4 Result of the sensitivity.

Methods	Sensitivity (%)
ANN	83
CNN	79
RNN	80
FI-OCNN [Proposed]	96

3.5. Specificity

The percentage of non-fatigue occurrences that the system properly classifies as such is known as the specificity of the system's ability to identify driver weariness during driving events. It shows how well the algorithm can distinguish between tiredness and other states, hence reducing false positives. A low proportion of false positives show that the system has high specificity, which means that it properly detects situations when drivers are not tired. On the other hand, poor specificity suggests a greater chance of false positives when the system mistakenly labels non-fatigue events as weariness. Figure 6 and table 5 denote the specificity of the proposed method. It denotes that the suggested method is high specificity than the existing one. These numbers suggest that the systems are capable of successfully differentiating between tiredness and non-fatigue states, although false positives are still a possibility.

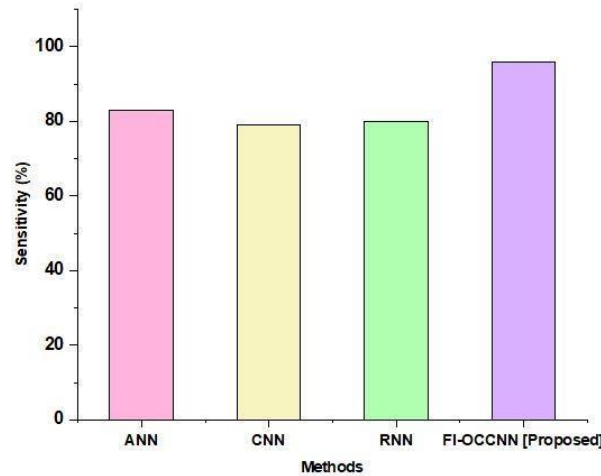


Figure 6 Sensitivity of the proposed method.

Table 5 Result of the Specificity.

Number of Datasets	Specificity (%)			
	ANN	CNN	RNN	FI-OCNN [Proposed]
1	72	82	90	91
2	79	86	92	96
3	82	89	93	97
4	85	80	81	95
5	81	85	87	94

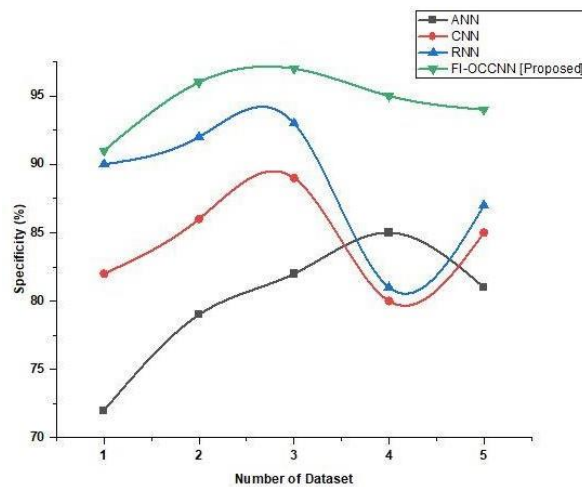


Figure 7 Specificity of the proposed method.

4. Conclusions

Despite tiredness detection systems may be helpful in spotting possible driver drowsiness, they are not perfect and should be seen as supporting tools rather than the only means of avoiding accidents. The effectiveness of these systems may be impacted by variables, including the amount of illumination, the state of the road, distractions, and individual driver variances. According to studies, the specificity rates for various tiredness detection methods range from 94%. These results indicate that the systems can distinguish between weariness and non-fatigue states with reasonable accuracy, although false positives are still a possibility. By using this variation, the suggested algorithm was able to attain the greatest performance, as shown by the best detecting speed and accuracy, with a high weight for the accuracy metric.

Ethical considerations

Not applicable.



Declaration of interest

The authors declare no conflicts of interest.

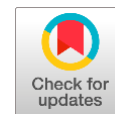
Funding

This research did not receive any financial support.

References

- Anderson G, Ebersole D, Covington D, Denoble PJ (2019) The effectiveness of risk mitigation interventions in divers with persistent (patent) foramen ovale. *Diving and Hyperbaric Medicine* 49:80.
- Ansari S, Naghdy F, Du H, Pahnwar YN (2021) Driver mental fatigue detection based on head posture using new modified reLU-BiLSTM deep neural network. *IEEE Transactions on Intelligent Transportation Systems* 23:10957-10969.
- Chitra K, Shanthy C (2022) A Novel Approach for Fatigue Driver Prediction using Deep Learning Model. In 2022 11th International Conference on System Modeling & Advancement in Research Trends (SMART), pp. 1262-1265. IEEE.
- Flores-Monroy J, Nakano-Miyatake M, Sanchez-Perez G, Perez-Meana H (2021) Visual-based real time driver drowsiness detection system using CNN. In 2021 18th International Conference on Electrical Engineering, Computing Science and Automatic Control (CCE), pp. 1-5. IEEE.
- Horberry T, Mulvihill C, Fitzharris M, Lawrence B, Lenné M, Kuo J, Wood D (2021) Human-centered design for an in-vehicle truck driver fatigue and distraction warning system. *IEEE Transactions on Intelligent Transportation Systems*.
- Hu X, Lodewijks G (2020) Detecting fatigue in car drivers and aircraft pilots by using non-invasive measures: The value of differentiation of sleepiness and mental fatigue. *Journal of safety research*, 72, pp.173-187.
- Khan MA, Nawaz T, Khan US, Hamza A, Rashid N (2023) IoT-Based Non-Intrusive Automated Driver Drowsiness Monitoring Framework for Logistics and Public Transport Applications to Enhance Road Safety. *IEEE Access* 11:14385-14397.
- Li Z, Yang Q, Chen S, Zhou W, Chen L, Song L (2019) A fuzzy recurrent neural network for driver fatigue detection based on steering-wheel angle sensor data. *International Journal of Distributed Sensor Networks* 15:1550147719872452.
- Majumder S, Guragain B, Wang C, Wilson N (2019) On-board drowsiness detection using EEG: Current status and future prospects. In 2019 IEEE International Conference on Electro Information Technology (EIT), pp 483-490. IEEE.
- Nasiri S, Khosravani MR (2022) Applications of data-driven approaches in prediction of fatigue and fracture. *Materials Today Communications* 33:104437.
- Navastara DA, Putra WYM, Fatichah C (2020) Drowsiness detection based on facial landmark and uniform local binary pattern. In *Journal of Physics: Conference Series* 1529:052015.
- Pandey NN, Muppalaneni NB (2021) Temporal and spatial feature based approaches in drowsiness detection using deep learning technique. *Journal of Real-Time Image Processing* 18:2287-2299.
- Reddy TK, Behera L (2022) Driver drowsiness detection: An approach based on intelligent brain-computer interfaces. *IEEE Systems, Man, and Cybernetics Magazine* 8:16-28.
- Sathesh S, Maheswaran S, Mohanavenkatesan P, Mohammed Azarudeen M, Sowmitha K, Subash S (2022) Allowance of Driving Based on Drowsiness Detection Using Audio and Video Processing. In *Computational Intelligence in Data Science: 5th IFIP TC 12 International Conference, ICCIDS 2022, Virtual Event, March 24–26, 2022, Revised Selected Papers*, pp 235-250. Cham: Springer International Publishing.
- Song Y, Yin H, Wang X, Sun C, Ma Y, Zhang Y, Zhong X, Zhao Z, Zhang M (2022) Design of a Wireless Distributed Real-time Muscle Fatigue Detection System. In 2022 IEEE Biomedical Circuits and Systems Conference (BioCAS), pp 709-713. IEEE.
- Zablocki E, Ben-Younes H, Pérez P, Cord M (2022) Explainability of deep vision-based autonomous driving systems: Review and challenges. *International Journal of Computer Vision* 130:2425-2452.
- Zhang W, Yang D, Wang H (2019) Data-driven methods for predictive maintenance of industrial equipment: A survey. *IEEE Systems Journal* 13:2213-2227.

Effect of quality of sleep on psychological health among college students with healthy patterns of sleeping



Sachin Gupta^a ✉ | Prerana Gupta^b | Vikas Gaur^c

^aSanskriti University, Mathura, Uttar Pradesh, India, Chancellor, Department of Management.

^bTeerthanker Mahaveer University, Moradabad, Uttar Pradesh, India, Professor, Department of Psychiatry.

^cJaipur National University, Jaipur, India, Professor, Department of Psychiatry.

Abstract Surprisingly little, nevertheless is known about the connections between college students' usually healthy sleep habits and their state of mind. Previous studies have demonstrated a strong correlation between students' sleep problems and more severe mental health problems. It is critical to notice the connections between sleep and mental health in persons with usually sound sleeping routines since pupils' sleeping habits tend to decline as they get older, and even brief sleep troubles can have a substantial influence on the beginning of mental illnesses. 73 college students who typically had decent sleep patterns participated in the current study and provided information on their state of mind and sleeping habits. Despite the fact that people as a whole did not report any clinically relevant mental health issues, the general quality of sleep was associated with psychological wellness. A regression study shows that the link between total problems and clinically important indicators of psychological distress differs depending on the number of nocturnal sleep disruptions and the duration of the night's sleeping. These results highlight the importance of understanding the relationship between sleep and mental health among college students who typically get enough sleep. Not just because so many college students eventually have psychological issues and sleep troubles but also because, before they reach clinically concerning levels, it would be able to intervene and enhance psychological results.

Keywords: quality of sleep, students, healthy sleep, mental health

1. Introduction

College years are especially susceptible to sleep issues and issues with one's mental wellness. College students' sleep issues frequently get worse as time passes, which is problematic because even a brief presentation of severe sleep issues is linked to deteriorating psychological effects (Minihan et al 2020). According to the survey, Pan et al (2021) around 25% of college students who initially did not disclose a mental health condition did so two years later. About 60% of pupils reported having at least one mental health issue. Around fifty percent of the children who regularly reported psychological problems throughout examinations chose not to obtain assistance. Overall, the results suggest that college students sleep problems may not only be minor annoyances; they may get worse over time and affect their mental health. Poor sleep has been associated with more serious mental health problems from infancy through growing up, including an increase in aggressive, delinquent, and depressive behaviors, according to prior studies. Understanding (Chang et al 2019) the connections between sleep and psychological well-being in this group may be crucial because it could assist and enhance students' psychological results before they turn clinically problematic. College students with normally sound sleep patterns might benefit from more research into the general state of their sleep, an indicator that often contains objective and subjective elements. According to a previous study, sleep problems are related to poor mental health in adults. For instance, toddlers with superior nighttime sleep patterns were less prone than 2- to 3-year-olds to experience expressing and internalizing difficulties.

According to Tamana et al (2019) study, children aged 2 to 5 with sleep issues are more likely to experience externalizing and overall difficulties, especially if they get less than 11 hours of sleep each day. Work done with children who are in school repeats and expands upon these discoveries. In Karjalainen (2021) study, parents' ratings of their 7 to 12-year-old children's delinquent behaviors, thinking issues, and overall problems were considerably higher for those with more fragmented nocturnal sleep than those with better sleep patterns. Interestingly, children who slept less soundly at night had slightly higher scores on each of the increases used, which may indicate problems with violence, interest, withdrawal, physical complaints, anxiety-depression, relationships with others, and general externalizing and internalizing signs.

It has been proven and reinforced that there is a link between sleep quality and mental health in young people and adolescents (Sohn et al 2019). For instance, according to one study, Adolescents with many sleep problems were found to have an anxious or depressed state in 67% of cases, according to the DSM (Haynes et al 2018). In these situations, particular aspects of sleep quality have also been connected to achieving mental health. In Monzon et al (2019) study, young people's lower mood and greater anxiety were linked to shorter nocturnal hours of sleep. Nocturnal sleep disturbances, defined as having problems falling asleep, sleeping through the night, or getting up too early, are linked to higher levels of sadness and anxiety. Prior studies have repeatedly shown that college students have a significant frequency of sleep disorders and mental health concerns (Li et al 2018). About 2000 college students in Taiwan reported having sleep disorders, with inadequate sleep being the most often cited concern. Almost fifty percent of these students said they had these issues. Most American young adults polled in nationwide cross-sectional research who were asked about their psychological health said they had experienced a clinically significant psychiatric condition.

Within the last year, Rahban et al (2019), based on DSM-IV criteria. As was already said, more college students than those who satisfy the criteria for clinically significant sleep problems occasionally have trouble sleeping. It is important to notice the links between sleep and psychological well-being in people with regular sleeping schedules since college students' sleeping habits tend to deteriorate with time, and even little sleep disruptions can substantially influence the beginning of mental health difficulties (McMahon et al 2018). The questionnaire was created by the researchers and had two main pieces. The first portion asked for demographic details such as gender, level/year, age, and cumulative average (Haider and Salman 2020). The study fills a gap in the literature by investigating the relationship between the use of smartphone and mental health among Thai undergraduates (Tangmunkongvorakul et al 2019). Identifying the frequency of and contributing variables to adolescents' mental health problems, Sheldon et al (2021) conducted a comprehensive review and meta-analysis. Results on how sleep and mental health are related among college students who normally have decent sleeping patterns point to the possible advantages of early intervention to improve mental well-being before it becomes clinically troubling (Ghrouz et al 2019). Therefore, sleep patterns may significantly impact psychological health practices on college campuses.

This study sought to determine if college students' self-reported sleep schedules and mental health were related to their overall amount of sleep. A student was deemed to have typically decent sleeping routines if they had a fatigue score of 10 or less at enrolment and went to bed by 2:00 am a minimum of 4 nights per week, in addition to having 6 or more hours of sleep each night. Furthermore, pupils with typically healthy sleep patterns did not have unusual sleeping habits, had never previously had sleep issues identified, or used nighttime tranquilizers more than three times per week. Another goal was to determine if these components of overall sleep quality differed in their contributions to self-reported mental health because prior studies concentrated on the different impacts of nocturnal sleep length and disturbances on psychological results. Finally, we proposed that several of the assessed results related to mental health, notably overall issues and clinically significant symptoms of psychological distress, would be differently predicted depending on individual variability in overnight sleep length and regularity.

The following sections make up the remainder of the paper. The method is described in Part 2. The data analysis is in Part 3. The results in part 4 and the conclusions are covered in Part 5.

2. Materials and Methods

The University of California, Irvine's Institutional Review Board approved this study's completion. For the online screening section of the trial, formal informed consent was waived; participants with eligibility signed consent forms that were informed before finishing the battery of questions. Table 1 shows the Participant's details.

Table 1 Participants' details.

Category	Number of Participants
Total Participants	73
Female Participants	39
Male Participants	34
Age Range	19 to 26 years (Mean age = 21)
Asian Descent	35
Caucasian Descent	27
Mixed Race	6
African American	2
Race Not Reported	3
Hispanic	10
Ethnicity Not Reported	2
Compensation Option	Cash: \$30 or Extra Course Credit: 4 points

2.1. Procedure

Depending on their replies to an online evaluation form specially created for the study's objectives based on prior research, respondents were chosen for the inquiry. We asked them about their sleeping patterns, if they had ever been diagnosed with a sleeping disorder and whether they were presently getting treatment for one if they had ever been diagnosed with a sleeping disorder and whether they were presently receiving treatment for one, whether they presently used any psychoactive medicines, or if they had ever taken any other kinds of prescribed sleeping pills. Participants were asked if they intended to abstain from using illegal substances, alcohol, coffee, and cigarettes in addition to the Epworth Sleepiness Scale (ESS) Throughout the twelve hours of the two lessons. Those who weren't fluent in English as their mother tongue were asked which language they felt most at ease with while reading and speaking. English was questioned whether the respondents' first language. According to the objectives of the broader study that provided the source of the given data, these selection requirements were considered.

College students who normally have decent sleep habits were chosen because they went to bed by 2:00 am at least four nights per week, slept for six hours or more each night, and had an ESS score of nine or less. This was done to learn more about the connections between sleep and mental health in college students. Additionally, many claimed to be native English speakers or feel at ease speaking and reading in English as they did in their mother tongue. The researchers did not classify the suitable students' observed aberrant sleep patterns as abnormal or had no history of documented sleep problems. Despite not being qualified for the assignment, 558 students finished the online assessment questionnaire: 129 individuals scored 10 or above on the ESS; 11 did not speak English as a first language or preferred to converse in their home dialect; 6 people used nightly sleep aids, 5 smoked marijuana, one had a sleeping disorder, three noticed unusual sleep patterns that the researchers either didn't know about or couldn't confirm were unusual. Less than three evenings each week, 38 went to bed before 2:00 am.

A phone call or email was sent to those eligible with information about how to continue participating in the research project. Randomly chosen participants were allocated to show up at the lab for their first session at 9:00 am or 9:00 pm according to the broader aims of the study, from which the presented findings were drawn.

The University of California, Irvine's Institutional Review Board (IRB) approved the research's execution. The IRB decided not to seek formal informed permission during the trial's online assessment phase. Instead, before starting the battery of inquiries, those who satisfied the eligibility requirements were given consent papers with every necessary detail. This method preserved adherence to ethical principles and research standards while ensuring that those involved had the chance to evaluate and comprehend the specifics of the study before freely consenting to participate in it.

2.2. Measures

2.2.1. Epworth Sleepiness Scale (ESS)

The Epworth Sleepiness Scale (ESS) is a brief questionnaire with 8 items that measure a person's propensity to nod off or feel tired under different conditions. On a scale from 0 to 3, each item is scored, with higher ratings suggesting an increased predisposition for sleepiness. The ESS has good test-retest reliability, with a value of 0.72 in the specific sample under study, and strong internal coherence, suggesting that the items inside the survey are closely connected. The results from all 8 questions are added together to estimate the initial state of weariness at the start of the first period. Higher ratings indicate a person is more fatigued overall, which can be used as a measure of how much exhaustion they are now experiencing.

2.2.2. Pittsburgh Sleep Quality Index (PSQI)

The PSQI is a 19-item questionnaire that evaluates the quantitative and qualitative elements of sleeping habits over the previous 30 days. Qualitative questions focus on the subjective nature of sleep and motivation to do daily tasks, whereas quantitative inquiries gather information on bedtime, wake-up time, sleep duration, and sleep interruptions. The inventory has received good internal consistency and test-retest stability (0.61 in this sample) and has been verified over a wide range of sleep patterns. It is regarded as the benchmark for assessing perceived sleep quality. Seven aspects of sleep were broken down into scores from the 19 questions, and a combined score for total sleep quality was computed. Higher scores signify worse sleep, with values above five indicating poor sleep. Two additional factors related to mental well-being were examined: the normal nocturnal sleep length and the frequency of sleep interruptions. Responses ranged from 0 to 3, and the total of the codes yielded a constant score for sleep disruption.

2.2.3. Adult Self-Report Form (ASR)

The ASR (Adult Self-Report) questionnaire was used to evaluate mental health. It records the actions and drug use reported by participants throughout six months. Numerous ASR questions call for rating answers on a scale of 0 to 2. According to the DSM-IV categories, actions including hostility, violating rules, anxiousness, somatic symptoms, and withdrawal are rated based on questionnaires. The ASR has strong test-retest reliability and internal consistency. The publisher's Assessment Data Management (ADM) software was used to compress the ASR data and provide clinically

applicable measures of emotional distress and overall evaluations for different syndrome evaluations. Psychiatrists and psychologists created DSM-relevant measures corresponding with certain DSM-IV diagnostic groupings, whereas statisticians constructed syndrome measures based on co-occurring behaviors. By looking at the total ASR rankings, outliers were found. Values that deviated more than three standard deviations from the mean were deemed outliers and reduced to the dataset's maximum permitted value plus one. The ASR data reduction handbook's instructions were followed to analyze the total results from each scale, and the results were z-scored.

3. Data analysis

SPSS Version 20 is used for the data evaluation. A broad analytic methodology examined the relationships between participant sleep quality, its components, and personality. To investigate the relationships among group assignment, race, ethnicity, respondent sleepiness in the first period, total sleep quality, and mental wellness, preliminary analyses of variance (ANOVAs) were carried out. ASR-measured clinically relevant indicators of psychological distress were then correlated with total sleep quality, sleep duration, sleep interruptions, syndrome scales, and other variables. The effects of sleep length and interruptions on self-reported mental health were examined using multiple regression analyses. Due to prior studies connecting these characteristics to mental health, they were selected as prospective indicators. Based on their associations with sleep time frame, sleep quality, and sleep interruptions at preset significance thresholds ($p \leq 0.5$ and $p \leq 0.10$), a selection of ASR and DSM-relevant measures was chosen for regression analysis. This method assisted in lowering the volume of regressions run.

4. Results

The percentage of people who fell into each ASR variable's clinical range is included in Table 2's descriptive data for the main research factors.

Table 2 Descriptive information about the primary research variables; 73 individuals.

Variables	Mean	SD	Clinical Range (%)
The scale of Epworth sleepiness			
Sleepiness Rating	6.72	3.72	NA
The Measure of Pittsburgh's Sleep Quality			
the overall level of slumber	4.67	2.37	NA
Self-Report by Adult			
Making Issues External	47.28	8.38	0%
aggressive issues	51.92	2.95	0%
Issues of Intrusive	52.92	5.14	2%
Rule-Breaking Problems	53.73	4.23	0%
Inside-Out Problems	49.43	8.75	7%
Anxious issues	56.02	6.05	5%
Somatic issues	53.03	5.42	1%
Withdrawn issues	54.38	5.84	4%
Total Problems	48.98	7.28	0%
DSM-Oriented Scales			
Issues with an antisocial character	52.89	4.08	0%
Anxiety issues	54.18	6.26	5%
Attention Deficit/Hyperactivity issues	53.56	4.72	2%
Avoidant Personality issues	55.44	6.69	6%
Depressive issues	53.39	4.39	2%
somatic conditions	52.56	5.32	2%

4.1. Result of ANOVA

Information from three individuals without values for race and one Participant without values for ethnicity were thus disregarded in the following analyses. When $p \leq 0.05$., substantial results are shown.

4.2. Bivariate Relationships between Mental Health and Sleep Quality

Table 3 displays partial relationships between continuous sleep quality measurements PSQI factors and self-reported mental wellness.

4.3. Examining the length of sleep during the night and interruptions as indicators of mental health

We ran one regression on the symptom scales for overall issues to investigate the relationship between the amount of time spent sleeping at night and the number of nocturnal sleep interruptions (Table 4).

The DSM-relevant measures for anxiety difficulties, depressive disorders, and somatic complaints were subsequently the subject of 3 further regression evaluations (Table 5). Race, ethnicity, the length of nightly sleep, and the frequency of sleep interruptions were all indicators.

Table 3 Measurements of continuous sleep and PSQI elements (self-reported).

ASR factors and Scales	Worldwide sleep standard	At night, sleep duration	Sleep disruptions during the night	Disruptions	Duration	Dysfunction	Efficiency	Latency	Medication	Quality
Suffering Scales										
Making Issues External	.41*	-.22	.17	.15	.23	.27*	.13	.34*	.12	.35*
aggressive issues	.40*	-.24	.04	-0.9	.30*	.27	.10	.36*	.08	.39*
Intrusive issues	.05	-.04	.16	.08	-0.3	-.08	-.05	.12	-.03	-.06
Rule-Breaking issues	.044*	-.18	.19	.28*	.17	.34*	.22	.26	.014	.36*
Internalizing issues	.37*	-.20	.18	.08	.21	.17	.41*	.21	-.03	.32*
Anxious issues	.33*	-.21	.08	-0.7	.24	.20	.37*	.19	-.14	.32*
Somatic issues	.46*	-.13	.52*	.46*	.21	.04	.38*	.26	.23	.35*
Withdrawn issues	-.05	-.08	-.22	-.29*	-0.4	.00	.15	-.06	.00	.05
Total Problems	.48*	-.26	.26	.18	.27	.27*	.32*	.31*	.06	.43*
DSM-Oriented Scales										
Antisocial Personality Problems	.39*	-.14*	.09	.08	.24	.22	.13	.34*	.13	.37*
Anxiety Problems Attention	.43*	-.23	.29*	.16	.23	.09	.23	.39*	.01	.46*
Deficit/Hyperactivity Problems	.39*	-.19	.22	.22	.19	.34*	.16	.29*	.00	.28*
Avoidant Personality Problems	.14	-.09	-.04	-.14	.09	.09	.25	.09	-.06	.14
Depressive issues	.48*	-.25	.22	.12	.31*	-2.3	.41*	.32*	-.09	.42*
Somatic issues	.29*	.00	.57	.53*	.04	-0.4	.27*	.09	.28*	.20

Table 4 Regression analyses between Total Issues and Constant Sleep Measurements (ASR)

	b	SE(b)
Model-1		
Race	-.28	.28
Ethnicity	-.34	.40
Model-2		
Race	-.32	.27
Ethnicity	-.34	.38
Length of night sleep	-.25*	.13
Sleep interruptions at night	.08*	.06
<i>R</i> ²		.17
ΔR^2		.14*

Scales of the syndrome: The length of the night's sleep was adversely correlated with overall issues, whereas the frequency of nocturnal sleep interruptions was correlated favorably with overall troubles. Difficulties, in general, were not correlated to race or ethnicity.

DSM-related scales: This approach was effective in keeping dedication to ethical norms and research practices while giving each Participant's freedom and well-being a top priority. By using this strategy, people were given a chance to carefully evaluate and comprehend the specifics of the study, enabling them to make judgments and freely offer their permission. The freedoms and worth of those who participated were protected at all stages of the procedure thanks to the careful consideration of ethical rules and study methods. As a result, our approach achieved a balance between individual freedom and ethical honesty, promoting an open and responsible environment for the study.

5. Conclusions

The primary objectives of the current study were to (I) examine the association between respondents' reported mental health and the amount of sleep they had among college students who typically get enough rest and (II) examine the association between two elements of respondents' sleep quality, Specifically, as significant determinants of psychological outcomes, nocturnal sleep length and the frequency of nighttime sleep interruptions. The findings of this study shed light on the relationships between psychological health and sleep in a group that is predisposed to both sleep disorders and mental health conditions. The use of the ASR as a gauge of respondent mental health was one of the study's significant gains. In order to boost mental wellness impacts before they are clinically relevant, additional studies should examine if present sleep



therapies could improve sleep and psychological results in college pupils with generally favorable sleep schedules. These preventative measures might have a significant influence on both individual students and college campuses in general if they are successful.

Table 5 Regression analyses between selected DSM-relevant factor evaluations and continuous sleep measurements.

8	Anxiety issues		Depressive issues		Somatic issues	
	b	SE(b)	b	SE(b)	b	SE(b)
Model-1						
Race	.36	.28	-.27	.28	.30	.28
Ethnicity	-.11	.40	.07	.40	.18	.40
Model-2						
Race	.32	.27	-0.32	.27	.30	.25
Ethnicity	-.12	.38	.07	.39	.06	.34
Length of night sleep	-.23	.13	-.24	.13	-0.5	-.12
Sleep interruptions at night	.09*	.06	.08	.06	.18*	.05
R^2		.16		.13		.35
ΔR^2		.14*		.12*		.32*

Ethical considerations

Not applicable.

Declaration of interest

The authors declare no conflicts of interest.

Funding

This research did not receive any financial support.

References

- Chang X, Jiang X, Mkandarwire T, Shen M (2019) Associations between adverse childhood experiences and health outcomes in adults aged 18–59. *PLoS one* 14:e0211850.
- Ghrouz AK, Noohu MM, Dilshad Manzar M, Warren Spence D, BaHammam AS, Pandi-Perumal SR (2019) Physical activity and sleep quality about mental health among college students. *Sleep and Breathing* 23:627-634.
- Haider AS, Al-Salman S, (2020) Dataset of Jordanian university students' psychological health impacted by using e-learning tools during COVID-19. *Data in brief* 32:106104.
- Haynes SN, Kaholokula JKA, Tanaka-Matsumi J (2018) Psychometric foundations of psychological assessment with diverse cultures: What are the concepts, methods, and evidence? *Cultural competence in applied psychology: An evaluation of current status and future directions* 441-472.
- Karjalainen P (2021) Parenting intervention to help children with behavior problems in child protection and other family support services.
- Li L, Wang YY, Wang SB, Zhang L, Li L, Xu DD, Ng CH, Ungvari GS, Cui X, Liu ZM, De Li S (2018) Prevalence of sleep disturbances in Chinese university students: a comprehensive meta-analysis. *Journal of sleep research* 27:e12648.
- McMahon DM, Burch JB, Wirth MD, Youngstedt SD, Hardin JW, Hurley TG, Blair SN, Hand GA, Shook RP, Drenowatz C, Burgess S (2018) Persistence of social jetlag and sleep disruption in healthy young adults. *Chronobiology International*, 35:312-328.
- Minihan E, Gavin B, Kelly BD, McNicholas F (2020) COVID-19, mental health and psychological first aid. *Irish Journal of Psychological Medicine* 37:259-263.
- Monzon A, McDonough R, Meltzer LJ, Patton SR (2019) Sleep and type 1 diabetes in children and adolescents: A proposed theoretical model and clinical implications. *Pediatric diabetes* 20:78-85.
- Pan KY, Kok AA, Eikelenboom M, Horsfall M, Jörg F, Luteijn RA, Rhebergen D, van Oppen P, Giltay EJ, Penninx BW (2021) The mental health impact of the COVID-19 pandemic on people with and without depressive, anxiety, or obsessive-compulsive disorders: a longitudinal study of three Dutch case-control cohorts. *The Lancet Psychiatry* 8:121-129.
- Rahban R, Priskorn L, Senn A, Stettler E, Galli F, Vargas J, Van den Bergh M, Fusconi A, Garlantezec R, Jensen TK, Multigner L (2019) Semen quality of young men in Switzerland: a nationwide cross-sectional population-based study. *Andrology* 7:818-826.
- Sheldon E, Simmonds-Buckley M, Bone C, Mascarenhas T, Chan N, Wincott M, Gleeson H, Sow K, Hind D, Barkham M (2021) Prevalence and risk factors for mental health problems in university undergraduate students: A systematic review with meta-analysis. *Journal of Affective Disorders* 287:282-292.
- Sohn SY, Rees P, Wildridge B, Kalk NJ, Carter B, (2019) Prevalence of problematic smartphone usage and associated mental health outcomes amongst children and young people: a systematic review, meta-analysis and GRADE of the evidence. *BMC Psychiatry* 19:1-10.
- Tamana SK, Ezeugwu V, Chikuma J, Lefebvre DL, Azad MB, Moraes TJ, Subbarao P, Becker AB, Turvey SE, Sears MR, Dick BD (2019) Screen-time is associated with inattention problems in preschoolers: Results from the CHILD birth cohort study. *PLoS one* 14:0213995.
- Tangmunkongvorakul A, Musumari PM, Thongpibul K, Srithanaviboonchai K, Techarivichien T, Sugimoto SP, Ono-Kihara M, Kihara M (2019) Association of excessive smartphone use with psychological well-being among Chiang Mai, Thailand university students. *PLoS one* 14:0210294.

Type-2 Diabetes prediction with cuttlefish search optimization and hybrid model



Dilip Kumar Pati^a | Saubhagya Mishra^b | Aditya Mishra^c

^aSanskriti University, Mathura, Uttar Pradesh, India, Professor, Department of Ayurveda.

^bTeerthanker Mahaveer University, Moradabad, Uttar Pradesh, India, Professor, Department of Medicine.

^cJaipur National University, Jaipur, India, Assistant Professor, Department of Microbiology.

Abstract In India, there are over 30 million individuals with diabetes and many more who are at risk. Diabetes and related health issues must be detected and treated early to be prevented. This study looks at a person's lifestyle and family history to determine their risk of having diabetes. The suggested hybrid machine learning approach, which combines the Support Vector Machine (SVM) classifier and Naive Bayes (NB) classifier, was used to forecast the probability of Type 2 diabetes. We incorporate Cuttlefish Search Optimization (CFSO) to increase prediction accuracy. After the model has been successfully trained, individuals may evaluate their own risk of developing diabetes. 952 times the information required for the question using an online and offline survey along with 18 questions about your habits, health, and family history. Preprocessing was done using min-max normalization, and feature extraction was done using linear discriminant analysis (LDA). The recommended approach was also examined using the Pima Indian Diabetes database. The performance of the provided approach is proved to be the most accurate for both datasets. The term "Type 2 Diabetes prediction with Cuttlefish Search optimization and a hybrid model" refers to the employment of a particular optimization technique called Cuttlefish Search in conjunction with a hybrid model to forecast a person's chance of getting Type 2 Diabetes.

Keywords: Support Vector Machine, type 2 diabetes, Naïve Bayes, cuttlefish search optimization

1. Introduction

Diabetes is one of the most common chronic illnesses that are not contagious in the world. Researchers have looked at medical data utilizing data mining and machine learning techniques to enhance the efficacy and accuracy of type 2 diabetes predictions. Preparing datasets using data-mining techniques allows the discovery of hidden patterns and the selection of the most relevant feature datasets. Chronic non-communicable diseases are the leading causes of death worldwide. A class of ailments known as non-communicable chronic diseases does not include viruses or other infectious agents, making them incapable of being passed from one person to another. People with these conditions do not display any indications of illness, and they progress slowly. Both the Hospital Frankfurt Diabetes (HFD) and Pima Indian Diabetes (PID) datasets were acquired from the UCI repository and utilized in the development of the algorithm (Al-Tawil et al 2023). Disease diagnosis is the process of determining which ailment best fits a person's symptoms. Since certain symptoms and indicators are general, the most difficult issue is the prognosis. Disease identification is the most crucial stage in the treatment of any disorder. Machine learning is a discipline that may help in predicting the diagnosis of an illness based on previously trained data. Many scientists have created a range of machine-learning approaches to accurately diagnose a number of ailments. Due to machine learning, robots can learn even without being explicitly programmed (Ibrahim et al 2021). When a person has diabetes mellitus type 1, sometimes referred to as "insulin-subordinate diabetes mellitus" (IDDM), their pancreas does not generate as much insulin as their body needs. Exogenous insulin dosage is required to make up for the pancreas' decreased insulin production in persons with type-1 DM. The pancreas generates less insulin than what the body needs when a person has diabetes mellitus type 1, sometimes referred to as "insulin-subordinate diabetes mellitus" (IDDM). Insulin resistance is a feature of diabetes mellitus type 2 because the body's cells react to the hormone otherwise than they would ordinarily. The body can ultimately stop manufacturing insulin as a consequence of this. "Adult starting diabetes" (ASD) and "non-insulin subordinate diabetes mellitus" (NIDDM) are other terms for this. These types of diabetics often have high BMIs or have sedentary lives. Globally, more than 50 million individuals, mostly adults, have chronic liver disease. The sickness, however, could be cured if it is found in its early stages. Common illnesses might be identified early by using machine learning-based sickness prediction. Health is now seen as a secondary priority, which has resulted in several issues. A medical diagnostic is an example of a problem that must be solved in the real world and is very important. The process of turning observational data into disease designations is known as illness diagnosis. Data obtained from assessing a



patient and chemicals produced by the patient make up the evidence; diseases are theoretical medical entities that look for abnormalities in the evidence that has been collected (Badawy et al 2022).

A broad definition of hypertension includes not only blood pressure but also its connection to structural and functional cardiac and vascular abnormalities that harm the target organs and result in early morbidity and mortality. Approximately 972 million people worldwide had hypertension in 2000, and by 2025, that number is expected to rise to 1.56 billion. Additionally, immune system changes have an impact on pre-hypertension, an inflammatory-related syndrome that starts a more severe hypertensive state (Abachi et al (2019)). One of the most serious microvascular issues that people with diabetes experience is Diabetic Kidney Disease (DKD), and its prevalence is increasing annually. Notably, recent research has shown that some pattern recognition receptors (PRRs) in cells may be able to recognize hyperglycemia, fatty acids, and other compounds linked to damage, inducing pyroptosis. We think that the pathophysiology of DKD is intrinsically linked to the signal transduction pathways of pyroptosis (Lin et al (2020)). Through the use of computational data extraction tools, key diabetic traits may be examined in order to predict and prevent diabetes. The pathogenic process was studied using a system biology approach in this study to discover crucial indicators that may serve as therapeutic targets. Data mining is critical to the healthcare sector since identifying and studying illnesses requires a plethora of information (Abdulqadir et al 2021). Hemanth et al 2020 goal are to provide a different, hybrid approach to using retinal fundus pictures to diagnose diabetic retinopathy. In order to get better outcomes, the hybrid approach is built on combining deep learning with image processing. It is a recognized open challenge in medical image processing those alternative methods must be developed in order to accurately diagnose diabetic retinopathy from digital fundus pictures. Here, manual interpretation of retinal fundus images requires substantial time, expertise, and effort commitment. As a result, imaging and computer vision systems are necessary for doctors, and the adoption of intelligent diagnostic technologies is commonly seen as the next phase. Type 2 diabetes and/or insulin resistance have a high correlation with the complex condition of obesity. An effective method to combat these dysmetabolic disorders that cause many illnesses, including inflammatory and cardiovascular ones, is via proper diet (Ivan et al 2022). In order to successfully treat chronic diabetes wounds, which often have complex microenvironments, a hydrogel wound dressing must have more than one function. Thus, a multifunctional hydrogel is ideal for better therapeutic therapy. (Yang et al 2023). One of the most prevalent illnesses in the world is diabetes. Numerous Machine Learning (ML) techniques have been put to use in recent years to predict diabetes (Larabi-Marie-Sainte et al 2019). Considering metabolic diseases as a group, diabetes is characterized by chronically high blood sugar levels, which makes it a chronic condition. It is highly challenging to produce a reliable and accurate diabetes prediction due to the small amount of labeled data and outliers contained in the diabetes datasets (Hasan et al 2020). Early detection is crucial for diabetes since there is presently no cure. In this study, methods for predicting diabetes include data mining, machine learning (ML), and neural networks (NN). For this experiment, the UC Irvine Unique Client Identifier (UCI) machine learning repository provided the Pima Indian Diabetes (PID) dataset (Khanam et al 2021). In this section, we discuss Type -2 Diabetes prediction with a hybrid model and cuttlefish search optimization.

2. Materials and Methods

In this part, we talk about predicting Type 2 Diabetes using a hybrid model with cuttlefish search optimization (CFSO).

2.1. Data set

The dataset comprises the names of the characteristics as well as their descriptions, which are provided in Table 1. There are 520 instances in the collection, and each one has 17 characteristics. The dataset also contains one class with two potential outcomes that were tested positively and negatively.

2.2. Preprocessing using Min-Max Normalization

Scaling numerical characteristics within a certain range is often done using min-max normalization. It is often used to get data ready for models in machine learning. Min-max normalization may be used to normalize the input characteristics of the dataset for diabetes prediction.

Min-Max normalization is a technique of normalizing that uses linear modifications to the original data to provide a fair comparison of values before and after the procedure.

$$Z_{new} = \frac{z - \min}{\max(z) - \min(z)} \quad (1)$$

Where:

Z_{new} = The adjusted value obtained after scaling the data

Y = outdated value

$Max(Y)$ = Dataset's highest possible value

$Min(Y)$ = Dataset's lowest possible value

2.3. Feature Extraction using Linear Discriminant Analysis (LDA)

The situation where the within-class frequencies are variable may be handled with simplicity using linear discriminant analysis. Results from randomized testing have been used to evaluate their efficacy. By lowering the ratio of within-class variance to between-class variation in any given batch of data, the maximum separability is offered by this technique. When using linear discriminant analysis to categorize data, the classification problem in speech recognition is taken into consideration. We decided to develop a technique for LDA in an attempt to give a better classification than Principal Components Analysis. The primary difference between the two methods is that Principal Component Analysis (PCA) does more feature classification than LDA. PCA suggests relocating the original data sets into a new location without altering their size, location, or form; LDA, on the other hand, just seeks to improve class separability and create a decision area between the existing classes.

When using the LDA method to solve two-class problems, a projection vector in the feature space is found that maximizes the between-class scatter matrix and minimizes the within-class scatter matrix. Here, the objective is to locate a linear function.

$$z = b_1v_{j_1} + b_2v_{j_2} + b_3v_{j_3} + \dots .b_rv_{j_r} \tag{2}$$

Where:

$$b^s = \{b_1, b_2, \dots, b_r\}$$

is a vector of coefficients that has to be determined, while

$$v_j = [v_{j_1}, v_{j_2}, \dots, v_{j_r}] \tag{3}$$

$$v_i = [v_{i_1}, v_{i_2}, \dots, v_{i_r}] \tag{4}$$

The following multivariate analysis of variance assumptions is required in order to estimate the dataset's mean and variance.

Normality: Each level of the grouping variable has a normal distribution for independent variables.

Collinearity: If two variables have a strong correlation, the predictive potential may be reduced.

Table 1 Dataset Description.

Attribute Number	Attribute Number	Answer
1	Age	21.66
2	Gender	Male Female
3	Obesity	Yes No
4	Class	Positive negative
5	Partially paralyzed	Yes No
6	Polyphagia	Yes No
7	stiff muscles	Yes No
8	Mouth thrush	Yes No
9	Fuzziness in the vision	Yes No
10	Itching	Yes No
11	Irritability	Yes No
12	Delayed Recovery	Yes No
13	Alopecia	Yes No
14	Polyuria	Yes No
15	Polydipsia	Yes No
16	Unexpected weight reduction	Yes No
17	Weakness	Yes No

3. Classification

Three bio-inspired methods for identifying type 2 diabetes are covered in this section: the cuttlefish algorithm, support vector machine technique, and naive Bayes algorithm.

3.1. Naive Bayes Classifier

The assumptions behind the classification method known as Naive Bayes are that all features are independent and different from one another.

It works well with data that contains missing numbers and imbalance problems. The Bayes Theorem is used by the Naive Bayes machine learning classifier. The posterior probability $P(C|X)$ may be derived using the Bayes theorem from $P(C), P(X)$, and $P(X|C)$. Consequently,



$$P(C|X) \text{ equals } (P(X|C) P(C))/P(X) \quad (5)$$

The posterior probability for the intended class is $P(C|X)$.

Class prediction probability is $P(X|C)$.

The probability that class C is true is $P(C)$.

$P(X)$ Represents the predictor's prior probability.

3.2. Support Vector Machines (SVM)

Support Vector Machines (SVM) is used to assess the correctness of the data used in regression and classification studies. Supervised learning models, or SVMs, have equivalent learning processes.

Although it has been stated that the main justification for adopting an SVM rather is that the problem may not be linearly separable, it has often been observed that the SVM technique yields better outcomes than other classifiers.

The Radial Basis Function (RBF) or another non-linear kernel SVM would be appropriate in this situation. In a linked high-dimensional space, SVMs are required. For example, SVMs are said to categorize text more accurately, even when training takes some time.

The SVM, a variation of the support vector classifier, is derived from a particular method of kernel-based feature space expansion.

Equation (6) illustrates how a linear support vector classifier is represented.

$$e(v) = \beta_0 + \sum_{j=1}^m \alpha_j \langle v, v_j \rangle \quad (6)$$

where $\alpha_1, \dots, \alpha_n$ and β_0 variables that are estimated by $\left(\frac{m}{2}\right)$ inner products $\langle v_j, v'_j \rangle$ among all sets of training observational pairs. Changing the internal component with $L(v_i, v'_i)$, where L is a process known as the kernel. Equation (7) illustrates the representation of the linear kernel.

$$L(v_j, v'_j) = \sum_{i=1}^o v_{ji} v'_{ji} \quad (7)$$

The following equation (8) may be used to describe a polynomial kernel of degree c :

$$L(v_j, v'_j) = \left(1 + \sum_{i=1}^o v_{ji} v'_{ji}\right)^c \quad (8)$$

The SVM classifier is a supervised learning method based on kernels that were created primarily for binary classification. Since it splits the data into two or more groups when there are many training samples, it is not advised. The SVM classifier is a supervised learning technique based on a kernel intended for binary classification. Using a kernel function, the training set is mapped to resemble a set of data that can be separated linearly. The reason for mapping is to increase the dimension of the data collection, and a kernel function is employed to do this successfully. Several kernel functions, including the linear, RBF, quadratic, multilayer perceptron, and polynomial kernels, are often used. Furthermore, compared to the RBF kernel function, the linear kernel function is less susceptible to overfitting. The regularization parameter C , also known as the box constraint, and the kernel parameter, commonly known as the scaling factor, govern how well the SVM classifier performs. The hyperplane parameter is used to refer to them all combined. SVM creates a model, maps the decision boundaries for each class, and finds the hyperplane dividing the various classes through the training stage. SVMs may be used for non-linear classification as well.

SVMs have been effectively utilized for a variety of tasks involving text and hypertext categorization, speech recognition, image retrieval, bankruptcy prediction, remote sensing analysis of visual data and biological, time series forecasting, information security, including bioinformatics and protein classification, and science of chemicals, such as the findings of spectroscopy, such as chromatography-mass spectrometry.

3.3. Cuttlefish Search Optimization

In earlier work, we developed a brand-new optimization technique known as the CFA. The program imitates the processes a cuttlefish uses to alter its color. Reflected light from the cuttlefish's many cell layers, including the chromatophores, leucophores, and iridophores, creates the patterns and colors that are visible. The CFA takes into consideration visibility and reflection. While the reflection process is used to mimic the method by which light reflects off surfaces, visibility is used to mimic the visibility of matching patterns. As a search method, these two procedures are employed to locate the overall ideal answer.

$$\text{new_population} = \text{ref} \quad (9)$$

Six distinct situations are produced by the visibility and reflection processes together, and Equation (9) suggests a new potential resolution.

Algorithm 1 The cuttlefish algorithm

```

Input: Maximum Iteration  $x_1, x_2, q_1, q_2$ , Higher, Lower
Output: learn about the top 4 characteristics
//f = fitness, best = bs, new solution = ns//
Start measuring populations and counting them
Examine the healthiness of the populace
Save the superior option
separate cells into four groups  $H_1, H_2, H_3$ , and  $H_4$ 
while  $I \leq \text{Max iteration}$ , do
Calculate the average of the best answer and save it in the best
For each cell in  $H_1$  do //cases 3&4
create new solution using (1), (2), and (3)
 $ref = rand(q_1, q_2) \times H_1[j].points[i]$ 
 $Vis = rand(q_1, q_2) \times (Best.Points[i]) - H_1[j].points[i]$ 
Evaluate f for ns
if ( $f > bs$ ) then present = new Sol
End if
End for
Do this for every cell in  $H_2$ 
Generate a new method based on (1) and (3)
 $Ref = Best.Point[i]$ 
 $Vis = rand(x_1, x_2) \times (Best.Points[i]) - H_2[j].points[i]$ 
Evaluate the f for the ns
if ( $f > bs$ ) then current = new sol
end if
end for
For every cell in  $H_3$  do //case 5
Create a new solution using (1) and (7)
 $Ref = Best.Point[i]$ 
 $Vis = rand(x_1, x_2) \times (Best.Points[i]) - AVbest$ 
Evaluate the fitness of the new_sol
if ( $f > bs$ ) then current = new_sol
End it
End for
For every cell in  $H_4$  do //cases 6
create a random solution using (1)
 $O[j].points[i] = rand \times (Upper - Lower) + lower$ 
Evaluate the f for the new_sol
if ( $f > bs$ ) then current = new_sol
end it
end for
I=I+1;

```

Cases 1 and 2 illustrate instances of interactions between chromatophores and iridophore cells, which result in a novel solution to equation (10). In these cases, G1 is a group of cells, and i and $Points[j]$ stand for the i th cell and the j th point of the i th cell, respectively.

$$ref[i] = Q \times H_1[j].points[i] \quad (10)$$

$$vis = W \times (Best.Points[i] - Q \times H_1[j].points[i]) \quad (11)$$

The values of $Rand$ (q_1 and q_2) are obtained using equations (11) and (12), respectively.

$$R = rand() \times (q_1 - q_2) + q_2 \tag{12}$$

$$W = rand() \times (x_1 - x_2) + x_2 \tag{13}$$

To calculate how visible the relevant background is, utilize equation (13). The places of the optimum solutions are shown by points. *R* governs the saccule's stretch or shrink interval, while *V* determines how visible the pattern is.

In cases 3 and 4, the visibility of the matching pattern and the light reflected from the best response is considered in order to arrive at a new solution. A new search area is created as an interval around the best response by equation(14).

$$ref[i] = Q \times Best.points[i] \tag{14}$$

Leucophore cells are employed in equation (13), where AVbest is the Best, analogous to equation (15), to reflect light from the area of the best solution and increase the pattern's visibility. The usual point value. Using the leucophore cell operator, a random solution was produced in instance 6.

$$vis[i] = X \times (Best.Points[i] - BXbest) \tag{15}$$

4. Results

To demonstrate the effectiveness and reliability of a suggested approach, its performance is compared with that of conventional methods such as Artificial Neural Networks (ANN) (Srivastava et al (2019), Long Short-Term Memory Networks (LSTM) (Yahyaoui et al (2019), and Convolutional Neural Networks (CNN) (Massaro et al (2019). The usage of SVM + NB in the creation of diabetes prediction models has been advised. These techniques are evaluated against traditional ones using a number of criteria, such as accuracy, precision, recall, and cost of implementation.

4.1. Accuracy

In the design of industrial items, accuracy is defined as the usage of being accurately categorized to the overall number of occurrences.

$$Accuracy\% = \frac{TP+TN}{TP+FP+FN+TN} (\%) \tag{16}$$

Figure 1 displays the accuracy of the present and existing methods. The accuracy of the proposed SVM+NB has been suggested for diabetes prediction. The suggested method achieves 97% accuracy compared to ANN's 90% and LSTM's 93%. It demonstrates that the suggested method is more accurate than the current one. The values of accuracy are shown in Table 2.

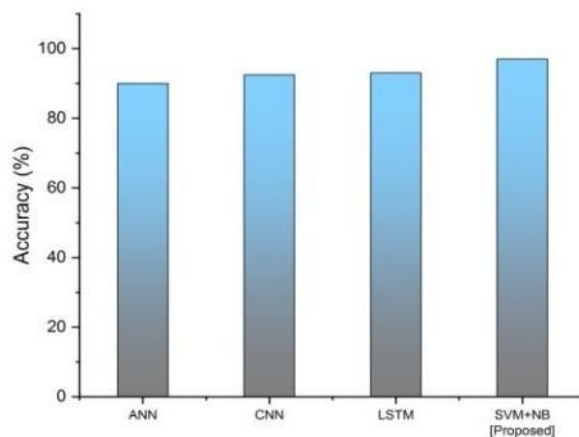


Figure 1 Accuracy of the proposed method.

Table 2 Comparison of Accuracy.

Techniques	Accuracy (%)
ANN	90
CNN	92.5
LSTM	93
SVM+NB [Proposed]	97



4.2. Precision

In order to forecast diabetes, the capability of a classification model is employed to pinpoint just the relevant data points.

$$Precision = \frac{TP}{TP+FP} \quad (17)$$

Figure 2 displays the accuracy of the proposed and existing systems. The accuracy of the proposed SVM + NB has been suggested for usage in diabetes prediction. The suggested method achieves 96.2% accuracy, compared to ANN's 91% and LSTM's 95.4%. It demonstrates that the suggested method is more precise than the current one. The accuracy values are shown in Table 3.

Table 3 Result of Precision.

Techniques	Precision (%)
ANN	91
CNN	93.6
LSTM	95.4
SVM+NB [Proposed]	96.2

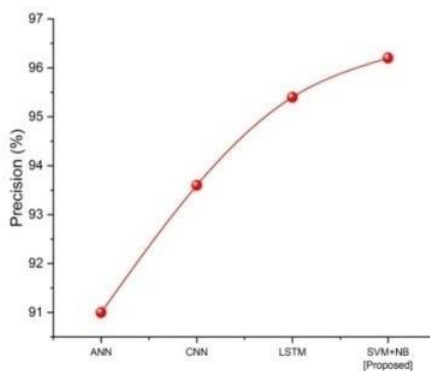


Figure 2 Precision of the proposed method.

4.3. Recall

Mathematically, the recall is determined as the sum of true positives minus false negatives. A model's capacity to locate all relevant events in a set of data for diabetes prediction may be employed.

$$Recall = \frac{TP}{TP+FN} \quad (18)$$

The recalls for the present and proposed systems are shown in Figure 3. The projected SVM + NB recall has been suggested for usage in the diabetes prediction. In comparison to ANN's 89% and LSTM's 94.2% recall rate, the suggested method achieves 95%. It demonstrates that the suggested method has a higher recall rate than the current one. The recall values are shown in Table 4.

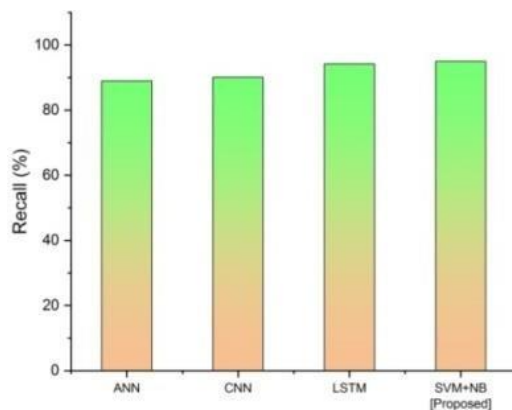


Figure 3 Recall of the proposed method.



Table 4 Result of Recall.

Techniques	Recall (%)
ANN	89
CNN	90.1
LSTM	94.2
SVM+NB [Proposed]	95

4.4. F1-measure

The F1-measure is a statistic that evaluates the overall effectiveness of a classification model or system by combining accuracy and recall. It is often used to evaluate a model's capability of correctly identifying and classifying diabetes prediction. The F1-measure is the harmonic mean of recall and accuracy, which adds the two metrics to get a single value. This formula is used to compute it:

$$F1 - measure = 2 \times \frac{(Precision \times Recall)}{(Precision + Recall)} \tag{19}$$

The F1-measure for the proposed and existing systems is shown in Figure 4. It has been recommended to use the F1measure of the proposed SVM + NB in the Diabetes Prediction. The suggested system achieves 92.6% of F1-measure, whereas ANN has obtained 85.4% and LSTM has attained 90.2%. It demonstrates that the suggested strategy has a higher F1-measure than the existing one. The F1-measure values are shown in Table 5.

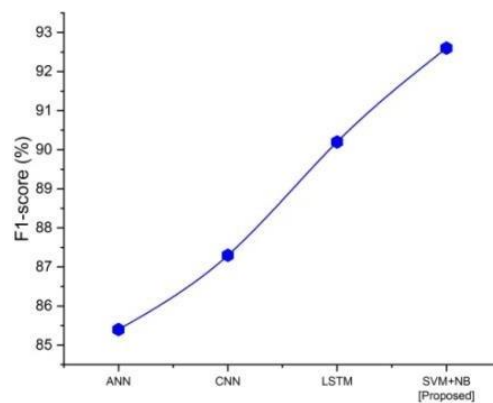


Figure 4 F1 score of the proposed method.

Table 5 F1-measure values.

Techniques	F1 score (%)
ANN	85.4
CNN	87.4
LSTM	90.2
SVM+NB [Proposed]	92.6

5. Conclusions

In the future, any additional ailment may be predicted using this result. One area where this study might be enhanced is the use of additional machine learning techniques to forecast diabetes or any other ailment. The PIMA database also used the same methods. This result might be used in the future to predict any additional illnesses. The application of additional machine learning methods to predict diabetes or any other illness is one way that this work might be improved. Future potential for predicting Type 2 Diabetes utilizing CFSO and a hybrid model is encouraging. To fully explore and fulfill the promise of Type 2 Diabetes prediction utilizing CFSO and hybrid models, further study, validation, and technology developments will be needed.

Ethical considerations

Not applicable.

Declaration of interest



The authors declare no conflicts of interest.

Funding

This research did not receive any financial support.

References

- Al-Tawil M, Mahafzah BA, Al Tawil A, Aljarah I (2023) Bio-Inspired Machine Learning Approach to Type 2 Diabetes Detection. *Symmetry* 15:764.
- Ibrahim I, Abdulazeez A (2021) The role of machine learning algorithms for diagnosing diseases. *Journal of Applied Science and Technology Trends* 2:10-19.
- Badawy M, Ramadan N, Hefny HA (2022) Healthcare Predictive Analytics Using Machine Learning and Deep Learning Techniques: A Survey.
- Abachi S, Bazinet L, Beaulieu L, (2019) An antihypertensive and angiotensin-I-converting enzyme (ACE)-inhibitory peptide from fish as potential cardioprotective compounds. *Marine drugs* 17:613.
- Lin J, Cheng A, Cheng K, Deng Q, Zhang S, Lan Z, Wang W, Chen J (2020) New insights into the mechanisms of pyroptosis and implications for diabetic kidney disease. *International journal of molecular sciences* 21:7057.
- Abdulqadir HR, Abdulazeez AM, Zebari DA (2021) Data mining classification techniques for diabetes prediction. *Qubahan Academic Journal* 1:125-133.
- Hemant DJ, Deperlioglu O, Kose U (2020) An enhanced diabetic retinopathy detection and classification approach using deep convolutional neural network. *Neural Computing and Applications* 32:707-721.
- Ivan CR, Messina A, Cibelli G, Messina G, Polito R, Losavio F, Torre EL, Monda V, Monda M, Quiete S, Casula E (2022) Italian Ketogenic Mediterranean Diet in Overweight and Obese Patients with Prediabetes or Type 2 Diabetes. *Nutrients* 14:4361.
- Yang X, He S, Wang J, Liu Y, Ma W, Yu CY, Wei H (2023) Hyaluronic acid-based injectable nanocomposite hydrogels with photo-thermal antibacterial properties for infected chronic diabetic wound healing. *International Journal of Biological Macromolecules* 124872.
- Larabi-Marie-Sainte S, Aburahmah L, Almohaini R, Saba T (2019) Current techniques for diabetes prediction: review and case study. *Applied Sciences* 9:4604.
- Hasan MK, Alam MA, Das D, Hossain E, Hasan M (2020) Diabetes prediction using ensembling of different machine learning classifiers. *IEEE Access* 8:76516-76531.
- Khanam JJ, Foo SY (2021) A comparison of machine learning algorithms for diabetes prediction. *ICT Express* 7:432-439.
- Srivastava S, Sharma L, Sharma V, Kumar A, Darbari H (2019) Prediction of diabetes using an artificial neural network approach. In *Engineering Vibration, Communication and Information Processing: ICoEVCI 2018, India*, pp 679-687. Springer Singapore.
- Yahyaoui A, Jamil A, Rasheed J, Yesiltepe M (2019) A decision support system for diabetes prediction using machine learning and deep learning techniques. In *2019 1st International Informatics and software engineering conference (UBMYK)*, pp 1-4. IEEE.
- Massaro A, Maritati V, Giannone D, Convertini D, Galiano A (2019) LSTM DSS automatism and dataset optimization for diabetes prediction. *Applied Sciences* 9:3532.

Swarm-intelligent elephant herding optimized support vector machine for predicting heart disease



Deepthi Krishna^a ✉ | Md Mazhar Alam^b | Murari Dhanatwal^c

^aSanskriti University, Mathura, Uttar Pradesh, India, Associate Professor, Department of Ayurveda.

^bTeerthanker Mahaveer University, Moradabad, Uttar Pradesh, India, Assistant Professor, Department of T.B. & Chest.

^cJaipur National University, Jaipur, India, Assistant Professor, Department of Pathology.

Abstract Considering the significant worldwide mortality rate of cardiac disease, early and precise prognosis is essential to enhancing patient outcomes. The accuracy, effectiveness, and dependability of the heart disease prediction techniques currently in use, however, continue to encounter difficulties. Therefore, it is essential to create novel strategies that can get beyond these constraints and offer a better way to forecast cardiac disease. A novel advanced elephant herding optimised support vector machine (AEHO-SVM) technique utilized for the study in suggest method for predicting cardiovascular disease. A heart disease dataset is used to assess the efficacy of the suggested AEHO-SVM algorithm. To deal with missing values, normalise the data, and minimise dimensionality, the dataset is pre-processed. The AEHO-SVM approach aims to maximise classification accuracy while lowering the possibility of misdiagnosis by optimising the hyperplane separation and changing the support vectors iteratively. A number of metrics, like sensitivity, accuracy, f-measure, and specificity are used for assess model's performance. The experiment show that the AEHO-SVM technique works better than conventional methods and achieves good predictive accuracy for the diagnosis of heart disease. A suggested AEHO-SVM technique makes use of the collective thinking of elephant herding and its built-in optimisation skills to provide a more effective and trustworthy prediction method.

Keywords: heart disease, prediction, patient outcomes, accuracy, AEHO-SVM

1. Introduction

Heart disease is a major global health issue that claims many lives and puts a heavy cost on healthcare systems around the world. For effective prevention and early intervention efforts, accurate and timely cardiac disease prediction is essential (Monga et al 2022). By utilising the strength of data analysis and pattern identification, improvements in machine learning approaches have recently demonstrated promise in the prediction of cardiac disease. Novel methodologies are needed, nonetheless, to further improve the forecast accuracy. The swarm-intelligent elephant herding optimised support vector machine (SIEH-SVM), which combines swarm intelligence and machine learning to enhance heart disease prediction, is the novel method suggested by Amin et al (2019). Innovative approach tries to optimise the SVM model, ultimately improving its performance and dependability by harnessing the collective wisdom of a virtual swarm of elephants. In order to enhance the diagnosis and treatment of cardiac disease, our research intends to contribute to the creation of more precise and effective predictive models (Subhadra and vikas, 2019).

A significant percentage of illnesses and fatalities are brought on by cardiovascular disease, which is a serious global health concern. The healthcare industry produces enormous amounts of data, and data mining is essential in turning this unstructured data into information that can be used. Cardiovascular disease prognosis prediction and decision-making are significant areas of medical research (Spencer et al 2020). A number of factors, including dietary choices and genetic predisposition, contribute to the rising prevalence of diseases, including cardiovascular disorders. Particularly among all diseases, heart disease is the most prevalent and lethal. It includes a variety of cardiac and blood vascular dysfunctions. It might be difficult for doctors and medical professionals to make an accurate diagnosis of heart disease. Modern healthcare relies heavily on data science to make early predictions and address problems brought on by massive datasets. Clinical and pathological data are frequently combined to diagnose heart illness. Because of this intricacy, clinical professionals and researchers have a keen interest in creating accurate tools for heart disease prognosis (Repaka et al 2019).

This paper goal is to increase classification accuracy and decrease misdiagnosis by optimising hyperplane separation and modifying support vectors iteratively. The model's performance is evaluated to utilizing a variety of metrics, including sensitivity, accuracy, specificity, f-measure and sensitivity.

The main goal of this paper are as follows: part 2 describe the related works, part 3 explain the material and methods, part 4 discuss about the result and discussion and part 5 concludes the paper.



2. Related works

Monga et al (2022) suggested a unique method for improving the precision of cardiovascular disease prediction through the use of machine learning techniques to identify essential variables. To introduce the prediction model, numerous feature combinations and well-known categorization techniques were used. The study showed how these suggested techniques were widely used to a range of problems. Amin et al (2019) found an important characteristics and data mining techniques to improve the accuracy of cardiovascular disease prediction. The prediction models were created using seven classification methods, including k-NN, Decision Tree, Support Vector Machine (SVM), Naive Bayes, Logistic Regression (LR), Neural Network, and Vote. These methods were investigated to raise the reliability of cardiovascular disease prediction. A diagnostic technique for foretelling heart disease was suggested by Subhadra and vikas (2019). The created technique accurately evaluates the risk level of heart disease using 14 key variables, as demonstrated by comparisons with existing approaches. The outcomes show how well the diagnostic system performs in determining the likelihood of heart disease. The performance of model was created using machine learning approaches was experimentally evaluated in the research of Spencer et al 2020. Utilising pertinent features selected using a variety of feature-selection techniques. Chi squared testing, ReliefF, and symmetrical uncertainty have all been used to examine four widely-used heart disease datasets in order to produce different feature sets. Repaka et al (2019), created a Smart Heart Disease Prediction (SHDP) system utilizing Naive Bayes and focuses on using past data to diagnose cardiac sickness. The report emphasizes how quickly technology is evolving, particularly in the field of mobile health, where this technology has seen a considerable uptick. The UCI repository dataset was used by Singh and kumar (2020) to train and test machine learning techniques for forecasting heart illness. They evaluated the precision of a number of techniques, including SVM, DT, k-nearest neighbour and linear regression. The study assessed how well different algorithms performed at correctly predicting heart disease.

Predicting the risk that patients would acquire cardiac disease was the aim of Shah et al (2020). The results demonstrate that K-nearest Neighbour has the highest accuracy rating. A collection has 76 attributes and 303 occurrences. These 76 qualities, which are essential for proving the efficacy of different algorithms, are just 14 of them that were tested. When compared to RF and ET classifiers, the proposed model's effectiveness was assessed using data on Cleveland heart disease. The following five evaluation measures were utilised to assess performance: sensitivity, F1-score, accuracy, specificity (Budholiya et al 2022). For a more precise assessment of cardiac illness, Khan and M.A (2020), suggested an Internet of Things architecture based on Modified Deep Convolutional Neural Networks (MDCNN). Data from the patient's electrocardiogram (ECG) and blood pressure are monitored by their smartwatch and heart monitor. The outcomes show that the proposed MDCNN-based system performs better at predicting cardiac disease than earlier methods. Overall, the suggested strategy consistently outperforms alternatives. Fitriyani et al (2020) presented a useful CDSS heart disease prediction model (HDPM). In order to balance the distribution of training data, the Synthetic Minority Oversampling Technique-Edited Nearest Neighbor (SMOTE-ENN) hybrid approach, XGBoost for heart disease prediction, and Density-Based Spatial Clustering of Applications with Noise (DBSCAN) to locate and eliminate outliers are all incorporated into the HDPM. In the medical sector, data science was used to anticipate cardiac issues. Although there have been a number of studies on this subject, further study is required to improve forecast accuracy. To analyse the experiments and demonstrated accuracy improvements, the research analyses numerous heart disease datasets. It then focuses on feature selection strategies and algorithms (Bashir et al 2019). A more effective machine learning technique was suggested by Mienye et al (2020), for the risk prediction of heart disease. The dataset was split into smaller subgroups at random using a mean-based splitting method. The classification and regression tree (CART) approach was then used to represent the divisions. In order to predict coronary artery disease, Ayon et al (2020) analyzed seven computational intelligence techniques: Naive Bayes (NB), Random Forest (RF), Deep Neural Network (DNN), Decision Tree (DT), Logistic Regression (LR), Support Vector Machine (SVM), and K-Nearest Neighbor (K-NN). These strategies' effectiveness was assessed and contrasted. Early convergence and local optimum problems in optimization are addressed by the HEHO-HSA-PLB-CE approach. Additionally, Ali et al (2022), concentrated on accomplishing resource optimization and load balancing in cloud computing settings. Load balance rate, scheduling time, Response time and delay evaluation metrics were used to gauge the effectiveness of the technique after it was deployed in CloudSim. The Elephant and Dolphin Herding algorithms, in particular, have various benefits such as cheap total cost, derivative-free optimization, resilience, ease of implementation, and adaptability. These algorithms were suggested by Kamal et al (2020) to enhance the detection and scalable of attacks by the Neris botnet. The proposed approach efficiently and successfully located the Neris botnet, proving its quick and precise detection capability.

3. Materials and Methods

3.1. Dataset

The dataset employed in this investigation consists of 75,000 patient records, each of which has 14 unique attributes. These characteristics cover a wide range of characteristics, including age, gender, systolic and diastolic blood pressure. The target class, "cardio," specifies whether a patient has cardiovascular illness or is thought to be in good health (expressed as

0). Based on the specified attributes, this dataset offers useful information for assessing and predicting the presence of cardiovascular disease.

3.2. Support vector machines (SVM)

A model used for regression analysis and classification is called a support vector machine (SVM). When the data contains two classes, it functions properly. In order to get a wider gap between the two classes, the SVM selects the optimal hyperplane to divide them. The data points at the margin's edge form support vectors. SVM is appropriate for multi-attribute, complex real-world situations, such as CHDD (probably alluding to coronary heart disease). SVM employs a variety of kernel spaces, including radial basis function (RBF), linear, quadratic, and polynomial. For SVM, choosing the right kernel and technique might be difficult in order to prevent the model from being unduly optimistic or pessimistic. It is controversial whether RBF or linear kernels are better for CHDD (Cleveland Heart Disease database), which has a huge number of instances and features. Although the link between characteristics and class labels is nonlinear, the RBF kernel could not be useful due to the vast number of features. It is advised to try both kernels and pick the one with the best performance.

SVM prediction uses optimal separation hyperplanes to separate classes, maximising the distance between the nearest data points. SVM classification relies heavily on kernels, and choosing the best kernel can have a big impact on how well a classification algorithm performs, as demonstrated in the following equations 1,2,3,4,5. The SVM method aims to determine the maximum distance around a hyperplane to distinguish between positive and negative classes.

$$e(w) = (W \cdot \phi(w)) + a \quad (1)$$

$$Q_{TUN}(D) = d \frac{1}{M} \sum_{j=1}^M K_s(z_j, z_j^\Delta) + \frac{1}{2} X_s \cdot X \quad (2)$$

$$K_s(z_j, z_j^\Delta) = \begin{cases} |z_j - z_j^\Delta| - \varepsilon |z_j - z_j^\Delta|, & \geq \varepsilon \\ 0, & \text{Otherwise} \end{cases} \quad (3)$$

$$z^\Delta = e(w) = \sum_{j=1}^M (\alpha_j - \alpha_j^*) L(w_j, W) + a \quad (4)$$

$$L(w_j, W) = \exp\left(-\frac{1}{\delta^2} (w_j - w_i)^2\right) \quad (5)$$

Where,

$(\phi(w))$ = Nonlinear High Dimension Feature Space, W - Space of the input, w - flexible method and a - Threshold, D - positive real constant, $\alpha_j - \alpha_j^*$ = Lagrange multipliers, $L(w_j, W)$ defines the Gaussian kernel, δ^2 = width of the kernel function.

3.3. EHO

EHO (Elephant Herding Optimization) has not been widely applied specifically for heart disease prediction. EHO can, however, be used as an optimization approach in conjunction with machine learning methods for heart disease prediction applications. In such a case, EHO could be utilized to improve the parameters or feature selection process of a machine learning model for heart disease prediction. EHO can aid in identifying the ideal set of characteristics or fine-tuning a predictive model's hyperparameters, potentially enhancing the system's performance and accuracy in predicting heart disease. In order to implement EHO specifically for heart disease prediction, the problem must be formulated, the fitness function must be defined, and the parameters that must be optimized must be identified. The search space would then be explored using EHO, leading to optimal or nearly optimal solutions for heart disease prediction. It is crucial to remember that the success of using EHO to predict heart disease will depend on a number of variables, including the caliber and relevance of the dataset, how the problem is formulated, and how carefully the EHO algorithm is designed and integrated into the machine learning model. Assessing the precision and dependability of the heart disease predictions would also require a thorough validation and performance evaluation of the predictive model.

3.4. AEHO

Improvements to the original Elephant Herding Optimisation (EHO) algorithm are included in the proposed improved EHO algorithm. A fresh elephant is initialised next to the clan's worst member or leader. This substitution helps to preserve population diversity and keeps the algorithm from becoming stuck on less-than-ideal solutions. This approach ensures that promising answers are not destroyed and helps the algorithm's overall performance by maintaining the best solutions thus far.

3.4.1. Modified separation operator

To encourage population diversity and prevent local optima, the worst elephant of each clan is substituted in the traditional EHO algorithm with a randomly initialised individual. This tactic, meanwhile, is unguided and might steer the algorithm in the incorrect direction. The worst elephant of clans is replaced by a new strategy in the suggested algorithm. A new person is initialised next to the clan head or the clan's worst elephant instead of at random. It is possible to explore uncharted territory and potentially improve on current methods of problem-solving thanks to this well planned population diversity. The suggested approach calculates the separation operator by performing an equation evaluation. Sadly, the offered material does not provide any details about the equation itself. To determine the separation or distance between various people or clusters inside the algorithm, the separating operator is most likely to play a part. The suggested approach intends to enhance the search process, boost exploration of the solution space, and maybe uncover better solutions for the optimisation problem at hand. It does this by adding guided population diversification and a suitable separation operator.

4. Result and Analysis

The AEHO-SVM approach optimizes the hyperplane separation and iteratively modifies the support vectors in order to increase classification accuracy while decreasing the likelihood of misdiagnosis. Performance of the model is evaluated using a variety of metrics, including sensitivity, accuracy, f-measure, and specificity. The results of the trial demonstrate that the AEHO-SVM technique achieves good prediction accuracy, sensitivity, f-measures for the diagnosis of heart disease and performs better than traditional methods like naive blaise (NB), deep neural network (DNN), logistic regression (LR).

Sensitivity, sometimes referred to as true positive rate or recall, is a metric used to evaluate how well a diagnostic test or predictive model is working, the formula for the sensitivity as shown in equation (6). It measures the percentage of real positive cases that the model or test successfully detected. A high sensitivity score means that the model is successful in identifying people with cardiovascular illness and denotes a low occurrence of false negatives. It reveals that our suggested method, AEHO-SVM has better than existing work NB (82.17), DNN (85.25), LR (90.75) in prediction of the heart disease (95.17%).

$$Sensitivity = TP / (TP + FN) \quad (6)$$

We build the FM assessment system from the viewpoints of the external environment and decision-making in order to create an accurate evaluation of FM, as illustrated in Figure 1. There are specific connected components in managerial decision-making, evaluation of the external environment, and corporate governance structure.

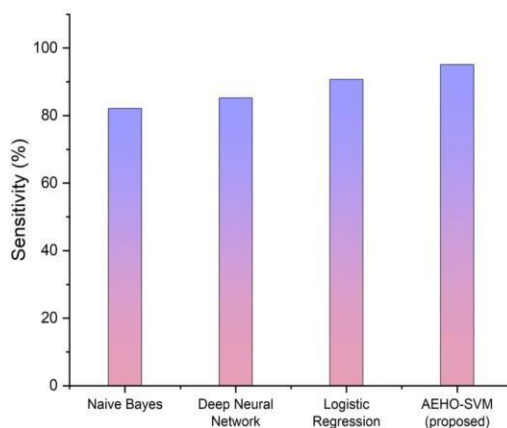


Figure 1 Sensitivity.

To calculate the percentage of all data points that were successfully anticipated, accuracy is used. It is derived by dividing the overall number of outcomes that were successfully predicted by the overall number of forecasts.

$$Accuracy = (TP + TN) / (TP + TN + FP + FN) \quad (7)$$

The accuracy result is analyzed using Equation (7). The accuracy results are shown in Figure 2. It reveals that our suggested method, AEHO-SVM has greater accuracy (98.85%) than traditional techniques NB (88.75), DNN (89.90), LR (94.75).

As the harmonic mean of memory and specificity, the F1 measure is described. The harmonic mean is an alternate metric to the more often used arithmetic mean, in case you forgot. Calculating an average rate often makes use of it. By using the equation (8), we have analyzed the result of the F1-measure. Figure 3 shows that when compared to the currently



in use approaches, NB, DNN, and LR, our recommended methodology (AEHO-SVM) performance measure (93.25%) is better and more effective. Than existing approach NB (83.25 %), DNN (85.75 %), LR (88.90 %).

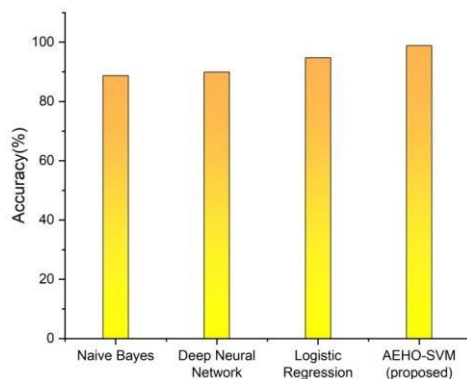


Figure 2 Accuracy.

$$F1 \text{ measure} = 2 * (\text{specificity} * \text{sensitivity}) / (\text{specificity} + \text{sensitivity}) \quad (8)$$

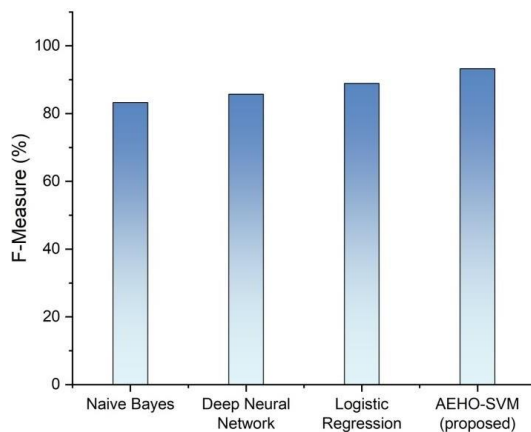


Figure 3 F-measure.

$$\text{specificity} = TP / (TP + FP) \quad (9)$$

By using equation (9), we have analyzed the result of the specificity. This metric is primarily used to indicate the reliability of the positive samples. Figure 4 depicts the specificity result. This demonstrates that our suggested technique, AEHO-SVM has a better performance (95.50%) than existing work including naive bayes (85.75 %), Deep neural network (87.15%), logistics regression (89.90%).

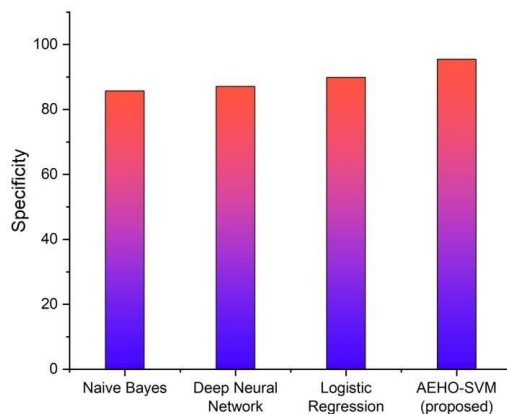


Figure 4 Specificity.



5. Conclusions

A dataset on heart disease is used to test the AEHO-SVM method after it has been pre-processed to manage missing values, normalise the data, and reduce dimensionality. By optimising hyperplane separation and iteratively changing support vectors, the method seeks to maximise classification accuracy while reducing the chance of misdiagnosis. The AEHO-SVM model's performance was assessed using a number of metrics, including f-measure, sensitivity, accuracy, and specificity. These metrics allow for an evaluation of the model's performance in terms of its capacity to categorize instances accurately, overall accuracy, capability to recognize genuine negatives, and harmony between precision and recall. The experimental findings show that the AEHO-SVM technique performs better than traditional approaches and achieves a high level of prediction accuracy in order to identify heart illness. A suggested AEHO-SVM method uses elephant herding's collective intelligence and its built-in optimisation capabilities to offer a more accurate and dependable prediction strategy. The AEHO-SVM technology presents a promising approach for precise cardiac disease prediction by integrating the advantages of both the AEHO algorithm and support vector machines.

Ethical considerations

Not applicable.

Declaration of interest

The authors declare no conflicts of interest.

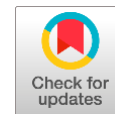
Funding

This research did not receive any financial support.

Reference

- Ali SM, Kumaran N, Balaji GN (2022) A hybrid elephant herding optimization and harmony search algorithm for potential load balancing in cloud environments. *International Journal of Modeling, Simulation, and Scientific Computing* 13:2250042.
- Amin MS, Chiam YK, Varathan KD (2019) Identification of significant features and data mining techniques in predicting heart disease. *Telematics and Informatics* 36:82-93.
- Ayon SI, Islam MM, Hossain MR (2022) Coronary artery heart disease prediction: a comparative study of computational intelligence techniques. *IETE Journal of Research* 68:2488-2507.
- Bashir S, Khan ZS, Khan FH, Anjum A, Bashir K (2019) Improving heart disease prediction using feature selection approaches. In 2019 16th international bhurban conference on applied sciences and technology (IBCAST), pp 619-623. IEEE.
- Budholiya K, Shrivastava SK, Sharma V (2022) An optimized XGBoost based diagnostic system for effective prediction of heart disease. *Journal of King Saud University-Computer and Information Sciences* 34:4514-4523.
- Fitriyani NL, Syafrudin M, Alfian G, Rhee J (2020) HDPm: an effective heart disease prediction model for a clinical decision support system. *IEEE Access* 8:133034-133050.
- KAMAL MA, IBRAHIM LM, AL-ALUSI AA (2020) Dolphin and elephant herding optimization swarm intelligence algorithms used to detect neris botnet. *Journal of Engineering Science and Technology* 15:2906-2923.
- Khan MA (2020) An IoT framework for heart disease prediction based on MDCNN classifier. *IEEE Access* 8:34717-34727.
- Mienye ID, Sun Y, Wang Z (2020) An improved ensemble learning approach for the prediction of heart disease risk. *Informatics in Medicine Unlocked* 20:100402.
- Monga P, Sharma M, Sharma SK (2022) A comprehensive meta-analysis of emerging swarm intelligent computing techniques and their research trend. *Journal of King Saud University-Computer and Information Sciences* 34:9622-9643.
- Repaka AN, Ravikanti SD, Franklin RG (2019) Design and implementing heart disease prediction using naives Bayesian. In 2019 3rd International conference on trends in electronics and informatics (ICOEI), pp 292-297. IEEE.
- Shah D, Patel S, Bharti SK (2020) Heart disease prediction using machine learning techniques. *SN Computer Science* 1:1-6.
- Singh A, Kumar R (2020) Heart disease prediction using machine learning algorithms. In 2020 international conference on electrical and electronics engineering (ICE3), pp 452-457. IEEE.
- Spencer R, Thabtah F, Abdelhamid N, Thompson M (2020) Exploring feature selection and classification methods for predicting heart disease. *Digital health* 6:2055207620914777.
- Subhadra K, Vikas B (2019) Neural network based intelligent system for predicting heart disease. *International Journal of Innovative Technology and Exploring Engineering* 8:484-487.

A significant review on the performance of microbial concrete in compartment of diverse nutrients



Gouthami Patnaik Palter^a   | Misbah Syeda^a  | Kanaka Durga Sambhana^a  |
Potharaju Malasani^b  | Venkata Giridhar Poosarla^c 

^aDept. of Civil Engineering, GITAM School of Technology, GITAM (Deemed to be University), Visakhapatnam, Andhra Pradesh, 530045, India.

^bApollo University, Chittoor, Andhra Pradesh, 517127, India.

^cDept. of Microbiology and FST (Food Science & Technology), GITAM School of Technology, GITAM (Deemed to be University), Visakhapatnam, Andhra Pradesh, 530045, India.

Abstract Concrete is substantially a prerequisite material being used but as the year's pass, the concrete structures due to external load application might be subjected to the inevitable crack formation that can degrade their durability and strength. The addition of bacteria and the supplementary calcium source creates a pervious layer over concrete fissures similar to calcite precipitation in sealing pores and micro-cracks in the concrete. This review exemplifies the usage of several species of calcite-precipitating, alkali-resistant *Bacillus* bacteria as crack healing agents and nutrients added for bacteria sustainability in the concrete and mortar at diverse age periods. Various strategies have been proposed to endow self-healing in concrete in past decades. This review summarizes the effect of micro-capsules, hydrogels, cellulose fiber, polymers, mineral admixtures and bacteria type when employed in cementitious materials. This study exuviates light on the advantages of bio minerals produced via bacteria metabolism that improves mechanical properties, durability parameters and microstructure behaviour. It can be summarized that the inclusion of bacteria in concrete and mortar improves its properties resulting in crack healing, making it more sustainable and reducing maintenance cost. Furthermore, research can be a promising investigation into the longevity of the bacteria for its extensive practical outcome-based application.

Keywords: bio-mineralization, self-healing concrete, microbial CaCO_3 , strength properties, microstructure analysis

1. Introduction

Concrete is an inherent construction material used in most infrastructures worldwide at a large scale. A structure's service life is typically 50 years; however, it can be increased to 100 years in intricate structures. In this regard, materials performance in durability aspects needs to ensure their realistic alimony (Roig-Flores et al 2021). Despite its benefits, it is sometimes prone to cracking because of shrinking, thermal stress, chemical reactions, incessant overload, and external load in the hardened state and causes detrimental effects on the life span of the structures in the long term. When exposed to water, CO_2 , and chemicals from the environment, crack formation reduces the structure's lifetime and strength and impairs the reinforcement (Prasad and Lakshmi 2018). It is crucial to cease the cracks in the advanced stage. Various crack repair techniques have been developed, but they were expended at the high cost and life span of the structures anticipated to be around 15 years and hazardous to the human environment (De Belie and Wang 2016; Van Breugel 2007). Cracks can be treated in two-way classification passive and active methods (Seifan et al 2016). In the former case, surface cracks can be healed by providing external coatings either by injecting or spraying but due to poor resistance to heat, sensitivity to moisture, differential coefficient of thermal expansion, and it is limited (De Muynek et al 2008a; Qian et al 2015; Wang et al 2012a). The latter method, regardless of crack position, can be treated with the aid of a technique termed a self-healing approach for a cement-based matrix, as shown in (Figure 1). In an autogenous process, concrete itself can self-heal crack after several weeks and months for a maximum closure of crack width up to 150 μm , as seen in (Figure 2), calcium carbonate is generated when unhydrated cement particles are hydrated in the presence of moisture seen in the (Eq. (1), (2)) (Hearn 1998). However, these micro-cracks do not influence the strength of the structure but will impart to material porosity and permeability (Jonkers et al 2010). The autogenous healing process can be ameliorated by bringing down the water/cement (w/c) ratio, but simultaneously cement content comes into demand, reflecting on the workability and shrinkage properties (Seifan et al 2016). The maximum crack healing was reported to be 0.30 mm during one year and about 0.45 mm when immersed in CO_2 water for 90 days (Suleiman and Nehdi 2018; Yıldırım et al 2018). Additionally, reinforcing bars implanted in

concrete can slow the rate of fracture propagation but cannot prevent crack initiation, which has an adverse effect on the structure's lifespan and maintenance costs (Seifan 2018).

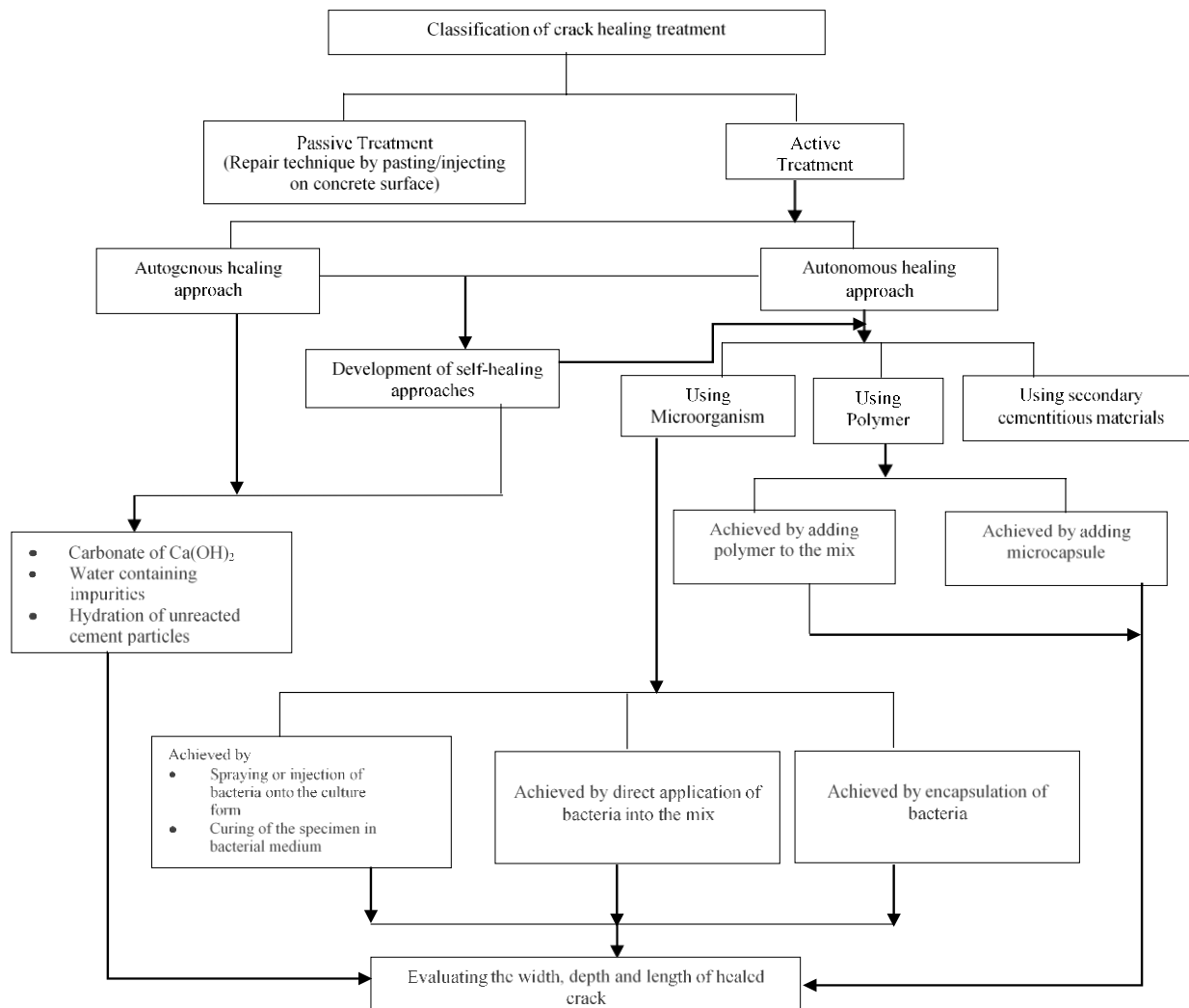
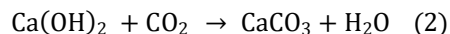
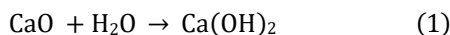


Figure 1 Hierarchy of self-healing strategies for cementitious based material (Muhammad et al 2016).

Hence, the autogenous healing method is a naturally occurring process. It is intractable to anticipate or rely on as they depend heavily on environmental conditions and occur only in water. To surmount the above drawbacks, the invention of an autonomous healing mechanism came into existence. In this system, methods comprising expansive agents, encapsulation, and bacteria (microorganism) have been pioneered by several researchers (Qian et al 2009). Various self-healing (autonomous) approaches have been adopted, that could spring up the encapsulation method by carrying out the self-healing mechanism using polymeric materials (Kessler et al 2003; Muhammad et al 2016; White et al 2001). The micro- or macro-encapsulated polymers/minerals, bacteria-based system, and other designed agents are to be combined directly with the cement matrix or implanted in an encapsulation system throughout the autonomous healing process (Han and Xing 2017). This mechanism can heal the crack of about 300 μm, or even up to 1 mm at a faster time span minimum of 1 day up to 4 weeks. A cementitious composite specimen cement: slag: sand) (1:0.67:0.67) using urea-formaldehyde/epoxy resin microcapsule was designed (Dong et al 2013). In this, different particle sizes of microcapsule were considered (132μm, 180μm, and 230μm), and for recovery of strength at 60 % pre-loading, maximum self-healing efficiency ascends to 6.11, 9.63, and 10.23 %, respectively. A major concern was the semi-permanent stability when encapsulated polymers are used as the shell has inescapable permeability. Delay in hydration reaction can also depict a significant crack healing property when there is presence of high binder mixtures but the limitation of the crack width is less than 0.2 mm (Li and Yang 2007). Additionally, higher the binder content more is the emissions of CO₂ (Wiktor and Jonkers 2011). To reduce all the issues mentioned earlier, currently, one mechanism is being considered: application of bacterial spores (encapsulated or not) or mineral additives.



Altogether, around 200 studies are being made using a bacteria-based system on the durability aspects but limited to a short-term period (De Belie et al 2019). Novel methods like biotechnology and nanotechnology are employed to improve concrete's durability and other qualities. With the aid of the biotechnology approach, microbially-induced calcite precipitation (MICP) produced due to the addition of bio-cultures (bacteria) became an assuring path to encounter the consequences pertinent to passive and active treatments (Zhang et al 2023). In this mechanism, cracks with efficient self-healing by mineral-precipitation was observed by spraying or applying the bacteria-based mixtures into the cracks (Bang et al 2001; De Muynck et al 2008a; De Muynck et al 2008b; Ramachandran et al 2001). This modality of repair cannot be asserted as truly self-healing hence, applying the microbes in the concrete matrix has overreached various other processes due to its benefits eco-friendly, durable and economical (Jonkers and Schlangen 2008; Jonkers 2007; Jonkers et al 2010; Vijay and Murmu 2020). This study was initiated on assessing the self-healing of minor damages in a human body. This led to the development of bio-cement or bio-influenced self-healing concrete, which serves as a practical healing agent to stop crack growth (Elkhateeb et al 2021). This review aims to describe the state-of-the-art mechanisms/strategies involved in producing MICP through bacteria metabolism. Also, it discusses the bacteria effect on concrete properties elaborately.

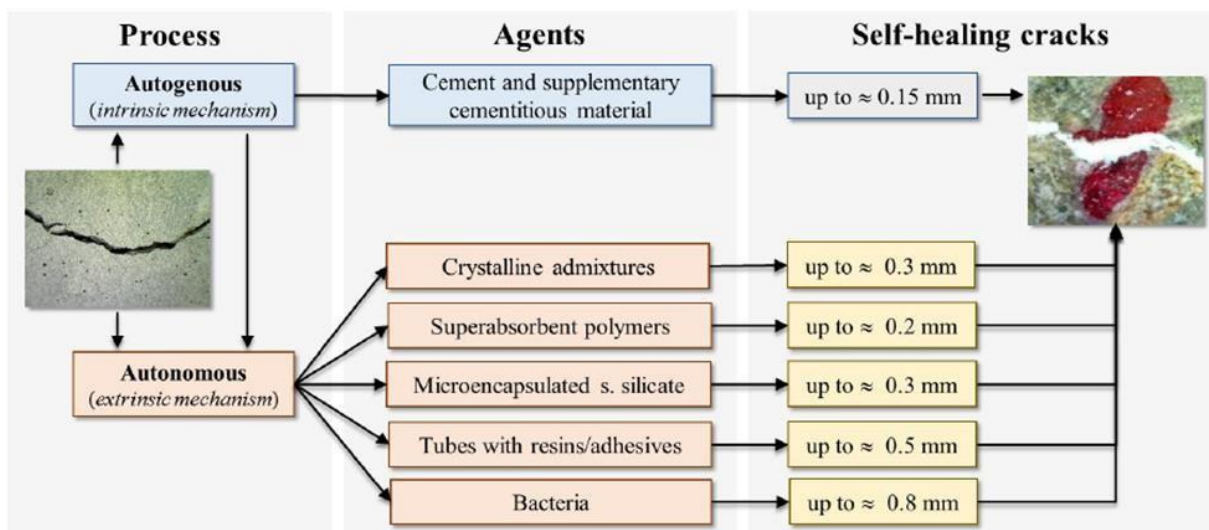


Figure 2 Self-healing concrete mechanisms and potential extent of healing of some of the most used self-healing system (Roig-Flores et al 2021).

2. Biological agents: Metabolic conversions of organic acid using bacterial and enzymatic ureolysis

Microscopically small, unicellular rod-shaped bacteria with a diameter of around 0.5 μm and a length of 1 μm are found in low-nutrient settings (Beveridge 1981). Hence, they have a larger surface to volume ratio; thereby larger contact area can be developed to perform interactions within the environmental surroundings (Ghosh et al 2009). Microorganisms, particularly bacteria, have a geochemical activity responsible for the deposition of minerals like carbonates, phosphates, oxides, sulphates, etc., to a great degree (Wang et al 2016). Inhomogeneous materials made of organic and inorganic compounds, such as carbonate, phosphate, oxalate, silica, iron, or sulphur-containing minerals, with non-uniform distributions are created through the process of biomineralization by reflecting the environment (Skinner and Jahren 2003). It has been discovered to be the most promising method, also known as self-healing concrete or bio concrete (Seifan et al 2016). This includes incorporating a unique self-healing mechanism into the concrete in which bacteria aids in mineral production swiftly closes newly created cracks, reducing concrete permeability, improving durability, and preserving embedded steel reinforcement from corrosion (Bashir et al 2016). The influence of microorganisms in mortar or concrete has become immense potential in research. This naturally occurring, pollution-free mineral precipitation created by the bacterial metabolism is highly sought-after (Ramakrishnan 2007). Mineralization is the result of the ongoing metabolic activity of microbes and reaction with their generated metabolic products with an adjoining environment (Afifudin et al 2011). The underpinning metabolic theory of bacterial crack healing is that the bacteria themselves work largely as a catalyst, converting a precursor component into suitable filler material. This compound now serves as a bio-cement and healing the crack. With various metabolic routes, several microorganisms can obstruct the synthesis of calcium carbonate, as seen in (Table 1), such as photosynthesis, sulphates reduction, urea hydrolysis or denitrification, and for these pathways to start, bacteria need nutrients. The process in which the self-healing mechanism develops in the concrete by MICP is the bacterial respiration process to produce CO_2 or urea hydrolysis by ureolytic bacteria or reduction of nitrates (Roig-Flores et al 2021; Soysal et al 2020). In the first mechanism, bacteria convert the precursor by acting as a catalyst to calcium carbonate, a hard filler material. These materials are formed as seen in (Eq. (3)) and seal the formed cracks (Rajczakowska 2019).

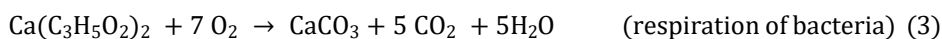


Table 1 Different metabolic pathways of bacterial calcium carbonate precipitation (De Belie and Wang 2016).

Autotrophic bacteria		Heterotrophic bacteria			
Non-Methylotrophic methanogenesis	Assimilatory pathways	Dissimilatory pathways			
	Urea decomposition	Oxidation of organic carbon			
An oxygenic photosynthesis		Aerobic Process	e-acceptor	Anaerobic Process	e-acceptor
oxygenic photosynthesis	Ammonification of amino acids	Respiration	O ₂	NO _x reduction	NO ₃ ⁻ /NO ₂ ⁻
		Methane oxidation	CH ₄ /O ₂	Sulfate reduction	SO ₄ ²⁻

Carbon dioxide and calcium hydroxide react to produce calcium carbonate, which is more in quantity in this process when compared to autogenous healing techniques. This process of oxidation of organic salt compounds under aerobic conditions leads to carbon dioxide production, further producing calcium carbonate in an alkaline environment (Sierra-Beltran et al 2014; Wiktor and Jonkers 2011). In the second mechanism, micro-organisms give urease enzyme during the microbial urease movement, which catalyzes urea to ammonium and carbonates NH₄⁺ and HCO₃⁻ (Murari and Kaur 2021; Vijay and Murmu 2020). One mole of urea is hydrolyzed intracranial to a mole of NH₃ and carbonate each. The constitution of NH₃ mol and H₂CO₃ mol takes place through impulsive hydrolysis of carbamate as seen in (Eq. (4), (5)). These substances also generate bimolecular ammonium and hydroxide ions, as well as unimolecular bicarbonate ions, as seen in (Eq. (6), (7)). Bicarbonate equilibrium gets shifted as a rise in pH leads to the formation of carbonate ions (Eq. (8)). Once the supersaturation level is attained in the presence of calcium ions, calcium carbonate precipitation is formed, as seen in (Eq. (9)). A schematic diagram for the structure of the bacteria and precipitation of calcium carbonate are shown in (Figure 3). Microbial cell walls are negatively charged, and it attracts positively charged ions of the environment such as Ca²⁺, facilitating the mineral precipitation. This could be understood from (Eq. (10), (11)) (Seifan et al 2016). Hence, the second mechanism is not suitable as it releases excess ammonium, which is detrimental to the concrete environment through the leaching action of calcium hydroxide analogous to acid attack (Singh and Gupta 2020; Soysal et al 2020). In the third mechanism, bacteria respire nitrogen instead of oxygen. During this denitrification, there will be a metabolic conversion of the organic salts, thereby producing carbonates that will produce calcium carbonate upon reaction with calcium ions.

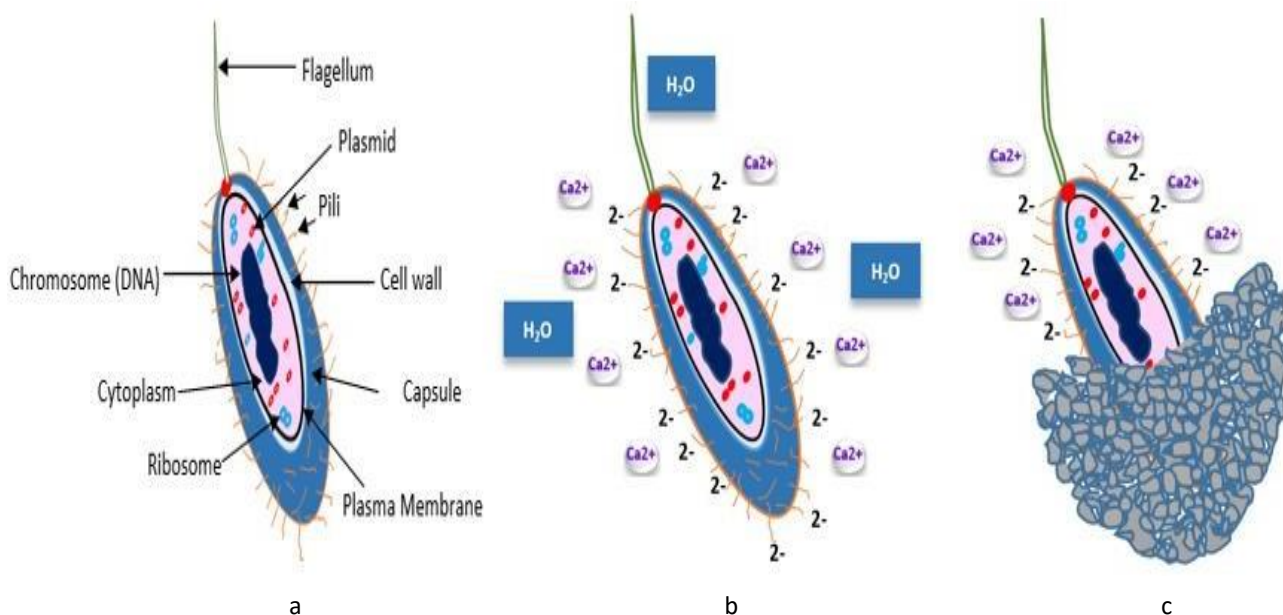
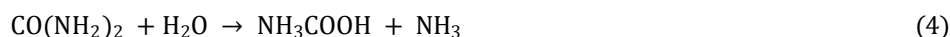
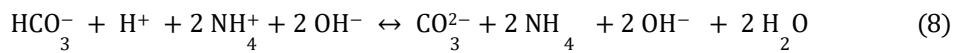


Figure 3 Formation of calcium carbonate on bacteria cell wall (a) Structure of bacteria (b) Presence of positive charged ions and negative charged cell wall (c) Binding ions to cell wall leading to bio mineral production (Seifan et al 2016; Vijay and Murmu 2020).





3. Enforcement of the bacteria in different self-healing approaches and nutrient types

Various alkali-resisting spore-forming bacteria are useful for self-healing: *Bacillus pasteurii*, *Bacillus subtilis*, *Sporosarcina pasteurii*, *Enterococcus faecalis*, *Bacillus sphaericus*, *Bacillus cereus*, *Bacillus lentus*, *Bacillus megaterium* (El Enshasy et al 2020). An intrinsic bio-culture (bacteria) material acting as a self-healing agent is applied into the cement matrix to circumvent the cracks (Vijay and Murmu 2020; Zawad et al 2021). Cracks in concrete can be healed in three primary ways. The first is autogenous healing, and the second is polymeric encapsulation (Van Tittelboom and De Belie 2013). The third is being microbial production of calcium carbonate by biomineralization. MICP develops an environment that produces mineral calcium carbonate at a specified pH, ion concentration, and nucleation site (Hoffmann et al 2021). In an autonomous self-healing process, incorporation of the bacteria can be done in two techniques, as mentioned above, direct and encapsulation. Either of these methods envisages the capability of self-healing performance and the specimen's compressive strength. In the direct method, either the bacteria spores instead of living cells or bacterial solution will be added into the concrete and mortar during mixing along with the bacteria, organic mineral precursors or the carriers are incorporated to enhance the efficiency of self-healing property and also the bacterial survival (Tang and Xu 2021). Adopting spores directly into the mixture can resist the mechanical and chemical stresses induced, but the longevity and survival of spores are highly concerned, especially in an abrasive environment, as they will be crushed to death at an increasing age of concrete. To devoid this, bacteria must be protected to remain viable in the concrete or mortar, and this can be done by immobilizing the spores, nutrients, calcium-based sources, either organic or inorganic carriers like lightweight aggregates (LWA), expanded clay (EC), expanded perlite (EP), diatomaceous earth (DE), graphite nanoplatelets (GNA), glycerol (GL), metakaolin, granular activated carbon, zeolite. In the latter method, impregnation of carriers in bacteria solution and then encapsulating a polymer-based coating layer will be done (Erşan et al 2015a). In this microencapsulation process, bacteria spores are immobilized with silica gel, polyurethane (PU), polymeric membrane, microcapsules, hydrogel, and then to provide better protection to the bacteria, as shown in (Figure 4) and they are encapsulated in a glass tube (Bundur et al 2017; Khaliq and Ehsan 2016). Based on thermogravimetric analysis (TGA), when concrete is embedded with bacteria encapsulated with silica gel produces more amount of CaCO_3 precipitation compared to PU (Wang et al 2012b). But most of these encapsulated materials were highly-priced excepting DE, EC (Silva et al 2015; Wang et al 2012a). It has been determined to what extent self-healing concrete contains organic precursors calcium lactate and calcium glutamate and non-ureolytic bacteria (Xu and Yao 2014). When Bacterial spores were applied directly to the cement matrix, the viable duration lasted up to 4 months, but as the crack closure potential increased, its application reached out to be anticipated (Jonkers et al 2010). Under concealed marine and tidal environmental circumstances, the activity of the bio-concrete made with *Halobacillus halophilus* bacteria and carriers such as calcium lactate and EP was examined (Khan et al 2021). The proposed bio-mineral CaCO_3 is more congenial with the concrete matrix and eco-friendly compared with expanded additives and polymer healing agents (Wang et al 2012b). *Bacillus subtilis*, *B. sphaericus*, *B. pasteurii*, *B. cohnii*, and *B. megaterium* are among the *Bacillus* bacteria that can withstand extremely alkaline conditions. *Diaphorobacter nitroreducens* and *B. pseudofirmus* are the candidates mostly used for the metabolic conversion of organic acids and denitrification (Erşan et al 2015b; Jonkers et al 2010). The nutrients added to concrete before mixing are calcium-based sources to ensure the alkaline condition. Most of the studies adopted calcium lactate and nitrate, and apart from the two mentioned, calcium acetate, calcium chloride, and calcium formate are also used (Kevin Paine 2016). The nutrients like urea and yeast extract (YE) also assist in spore germination when added to the concrete mix and offer a source for developing bacterial cells, significantly influencing the self-healing efficiency and concrete characteristics (Rajczakowska 2019). Water penetrates through cracks in concrete buildings and activates bacterium spores, which subsequently feed on minerals like calcium lactate. Insoluble limestone is the transformed form of the soluble calcium lactate being produced due to the oxygen deficit (Prasad and Lakshmi 2018). This limestone hardens over time, filling up the fractures in the damaged surface. Calcium chloride was not found to be optimal due to chloride, but calcium lactate was seen to produce more calcium ions, thus increasing the strength of concrete (Rajczakowska 2019). Due to the abrasive environmental conditions in cement matrix, there is a negative stimulus towards the bacterial survival. The competent way to conserve the microbial activity of bacteria is to protect it (Tang and Xu 2021). Some self-healing bacteria can tolerate extreme conditions and survive up to 200 years in concrete under a dormant state (Jonkers 2007).

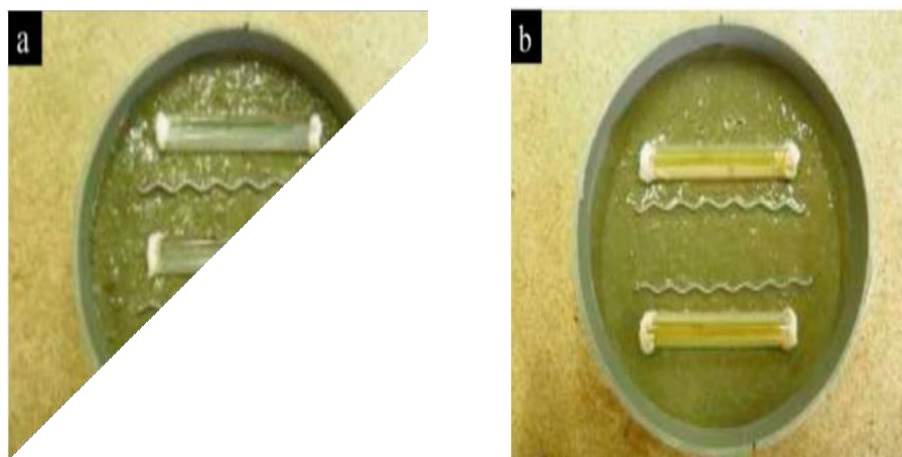


Figure 4 Bacteria spore immobilized with a) silica gel b) PU and encapsulated in glass tube (Tang and Xu 2021).

4. Overview of the subsisting research on the effect of bacteria on properties and performance of concrete

Immobilization of bacteria, either intrinsic or extrinsic, would lead to the precipitation of calcium carbonate. Though it is a prolonged process in the presence of high pH value of surrounding cement matrix, once it indurates to the alkali environment, it tries to develop cell growth. When bacteria cells receive sufficient nutrients and oxygen, they get activated, thereby plugging the pores, leading to lesser porosity and permeability in concrete or cement mortar. Later, the spores will retrieve to the dormant state or form endospores when all the pores in the matrix are filled. This microbially induced self-healing mechanism influences the healing capacity of the concrete and triggers the mechanical properties and the performance of the bio concrete (Khaudiyal et al 2022). In order to protect the bacterial spores from crushing or shearing, protective carriers must be induced to ensure the viability of the microbes in the concrete (Tang and Xu 2021). Compressive strength is the most widely tested parameter. Indirect tensile tests were also studied, i.e., flexure and split tensile. The significant durability aspects covered are the rapid chloride permeability test (RCPT) and water absorption. SEM images were analyzed by many researchers apart from X-Ray diffraction (XRD).

5. Effect of biocementation on concrete properties, durability parameters

Optimization of bio concrete properties for M30 grade concrete by the response of calcium lactate (CL) content (0.22–2.18 g/L) using response surface methodology (RSM) was investigated (Abo Sabah et al 2021). In this study, *B. sphaericus* was isolated from fresh urine and was sub-cultured. With an increase in CL and age of curing period, compressive strength, split tensile strength, and flexural strength increased proportionally. On the 28th day, specimen denoting 2.18 *B. sphaericus* the compressive, split and flexural strength increments were 13.4, 18.5 and 2.2%, respectively. At 23.4 days of curing period and CL content (2.18 g/L), the operating parameters for improving the compressive, split and flexural strength were 43.51 vs 43.43 MPa, 3.19 vs 3.19 MPa, 6.93 vs 5.50 respectively, and water absorption was 7.55 vs 7.55 mm. Cement mortar cubes specimens (50.8 x 50.8 x 50.8 mm) were prepared, one being control and the other containing biomass *B. pasteurii*, *Pseudomonas aeruginosa* (live or dead) suspended in (saline, phosphate solution) with different concentrations of 7.6×10^3 , 7.6×10^5 , 7.6×10^7 cells/cm³ (Ramachandran et al 2001). Compressive strength of mortar cubes in phosphate solution at different cell concentrations gave higher strengths at 28 days than cubes in saline condition and control. Live cell forms showed enhanced strength of 65% compared to lower concentrations. *Sporosarcina pasteurii* PTCC 1645 bacterial concentration of 10^7 cells/mL was used to prepare a concrete mix of M25 grade (Parastegari et al 2019). Three curing mediums were considered, freshwater, urea-calcium lactate, and seawater. Specimens cured in urea-calcium lactate solution possess better performance than the rest two. The addition of bacteria to mixing water at 5% air-entrained concrete (AEC) resulted in 25% of electrical resistivity, and the chloride ion penetration has reduced to 28% by the addition of bacteria with nutrients in water mixing concrete. *B. sphaericus* LMG of 10^7 cells/mL was used in the mortar specimens with varying w/c ratios 0.5, 0.7. Because the specimen is porous, the development of calcium carbonate crystals on the surface reduced the water absorption by 65–90%. The carbonation rate and resistance to chloride penetration decreased to around 25–30% and 10–40%, respectively (De Muynck et al 2008b). The study also denoted that bio deposition of calcite was in line with the surface treatment. It was recommended to further research on the surface treatment method in distinct environmental conditions. *B. Subtilis* JC3 suspension (10^8 cells/mL) was procured and sample concentrations of 10^3 , 10^4 , 10^5 , and 10^6 cells/mL had been derived (Meera and Subha 2016). A concrete mix of M20 grade cube specimens (150 X 150 X 150 mm) was prepared. The substantial increment was observed at 42% and 63% in compressive and tensile strength, respectively, at 28 days for 10^5 cells/mL concentration. Water absorption and percentage weight loss due to acid and chloride attack after 90

days contributed to diminishing growth of 17, 44, and 58%, respectively, for the same concentration. The effect of bacterium *S. pasteurii* in fly ash (FA) concrete (M20 grade) as a replacement in cement at 10, 20, and 30% for cell concentrations of 0, 10^3 , 10^5 , and 10^7 cells/mL was investigated (Chahal et al 2012a). Compressive strength has increased to 22% for 0% FA, and there was a reduction in water absorption about four times, i.e., 26% for 10% FA and chloride penetration has shown charge reduction to 762 C (in coulomb) for 10% FA at 28 days at an optimum concentration of 10^5 cells/mL. A study showed that aerobic *S. pasteurii* with an optical density (OD) (0.5, 1.0, and 1.5) was incorporated into the cement mortar (CM), and there was an escalation of compressive strength of 33% for CM specimens with 1 OD than 1.5 OD and control specimens at 28 days of curing (Abo-El-Enein et al 2013). Water absorption at all concentrations of OD resulted in lesser values. The relative water permeability of the reference concrete specimens at an age period of 56 days before and after 28 days of healing time was 82.2%, and for spore and microbial groups, it was 71.8 and 4.23%, respectively. The initial and final setting time of the microbial group (235 and 490 min) was the smallest due to calcium nitrate, which accelerates the hydration of cement. The compressive strength of the spore group has shown a consistent growth compared to the microbial group at 14 and 28 days due to a lack of the grain strength of the agents in line with the curing period (Zheng et al 2020). Table 2 provides summarized outcome on bacteria types, concentration and their effect on the properties of concrete. Two bacterial strains, namely, *B. pseudofirmus* and *D. nitroreducens* were considered, and calcium alginate hydrogel was encapsulated into the bacterial suspension at varying dosages (0, 0.5, 1.5, and 3.0 %) each along with (38 mm) polymers, calcium nitrate (2% by cement weight) and concrete beams were casted (Soysal et al 2020). Specimens with *B. pseudofirmus* of 0.5%, for *D. nitroreducens* of 0.5% yielded greater strength compared to rest similar to the control samples. Significantly, modulus of elasticity did not result in much variation for all dosages. Stiffness recovery was maximum depicted for the control specimen consisting 3% micro-capsule and DN 3.0% post being exposed to wet-dry cycles (in absence of bacteria).

6. Microstructure

Table 3 and Figure 5 presents major outcomes on self-healing effect by incorporating various types of bacteria, nutrients/ carriers. Mortar specimens containing *B. pasteurii* were suspended in a phosphate solution and cured in urea- CaCl_2 solution; the ratio of calcite to sand components was 0.3 (Ramachandran et al 2001).

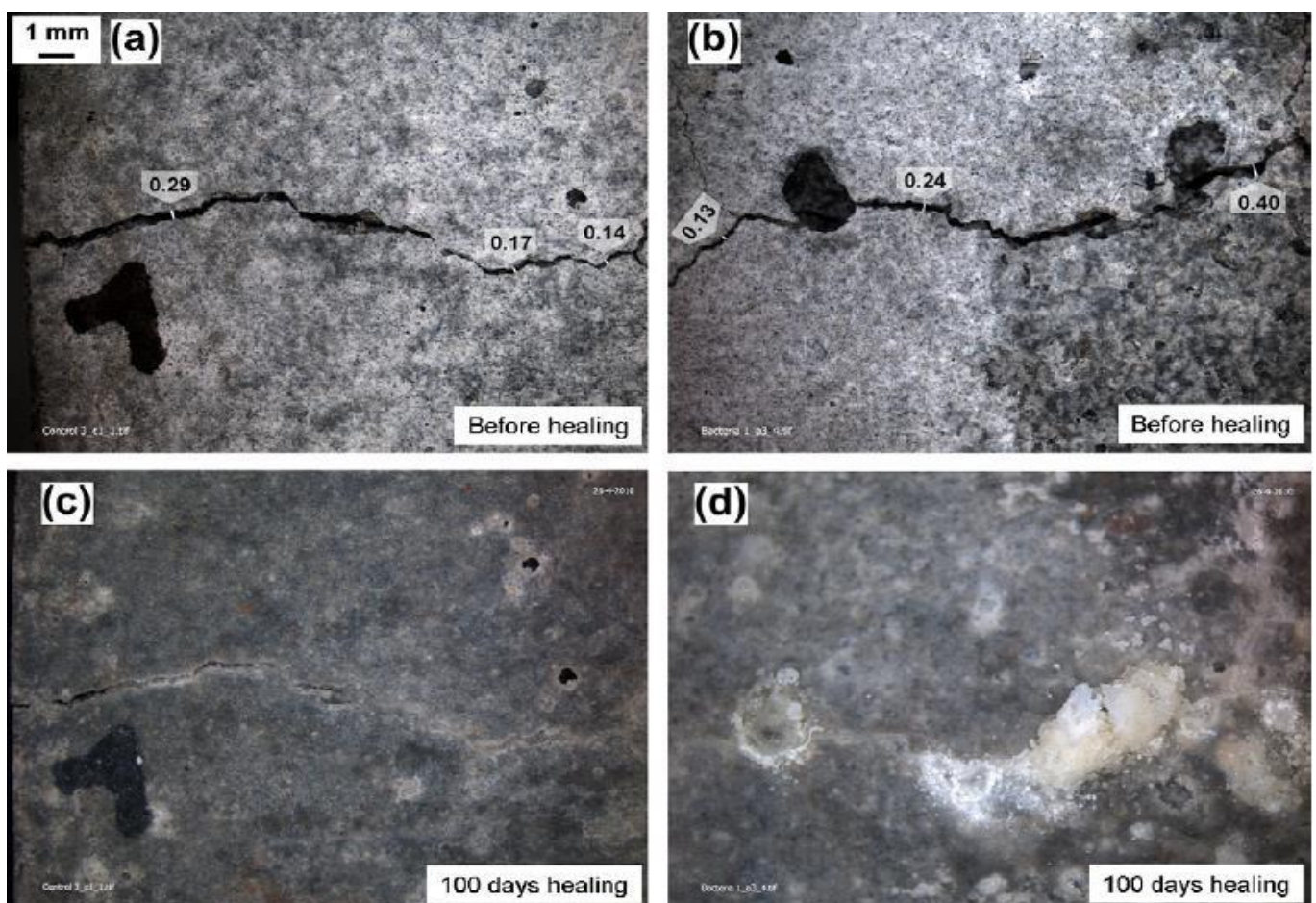


Figure 5 Stereomicroscopic images of crack-healing process in control mortar specimen before (a) and after 100 days healing (c), in bio-chemical agent-based specimen before (b) and after 100 days healing (d) (Wiktor and Jonkers 2011).

The SEM and Energy-dispersive X-ray analyzer (EDAX) presented morphology and size of calcite crystals for control and (CM) with an OD (0.5, 1.0, 1.5) specimens (Abo-El-Enein et al 2013). They ensued calcium carbonate (CC) precipitation of 0.5 OD as spherical calcite crystals smaller than 1.0 OD bacteria cells of rod-shaped crystals. 1.5 OD cells have displayed amorphous calcite and a small amount of spherical calcite crystals. Morphology characteristics were determined by using *Bacillus mucilaginosus* L3 which has vegetative cells (10^9 cells/mL), spores (1.0×10^{10} cfu/g) as shown in (Figure 6). Concrete cylindrical specimens of size 100 X 50 mm were prepared using sulfoaluminate cement (SC), water reducer, calcium nitrate, sand, water, and microbial self-healing agents. When subjected to a loading 0.1-0.2 kN/s under electrohydraulic pressure testing machine width of the cracks created, these specimens were observed to be around 0.3-0.5 mm. Different curing age periods of (7, 14, 28, and 56) days, the morphology and calcite precipitated at the mouth of the crack was analysed prior and later to 28 days of healing time using SEM, energy-dispersive spectrometer (EDS), and X-ray diffraction. The area repair ratio was below 10% for the reference group of all ages. As the spores are not viable unless they are protected, the precipitation gradually decreases in the spore group. The ratio has shown 93% at an age period of 7 and 14 days. Beyond 14 days, the spores are dead, and the ratio falls below 30%. In the microbial group, the precipitation was observed with the increase in age period, and the ratio was 90% throughout. *Lysinibacillus boronitolerans* YS11 optimum proliferation was arrived (1×10^8 cfu/mL) using the components at 1% of rice bran, malt, corn syrup, and ammonium sulfate each (Ryu et al 2020). The bacterial sporulation was investigated, and the highest observed with Fe^{2+} compared to Ca^{2+} , Mn^{2+} divalent cations have been chosen as the promoter. Initially, the width of the crack on average was observed to be 0.34 mm, after 28 days, in the case of control mortar cubes, a crack of 0.11 mm was healed, and for cubes with nutrients 0.15 mm. After 7 days itself, mortar cubes containing spore powder plus nutrient healed completely.

Table 2 Summarized outcomes on bacteria- its types, concentration and their effect on properties of concrete.

Bio-culture used	Bacterial cell concentration	Major studies on the impact of concrete properties/ microstructure	References
<i>Bacillus megaterium</i>	30×10^5 cfu/mL	Compressive strength improved by 24% for the highest grade (50 MPa) bacterial concrete. It was found that concrete was filled by the mineral calcite precipitation was 38.76% and had less porosity.	(Andalib et al 2016)
<i>Bacillus subtilis</i>	2.8×10^8 cells/mL	12% increase in compressive strength was found when incorporated along with LWA carrier in the concrete mix. Calcium carbonate formation is mainly due to bacteria and calcium lactate.	(Khaliq and Ehsan 2016)
<i>Bacillus subtilis</i> HU58	10^9 cfu/g	Compressive strength was increased to 14% when bacteria were incorporated with diatomite pellets.	(Huynh et al 2017)
<i>Bacillus pasteurii</i>	5×10^9 cells /mL	Compressive strength of 9.16% increment was found at 10SF20BC optimal mixing material ratio. 9.49% was found to be the highest calcium carbonate precipitate at same optimal mix.	(Metwally et al 2020)
Spore-forming alkali-resistant bacteria	10^9 cells/mL	The white crystals at the crack surface showed lamellar closed morphology.	(Luo et al 2015)
<i>Bacillus pasteurii</i>	-	Bacterial concrete casted using LWA, calcium lactate and cured in urea+ calcium acetate gave a large amount of precipitate at outer edges than at centre.	(Chen et al 2019)
<i>Bacillus Sp. BY1</i>	10^6 CFU/mL	Compressive strength increased by 9.5%, 9.9%, and 16.4% with addition of calcium formate, calcium acetate, and calcium lactate respectively. The crystals formed were rhombohedral, rugged structures usual shape of calcite formed in the presence of calcium formate or calcium lactate. Polymorph resulted in 95% calcite by weight for calcium formate, 78.61% by weight for calcium acetate, and 94.26% by weight for calcium lactate.	(Jeong et al 2019)
<i>Bacillus sphaericus</i>	-	Bacterial concrete with 20 mL solution and at 8% micronized biomass silica (MBS) gave 13.53% higher compressive strength, 15.46% low water absorption and 15.46% low water sorptivity.	(Priya et al 2019)
<i>S. pasteurii</i>	10^5 cells/mL	Concrete with 10% fly ash concrete gave minimum of 3.25% water absorption. Capacity of chloride ingress in fly ash concretes decreased with increase in bacterial concentration, maximum reduction in chloride ions was observed with 10^5 cells/mL for all 0, 10, 20, and 30% fly ash concretes. Compressive strength of fly ash concrete increased up to 10^5 cells/mL, and then there was reduction in the strength at 10^7 cells/mL cell concentration.	(Chahal et al 2012b)
<i>Bacillus subtilis</i>	10^7 cells/mL	Application of bacteria and steel fibers in the LWAC cured in a urea-calcium lactate environment was found to decrease its water absorption significantly by 13.1% and also gave the highest reduction in the chloride penetration by 20.5%	(Salmasi and Mostofinejad 2020)
<i>S. pasteurii</i> and <i>B. subtilis</i>	10^7 and 10^5 cells/mL	Decrease in water absorption of 19.5% in specimens containing silica fume and <i>S. pasteurii</i> in the mix and cured in the urea-calcium lactate solution compared to the specimens prepared without bacteria and cured in tap water. <i>S. pasteurii</i> had a greater effect than <i>B. subtilis</i> on the resistance against penetration when specimens cured in the urea-calcium chloride and urea-calcium lactate media.	(Tayebani and Mostofinejad 2019)

Table 3 Key literature portraying different micro-organisms (biomass) along with various nutrient/carriers and their self-healing function.

Method of application; mechanism of precipitation	Type of micro-organism	Nutrient	Carriers	Major Outcome	References
Immobilisation; Bacteria metabolic conversion of organic solid	<i>Bacillus alkalinitrilicus</i>	YE and calcium lactate	LWA, EC	After 100 th day of curing, crack closure in bacterial concrete was 0.46 mm and control was 0.18 mm (Figure 5)	(Wiktor and Jonkers 2011)
Direct; ureolytic activity	<i>Bacillus sp.</i> CT-5	Nutrient (NB), calcium chloride	broth Urea, calcium chloride	When stimulated a crack of maximum width 3mm and depth 27.2mm, on 28th day maximum depth of 27.2mm was filled	(Achal et al 2013)
Immobilization and passive; Bacteria metabolic activity	<i>Bacillus subtilis</i> M9	Beef extract, peptone, sodium carbonate, calcium lactate	Polyvinyl alcohol fibers (PVA)	With an aid of 3-point bend test 0.3 mm crack was created. Self-healing concrete was produced with flexural strength of 4.2 MPa. Yet to study the fiber pull out conduct.	(Feng et al 2021)
Direct and Immobilisation ; Bacteria metabolic conversion of organic solid	<i>Halobacillus halophilus</i>	Calcium lactate, calcium acetate, magnesium acetate	LWA, EP, GL	Calcium lactate was the optimum nutrient. Submerged freshwater (FW) FW control specimens showed overall healing of 37% after 90 days similar to specimens under marine water magnesium acetate (MW MA). Bacteria effectively increased healing from 33% in tidal condition with nutrients (TR NU) to 50% in TR BA specimens	(Khan et al 2021)
Direct; Bacteria metabolic activity	<i>Bacillus mucilaginosus</i>	Calcium nitrate, magnesium sulfate, potassium chloride, YE, ammonium sulfate	-	Direct addition of bacterial self-healing agents has enhanced the mineralization products by analysing zeta potential, electrical resistivity, SEM etc. Yet to carry out optimization of self-healing agent dosage.	(Su et al 2019)
Directly; ureolytic activity	<i>B. pasteurii</i> , <i>B. sphaericus</i> and <i>D. salina</i> alga	Calcium lactate powder, beef extract, peptone, magnesium sulfate, Urea	-	Control mix (CS) exhibited compressive strengths 18.32, 22.54, and 29 MPa respectively when cured under sea-water. At all ages alga has shown gain in strength value and corrosion rate. Specimens with either of the bacteria cells in pre-curing sea water exhibited good self-healing efficiency.	(Osman et al 2021)
Immobilization; Denitrification and ureolytic activity	<i>Bacillus sphaericus</i> , <i>Diaphorobacter nitroreducens</i>	Calcium nitrate, Calcium formate, Urea, YE	DE, EC, metakaolin, zeolite, granular activated carbon	Under denitrification, nutrients found out to be advantageous. Combination of encapsulated materials+ denitrifying pack showed better properties. Direct incorporation of bacteria spores or cells of <i>D. nitroreducens</i> led to decrease in compressive strength.	(Erşan et al 2015a)
Immobilization; Bacteria metabolic activity	<i>Bacillus subtilis</i> 168	Calcium lactate, peptone, NaCl, YE	Cellulose fiber	Cellulose fiber has depicted 12.04% betterment in self-healing on 14 th day of pre-cracked curing and on 28 th day it was 15.2% for threshold damage about 0.1-0.2. Further scope for higher degree of damage is suggested.	(Singh and Gupta 2020)
Microencapsulation process	<i>Bacillus sphaericus</i>	Calcium YE, urea	nitrate, Micro-capsule	Bio-microcapsule specimens have led to higher healing ratio of (48-80) % i.e., the maximum crack width healed was 970µm wider than non-bacteria specimens showing 250 µm. Treating the bacteria specimens under wet-dry cycle has been proven to be best incubation pathway.	(Wang et al 2014)
Encapsulation; Denitrification and metabolic conversion of organic acids	<i>Diaphorobacter nitroreducens</i> and <i>Bacillus pseudofirmus</i>	Calcium nitrate	Calcium alginate hydrogel beads, polymers	Higher the concentration of alginate beads more was the self-healing efficiency. For control 3% micro-capsule, DN 0.5% and DN 3.0% maximum crack width was healed about (80 µm and 90 µm respectively).	(Soysal et al 2020)
Encapsulation; Urea hydrolysis	<i>Lysinibacillus sphaericus</i>	Calcium, nutrient	urea (stored in capsule)	A numerical model developed to predict the evolution of calcite. Finite element method (FEM) was adopted to solve the differential equations. After 70 days, crack width of 0.4 mm was healed whilst predicted healing of crack at the time of 42 days was reaching to 58%.	(Algaifi et al 2018)

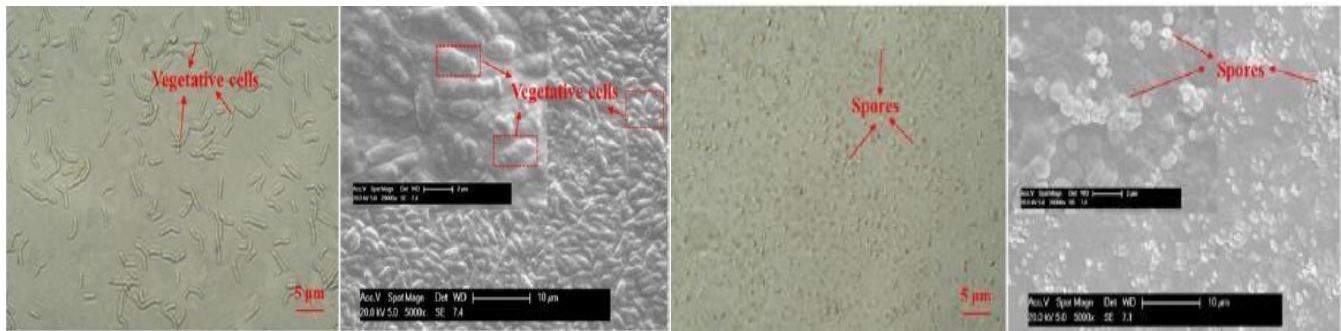


Figure 6 Stereomicroscopic images of crack-healing process in control mortar specimen before (a) and after 100 days healing (c), in bio-chemical agent-based specimen (Zheng et al 2020).

7. Considerations and practical applications

Integration of the microbial biomass either by immobilization or encapsulation way and their viability, the modality has been explicated comprehensively. The scope for visualizing metabolic calcite production was intensively studied under numerous applications, but distinct investigations on the survivability of bacteria in real life need to be examined. The addition of LWA has also implemented various protection strategies, GNP, micro-capsules, hydrogels etc., to safeguard the bio-culture against the pressure or forces endorsed in the concrete (Tang and Xu 2021; Wang et al 2014a). Their suitability in versatile environments and their effect on concrete properties like stiffness, modulus of elasticity, stress-strain behavior, shrinkage, and corrosion are to be assessed heretofore to achieve microbial self-healing concrete. All the tests performed in the lab affirmed promising output in the wide-scale range to date, but when we adapt to massive concrete structures its elements necessitate analyzing at longer service life and marine environmental conditions. Further study may also focus on choosing certain routes or processes, carriers, and nutrients that can enhance the resilience and self-healing capability of the microbial concrete as well as creating a theoretical model simulation to reduce the expense and time. Fatherly, to surmount the cost-effectiveness in production cost of bacterial concrete an inexpensive industrial waste with a high protein content can be adopted as the nutrient ingredients (Stanaszek-Tomal 2020).

8. Conclusion

This paper aims to stipulate an overview of the various types of bacteria or micro-organisms mostly used as self-healing agents, their metabolic function, different types of nutrients to enhance bacterial cell growth, and carrier's requisite for acting as protective cover aids in healing cracks in concrete. This review elucidates the self-healing mechanisms or strategies, their pros and cons, and different incorporating bacteria into the cement matrix. The study has reviewed various properties, including compressive strength, water absorption, split tensile strength, sorptivity, chloride ion penetration, water permeability, and microstructure analysis using SEM, EDS, TGA, XRD, and EDAX. Imbibing the bio-based material in concrete has reduced to very much extent the durability parameters, enhanced the mechanical properties, and the efficiency of self-healing has given a remarkable outcome. Compared to other species, a few of the ureolytic bacteria like *Bacillus subtilis*, *B. pasteurii*, and *B. sphaericus* exhibited an increasing trend in compressive, flexural, and split tensile strengths. Application of the microbes in the concrete, under mechanism of bacterial metabolic conversion, crack healing of 0.46 mm was significant post 100 days of curing. On subsidiary, in micro-encapsulation process, for a combination of micro-capsule and nutrients maximum crack width of 970 µm was healed but on other hand it rendered adverse effect on degree of hydration and compressive strength loss up to 47% after 90 days. But taking utmost care during selecting a suitable self-healing agent and preferable strategy to arrive at authentic self-healing in concrete is of great concern regarding prevailing favorable or unfavorable conditions. Furtherly, investigating the bacterial activity and its survivability at a more extended age period pertaining to concrete in a real-life time basis, its cost effectiveness is not yet discoursed. This microbial approach of self-healing concrete is proven to be the best way as the bacteria is harmless, eco-friendly and sustainable.

Ethical considerations

Not applicable.

Declaration of interest

The authors declare no conflicts of interest.

Funding

This research did not receive any financial support.

References

- Abo Sabah SH, Anneza LH, Juki MI, Abduljabbar H, Othman N, Al-Gheethi AA, Al-Shalif AF (2021) The use of calcium lactate to enhance the durability and engineering properties of bioconcrete. *Sustain Sci* 13. DOI: 10.3390/su13169269
- Abo-El-Enein SA, Ali AH, Talkhan FN, Abdel-Gawwad HA (2013) Application of microbial biocementation to improve the physico-mechanical properties of cement mortar. *HBRC Journal* 9:36-40. DOI: 10.1016/j.hbrj.2012.10.004
- Achal V, Mukerjee A, Sudhakara Reddy M (2013) Biogenic treatment improves the durability and remediates the cracks of concrete structures. *Constr Build Mater* 48:1-5. DOI: 10.1016/j.conbuildmat.2013.06.061
- Affudin H, Hamidah M, Hana H, Kamaruddin K (2011) Microorganism precipitation in enhancing concrete properties. *Appl Mech Mater* 99:1157-1165. DOI: 10.4028/www.scientific.net/AMM.99-100.1157
- Algaifi HA, Bakar SA, Sam ARM, Abidin ARZ, Shahir S, AL-Towayti WAH (2018) Numerical modeling for crack self-healing concrete by microbial calcium carbonate. *Constr Build Mater* 189:816-824. DOI: 10.1016/j.conbuildmat.2018.08.218
- Andalib R, Abd Majid MZ, Hussin MW, Ponraj M, Keyvanfar A, Mirza J, Lee H-S (2016) Optimum concentration of *Bacillus megaterium* for strengthening structural concrete. *Constr Build Mater* 118:180-193. DOI: 10.1016/j.conbuildmat.2016.04.142
- Bang SS, Galinat JK, Ramakrishnan V (2001) Calcite precipitation induced by polyurethane-immobilized *Bacillus pasteurii*. *Enzyme Microb Technol* 28:404-409. DOI: 10.1016/S0141-0229(00)00348-3
- Bashir J, Kathwari I, Tiwary A, Singh K (2016) Bio concrete- the self-healing concrete. *Indian J Sci Technol* 9:1-5. DOI: 10.17485/ijst/2015/v8i1/105252
- Beveridge T (1981) Ultrastructure, chemistry, and function of the bacterial wall. *Int Rev Cytol* 72:229-317. DOI: 10.1016/S0074-7696(08)61198-5
- Bundur ZB, Amiri A, Ersan YC, Boon N, De Belie N (2017) Impact of air entraining admixtures on biogenic calcium carbonate precipitation and bacterial viability. *Cem Concr Res* 98:44-49. DOI: 10.1016/j.cemconres.2017.04.005
- Chahal N, Siddique R, Rajor A (2012) Influence of bacteria on the compressive strength, water absorption and rapid chloride permeability of concrete incorporating silica fume. *Constr Build Mater* 37:645-651. DOI: 10.1016/j.conbuildmat.2012.07.029
- Chahal N, Siddique R, Rajor A (2012) Influence of bacteria on the compressive strength, water absorption and rapid chloride permeability of fly ash concrete. *Constr Build Mater* 28:351-356. DOI: 10.1016/j.conbuildmat.2011.07.042
- Chen H-J, Peng C-F, Tang C-W, Chen Y-T (2019) Self-healing concrete by biological substrate. *Mater* 12. DOI: 10.3390/ma12244099
- De Belie N, Van Belleghem B, Erşan YÇ, Van Tittelboom K (2019) Durability of self-healing concrete. In: *Concrete Solutions -7th International Conference on Concrete Repair* pp 1-8. DOI: 10.1051/mateconf/201928901003
- De Belie N, Wang J (2016) Bacteria-based repair and self-healing of concrete. *J Sustain Cem Based Mater* 5:35-56. DOI: 10.1080/21650373.2015.1077754
- De Muynck W, Cox K, Belie ND, Verstraete W (2008a) Bacterial carbonate precipitation as an alternative surface treatment for concrete. *Constr Build Mater* 22:875-885. DOI: 10.1016/j.conbuildmat.2006.12.011
- De Muynck W, Debrouwer D, De Belie N, Verstraete W (2008) Bacterial carbonate precipitation improves the durability of cementitious materials. *Cem Concr Res* 38:1005-1014. DOI: 10.1016/j.cemconres.2008.03.005
- Dong B, Han N, Zhang M, Wang X, Cui H, Xing F (2013) A microcapsule technology based self-healing system for concrete structures. *J Earthq Tsunami* 7:1350014. DOI: 10.1142/S1793431113500140
- El Enshasy H, Dailin DJ, Malek RA, Nordin NZ, Keat HC, Eyahmalay J, Ramchuran S, Chee Ghong JN, Ramdas VM, Laloo R (2020) Biocement: A novel approach in the restoration of construction materials. In: Yadav AN, Rastegari AA, Gupta VK, Yadav N (ed) *Microbial Biotechnology Approaches to Monuments of Cultural Heritage*. Springer, Singapore, pp 177-198. DOI: 10.1007/978-981-15-3401-0_10
- Elkhateeb W, Elnahas MO, Daba G (2021) Microbial induced mineralization of calcium carbonate for self-healing concrete. *Asian J Nat Prod Biochem* 19:1-9. DOI: 10.13057/biofar/f190101
- Erşan YÇ, Da Silva FB, Boon N, Verstraete W, De Belie N (2015) Screening of bacteria and concrete compatible protection materials. *Constr Build Mater* 88:196-203. DOI: 10.1016/j.conbuildmat.2015.04.027
- Erşan YÇ, De Belie N, Boon N (2015) Microbially induced CaCO₃ precipitation through denitrification: an optimization study in minimal nutrient environment. *Biochem Eng J* 101:108-118. DOI: 10.1016/j.bej.2015.05.006
- Feng J, Chen B, Sun W, Wang Y (2021) Microbial induced calcium carbonate precipitation study using *Bacillus subtilis* with application to self-healing concrete preparation and characterization. *Constr Build Mater* 280:122460. DOI: 10.1016/j.conbuildmat.2021.122460
- Ghosh S, Biswas M, Chattopadhyay B, Mandal S (2009) Microbial activity on the microstructure of bacteria modified mortar. *Cem Concr Compos* 31:93-98. DOI: 10.1016/j.cemconcomp.2009.01.001
- Han N-X, Xing F (2017) A comprehensive review of the study and development of microcapsule based self-resilience systems for concrete structures at Shenzhen University. *Mater* 10:2. DOI: 10.3390/ma10010002
- Hearn N (1998) Self-sealing, autogenous healing and continued hydration: what is the difference? *Mat Struct* 31:563-567. DOI: 10.1007/BF02481539
- Hoffmann TD, Paine K, Gebhard S (2021) Genetic optimisation of bacteria-induced calcite precipitation in *Bacillus subtilis*. *Microb Cell Factories* 20:1-19. DOI: 10.1186/s12934-021-01704-1
- Huynh NNT, Phuong NM, Toan NPA, Son NK (2017) *Bacillus subtilis* HU58 immobilized in micropores of diatomite for using in self-healing concrete. *Procedia Eng* 171:598-605. DOI: 10.1016/j.proeng.2017.01.385
- Jeong B, Jho EH, Kim SH, Nam K (2019) Effect of calcium organic additives on the self-healing of concrete microcracks in the presence of a new isolate *Bacillus sp.* BY1. *J Mater Civ Eng* 31:04019227. DOI: 10.1061/(ASCE)MT.1943-5533.0002711
- Jonkers H, Schlangen E (2008) Development of a bacteria-based self-healing concrete. Taylor & Francis Group. DOI:10.1201/9781439828410.ch72
- Jonkers HM (2007) Self-healing concrete: A biological approach. In: van der Zwaag S (ed) *Self-healing materials: an alternative approach to 20 centuries of materials science*. Springer, Netherlands, Dordrecht, pp 195-204



- Jonkers HM, Thijssen A, Muyzer G, Copuroglu O, Schlangen E (2010) Application of bacteria as self-healing agent for the development of sustainable concrete. *Ecol Eng* 36:230-235. DOI: 10.1016/j.ecoleng.2008.12.036
- Kessler M, Sottos N, White S (2003) Self-healing structural composite materials. *Compos Part A Appl Sci Manuf* 34(8):743-753. DOI: 10.1016/S1359-835X(03)00138-6
- Kevin Paine MA, Trupti S, Richard C, Heath A (2016) Design and performance of bacteria-based self-healing Concrete. In: the 9th International Concrete Conference, Materials Science, pp 545-554.
- Khaliq W, Ehsan MB (2016) Crack healing in concrete using various bio influenced self-healing techniques. *Constr Build Mater* 102:349-357. DOI: 10.1016/j.conbuildmat.2015.11.006
- Khan MBE, Shen L, Dias-da-Costa D (2021) Self-healing behaviour of bio-concrete in submerged and tidal marine environments. *Constr Build Mater* 277:122332. DOI: 10.1016/j.conbuildmat.2021.122332
- Khaudiyal S, Rawat A, Das SK, Garg N (2022) Bacterial concrete: A review on self-healing properties in the light of sustainability. *Mater. Today: Proc* 60:136-143. DOI: 10.1016/j.matpr.2021.12.277
- Li VC, Yang E-H (2007) Self-healing in concrete materials. In: van der Zwaag S (ed) *Self-Healing Materials: An Alternative Approach to 20 Centuries of Materials Science*. Springer, Netherlands, Dordrecht, pp 161-193.
- Luo M, Qian CX, Li RY (2015) Factors affecting crack repairing capacity of bacteria-based self-healing concrete. *Constr Build Mater* 87:1-7. DOI: 10.1016/j.conbuildmat.2015.03.117
- Meera C, Subha V (2016) Strength and durability assessment of bacteria based self-healing concrete. *IOSR J Mech Civ Eng* pp 01-07.
- Metwally GA, Mahdy M, Abd El AE-RH (2020) Performance of Bio concrete by using *Bacillus pasteurii* bacteria. *Civ Eng J* 6:1443-1456. DOI: 10.28991/cej-2020-03091559
- Muhammad NZ, Shafaghat A, Keyvanfar A, Abd. Majid MZ, Ghoshal SK, Mohammadyan Yasouj SE, Ganiyu AA, Samadi Kouchaksaraei M, Kamyab H, Taheri MM, Rezazadeh Shirdar M, McCaffery R (2016) Tests and methods of evaluating the self-healing efficiency of concrete: A review. *Constr Build Mater* 112:1123-1132. DOI: 10.1016/j.conbuildmat.2016.03.017
- Murari K, Kaur P (2021) Development of sustainable concrete using bacteria as self-healing agent. In: *Select Proceedings of SDEI 2020, Sustainable Development Through Engineering Innovations*, Springer, Singapore, pp 444 693-700
- Osman KM, Taher FM, Abd El-Tawab A, Faried AS (2021) Role of different microorganisms on the mechanical characteristics, self-healing efficiency, and corrosion protection of concrete under different curing conditions. *J Build Eng* 41:102414. DOI: 10.1016/j.jobe.2021.102414
- Parastegari N, Mostofinejad D, Poursina D (2019) Use of bacteria to improve electrical resistivity and chloride penetration of air-entrained concrete. *Constr Build Mater* 210:588-595. DOI: 10.1016/j.conbuildmat.2019.03.150
- Prasad CVS, Lakshmi TV (2018) Effect of *Bacillus subtilis* on mechanical behavior of bacterial concrete. *ARPN J Eng Appl Sci* 13:4873-81
- Priya TS, Ramesh N, Agarwal A, Bhusnur S, Chaudhary K (2019) Strength and durability characteristics of concrete made by micronized biomass silica and *Bacteria-Bacillus sphaericus*. *Constr Build Mater* 226:827-838. DOI: 10.1016/j.conbuildmat.2019.07.172
- Qian CX, Luo M, Ren LF, Wang RX, Li RY, Pan QF, Chen HC (2015) Self-healing and repairing concrete cracks based on bio-mineralization. In: *Trans Tech Publ Ltd, Key Engineering Materials*, 629:494-503. DOI: 10.4028/www.scientific.net/KEM.629-630.494
- Qian S, Zhou J, de Rooij MR, Schlangen E, Ye G, van Breugel K (2009) Self-healing behavior of strain hardening cementitious composites incorporating local waste materials. *Cem Concr Compos* 31:613-621. DOI: 10.1016/j.cemconcomp.2009.03.003
- Rajczakowska M (2019) Self-healing concrete. Licentiate thesis, comprehensive summary, Luleå tekniska universitet.
- Ramachandran SK, Ramakrishnan V, Bang SS (2001) Remediation of concrete using micro-organisms. *ACI Mater J, American Concrete Institute*, 98(1):3-9
- Ramakrishnan V (2007) Performance characteristics of bacterial concrete—a smart biomaterial. In: *Proceedings of the First International Conference on Recent Advances in Concrete Technology*, DC: Washington, pp 67-78
- Roig-Flores M, Formagini S, Serna P (2021) Self-healing Concrete-What Is It Good for? *Mater de Construcción* 71:e237-e237. DOI: 10.3989/mc.2021.07320
- Ryu Y, Lee KE, Cha IT, Park W (2020) Optimization of bacterial sporulation using economic nutrient for self-healing concrete. *J Microbiol* 58(4):288-296. DOI: 10.1007/s12275-020-9580-y
- Salmasi F, Mostofinejad D (2020) Investigating the effects of bacterial activity on compressive strength and durability of natural lightweight aggregate concrete reinforced with steel fibers. *Constr Build Mater* 251:119032. DOI: 10.1016/j.conbuildmat.2020.119032
- Seifan M (2018) Self-healing concrete: a novel nanobiotechnological approach to heal the concrete cracks. Dissertation, University of Waikato, Hamilton, New Zealand
- Seifan M, Samani AK, Berenjian A (2016) Bioconcrete: next generation of self-healing concrete. *Appl Microbiol Biotechnol* 100:2591-2602. DOI: 10.1007/s00253-016-7316-z
- Sierra-Beltran MG, Jonkers H, Schlangen E (2014) Characterization of sustainable bio-based mortar for concrete repair. *Constr Build Mater* 67:344-352. DOI: 10.1016/j.conbuildmat.2014.01.012
- Silva FB, Boon N, Belie ND, Verstraete W (2015) Industrial application of biological self-healing concrete: Challenges and economical feasibility. *J Commer Biotechnol* 21.
- Singh H, Gupta R (2020) Cellulose fiber as bacteria-carrier in mortar: Self-healing quantification using UPV. *J Build Eng* 28:101090. DOI: 10.1016/j.jobe.2019.101090
- Skinner H, Jahren A (2003) Biomineralization. In: *Treatise on geochemistry*, 2nd edn. 8:117-184
- Soysal A, Milla J, King GM, Hassan M, Rupnow T (2020) Evaluating the self-healing efficiency of hydrogel-encapsulated bacteria in concrete. *Transp Res Rec* 2674:113-123. DOI: 10.1177/0361198120917973
- Stanaszek-Tomal E (2020) Bacterial concrete as a sustainable building material? *Sustain* 12:696. DOI: 10.3390/su12020696

- Su Y, Feng J, Jin P, Qian C (2019) Influence of bacterial self-healing agent on early age performance of cement- based materials. *Constr Build Mater* 218:224-234. DOI: 10.1016/j.conbuildmat.2019.05.077
- Suleiman A, Nehdi M (2018) Effect of environmental exposure on autogenous self-healing of cracked cement- based materials. *Cem Concr Res* 111:197-208. DOI: 10.1016/j.cemconres.2018.05.009
- Tang Y, Xu J (2021) Application of microbial precipitation in self-healing concrete: A review on the protection strategies for bacteria. *Const Build Mater* 306:1-11. DOI: 10.1016/j.conbuildmat.2021.124950
- Tayebani B, Mostofinejad D (2019) Penetrability, corrosion potential, and electrical resistivity of bacterial concrete. *J Mater Civ Eng* 31:04019002. DOI: 10.1061/(ASCE)MT.1943-5533.0002618
- Van Breugel K (2007) Is there a market for self-healing cement-based materials. In: *Proceedings of the first international conference on self-healing materials, Netherlands*, pp 1-9.
- Van Tittelboom K, De Belie N (2013) Self-healing in cementitious materials—A review. *Mater* 6. DOI: 10.3390/ma6062182
- Vijay K, Murmu M (2020) Experimental study on bacterial concrete using *Bacillus subtilis* micro-organism. In: *Select Proceedings of ICETCE 2018, Emerging Trends in Civil Engineering*, Springer, Singapore, pp 245-252.
- Wang J, Ersan YC, Boon N, De Belie N (2016) Application of microorganisms in concrete: a promising sustainable strategy to improve concrete durability. *Appl Microbiol Biotechnol* 100(7):2993-3007. DOI: 10.1007/s00253-016-7370-6
- Wang J, Snoeck D, Van Vlierberghe S, Verstraete W, De Belie N (2014) Application of hydrogel encapsulated carbonate precipitating bacteria for approaching a realistic self-healing in concrete. *Constr Build Mater* 68:110-512 119. DOI: 10.1016/j.conbuildmat.2014.06.018
- Wang J, Soens H, Verstraete W, De Belie N (2014) Self-healing concrete by use of microencapsulated bacterial spores. *Cem.Concr Res* 56:139-152. DOI: 10.1016/j.cemconres.2013.11.009
- Wang J, Van Tittelboom K, De Belie N, Verstraete W (2012) Use of silica gel or polyurethane immobilized bacteria for self-healing concrete. *Constr Build Mater* 26:532-540. DOI: 10.1016/j.conbuildmat.2011.06.054
- Wang J-Y, De Belie N, Verstraete W (2012) Diatomaceous earth as a protective vehicle for bacteria applied for self-healing concrete. *J Ind Microbiol Biotechnol* 39:567-577. DOI: 10.1007/s10295-011-1037-1
- White SR, Sottos NR, Geubelle PH, Moore JS, Kessler MR, Sriram SR, Brown EN, Viswanathan S (2001) Autonomic healing of polymer composites. *Nature* 409(6822):794-797. DOI: 10.1038/35057232
- Wiktor V, Jonkers HM (2011) Quantification of crack-healing in novel bacteria-based self-healing concrete. *Cem Concr Compos* 33:763-770. DOI: 10.1016/j.cemconcomp.2011.03.012
- Xu J, Yao W (2014) Multiscale mechanical quantification of self-healing concrete incorporating non-ureolytic bacteria-based healing agent. *Cem Concr Res* 64:1-10. DOI: 10.1016/j.cemconres.2014.06.003
- Yıldırım G, Khiavi AH, Yeşilmen S, Şahmaran M (2018) Self-healing performance of aged cementitious composites. *Cem Concr Compos* 87:172-186. DOI: 10.1016/j.cemconcomp.2018.01.004
- Zawad MFS, Rahman MA, Priyom SN (2021) Bio-engineered concrete: a critical review. On the next generation of durable concrete. *Journal of the Civil Engineering Forum Web* 335-358.
- Zhang K, Tang CS, Jiang NJ, Pan XH, Liu B, Wang YJ (2023) Microbial-induced carbonate precipitation (MICP) technology: a review on the fundamentals and engineering applications. *Environ. Earth Sci* 82:229.
- Zheng T, Su Y, Zhang X, Zhou H, Qian C (2020) Effect and mechanism of encapsulation-based spores on self- healing concrete at different curing ages. *ACS Appl Mater Interfaces* 12:52415-52432. DOI: 10.1021/acsami.0c16343

Use of occlusal splint in subjects with TMJ disorders by general dental practitioners in Indian scenario



Sneha Verma^a  | Charu Garg^b | H. Malathi^c

^aMaharishi University of Information Technology, Lucknow, Uttar Pradesh, India, Associate Professor, School of Science and Humanities.

^bTeerthanker Mahaveer University, Moradabad, Uttar Pradesh, India, Department of Orthodontics and Dentofacial Orthopedics.

^cJain (Deemed-to-be University), Bangalore, India, Assistant Professor, Department of Life Sciences.

Abstract Temporomandibular disorders (TMDs) constitute a global health concern, giving rise to both physical and financial burdens, as evidenced by symptoms and indications indicative of masticatory muscle imbalances. These symptoms encompass manifestations associated with disorders of the masticatory muscles. Scant literature exists regarding the utilization of occlusal splints by general dentists for addressing TMDs within the Indian context. Employing a cross-sectional questionnaire survey, the present study aimed to evaluate the application of occlusal splints in the treatment of temporomandibular issues by Indian dental practitioners. The inquiry involved the administration of a questionnaire designed to investigate the diagnosis, management, and treatment of TMDs by general dentists in India. Responses to the survey questions, provided by 314 general dental practitioners, were subjected to assessment and analysis through statistical methodologies. For practitioners with less than five years of experience, 77.63% (n=118) of participants reported no attendance at Certified Diabetes Educator (CDE) programs, whereas 14.47% (n=22) attended a single CDE session, and 7.89% (n=12) attended multiple CDE sessions related to TMDs. Among those practicing for five to ten years, 57.77% (n=52) did not participate in any TMD-related CDE programs, while 24.4% (n=22) attended one, and 17.7% (n=16) attended more than one. Among practitioners with over ten years of experience, 34.48% (n=20) did not attend any CDE, 24.13% (n=14) attended one, and 37.93% (n=22) attended multiple TMD-related CDE sessions. Diagnosis of TMDs was carried out by 64.33% (n=193) of participants using a combination of study models, imaging, patient history, and medical history. Among a total of 300 subjects, 64.6% (n=194) of participants responded affirmatively to the treatment of patients with TMDs. Hinge and mean value articulators were utilized in conjunction with soft materials for the fabrication of occlusal splints. The survey results suggest a paucity of knowledge among general dental practitioners regarding the application of occlusal splints in the treatment of TMDs.

Keywords: dentists, masticatory muscle disorders, occlusal splints, certified diabetes educators, temporomandibular disorder

1. Introduction

TMDs are a heterogeneous group of disorders in which a condition produces impaired, incomplete, or abnormal function of the muscles of mastication and/or the TMJ (temporomandibular joint). TMDs are identified among the most controversial disorders in the field of dentistry and contribute to a major concern in the healthcare field globally, including India, and have a great impact on expenses related to the healthcare sector (Deshpande et al 2023). The TMJ, masticatory system, and related muscles make up the TMJ stomatognathic system. The etiology of these disorders is mainly attributed to the multifactorial system, and the pathophysiology of TMJ disorders is not clearly understood (Sim et al 2019). The splint prevents bruxism, often known as teeth grinding or clenching, by acting as a barrier between the upper and lower teeth. The splint helps to prevent future harm to the joint and related tissues by decreasing bruxism, a key contributing cause to TMJ problems. The treatment of TMDs is performed using different modalities, including behavioral therapy, pharmacotherapy, physiotherapy, occlusal splint therapy, orthodontic treatment, and joint surgery (Fernández-de-Las-Peñas and Von Piekartz 2020).

A detachable oral device known as an occlusal splint is produced specifically for each patient by a dentist or dental expert. It is often composed of acrylic material and is intended to fit over either the upper or lower teeth. The splint was meticulously adjusted for the patient's ideal occlusion or bite. The use of an occlusal splint for treating TMDs is one of the most common management modalities because it is an economical, reversible, and noninvasive intervention performed to treat these disorders. Previous literature data have reported that nearly 50% to 75% of subjects globally have one or more signs of TMDs (Mommaerts et al 2020). In cases where daily activities are impaired due to TMDs, the tendency to seek



medical care increases proportionally. For accurate diagnosis of TMDs, it is vital to identify the signs of TMJ disorders (Jankar et al 2020).

Generally, occlusal splint therapy presents a challenging condition for both patients being treated and the dentist treating the subject. Additionally, it is difficult to identify TMDs and to provide appropriate treatment time for TMDs owing to varying symptoms from subject to subject. Figure 1 depicts the diagram of TMD disorder.

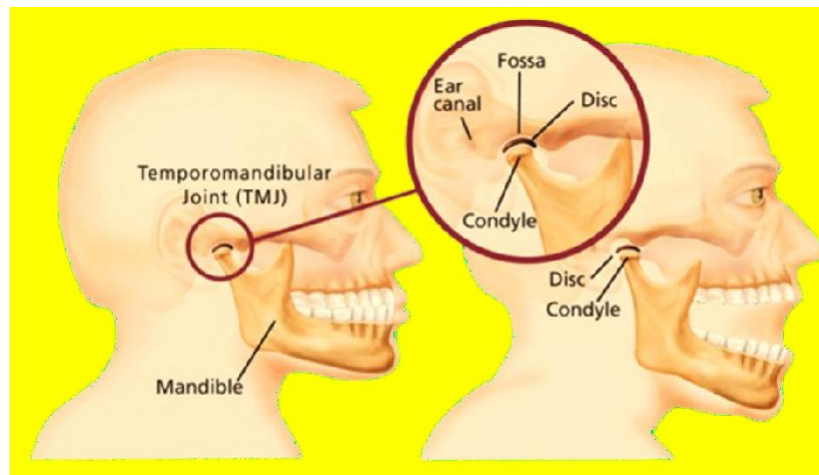


Figure 1 Diagram of TMD disorder.

After the symptoms related to TMDs are recognized, managed, and diagnosed with masticatory muscle dysfunction, occlusal splints are utilized (Ram and Shah 2021). The mandible is repositioned to the centric occlusion with the help of orthodontic appliances in occlusal adjustments. Occlusal splints are designed to be used intraorally to attain balanced and even occlusion without intentionally changing the rest position of the mandible. Occlusal splints are worn by the subjects, similar to removable dentures and retainer appliances (Furuchi et al 2022).

Despite being used as the most common management modality for temporomandibular disorder, the previous literature data about the approach of general dentists toward the use of occlusal splints in subjects with TMDs are scarce, especially in Indian subjects (Al-Moraissi et al 2020). Hence, the present study utilized a questionnaire survey in a cross-sectional manner to assess temporomandibular problems treated with occlusal splints by Indian dentists.

Saccomanno et al (2022) assessed how the pandemic might affect body mass index (BMI), obstructive sleep apnea syndrome (OSAS), and TMJ diseases. The patients spoke about their experiences living during the epidemic in this questionnaire. The paper noted that the sample under consideration gained weight throughout this health catastrophe. Bhardwaj et al (2022) investigated the connection between impacted third molars in the mandible and the emergence of TMJ abnormalities. For an accurate diagnosis, treatment, and prognosis of TMJ diseases, it is vital to be aware of the variables that negatively impact TMJ. Dong et al (2022) investigated the mechanism of cognitive-behavioral treatment (CBT) in adult women who have had discomfort from temporomandibular problems for more than three months. Between 2019 and 2021, eight patients were randomly chosen from adult patients with TMDs who had received a diagnosis for the first time. They received a 50-minute weekly psychological intervention in addition to physiological treatment and three- and one-month follow-up cortisol testing, and an effectiveness question was addressed. Repositioning the condyle may be essential throughout the patient's recovery, which has lost vertical dimension to prevent stress on the systematic region of the TMJ. The literature has a number of indications; however, moving the condyle inside the glenoid cavity is not a straightforward technique. Cone beam computed tomography (CBCT) is a tool for 3D visualization and digital approaches (Nota et al (2021). Monzani et al (2022) investigated 22 patients who had unidirectional, unmistakable Meniere's illness and concomitant temporomandibular joint conditions and had to stabilize occlusal splint treatment. Musa et al (2023) examined changes in condylar position, morphology, and bone mineral density (BMD) in participants with TMD in relation to condylar modifications, both quantitatively and qualitatively, after stabilization splint (SS) treatment. Orzeszek et al (2023) examined the effectiveness of occlusal splints in treating orofacial myalgia and myofascial pain (MP) in comparison to no treatment or alternative therapies.

2. Materials and Methods

The present survey-based cross-sectional research was carried out to evaluate the strategy of general dentists concerning the use of occlusal splints in the treatment of subjects with TMDs in India.

The study assessed subjects registered in the dental council of India, practicing in India, and eager to participate in the research. The exclusion criteria were contributors who did not give consent for study participation, subjects who did not fill out the questionnaire simultaneously, incomplete survey forms, and not registered practitioners. After explaining the study

design, informed consent in both verbal and written format was gathered from all the participants. Among 314 recruited subjects, 14 were eliminated from the survey for failing to respond.

The questionnaire for the survey was gathered and framed by two examiners with expertise in the field. The participating general dentists were from both academic and nonacademic backgrounds. The subjects were recruited in the study irrespective of the years in the practice, age, and gender of the dentists. The examiner collecting the data interacted with each participant personally to evaluate their knowledge of the participants. The questionnaire was formulated in the English language and comprised 15 questions in a multiple-choice format. The questionnaire comprised 2 parts: part 1 was related to the demographics and part 2 to the dentist's experience with using the occlusal splint to treat TMDs.

Questions 1-4 assessed gender, age, years of experience (<5, 5-10, and >10 years), and general or specialty practice. Questions 5-7 asked if subjects attended any CDE (continuing dental education program on TMDs), tools used for diagnosing TMDs (study models, imaging, physical history, medical history, or combination), and if they treat subjects with TMDs. Subjects responding positively to question 7 were only asked to respond to further questions, and subjects responding negatively were asked to submit the questionnaire.

In question 8, treatment rendered was asked (orthodontics, occlusal adjustments, occlusal splints, pharmacotherapy, physiotherapy, thermotherapy, diet plans, counseling, full-mouth rehabilitation, and/or combination). Question 9 assessed the purpose of using the occlusal splint (therapeutic, diagnostic, or both). Question 10 was on splint material as hard or soft, question 11 was on the articulator used (fully adjustable, semi adjustable, mean value, or hinge articulator), question 12 was on the splint duration as 6-12, >12 months, >1 year, or until TMDs were resolved, question 13 was on the time of wearing the splint as all the time, daytime, or night time, question 14 was on the time of occlusal correction (after or before the splint), and question 15 was on the situation of occlusal splint advised (myofascial pain, TMJ pain, bruxism, combination, or others).

The data were examined statistically with the chi-square test and SPSS version 21.0 (IBM cooperation, Armonk, NY, USA). The data are expressed as percentages, frequencies, means, and significance-level standard deviations of $p < 0.05$.

3. Results

Among the 314 subjects included in the present study, a complete survey questionnaire was completed by 300 participants, making the final sample size of 300 participants. The average age of the dentists was 33.42 ± 6.07 years, with 47.3% ($n=142$) females and 52.6% ($n=158$) males. A total of 18.66% ($n=56$) of the dentists were engaged in specialty practice, whereas 81.33% ($n=244$) of the subjects were engaged in general dental practice. Concerning the years of experience in dental practice, 50.6% ($n=152$) of participants had experience of <5 years, 30% ($n=90$) of subjects of 5-10 years, and 19.3% ($n=58$) of subjects had an experience of >10 years. The difference in specialty practice and experience was statistically significant in study participants with $p < 0.001$, as shown in Table 1.

Table 1 Demographic characteristics of the participating dentists in the study.

S. No	Characteristics	Percentage (%)	Number (n=300)
1.	Mean age (years)		33.42±6.07
2.	Gender		
a)	Females	47.3	142
b)	Males	52.6	158
3.	Type of practice		
a)	Specialty	18.66	56
b)	General	81.33	244
4.	Experience in years		
a)	<5	50.6	152
b)	5-10	30	90
c)	>10	19.3	58

For diagnosis and evaluation of the TMJ disorders, 64.33% ($n=193$) of study participants utilized the combination of study models, imaging, physical history, and medical history. For the subjects attending the CDE (continuing dental education) program on TMDs (temporomandibular disorders), it was reported that in subjects practicing for <5 years, 77.63% ($n=118$) of participants did not attend any CDE, 14.47% ($n=22$) of participants attended only 1 CDE, and 7.89% ($n=12$) of participants attended >1 CDE on TMDs. For participants practicing for 5-10 years, no CDE was attended on TMDs by 57.77% ($n=52$) of participants, 1 CDE by 24.4% ($n=22$) of participants, and >1 CDE by 17.7% ($n=16$) of participants. In the practice of >10 years, 34.48% ($n=20$) of participants attended no CDE, 24.13% ($n=14$) attended 1 CDE, and 37.93% ($n=22$) of subjects attended >1 CDE on TMDs, as summarized in Table 2 and Figure 2.

In participants with <5 years of experience, 51.31% ($n=78$) of subjects responded positively to treating subjects with TMDs, 75.55% ($n=68$) of subjects had 5-10 years of experience, and 82.75% ($n=48$) of subjects had >10 years of experience. In 300 subjects, 64.6% ($n=194$) of participants responded positively to treat patients with TMDs (Table 3 and Figure 3). This variance was also statistically significant, with $p < 0.001$. Concerning occlusal splint use for therapeutic and diagnostic

purposes, in <5, 5-10, and >10 years, 19.73% (n=30), 26.6% (n=24), and 20.68 (n=12) of subjects, respectively, used splints for both diagnostic and therapeutic purposes. The more commonly used material for splint fabrication was soft. The use of mean value and hinge articulators was more common in dentists with <5 and 5-10 years of experience, whereas for participants with >10 years of experience, semi adjustable and mean value articulators were used with statistically significant results and $p < 0.05$.

Table 2 Number of CDE programs attended by participants based on years of experience.

S. No	Number of CDE programs	Practice years			Total n=300 (%)
		<5 n=152 (%)	5-10 n=90 (%)	>10 n=58 (%)	
1. None		118 (77.63)	52 (57.77)	20 (34.48)	190 (63.33)
2. One		22 (14.47)	22 (24.4)	14 (24.13)	58 (19.3)
3. >1		12 (7.89)	16 (17.7)	22 (37.93)	52 (17.3)
4. Total		152 (100)	90 (100)	58 (100)	300 (100)

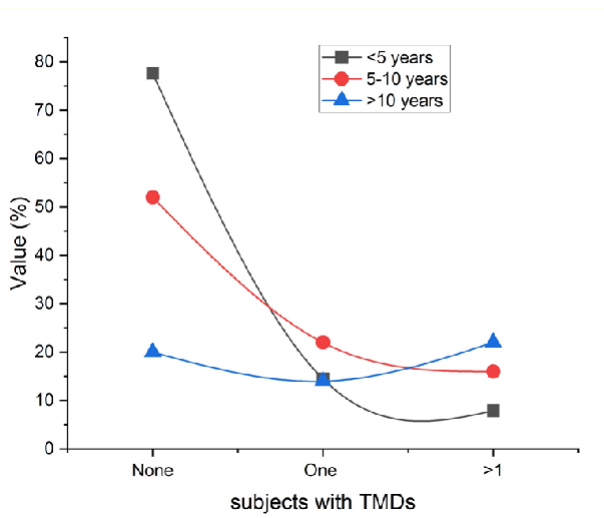


Figure 2 Participants' participation in CDE programs based on years of experience.

Table 3 Number of participants treating subjects with TMDs based on experience years.

S. No	Treating subjects with TMDs	Practice years			Total n=300 (%)
		<5 n=152 (%)	5-10 n=90 (%)	>10 n=58 (%)	
Yes		78 (51.31)	68 (75.55)	48 (82.75)	194 (64.6)
No		74 (48.68)	22 (24.4)	10 (17.24)	106 (35.3)
Total		152 (100)	90 (100)	58 (100)	300 (100)

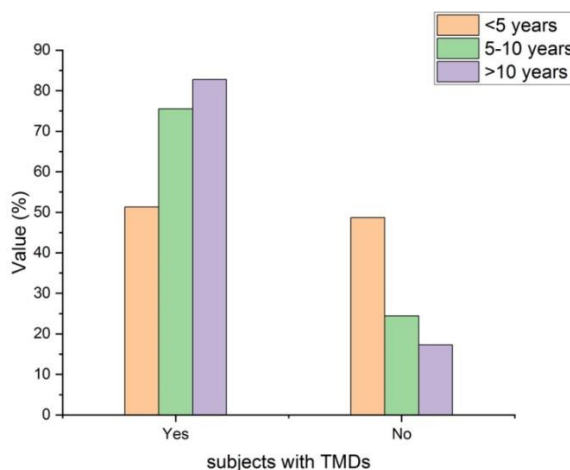


Figure 3 Number of participants who treat patients with TMDs by years of expertise.

In the participants with <5 years of experience, the majority (46.15%, n=36) of subjects recommended that occlusal splints be worn at night only; in the group with 5-10 years of experience, 47.05% of subjects suggested individual variation in the duration of wearing occlusal splints, and in the group with >10 years of experience, individual factors were considered by 66.6% (n=32) of subjects for occlusal splint wearing duration. The majority of 47.42% (n=92) of subjects suggested splints to be worn based on individual preferences (Table 4 and Figure 4).

Table 4 Suggestion on the duration of wearing occlusal splints for TMDs by study participants.

S. No	Treating subjects with TMDs	Practice years			Total n=194 (%)
		<5 n=78 (%)	5-10 n=68 (%)	>10 n=48 (%)	
1.	Individual subjects	28 (35.89)	32 (47.05)	32 (66.6)	92 (47.42)
2.	All the time	6 (7.69)	16 (23.52)	2 (4.16)	24 (12.37)
3.	Daytime	8 (10.25)	0	0	8 (4.12)
4.	Nighttime	36 (46.15)	20 (29.41)	14 (29.16)	70 (36.08)
5.	Total	78 (100)	68 (100)	48 (100)	194 (100)

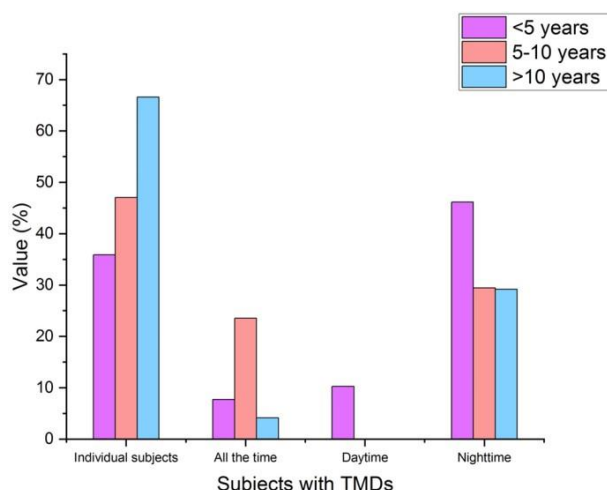


Figure 4 Study participants' recommendations for how long TMD patients should wear occlusal splints.

The majority of the study subjects having experience of either 5-10 or >10 years reported that in subjects with TMDs, before splint therapy, occlusal correction should be performed, as responded by 39.47% (n=60), 55.5% (n=50), and 55.17% (n=32) of participants, respectively. The use of an occlusal splint in a mixture with situations such as myofascial pain, TMJ pain, and bruxism was reported by 63.15% (n=96), 61.11% (n=55), and 70.68% (n=41) of subjects with <5, 5-10, and >10 years of experience, respectively.

3.1. Discussion

The current survey-based cross-sectional study was conducted to assess the approach of general dentists concerning the use of occlusal splints in the treatment of subjects with TMDs in India. The study included 314 dental practitioners of both sexes. Among 314 subjects, 14 participants either refused or did not finish the questionnaire and were disqualified. The participants were asked to fill out the questionnaire on the spot to assess their prompt knowledge of the management of subjects with TMDs. The obtained results and findings were compared with other studies and scientific evidence previously available in the literature.

For the study participants, the average age of the dentist was 33.42±6.07 years, with 47.3% (n=142) females and 52.6% (n=158) males. A total of 18.66% (n=56) of the dentists were engaged in specialty practice, whereas 81.33% (n=244) of the subjects were engaged in general dental practice. Concerning the years of experience in dental practice, 50.6% (n=152) of participants had experience of <5 years, 30% (n=90) of subjects of 5-10 years, and 19.3% (n=58) of subjects had an experience of >10 years. The difference in specialty practice and experience was statistically significant in study participants, with p<0.001. These demographics were comparable to previous studies by Sabhlok et al (2021) and Sam et al (2018), where the authors assessed dental practitioners concerning their knowledge about TMDs with demographic data comparable to those of the present study.



The current study's findings demonstrated that subjects with <5 years of practice experience were not treating subjects with TMDs, which can be attributed to their insufficient skills and knowledge of the treatment of TMDs compared to practitioners with more experience. These results were consistent with the studies of (SAJJANAR et al 2021) and (Sinclair et al 2022), where the authors reported that required efforts are not put in by the practitioners newer in practice to assess the etiology of TMDs and to diagnose TMDs; they rather decide to not treat the subject and refer them to a higher center or to the specialist that could treat TMDs. However, practitioners with more experience, as in the present study, of 5-10 years or >10 years, owing to more encounters of practitioners with TMDs, require clinicians to treat subjects with TMDs and increase their attendance in CDEs focused on TMDs, increasing their confidence and knowledge in treating subjects with TMDs.

The outcomes of the current study also showed that dentists participating in the study had fair knowledge concerning the identification and treatment of TMDs, and the methods used by the participants to treat subjects with TMJ disorders agreed with the study of Thambar et al (2020). It was also seen that most practitioners preferred soft material for occlusal splint fabrication, which may be due to its lack of need for occlusal adjustments and ease of use with less in-office dental time compared to splints made of hard material. Additionally, 47.42% (n=92) of participants recommended wearing the splint until the symptoms subsided, which was similar to the studies by Sabhlok et al (2021) and Macrì et al (2022), where authors reported more preference for dentists to fabricate occlusal splints using a soft material and their wearing time until the symptoms subsided by 42% of dentists in the study.

Insufficient and limited knowledge in participants with <5 years of experience can be due to the long protocol of wearing the occlusal splint. Additionally, the results varied concerning the recommendation on the duration of wearing the occlusal splint, showing insufficient knowledge. Additionally, as suggested by (Sullivan et al 2022), despite the accurate diagnosis, the long time needed for the initial screening of subjects with TMDs can lead to irreversible pathogenic modifications to the TMJ complex and masticatory system.

The study findings also reported a lack of awareness among dental practitioners concerning the use of the articulator while fabricating the occlusal splint. A semi adjustable articulator was not used during splint fabrication, and adjustments were made while splints were delivered. In participants with >10 years of experience, the individual condition of the patient was considered for the duration of wearing the splint, which was similar to (Al-Moraissi et al 2020), where the author reported that limited evidence in the literature exists on the duration of wearing the occlusal splint and that each condition might have a varying healing period, which was also confirmed by (Thambar et al 2020).

The study had a few limitations, including the caution needed to generalize the outcomes of the current study attributed to limited preexisting evidence in the literature that can help support the outcomes of the current study. The majority of participants were general practitioners, and the results cannot be applied to specialty practice.

4. Conclusion

The study, considering its limitations, concludes that the treatment and diagnosis of TMDs by practitioners were in agreement with the guidelines followed internationally. However, insufficient knowledge exists among dental practitioners concerning the timing, duration, types, and use of occlusal splints in subjects with TMDs. An increase in knowledge was seen with the increase in the practitioner's experience. Hence, national dental associations should work in collaboration with state dental associations to arrange more CDEs and symposiums at the state and national levels to enhance knowledge about TMDs.

Ethical considerations

Not applicable.

Declaration of interest

The authors declare no conflicts of interest.

Funding

This research did not receive any financial support.

References

- Al-Moraissi EA, Farea R, Qasem KA, Al-Wadeai MS, Al-Sabahi ME, Al-Iryani, GM (2020) Effectiveness of occlusal splint therapy in the management of temporomandibular disorders: network meta-analysis of randomized controlled trials International. Journal of oral and maxillofacial surgery 49:1042-1056.
- Bhardwaj A, Gupta S, Narula J (2022) Mischievous mandibular third molars are camouflaging temporomandibular joint disorders. Journal of the Korean Association of Oral and Maxillofacial Surgeons 48:155-158.
- Deshpande, S, Pande, N and Patil, P 2023 Stomatognathic Risk Factors and Clinical Manifestations of Temporomandibular Disorders in Indian Population: A Case-control Study The Journal of Contemporary Dental Practice 23:1195-1198.
- Dong S, Zhang Y, Cen X, Li X, Yu L, Li Z, Zhu X (2022) May Mechanism of action of cognitive behavioral therapy on pain in adult women with major TMJ



- disorders. In Proceedings of the 6th International Conference on Medical and Health Informatics 198-204.
- Fernández-de-Las-Peñas C, Von Piekartz H (2020) Clinical reasoning for the examination and physical therapy treatment of temporomandibular disorders (TMD): a narrative literature review. *Journal of Clinical Medicine* 9:3686.
- Furuchi M, Takeuchi Y, Kamimoto A, Koizumi H (2022) Usage of English prosthodontic terms 2019 in Japan. *Journal of Oral Science* 64:322-323.
- Jankar AS, Kamble SS, Sonawane SS, Fere S, Botwe SD (2020) Occlusal splints: an innovative treatment modality in temporomandibular disorders. *J Prosthodont Dent* 15:35-41.
- Macrì M, Murmura G, Scarano A, Festa F (2022) Prevalence of temporomandibular disorders and its association with malocclusion in children: a transversal study. *Frontiers in Public Health* 10:860833.
- Mommaerts MY, Nicolescu I, Dorobantu M, De Meurechy N (2020) Extended total temporomandibular joint replacement with occlusal adjustments: pitfalls, patient-reported outcomes, subclassification, and a new paradigm. *Annals of Maxillofacial Surgery* 10:73.
- Monzani D, Baraldi C, Apa E, Alicandri-Ciufelli M, Bertoldi C, Røggla E, Guerzoni S, Marchioni D, Pani L (2022) Occlusal splint therapy in patients with Ménière's disease and temporomandibular joint disorder. *Acta Otorhinolaryngologica Italica* 42:89.
- Musa M, Zhang Q, Awad R, Wang W, Ahmed MMS, Zhao Y, Almashraqi AA, Chen X, Alhammadi MS (2023) Quantitative and qualitative condylar changes following stabilization splint therapy in patients with temporomandibular joint disorders. *Clinical Oral Investigations* 1-12.
- Nota A, Ryakhovsky AN, Bosco F, Tecco S (2021) A full digital workflow to design and mill a splint for a patient with temporomandibular joint disorder. *Applied Sciences* 11:372.
- Orzeszek S, Waliszewska-Prosol M, Ettlin D, Seweryn P, Straburzynski M, Martelletti P Jr AJ, Wieckiewicz M (2023) Efficiency of occlusal splint therapy on orofacial muscle pain reduction: a systematic.
- Ram HK, Shah DN (2021) Comparative evaluation of occlusal splint therapy and muscle energy technique in the management of temporomandibular disorders: A randomized controlled clinical trial. *The Journal of Indian Prosthodontic Society* 21:356-365.
- Sabhlok A, Gupta S, Girish M, Ramesh KV, Shrivastava H, Hota S (2021) Practice of occlusal splint therapy for treating temporomandibular disorders by general dentists of Jabalpur – A cross-sectional survey. *J Pharm Bioall Sci* 2021:1079-83.
- Saccomanno S, Saran S, De Luca M, Mastrapasqua RF, Raffaelli L, Levrini L (2022) The Influence of SARS-CoV-2 Pandemic on TMJ Disorders, OSAS, and BMI International. *Journal of Environmental Research and Public Health* 19:7154.
- Sajjanar J, Soni M, Gade J, Agrawal M, Sajjanar AB (2021) Awareness and Knowledge of General Dental Practitioners in Central India Towards Management of Patients with Temporomandibular Disorder: A Questionnaire-based Survey. *Journal of Clinical & Diagnostic Research* 15.
- Sam P, Dhanraj M, Jain AR (2018) Treatment of temporomandibular disorders-Knowledge, attitude, and practice among general practicing dentists-A survey. *Drug Invention Today* 10
- Sim HY, Kim HS, Jung DU, Lee H, Han YS, Han K, Yun KI (2019) Investigation of the association between orthodontic treatment and temporomandibular joint pain and dysfunction in the South Korean population *The Korean Journal of Orthodontics* 49:181-187.
- Sinclair A, Wieckiewicz M, Ettlin D, Junior R, Guimarães AS, Gomes M, Meira e Cruz M (2022) Temporomandibular disorders in patients with the polysomnographic diagnosis of sleep bruxism: a case-control study. *Sleep and Breathing* 1-8.
- Sullivan DP, Martin PR, Boschen MJ, Bandarian-Balooch S (2022) Dysfunctional sleep beliefs and behaviours: Psychological factors in sleep-related headaches. *Behaviour Research and Therapy* 153:104094.
- Thambar S, Kulkarni S, Armstrong S, Nikolarakos D (2020) Botulinum toxin in the management of temporomandibular disorders: a systematic review. *British Journal of Oral and Maxillofacial Surgery* 58:508-519.

In vitro comparative assessment of the denture cleansers effectiveness on the surface hardness of permanent silicone denture line



Nidhi Srivastava^a  | Shalabh Kumar^b | Upendra Sharma US^c

^aMaharishi University of Information Technology, Lucknow, Uttar Pradesh, India, Associate Professor, School of Science and Humanities.

^bTeerthanker Mahaveer University, Moradabad, Uttar Pradesh, India, Department of Prosthodontics and Crown & Bridge.

^cJain (Deemed-to-be University), Bangalore, India, Assistant Professor, Department of Life Sciences.

Abstract The purpose of the current research was to evaluate the impact of various denture cleaners on the surface hardness of permanent silicone denture lines. In the present study, 124 specimens were included comprising of soft liners made of permanent silicone, which were made from the 15 mm x 10 mm custom metal mold dimensions, where 62 samples were made of Molossil™ and 62 other of Voco™ which are commercially available liners for permanent dentures. These samples were then divided into 4 groups of equal specimen numbers (n=32) depending on the cleansing treatments. Group I specimens were cleaned with water daily, and Group II Polident™ Group III was given Secure™ denture cleaning solution, while Group IV was given Periogard™ denture cleaning solution. The samples were assessed at 1st week, 1st month, and 6th month after cleanser use. The study results showed that at the 6th-month follow-up after the use of denture cleansers, all of the samples had considerably increased surface hardness compared to the baseline. Statistically significant results were seen with Periogard™, Secure™, and Polident™ compared to Group I controls. In Voco™ denture liners, minor changes were seen compared to Molossil™ soft liners with time in all the groups. The results of this investigation are significantly well cleansing action is seen with Voco™ soft denture lining material compared to Molossil™ soft denture lining material, and surface hardness is least affected by Polident™ denture cleanser compared to Secure™ and Periogard™ denture cleansing agents.

Keywords: cleansing agents, denture cleansers, shore a durometer, soft liners, surface hardness

1. Introduction

For the rehabilitation of completely and partially edentulous subjects, removable dentures are a widely used and accepted modality. A removable denture, whether partial or complete, transmits the forces by the mucous membrane to the underlying bone and largely depends on the tissue support for this force transmission. Owing to the presence of a thin mucous membrane, few areas are responsive to pressure exerted by the durable prosthetics on them. Mastication services are transmitted straight to the core bone after the absorbing shock capacity of the mucous membrane is surpassed. Dentures are prone to plaque, stains, the build-up of germs, and food particles, whether they are made of acrylic or another substance. Regular cleaning with a suitable denture cleaner aid in removing these deposits, getting rid of smells, and maintaining the look and performance of the dentures. This leads to increased stress on the residual ridge. In such cases, an absorbent coating on the component of the denture that comes in close proximity to the oral mucosa is formed with soft lining materials, leading to the transmission of fewer forces to the underlying bone (Khan et al 2022).

Denture cleaners come in a variety of formats, including tablets, powders, pastes, solutions, and solutions. To successfully remove stains, plaque, and germs from the denture surface, they are created with a mix of cleaning chemicals, disinfectants, and sometimes abrasive materials (Zhang et al 2022). However, the use of these soft lining materials presents clinicians with more problems, including porosity, color alterations, resiliency loss, and weakened bonds between dentures and lining materials. The resiliency loss can be due to the plasticizer and other elements leaking out. Additionally, the absorption of water in the denture until equilibrium is attained leads to an increase in the surface roughness of resilient denture liners (Rocha et al 2021).

The Shore A durometer is a measuring tool used to assess the stiffness or hardness of various materials, notably flexible plastics and elastomers. It offers a number that represents the material's resistance to being indented or penetrated by an indenter of a certain size and form. A specialized durometer gauge with a spring-loaded indenter and a blunt tip is used to conduct a Shore A durometer test. The gauge is applied to the surface of the material with a consistent amount of pressure, and the depth of the indentation is measured and shown on a scale in durometer units (Bartsch et al 2023). Plaque



control refers to the techniques and routines used to stop dental plaque from building up on teeth and gums. Dental plaque is a biofilm that adheres to tooth surfaces and gumlines and is made up of bacteria, saliva, and food particles. Plaque may cause dental issues, including tooth decay, gum disease, and poor breath, if it is not efficiently eliminated. Brushing, flossing, mouthwashing, a healthy diet, and regular dental appointments are all necessary for effective plaque management (Curto-Manrique et al (2019)). Plaque control in dentures using different chemical and mechanical control methods is vital to maintain good oral hygiene in denture wearers. In subjects with soft denture liners, mechanical plaque control measures are not advised because they can lead to damage to resiliency (Valkenburg et al 2019). The first choice for these soft denture liners is chemical plaque control agents such as denture cleansers. Denture cleansers help in cleaning when they are dentures outside the mouth. The purpose of denture cleaners is to control microorganisms on dentures, especially *C. albicans*, which, in turn, decreases the incidence of denture stomatitis (Saito et al 2020).

The objective of the current study is to evaluate the impact of various commercially available denture cleaners on the surface roughness of permanent silicone denture liners. The brands used in the present study were Mollosil™ and Voco™, whereas the denture cleansers used were PerioGuard™, Secure™, and Polident™. A surface toughness gauge (Shore A Durometer) was used to determine the surface hardness of the materials used.

Brown et al (2022) examined the effectiveness of brushing using a commercial denture cleaner. Using the Miles and Misra method, all treatment parameters were analyzed to identify live colony-forming units of bacteria and fungus, and images were captured using confocal laser scanning microscopy (CLSM). Over a period of seven days, daily DC therapy was the most successful in lowering the viable biofilm. Alfouzan et al (2021) examined the color durability in vitro of light-cured, heat-cured, and freshly invented prepolymerized computer-aided design (CAD) or computer-aided manufacturing (CAM) materials for acrylic resin bases once exposed to mechanical dental cleanings and chemical denture cleaners. Two heat-cured and prepolymerized polymethyl methacrylate (PMMA) and single urethane dimethacrylate-derived denture bases made of resin were exposed to mechanical brushing, chemical denture cleaners, and thermal cycling to replicate one year of typical prosthesis wear. The baseline and final color were determined using a benchtop UV light visible spectrophotometer; the assessments were made, and the color variance was then computed. Kaypetch et al (2023) examined the antimicrobial effects of a new vinegar-based denture cleaning solution on oral *Streptococci* and *Candida* species as well as the inhibitory effects on already-formed bacterial and *Candida* biofilms on denture bases. The time kill test and biofilm developed on denture bases were used to assess the antibacterial activity of the new vinegar solution. Coimbra et al (2021) determined the effectiveness of peroxide-based solutions for eliminating multispecies biofilms from denture base acrylic resin surfaces and for lowering the survival and metabolic activity of these biofilms. Herdman et al (2022) determined whether it would be feasible to create a cost-effectiveness model to evaluate denture washing techniques intended to avoid a user with dentures developing denture stomatitis viewpoints in the UK. To determine and gauge the costs and effects of three denture cleaning techniques, a model was created. Hidayati et al (2023) sought to ascertain the efficacy of employing tobacco leaf paste as denture cleaning to reduce the roughness of the surfaces of heat-cured acrylic resin (HCAR). Thirty-six samples were separated into 4 groups for this experimental laboratory investigation, with the posttest-only control group method being employed. The control group was brushed without toothpaste, Group A was brushed with HPAI herbal toothpaste, Group B was brushed with 50% tobacco leaf paste, and Group C was brushed with 75% TLP. When employed as an obturator material, silicon soft denture liner (SDL) and heat polymerization acrylic resin (PMMA) are often utilized because they can easily and permanently fill the undercut region of a wide defect. Despite this, the molecular structures of PMMA and silicon SDL vary, resulting in poor bond strengths for both materials. It is necessary to strengthen the binding between PMMA and SDL since prolonged usage may have an impact on the bond strength. Treatment of the surface is a technique to boost the bond strength (Chairunnisa 2023). Rajendran et al (2022) determined the optimum cleaning technique for removable partial dentures (RPDs) by measuring how well three different cleaning techniques can control *Candida* counts in RPD users.

2. Materials and Methods

The objective of the current study was to evaluate the impact of three commercially available denture cleaners on the surface hardness of permanent silicone denture liners. The study was carried out at the Department of Prosthodontics and Crown and Bridges of the Institute.

The present study used two commonly used resilient silicon-based liners in a total of 124 samples that were organized with a customized steel mold with dimensions of 15×10 mm. The manipulation of the soft-denture materials utilized instructions by the producer. After manipulation and setting of the materials, samples were removed, and excess material was trimmed. Throughout the study duration, the samples were kept immersed in synthetic saliva. The specimens were then divided into 4 groups of 32 subjects, each depending upon the cleansing treatments where Group I served as the control, Group II Polident™ Group III was given Secure™ denture cleaning solution, and Group IV was given PerioGuard™ denture cleaning solution. Furthermore, each group was broken down into two smaller groups of 16 subjects, each that was tested during the first week, first month, and sixth month after the use of the cleanser.

The cleansers were dissolved in water before use, following the instructions by the manufacturers. Group I specimens were immersed in water, Group II in Polident™ denture cleansing solution, Group III in Secure™ solution for cleaning

dentures, and Group IV in Periogard™ solution for cleaning dentures daily for 8 hours, followed by rinsing in the water for the rest of the day. Specimens were kept immersed in artificial saliva at room temperature.

The subgroup specimens were evaluated in the first week, first month, and sixth month for denture hardness using Shore a Durometer at a force of 8 N or 822 gf. The durometer had a blunt-point indenter with a scale (0-100 Shore A unit) using a lever arrangement. The greater the penetration of the indenter into the specimen depicted, the lower the toughness values. The highest reading was noted after the shaft was dropped to the center of the specimen.

The data gathered were statistically evaluated using SPSS software version 21 (Chicago, IL, USA) to create the findings. Data are presented as percentages and numbers, as well as their means and standard deviations. $P < 0.05$ was used as the significance threshold.

3. Results

This study's objective was to determine the impact of three different commercially available denture cleansers on the hardness of the surface of permanent silicone denture liners. The 124 study specimens were then divided into 4 groups of 32 subjects, each depending upon the cleansing treatments where Group I served control, Group II Polident™ cleaning solution for dentures, Group III with Secure™ cleaning solution for dentures, and Group IV with Periogard™ cleaning solution for dentures. Furthermore, each group was broken down into two smaller groups of 16 subjects, each that was tested during the first week, first month, and sixth month after the use of the cleanser. The ingredients of the three cleansers used are depicted in Table 1. Periogard had glycerine, propylene glycol, and chlorhexidine gluconate; secure had sodium perorate monohydrate, trisodium phosphate, and sodium bicarbonate; and Polident had tetraacetythylenediamine, sodium percarbonate, and potassium monopersulfate.

The study results showed that in Mollosil soft liners, the highest average surface hardness was seen for Periogard, followed by Polident, and the lowest values were seen for secure denture cleansers. This distinction was statistically significant at $p < 0.005$. For Mollosil, in the 1st week, no quantitatively significant difference in the hardness was seen for any group. However, in the 1st month, Periogard and Secure had surface hardness showing a statistically significant difference with $p < 0.005$. In the 6th month, all the surfaces showed significant differences in the mean surface hardness with $p < 0.005$ except for Polident and Group I control.

On comparing the surface roughness in two denture materials, Voco and Mollosil, it was seen that in the control group, the values were higher for the Mollosil group compared to Voco, which were statistically nonsignificant in the 1st week, 1st month, and 6th month with appropriate p values of 1.000, 0.414, and 0.492, respectively. For the Polident group, the values were significantly higher for Mollosil, which were 21.6 ± 0.546 , 24.6 ± 0.839 , and 30.02 ± 0.709 for Mollosil at the 1st week, 1st month, and 6th month, respectively, with appropriate p values of 0.02, 0.004, and < 0.001 . Figures 1 to 4 depict the control, secure, polident, and periogard groups of surface hardness in two denture materials. For Secure, the values were significantly higher for Mollosil in the 1st week and 1st month, with values of 21.6 ± 0.546 and 24.6 ± 1.16 and p values of 0.05. For a period, the value was significantly higher for Mollosil in the 6th month only, with a value of 35.8 ± 1.675 , and the p value was 0.01, which was 32.02 ± 2.02 for Voco (Table 2). Tables 3 to 6 denote the surface hardness of the two denture materials.

3.1. Discussion

The goal of the present research is to evaluate the impact of three different commercially available cleaners for dentures on the surface roughness of permanent silicone denture liners. The 124 study specimens were then divided into 4 groups of 32 subjects, each depending upon the cleansing treatments where Group I served control, Group II Polident™ solution for cleaning dentures, Group III with Secure™ solution for cleaning dentures, and Group IV with Periogard™ solution for cleaning dentures. Furthermore, each group was broken down into two smaller groups of 16 subjects, each that was tested during the first week, first month, and sixth month after the use of the cleanser. The ingredients of the three cleansers used are depicted in Table 1. Periogard had glycerine, propylene glycol, and chlorhexidine gluconate; secure had sodium perorate monohydrate, trisodium phosphate, and sodium bicarbonate; and Polident had tetraacetythylenediamine, sodium percarbonate, and potassium monopersulfate. These materials used were similar to the research of (Sameeh et al 2021) and (Kreve and Dos Reis, (2019), where authors used similar denture cleansers as in the present study.

The results of the present study showed that in Mollosil soft liners, the highest mean value of surface hardness was seen for Periogard, followed by Polident, and the lowest values were seen for secure denture cleansers. This difference was statistically significant, with $p < 0.005$. For Mollosil, in the 1st week, no statistically significant difference in the hardness was seen for any group. However, in the 1st month, Periogard and Secure had surface hardness showing a statistically significant difference with $p < 0.005$. In the 6th month, all the surfaces showed significant differences in the mean surface hardness with $p < 0.005$ except for Polident and Group I control. These results were consistent with the studies of (Tasopoulos et al 2023) and (Ghomi et al 2020), where the authors reported a higher surface hardness of Periogard, followed by Polident and Secure.

Table 1 Composition of three denture cleansers used in the present study.

S. No	Brand Name	Ingredients
1.	Periogard	
a)		Glycerin
b)		Propylene Glycol
c)		Chlorhexidine Gluconate
2.	Secure	
3.		Sodium perorate monohydrate
4.		Trisodium phosphate
5.		Sodium bicarbonate
6.	Polident	
7.		Tetraacetythylenediamine
8.		Sodium percarbonate
9.		Potassium monopersulfate

Table 2 Comparison of surface hardness in two denture materials.

S. No	Groups	Subgroups Voco	Subgroups Mollosil	p value
1.	Control			
2.	1 st week	20.6±0.546	20.6±1.12	1.000
3.	1 st month	25.4±1.306	25.6±0.839	0.414
4.	6 th month	31.4±1.485	31.6±1.097	0.492
5.	Polident			
6.	1 st week	20.4±0.839	21.6±0.546	0.02
7.	1 st month	22.8±0.896	24.6±0.839	0.004
8.	6 th month	26.6±0.839	30.02±0.709	<0.001
9.	Secure			
10.	1 st week	20.8±0.546	21.6±0.546	0.05
11.	1 st month	22.6±1.097	24.6±1.16	0.05
12.	6 th month	27.4±0.839	27.8±0.896	0.488
13.	Periogard			
14.	1 st week	21.4±1.097	21.6±1.16	0.786
15.	1 st month	26.02±0.709	26.6±1.16	0.526
16.	6 th month	32.02±2.02	35.8±1.675	0.01

Table 3 Results of the control groups in two denture materials.

Control Group	Value	
	Subgroups Voco	Subgroups Mollosil
1st Week	21.146	21.72
1st Month	26.706	26.439
6th Month	32.885	32.697

Table 4 Result of Polident groups in two denture materials.

Polident Group	Value	
	Subgroups Voco	Subgroups Mollosil
1st Week	21.239	22.146
1st Month	23.696	25.439
6th Month	27.439	30.729

Table 5 Result of secure groups in two denture materials.

Secure Group	Value	
	Subgroups Voco	Subgroups Mollosil
1st Week	21.346	22.146
1st Month	23.697	25.76
6th Month	28.696	28.696

Table 6 Results for the two denture materials in the Periogard groups.

Secure Group	Value	
	Subgroups Voco	Subgroups Mollosil
1st Week	21.346	22.146
1st Month	23.697	25.76
6th Month	28.696	28.696



Concerning the comparison of the surface roughness in two denture materials, Voco and Mollosil, it was seen that in the control group, the values were higher for the Mollosil group compared to Voco, which were statistically nonsignificant in the 1st week, 1st month, and 6th month, corresponding to p values of 1.000, 0.414, and 0.492, respectively. For the Polident group, the values were significantly higher for Mollosil, which were 21.6 ± 0.546 , 24.6 ± 0.839 , and 30.02 ± 0.709 for Mollosil at the 1st week, 1st month, and 6th month, respectively, with appropriate p values of 0.02, 0.004, and <0.001 . For Secure, the values were significantly higher for Mollosil at the 1st week and 1st month, with values of 21.6 ± 0.546 and 24.6 ± 1.16 and p values of 0.05. For periogard, the value was significantly higher for Mollosil in the 6th month only with a value of 35.8 ± 1.675 , and the p value was 0.01, which was 32.02 ± 2.02 for Voco. These outcomes matched the conclusions of (Babu et al 2017) and (Alsaggaf et al 2020), where higher surface roughness was reported with Mollosil compared to Voco, which was similar to the present study.

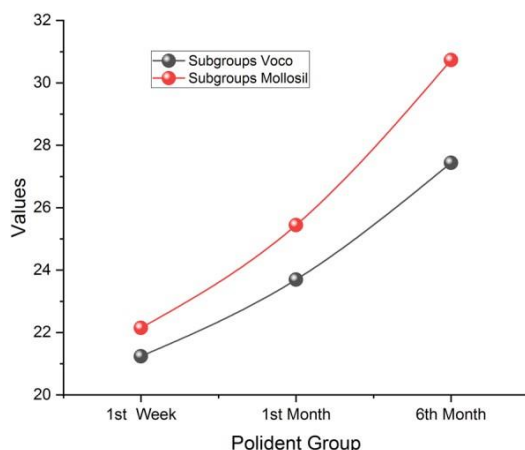


Figure 2 Polident groups of surface hardness in two denture materials.

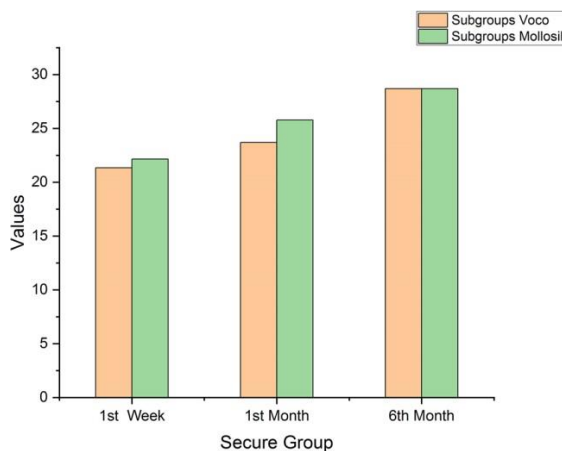


Figure 3 Secure groups of surface hardness in two denture materials.

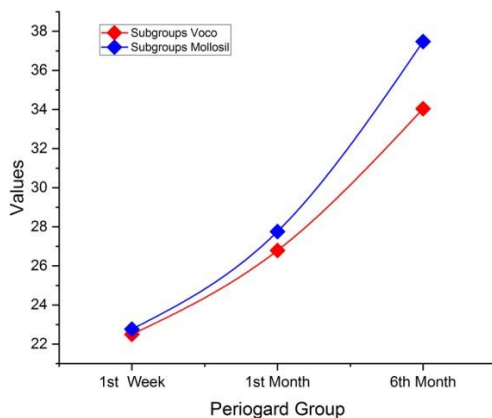


Figure 4 Periogard groups of surface hardness in two denture materials.



4. Conclusions

The present study concludes that significantly better cleansing action is seen with Voco™ soft denture lining material compared to Mollosil™ soft denture lining material, and surface hardness is least affected by Polident™ denture cleanser compared to Secure™ and Periogard™ denture cleansing agents. Better compatibility was seen with Voco compared to Mollosil. The findings of this research help to provide evidence-based dental care, empowering both denture users and dental professionals to choose the best denture cleaners. The lifetime of dentures can be maintained, oral health problems related to dirty dentures can be avoided, and optimum oral hygiene may be achieved by knowing the relative efficacy of various cleaners.

Ethical considerations

Not applicable.

Declaration of interest

The authors declare no conflicts of interest.

Funding

This research did not receive any financial support.

References

- Alfouzan AF, AlNouwaisar AN, AlAzzam NF, Al-Otaibi HN, Labban N, Alswaidan MH, Al Taweel SM, Alshehri HA (2021) Power brushing and chemical denture cleansers induced color changes in prepolymerized CAD/CAM denture acrylic resins. *Materials Research Express* 8:085402.
- Alsaggaf A, Fenlon MR (2020) A case-control study to investigate the effects of denture wear on residual alveolar ridge resorption in edentulous patients. *J Dent* 98:103373.
- Babu BD, Jain V, Pruthi G, Mangtani N, Pillai RS (2017) Effect of denture soft liner on mandibular ridge resorption in complete denture wearers after 6 and 12 months of denture insertion: A prospective randomized clinical study. *The Journal of the Indian Prosthodontic Society* 17:233.
- Bartsch K, Brandl A, Weber P, Wilke J, Bensamoun SF, Bauermeister W, Klingler W, Schleip R (2023) Assessing reliability and validity of different stiffness measurement tools on a multi-layered phantom tissue model. *Scientific Reports* 13:815.
- Brown JL, Young T, McCloud E, Butcher MC, Bradshaw D, Pratten JR, Ramage G (2022) An in vitro evaluation of denture cleansing regimens against a polymicrobial denture biofilm model. *Antibiotics* 11:113.
- Chairunnisa R (2023) The Effect of Surface Treatment And Thermocycling On Bond Strength Between Silicon Soft Denture Lining And Acrylic Resin Denture Base. *Journal of Pharmaceutical Negative Results* 14.
- Coimbra FC, Rocha MM, Oliveira VC, Macedo AP, Pagnano VO, Silva-Lovato CH, Paranhos HDF (2021) Antimicrobial activity of effervescent denture tablets on multispecies biofilms. *Gerodontology* 38:87-94.
- Curto-Manrique J, Malpartida-Carrillo V, Arriola-Guillén LE (2019) Efficacy of the lift-the-lip technique for dental plaque removal in preschool children. *Journal of Indian Society of Pedodontics and Preventive Dentistry* 37:162-166.
- Ghomi AJ, Soufdoost RS, Barzegar MS, Hemmati MA (2020) Oral rehabilitation with removable partial denture of a patient with cleidocranial dysplasia. *Case Reports in Dentistry* 2020.
- Herdman M, Johnson I, Mason S, Vernazza CR, Varghese R (2022) Development of a United Kingdom-centric cost-effectiveness model for denture cleaning strategies. *The Journal of Prosthetic Dentistry* 127:266-e1.
- Hidayati L, Parnaadji R, Malika KN (2023) The effectivity of tobacco leaf paste as denture cleanser to surface roughness of heat cured acrylic resin. *Makassar Dental Journal* 12:53-56.
- Kaypetch R, Anuwongnukroh N, Dechkunakorn S, Wichai W, Tua-Ngam P, Tantivitayakul P, Shrestha B (2023) Novel vinegar solution for denture-cleansing agent. *Journal of Oral Science* 65:117-120.
- Khan G, Roghani K, Muhammad N, Liaqat S, Khan MA (2022) Advancements in Polymeric Denture Lining Materials. In *Applications of Polymers in Surgery: Materials Research Forum LLC*, pp 175-194.
- Kreve S, Dos Reis AC (2019) Denture liners: A systematic review relative to adhesion and mechanical properties. *The scientific world journal* 2019.
- Rajendran A, George R, Mathew N, Ranjith M, Nazar NA (2022) Comparative evaluation of efficacy of three different denture cleansing methods in reducing *Candida albicans* count in removable partial denture wearers: A randomized controlled trial. *The Journal of Indian Prosthodontic Society* 22:256-261.
- Rocha MM, Carvalho AM, Coimbra FCT, Arruda CNFD, Oliveira VDC, Macedo AP, Silva-Lovato CH, Pagnano VO, Paranhos HDFO (2021) Complete denture hygiene solutions: antibiofilm activity and effects on physical and mechanical properties of acrylic resin. *Journal of Applied Oral Science* 29.
- Saito T, Wada T, Kubo K, Ueda T, Sakurai K (2020) Effect of mechanical and chemical cleaning on surface roughness of silicone soft relining material. *Journal of prosthodontic research* 64:373-379.
- Sameeh MA, Jyothsna MK, Nidhin R, Manohar P, Sreedevi S, Sasikumar TP (2021) Comparative evaluation of the effectiveness of denture cleansers on surface hardness of permanent silicone denture liners—An In vitro study. *Journal of Pharmacy & Bioallied Sciences* 13:S1102.
- Tasopoulos T, Vrioni G, Naka O, Diamantatou T, Zoidis P, Tsakris A (2023) Adherence of *Candida albicans* to Five Long-Term Silicone-Based Denture Lining Materials Bonded to CAD-CAM Denture Base. *Journal of Prosthodontics* 32:292-297.



Valkenburg C, Van der Weijden FA, Slot DE (2019) Plaque control and reduction of gingivitis: The evidence for dentifrices. *Periodontology 2000*, 79:221-232.

Zhang K, Zhang S, Shi Y, Zhang L, Fu B (2022) Effects of disinfectants on physical properties of denture base resins: A systematic review and meta-analysis. *The Journal of Prosthetic Dentistry*.

Determination of the retentive ability of different luting agents in titanium abutments on implant-supported crowns



Prakash Deep^a | Madhurima Sharma^b | Suhas Balla^c

^aMaharishi University of Information Technology, Lucknow, Uttar Pradesh, India, Associate Professor, School of Science and Humanities.

^bTeerthanker Mahaveer University, Moradabad, Uttar Pradesh, India, Professor, Department of Prosthodontics and Crown & Bridge.

^cJain (Deemed-to-be University), Bangalore, India, Assistant Professor, Department of Chemistry.

Abstract Implant-supported crowns are either cement-retained or screw-retained. Recently, function and esthetics have been given major focus as advances in implants have greatly improved the longevity of implant restoration. Superior esthetics is seen with cement-retained restoration and is more preferred. However, it is a controversial topic to select the ideal cement type for luting the implant-supported crown. The present study aimed to assess the retentive ability of different luting agents in titanium abutments on implant-supported crowns. The study assessed 60 samples divided into 3 groups of 20 subjects each where luting was done with three different types of cement, namely glass ionomer cement, zinc polycarboxylate, and zinc phosphate, respectively. A testing machine was used to assess the retentive strength of the three types of cement. The study results conclude that the highest retentive strength is seen with zinc polycarboxylate cement, followed by the glass ionomer and zinc phosphate cement.

Keywords: implant-supported crowns, luting agents, luting cement, retention, retentive ability

1. Introduction

The major mode of retention for dental implants was retention by the screws at the time when dental implants were introduced initially. At that time, the esthetics and occlusion were not given adequate attention and were compromised to compensate for the retention (Kapoor et al 2016). This was done owing to the poor rates of success associated with dental implants when dental implants were emerging. Another factor attributed was a need for surgery in cases with osseointegration failure and to repair the fractured parts of the prosthesis. It is important to remember that a number of elements, including abutment surface preparation, cement thickness, the fit of the crown, and occlusal stresses, may affect how well luting agents retain dental materials. Additionally, the total retention may vary depending on the composition of the substance and the cementing method utilized (Alvarez-Arenal et al 2016).

However, with the advances in the techniques and knowledge of implant dentistry, a rapid improvement was seen in the success rates of the implants with a significantly reduced need for crown retrieval (Saleh and Taşar-Faruk, 2019). Dental cement, commonly referred to as luting agents, is essential to the titanium abutments' final cementation procedure. Between the abutment and the prosthesis, they act as a bonding agent, giving the restoration stability, sealing, and retention. The appearance, robustness, and long-term achievement of the implant-supported prosthesis may also be impacted by luting chemicals. To replace the missing teeth, cement-retained crowns were then introduced with superior esthetics and optimal occlusion in comparison to the screw-retained prosthesis (Leung et al 2022).

Various factors affect the degree of retention for cement-retained prosthesis, including the type of cement used, roughness or surface finish, height and surface area, and the parallelism and the taper (Pjetursson et al 2022). For retention of the crowns on dental implants, definitive cement is not preferred as they make it difficult to retrieve the crown owing to its strongness (Kraus et al 2021). The long wall of abutment and ideal taper govern the provisional cement use for retention of the crowns over dental implants for a longer duration (Nastri et al 2021). However, further studies are needed to confirm the cement retention and to develop the cement specific to the implant-supported prosthesis (Strauss et al 2021). Consequently, this study's goal was to assess the retention ability of various luting agents used in titanium abutments on implant-supported crowns. In dental implantology, titanium abutments are often utilized as a dependable method of sustaining prosthetic restorations. These abutments serve as the link between the final crown or bridge and the dental implant. The right choice of luting chemicals is essential for a successful and long-lasting repair. For the present study, tensile strength was determined for the three different luting types of cement, including zinc polycarboxylate, zinc phosphate, and Glass Ionomer Cement (GIC) cement, which are used commonly as luting agents on crowns placed on titanium abutments.



The tensile strength of the types of cement was assessed with the universal testing machine, followed by the comparison of the values.

Karaokutan and Ozel (2022) investigated how various two ceramics' shear bond strength to commercially pure titanium was impacted by surface modifications and the kind of luting agent used. Titanium and all-ceramic specimens' cementation surfaces received a universal priming treatment. Titanium was adhered to using self-cure and dual-cure resin-based luting agents, and two all-ceramic cubes discs were created from Zirconia-reinforced Lithium Silicate Ceramic (ZLC) and Lithium Disilicate Ceramic (LDC). Rosas et al (2019) assessed the Marginal Discrepancy (MD) on the three luting agents on the calcinable copings in cemented prosthetic abutments. The titanium abutment's margin of preparation and the cast cylinder's free edge was used as the measurement points, and statistical significance levels were used to determine the measurement's accuracy. A titanium base and ceramic coping are the two halves of a two-part abutment. Mechanical strength is one of the main factors influencing their long-term success. A two-part implant abutment's retaining forces were the subject of the current study's investigation. A variety of surface treatments and resin-based luting agents were used on ceramic copings made of zirconia and lithium disilicate in the research (Freifrau et al 2019). Lugas et al (2020) the retrievability of dental prostheses attached to implants was examined while taking into account two of the most important issues that dentists must address: the geometry of the abutments and the luting agent. To replicate the retrievability of crowns in clinical settings, impulsive pressures were applied to dental bridge models. During each test, the number of impulses and the force with which they were given were counted and utilized as retrievability indices. The case's objective was to determine the persistence of specifically made-for-implant cement in addition to contrasting it using the widely used dental cement for implant systems. Abutments made of titanium were attached to auto-polymerizing acrylic resin blocks with twenty implant analogs placed within. The means and SDs of loads for cement failure were examined using the Bonferroni and ANOVA tests (Ahsan et al 2020).

Soares et al (2022) compared the capacity of various monolithic or bilayer ceramic materials of varying thicknesses to conceal surfaces designated for implant replacements using opaque and transparent assessment pastes. Ausiello et al (2023) assessed the effects of novel resin-based CAD-CAM implant-supported materials on stress and strain concentrations during posterior crown repair. All reliable models were imported into the engineering software that uses computers and subjected to a stress and strain finite element analysis. According to the manufacturer's information, material attributes were given to each solid with homogeneous and isotropic behavior. Zhang et al (2023) were to describe the occlusal variance of crowns supported only by a single posterior implant that had mild or no occlusion.

2. Materials and Methods

The purpose of the current investigation was to the retentive ability of different luting agents used in titanium abutments on implant-supported crowns. The study samples were comprised of the Department of Prosthodontics, crowns, and bridges of the Institute.

For the present study, 60 samples of 8mm height were taken and divided into 3 groups of 20 samples, each randomly. In an acrylic resin block, abutments were attached to the lab analogs, 1 mm above the margin. In the resin block, lab analogs were placed in a parallel manner with the dental surveyor. This was followed by tightening the abutments on their respective analogs at a torque of 35 N/cm using a wrench. Wax copings were made with the inlay wax with the addition of the wax rings on the occlusal surface of the wax copings to help remove the casting with the universal testing machine.

The study specimens were then invested in the investment material bonded with phosphate, and the casting was done in the base metal alloy. The copings were then placed on the abutments and were tested for adequate fit visually. In cases where misfit or marginal discrepancy was noted, the castings were repeated for those samples. Abutments and crowns were then cleaned. In the 3 groups, Group I samples were luted with the glass ionomer cement (GIC from GC Corp.); Group II specimens with zinc polycarboxylate (Dentsply), and Group III with zinc phosphate cement (Dentsply). All the 3 Cement kinds were combined following the instructions of the manufacturer, followed by crown cementation. After placing the copings on the abutments, the pressure was applied for 10 seconds using the finger, after which a weight of 6 kg was added; wait 10 minutes with the universal testing machine. With the explorer, the excess cement was removed, and the specimens were placed in artificial saliva for 24 hours at a temperature of 37°C. The tensile strength of the sample was evaluated then with a universal testing machine.

At a crosshead speed of 0.5mm/min and 500 kg load cell, tensile strength was tested for each study specimen with the universal testing machine. Crowns were removed from the abutment, and the final tensile strength was recorded when the cement failure occurred. The tensile strength was recorded by Newton.

ANOVA was used to statistically evaluate the collected data (analysis of variance) and Turkey's post hoc analysis with SPSS software version 19, IBM Company, Armonk, New York, USA. The importance levels were maintained at $p < 0.05$.

3. Results

The purpose of the current investigation was to the retentive ability of different luting agents used in titanium abutments on implant-supported crowns. For the present study, 60 samples of 8mm height were taken and divided into 3 groups of 20 samples each randomly. In the 3 groups, Group I samples were luted with the glass ionomer cement (GIC from GC Corp.), Group II specimens with zinc polycarboxylate (Dentsply), and Group III with zinc phosphate cement (Dentsply). On assessing the mean tensile strength of the three types of cement used, it was discovered in the current investigation that the mean strength was highest for zinc polycarboxylate cement with 631.804 ± 48.726 N followed by 472.018 ± 55.983 N for GIC and was least for zinc phosphate with 280.434000 ± 40.875 N. The upper bound for GIC, zinc polycarboxylate, and zinc phosphate was 513.498, 658.0.92, and 311.106, respectively, at 95% CI, whereas the lower bound was 430.537, 585.515, and 249.761 respectively, as shown in Table 1, figure 1 and figure 2 depicts the minimum and maximum strength of three luting cement.

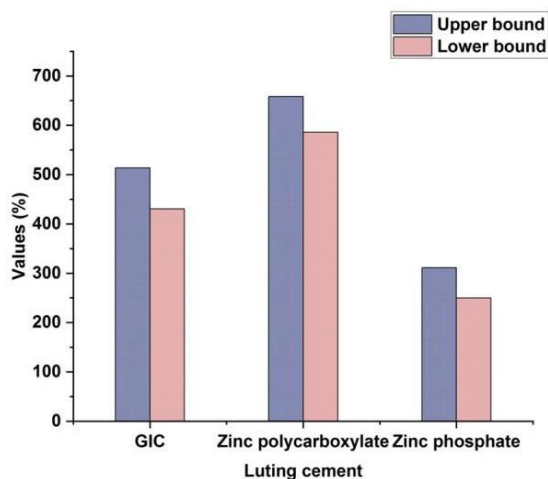


Figure 1 3 luting cement's average tensile strength.

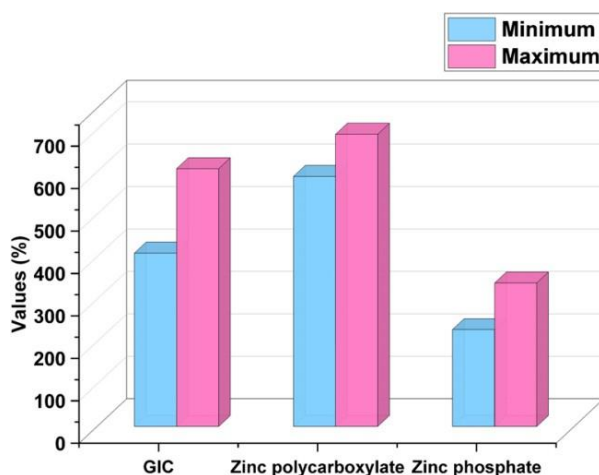


Figure 2 Mean Tensile minimum and maximum strength of 3 luting cement.

Table 1 Mean Tensile strength of 3 luting cement.

S. No	Cement	Mean± S. D	95% CI		Minimum	Maximum
			Upper bound	Lower bound		
1.	GIC	472.018±55.983	513.498	430.537	408.668	607.468
2.	Zinc polycarboxylate	631.804±48.726	658.092	585.515	589.168	688.678
3.	Zinc phosphate	280.434000±40.875	311.106	249.761	228.348	338.218

For the intergroup and intragroup comparison of the tensile strength among the three types of cement used in the study for luting the crowns on the titanium abutments, the study results are summarized in Table 2. It was noted that between the groups, the sum of squares was 583,577.171. Within the groups, the sum of squares was 67,965.146, and in the total study samples, the sum of squares was 653,544.319. The F value using the analysis of variance (ANOVA) was 110.984, and the p-value was 0.000, depicting the statistically significant difference (Table 2).



Table 2 ANOVA test for intergroup and intragroup comparison of tensile strength.

S. No	Groups	Sum of squares	F	p-value
1.	Between groups	583,577.171		
2.	Within groups	67,965.146	110.984	0.000
3.	Total	653,544.319		

In the intergroup comparison of the cement from one group to the cement from the other groups, Turkey's post hoc analysis was used. It was seen that for GIC, on comparison with zinc polycarboxylate, the mean difference was -147.784, the upper and lower bounds, respectively, were -204.229 and -91.338, and the p-value was 0.000. For GIC to zinc phosphate, the mean difference, upper bound, and lower bound were 189.582, 133.136, and 246.027, respectively, showing statistically significant results with p=0.000. For the comparison of Zinc polycarboxylate to GIC, the mean difference was 147.784 with a p-value of 0.000, showing a statistically significant result. Also, for zinc polycarboxylate to zinc phosphate, the mean difference and p-value were 339.368 and 0.000, respectively, depicting a statistically significant result. Concerning the intergroup comparison of zinc phosphate to GIC and zinc polycarboxylate, the difference was statistically significant, with p=0.000 for both. These results showed that the highest tensile strength was needed by zinc polycarboxylate to lead to cement failure compared to zinc phosphate and GIC (Table 3). Figure 3 and table 4 findings demonstrate that glass ionomer and zinc phosphate mean values were significantly outstripped by zinc polycarboxylate's mean value.

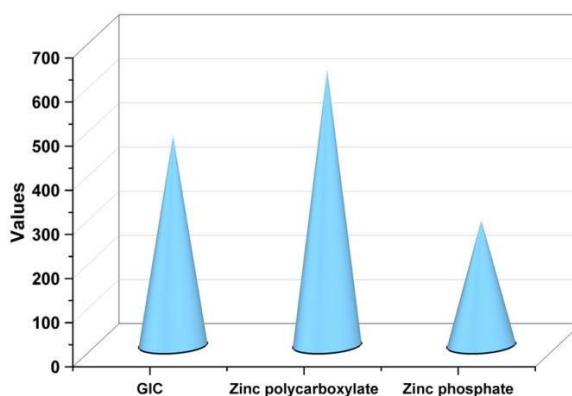


Figure 3 An average cement's tensile strength.

Table 3 Post hoc Turkey's analysis for intergroup comparison.

S. No	Groups	Comparison	Mean difference	p-value	95% CI	
					Upper bound	Lower bound
1.	GIC	Zinc polycarboxylate	-147.784	0.000	-204.229	-91.338
		Zinc phosphate	189.582	0.000	133.136	246.027
2.	Zinc polycarboxylate	GIC	147.784	0.000	91.338	204.229
		Zinc phosphate	339.368	0.000	282.922	395.813
3.	Zinc phosphate	GIC	-189.582	0.000	-246.027	-133.136
		Zinc polycarboxylate	-339.368	0.000	-395.813	-282.922

Table 4 An average cement's tensile strength.

S. No	Luting cement	Values
1.	GIC	475
2.	Zinc polycarboxylate	624.9
3.	Zinc phosphate	283.5

4. Discussion

The results of the present study showed that the highest retention is seen with the zinc polycarboxylate cement with 631.804 ± 48.726 N, followed by 472.018 ± 55.983 N for GIC and was the least for zinc phosphate with 280.434000 ± 40.875 N. The difference between the tensile strengths of the three groups was statistically significant, with p=0.000. The higher tensile strength for the zinc polycarboxylate compared to GIC and zinc phosphate can be attributed to the adhesive property associated with zinc polycarboxylate. While zinc polycarboxylate is setting, it has adhesiveness for the metal parts through the chelation of the metallic ions, as suggested by the previous study of (Jabbar and Alabodi, 2023).



It was also seen that the lowest retentive strength was noted with the zinc phosphate cement in the crowns placed on the implant titanium abutments in comparison to zinc polycarboxylate and GIC. This was similar to the results of the studies of Das et al (2023) and Ajay et al (2019) where less retentive ability was noted with the zinc phosphate cement.

The casting retention in the zinc phosphate cement is mainly caused by micromechanical interlocking into the irregularities on the abutment surface and to the castings, as reported by (Edachery et al 2021). This can be considered a vital fact for the prostheses retained by the cement. The author reported that cement gaining its casting retention and retentive ability from mechanical interlocking will have an increased roughness and more retention compared to adhesive cement. In the present study, the retentive strength was 472.018 ± 55.983 N which was lower when compared to zinc polycarboxylate, where the retentive strength was 631.804 ± 48.726 N. These findings were in line with earlier research (Ajay et al 2019; Reda et al 2021), where the writers reported the highest retentive strength with polycarboxylate cement compared to GIC and zinc phosphate used in the present study.

A vital factor in the selection of cement is the cement failure location. The cement failure in zinc phosphate and glass ionomer was mainly adhesive and is usually seen at the interface of cement and abutment. The retentive ability of the zinc phosphate is mainly by the micromechanical interlocking. The implant surface is comparatively smooth, causing the cement failure at the interface of crown and cement, as there were remains of zinc phosphate cement at the inner surface of the copings. No pre-treatment was done on the abutment or coping in the present study making the surface as inert as suggested by (Rengasamy et al 2023). Also, for GIC, the solubility was higher than the other cement, and the susceptibility was seen with the desiccation and the water contact in the initial stages that can drastically compromise the mechanical properties of the luting cement as reported by the previous studies (Kalla et al 2022).

For the zinc polycarboxylate cement, cohesive failure is usually seen. Cement was seen attached to both the coping and the abutment depicting that failure is usually seen within the cement. For polycarboxylate, cohesive failure can be attributed to the fact that higher bond strength to titanium abutments and high adhesion to the other casting alloys for the cement, as reported by (Saleh and Taşar-Faruk, 2019).

As in the present study, no modification was done on the abutment, and the surface was smooth, which could have been responsible for reduced micromechanical interlocking in the cement-abutment surface, leading to reduced values for cement retention. This can be the reason for failure in the adhesion of zinc phosphate and GIC, as reported by (Ebadian et al 2022). However, a chemical reaction can be seen with the inert surface of the abutment leading to the cohesive failure.

The limitations of the study are in-vitro nature which is not able to simulate the exact intra-oral condition due to thermocycling and storage in the water. Hence, further studies are warranted to assess the retentive ability of various types of cement in intra-oral environments.

4. Conclusions

Given its constraints, the current research comes to the conclusion that the highest retentive strength is seen with zinc polycarboxylate cement, followed by the GIC and zinc phosphate cement. The least tensile strength was seen with zinc phosphate cement, with a statistically significant difference. In cases with questionable implant prognosis, it is advised to use cement as a luting agent having lower tensile strength for the crown for crown retrieval. The clinical environment, restoration style, occlusal pressures, and clinician preference all have a role in the choice of luting agent. In order to get the best results, it is crucial to take into account the unique traits and indicators of each luting agent. The best luting agent for titanium abutments should be chosen depending on the requirements of each individual patient, and visiting a dental specialist or prosthodontist is strongly advised.

Ethical considerations

Not applicable.

Declaration of interest

The authors declare no conflicts of interest.

Funding

This research did not receive any financial support.

References

- Ahsan A, Khushboo B, Kumar A, Kumari S, Poojary B, Dixit A, Kumar A, Badiyani BK (2022) An In Vitro trial to estimate the retention ability of luting agents utilized with dental implant-supported prosthesis. *Journal of Pharmacy and Bioallied Sciences* 14:S541-S544.
- Ajay R, Rakshagan V, Kamatchi M, SelvaBalaji A, Sivakumar JSK, Kumar MS (2019) Effect of Implant abutment acid etching on the retention of crowns luted with different cements: an in vitro comparative evaluation. *Journal of Pharmacy & Bioallied Sciences* 11:S360.
- Alvarez-Arenal A, Gonzalez-Gonzalez I, deLlanos-Lanchares H, Brizuela-Velasco A, Ellacuria-Echebarria J (2016) The selection criteria of temporary or

- permanent luting agents in implant-supported prostheses: In vitro study. *J Adv Prosthodont* 8:144-9.
- Ausiello P, Di Lauro AE, Tribst JPM, Watts DC (2023) Stress distribution in resin-based CAD-CAM implant-supported crowns. *dental materials* 39:114-122.
- Das A, Alqahtani FA, Abdulaziz F, AlFadel M, AlJabri R, Elkhyat T (2023) Impact of Different Implant Abutment Geometry on Retention of Implant-supported Cement Retained Prosthesis: A Comparative Study. *World Journal of Dentistry* 14:259-262.
- Ebadian B, Abbasi M, Karbasi M (2022) Shear Bond Strength of Dental Cements on Titanium Alloy: Use of Different Restorative Materials. *Majalah Kedokteran Bandung* 54:63-68.
- Edachery V, Shashank R, Kailas SV (2021) Influence of surface texture directionality and roughness on wettability, sliding angle, contact angle hysteresis, and lubricant entrapment capability. *Tribology International* 158:106932.
- Freifrau von Maltzahn N, Bernard S, Kohorst P (2019) Two-part implant abutments with titanium and ceramic components: Surface modification affects retention forces—An in-vitro study. *Clinical Oral Implants Research* 30:903-909.
- Jabbar N, Alabodi (2023) Development of the properties of zinc polycarboxylate cement used as a basis for dental fillings using Alumina nanoparticles. *Journal of Population Therapeutics and Clinical Pharmacology* 30:257-266.
- Kalla K, Arunachalam S, Behera SSP, Konchada J, Lankapalli S, Vaniseti L (2022) Effect of Surface Modifications on the Retention of Implant-supported Cement-retained Crowns with Short Abutments: An In Vitro Study. *The Journal of Contemporary Dental Practice* 22:1451-1456.
- Kapoor R, Singh K, Kaur S, Arora A (2016) Retention of implant-supported metal crowns cemented with different luting agents: A comparative in vitro study. *J Clin Diagn Res* 10:61-4.
- Karaokutan I, Ozel GS (2022) Effect of surface treatment and luting agent type on shear bond strength of titanium to ceramic materials. *The journal of advanced prosthodontics* 14:78.
- Kraus RD, Espuelas C, Hämmerle CH, Jung RE, Sailer I, Thoma DS (2022) Five-year randomized controlled clinical study comparing cemented and screw-retained zirconia-based implant-supported single crowns. *Clinical oral implants research* 33:537-547.
- Leung GKH, Wong AWY, Chu CH, Yu OY (2022) Update on dental luting materials. *Dentistry Journal* 10:208.
- Lugas AT, Terzini M, Zanetti EM, Schierano G, Manzella C, Baldi D, Bignardi C, Audenino AL (2020) In vitro simulation of dental implant bridges removal: Influence of luting agent and abutments geometry on retrievability. *Materials* 13:2797.
- Nastri L, Nucci L, Grassia V, Miraldi R (2021) Aesthetic outcomes and peri-implant health of angled screw retained implant restorations compared with cement retained crowns: medium term follow-up. *Journal of Functional Biomaterials* 12:35.
- Pjetursson B E, Fehmer V, Sailer I (2022) EAO Position Paper: Material selection for implant-supported restorations. *The International Journal of Prosthodontics* 35:7-16.
- Reda R, Zanza A, Cicconetti A, Bhandi S, Guarnieri R, Testarelli L, Di Nardo D (2022) A systematic review of cementation techniques to minimize cement excess in cement-retained implant restorations. *Methods and Protocols* 5:9.
- Rengasamy S, Nair KC, Shetty J (2023) Effect of Luting Agents and Height of Implant Abutments on the Retentive Properties of Copings-an In Vitro Study. *Acta Scientific Dental Sciences* 7.
- Rosas J, Mayta-Tovalino F, Guerrero ME, Tinedo-López PL, Delgado C, Ccahuana-Vasquez VZ (2019) Marginal discrepancy of cast copings to abutments with three different luting agents. *International Journal of Dentistry* 2019.
- Saleh M, Taşar-Faruk S (2019) Comparing the marginal leakage and retention of implant-supported restorations cemented by four different dental cements. *Clinical Implant Dentistry and Related Research* 21:1181-1188.
- Soares PM, Cadore-Rodrigues AC, Packaesser MG, Bacchi A, Valandro LF, Pereira GKR, Rippe MP (2022) Masking ability of implant abutment substrates by using different ceramic restorative systems. *The Journal of Prosthetic Dentistry* 128:496-e1.
- Strauss FJ, Hämmerle CH, Thoma DS (2021) Cemented implant reconstructions are associated with less marginal bone loss than screw-retained reconstructions at 3 and 5 years of loading. *Clinical Oral Implants Research* 32:651-656.
- Zhang R, Hao X, Zhang K (2023) Evaluation of two different occlusal patterns on single posterior implant-supported crowns: A 12-month prospective study of occlusal analysis. *The Journal of Prosthetic Dentistry*.

Impact of acidic beverages on esthetic restorations concerning microhardness and color stability: a comparative assessment



Sneha Verma^a  | Abhinay Agarwal^b | Renuka Jyothi R.^c

^aMaharishi University of Information Technology, Lucknow, Uttar Pradesh, India, Associate Professor, School of Science and Humanities.

^bTeerthanker Mahaveer University, Moradabad, Uttar Pradesh, India, Professor, Department of Conservative Dentistry and Endodontics.

^cJain (Deemed-to-be University), Bangalore, India, Assistant Professor, Department of Life Sciences.

Abstract Recently, the focus has been placed on esthetic restorations by both clinicians and subjects. With the intake of acidic beverages popular these days, erosive wear of the esthetic restoration results in discoloration, raising a concern and affecting the cost. The objective of the current research was to assess how acidic drinks affected the microhardness and color stability of several esthetic restorative materials. 120 samples were split into three groups of 40 individuals. Each Group I had organically modified ceramics (ORMOCER), Group II had nanoceramics, and Group III had microhybrid composite restorations. The samples were made from the aluminum cylindrical mold of 5mm depth and 10mm diameter, followed by immersion in 25ml acidic beverages (Pepsi) for 10 minutes for 20 days. Microhardness was then assessed using a Vickers diamond indenter for each sample on the 10th and 20th day. At baseline, mean hardness was 58.12 ± 1.74 , 60.06 ± 0.36 , and 63.22 ± 0.44 , respectively, for ormocer, nanoceramics, and microhybrid composite. It was seen that the microhardness was higher for the microhybrid composite. However, the difference was statistically non-significant between the three groups with $p=0.864$. Microhardness on the 10th day was highest for the microhybrid composite, followed by nanoceramics and ormocer ($p=0.001$). However, on the 20th day, the difference was statistically non-significant between the three groups. The study, considering its limitations, concludes that the finest behavior and microhardness are associated with organically modified ceramics after immersion in acidic beverages. Nanoceramics showed the second-best behavior, and microhybrid composite resins were the least among the three.

Keywords: acidic beverages, composite, microhardness, ormocers, vickers microhardness

1. Introduction

In recent times, various clinicians and subjects have considered esthetic restorative materials to restore decayed/broken teeth, both in the anterior and posterior zone. This has globally increased the demand and use of the available aesthetic restorative materials of dentistry. A newer resin composite material, nanohybrid, owing to its esthetic value, is gaining popularity as a restorative material, which is further aided by its excellent esthetics, mechanical, and physical properties (Alauddin et al 2020). Unique combinations of nanofillers and micro fillers define nanohybrid composites. The nanofillers are very small particles with nanometer-scale dimensions, generally between 1 and 100 nanometers. These nanofillers, such as silica or zirconia nanoparticles, provide the composite material with a number of advantages. The particle size of nanohybrid composite is smaller than the micro-filled composite resins. Nanohybrid can be used for both posterior and anterior regions and has high wear strength, stain resistance, and color stability, making it a suitable esthetic restorative material (Elnour et al 2021). Modern dentistry relies heavily on aesthetic restorations since they work to repair a patient's teeth in both their functional and beautiful states. Microhardness and color stability are two important elements that affect the long-term success and patient satisfaction of esthetic restorations. Microhardness is the material's capacity to endure dents or scratches, whereas color stability is the capacity of a substance to retain its original color over time. Achieving long-lasting and aesthetically acceptable repairs depends on understanding and maximizing these features.

Recently, to improve concentration, athletic performance, stamina, weight loss, and energy, various energy and sports drinks have been marketed on a large scale. These beverages contain sweeteners, sugar, herbal supplements, vitamins, taurine, and caffeine. However, these sports and energy drinks are marketed under different names and brands, they usually have comparable ingredients and composition with acidic pH (Sato et al 2021). Microhardness is a crucial component of aesthetic restorations because it directly affects how resistant the restoration is to wear and abrasion. Dental materials with greater microhardness values usually have better lifetime and endurance, which lowers the chance of early failure. The low pH of these acidic beverages and food materials leads to the tendency of acidic wearing seen with these materials. For



clinical success, compositive restorative materials should have wear obstruction and toughness when placed in the oral environment. They are persistently or discontinuously uncovered to the compounds seen in beverages, foods, and saliva, which could lead to the leaching out of the composite resins' fillers due to the composite resin matrix softening (Bhatia et al 2016).

The term flowable consistency describes how fluid or viscous the composite material is. The viscosity of flowable composites is lower than that of conventional composite materials, enabling them to flow more freely into cavities, conform to the tooth structure, and access hard-to-reach places. They are especially well suited for the repair of cavities with intricate anatomical structures or hard-to-reach places when using conventional composite materials because of this property. Lately, high and flowable consistency bulk-fill resin-based composite restorative materials have gained popularity owing to their simple strategy of application, which was different from the regular composite resins (Tseng et al 2021). Also, they can be embedded in a single layer of 4mm, unlike regular composite resins. Vickers microhardness is a measurement of the tiny scale hardness or resistance to the indentation of a substance. The Vickers hardness test, which includes employing a diamond indenter with a square-based pyramid form to apply a regulated force to a material's surface, is used to ascertain it. To determine the hardness of materials, particularly dental restorative materials, the Vickers hardness test is often used in a variety of sectors, including dentistry. To incorporate further advancements in the composite resin materials, high-level composite fillers are incorporated by lesser filler components allowing more transmission of light and increasing the molecular size, which further improves the light-receptive photograph initiator system with the expanded size of the molecule (Unsal and Karaman, 2022; Veena Kumari et al 2019). The objective of the present research was to assess how acidic drinks affected the microhardness and color stability of different cosmetic repair materials.

The mechanical characteristics of various cosmetic restoration materials and found to be equivalent to those of CAD/CAM ceramic, but the impact of brushing your teeth on pressable ceramic has not been fully analyzed. Examining how simulated artificial toothbrushing affected the microhardness, color stability, and surface roughness of several ceramic materials was the goal of the present work (Mahrous et al 2023). Barve et al (2021) intended to determine the influence of popular drinks on the microhardness and color durability of microhybrid (MH) and nano filled (NF) resin composites. Due to their strength and aesthetic qualities, composite resins are among the most often used materials in dental restorative procedures. Bulk fill resins are becoming more and more common; however, since they are placed in a single 4-5 mm step, there is fear that some of their components may leak. The resins Opus Bulk Fill (OBF), Tetric N-Ceram Bulk Fill (TNC), and Filtek Bulk Fill (FBF), and are three that are used for restoration, were examined in this in vitro investigation to determine their microhardness, solubility, sorption, and color durability (Espíndola-Castro, 2020). Cangul et al (2022), two unique resources together with modeling resins. Molded in plastic, the composites were put. The surfaces of a pair of composite groupings were then treated with modeling resins. All of the groups' microhardness and color were assessed. To conduct the statistical analysis for the present research, Kruskal Wallis and One-Way ANOVA tests were utilized.

Alshali and Alqahtani (2022) determined how various bleaching agents affect the CAD/CAM ceramics with microhardness and color, including IPS CAD (lithium disilicate), VITA ENAMIC (polymer-infiltrated ceramic), and Celtra Duo CAD. Measurements of Spectrophotometric color were used to measure Vickers microhardness made at basis and upon bleaching. Head and Neck Cancer (HNC) treatment radiotherapy (RT) is linked to the routine of tobacco and has side effects that might affect the dental cavity, including a rise in the incidence of caries. Conti et al 2022) examined how high fluoride toothpastes affected the color, microhardness, and restoring ability of irradiation teeth. Muralidasan et al (2023) compared and assessed how home bleaching affected the flexural strength and microhardness of microhybrid and nanohybrid composite resins. Utilizing a specially created silicon rubber mold, the research material was created. 40 disc-shaped specimens were produced and separated into 4 groups for microhardness testing. The purpose of this in vitro research Bharathwaj et al 2023; Azmy et al 2022) assessed the impact of five different single-serve sachet powder drinks that have recently become popular among teenagers on the coloration of Nanohybrid composite resin.

2. Materials and Methods

The current in-vitro research aimed to estimate the impact of acidic drinks on the microhardness and color stability of various materials for aesthetic restoration. The study population was comprised of samples from the Department of Prosthodontics of the Institute. The study included 120 samples which were divided into 40 samples each. Group I had organically modified ceramics (ORMOCER), Group II had nanoceramics, and Group III had microhybrid composite restorations.

The 40 samples were made from each restorative material with the help of hollow and round aluminum forms having an inner breadth of 10mm and depth of 5mm. On the inner surface of the shape, Vaseline was applied as a lubricant to allow simple sample recuperation. Polyester matrix mylar strips were used to cover the base and top surface of the restorative material. The level was maintained with a glass slide which was inflexible to attain a bubble-free and uniformly polymerized surface of the restorative material following the curing of the material. Glass slide was pressed with the pressure of the finger to remove the extra material followed by polymerization of each side for 40 seconds. The curing unit with it only employed one light polymerization mode. At a 1.5mm distance, the light was positioned opposite the exterior of the sample. Fine

polishing disks were then used to clean the surface of every sample to simulate the clinical situation. All the samples from all three groups were immersed for 10 minutes in 25ml of an acidic beverage (Pepsi) each day for 20 days.

The samples were removed from the acidic beverage and were dried with dry tissue paper, and the readings for surface hardness were recorded at the baseline. Microhardness for each sample was recorded with the Vickers diamond indenter placed in the acidic beverage. A 15-second force was placed on the uncovered sample surface to record the surface hardness utilizing the conventional surface of (Wu et al 2022). Three readings were recorded consecutively at baseline, and the mean values were taken as VHN1 (Vickers hardness number). Towards the end of inundation or trial duration, on the 20th day, microhardness was recorded as the mean of three readings and recorded as VHN2 in a similar manner used at the baseline.

The collected data were statistically evaluated using one-way ANOVA (analysis of variance) and SPSS software, version 22.0, Chicago, IL, USA, for the flexure strength between the three groups, and the level of significance was kept at a p-value of <0.05.

3. Results

The present in-vitro study aimed to calculate the impact of acidic drinks on the microhardness and color stability of a variety of cosmetic restoration materials. The study included 120 samples which were divided into 40 samples each. Group I had organically modified ceramics (ORMOCER), Group II had nanoceramics, and Group III had microhybrid composite restorations. On assessing the mean surface hardness of the three study groups at baseline, before placing them in the acidic beverage, it was seen that the mean hardness was 58.12 ± 1.74 , 60.06 ± 0.36 , and 63.22 ± 0.44 respectively, for ormocer, nanoceramics, and microhybrid composite (Figure 1). It was seen that the microhardness was higher for the microhybrid composite. However, the difference was statistically non-significant between the three groups with $p=0.864$, as shown in Table 1.

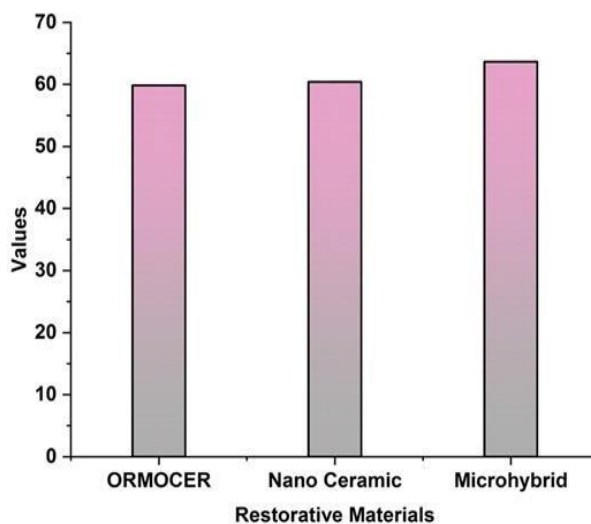


Figure 1 Baseline microhardness of three materials for aesthetic restoration.

Table 1 Microhardness of three esthetic restorative materials at baseline.

S. No	Material used	Mean± S. D	f-value	p-value
1.	ORMOCER	58.12±1.74	26.363	0.864
2.	Nanoceramics	60.06±0.36		
3.	Microhybrid composite	63.22±0.44		

On assessing the microhardness at 10th days after immersion in the acidic beverage, it was seen that the microhardness was 49.82 ± 0.81 , 51.16 ± 0.67 , and 56.33 ± 0.04 for ormocer, nanoceramics, and microhybrid composite respectively (Figure 2). The microhardness on the 10th day was highest for the microhybrid composite, followed by nanoceramics and ormocer. The variation in the three groups was significant using statistics, and the p-value was 0.001, as depicted in Table 2.

Table 2 Microhardness of three esthetic restorative materials on 10th day.

S. No	Material used	Mean± S. D	f-value	p-value
1.	ORMOCER	49.82±0.81	24.724	0.001
2.	Nanoceramics	51.16±0.67		
3.	Microhybrid composite	56.33±0.04		

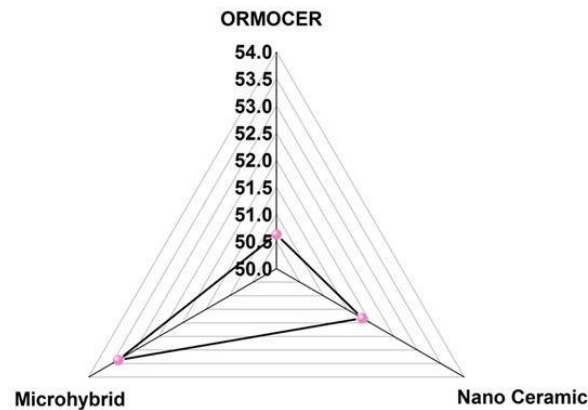


Figure 2 Three aesthetic restoration materials' microhardness after ten days.

After 20-day immersion of the study samples in the acidic beverage, it was seen that surface microhardness with the Vickers hardness intender was higher for Microhybrid composite and was 53.16 ± 0.21 followed by Group II (nanoceramics), where it was 50.34 ± 0.26 , and the least surface microhardness was seen for Group I, ORMOCER where microhardness was 48.12 ± 0.44 . However, as indicated in Table 3 and Figure 3, the alteration among the three research groups was statistically insignificant ($p = 0.6$).

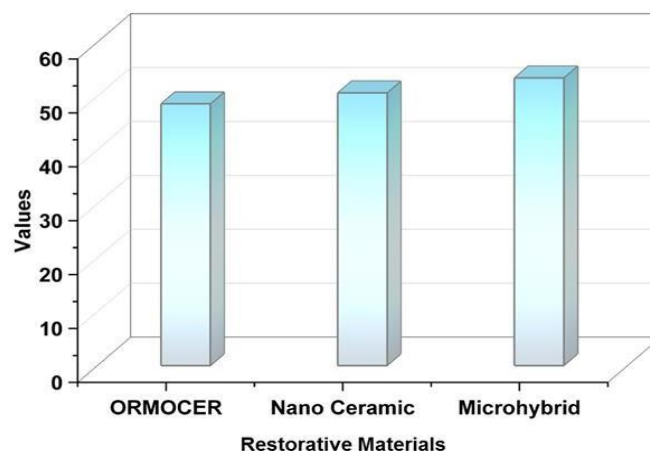


Figure 3 Three aesthetic restoration materials' 20-day microhardness.

Table 3 Microhardness of three esthetic restorative materials on 20th day.

S. No	Material used	Mean± S. D	f-value	p-value
1.	ORMOCER	48.12±0.44		
2.	Nanoceramics	50.34±0.26	26.644	0.06
3.	Microhybrid composite	53.16±0.21		

On the multiple comparisons of the three groups using Turkey's post hoc test, a statistically important difference was seen in the microhardness of Group I and Group III, Group II and Group III, and Group III and Group II with $p=0.001$. However, a statistically non-significant variance was seen in Group I and Group II with $p= 0.07$ and Group II to Group I with $p=0.07$, as depicted in Table 4.

Table 4 Comparison of mean surface hardness in different study groups.

S. No	Groups	Comparison	Mean difference	Significance
1.	Group I	Group II	-1.36	0.07
		Group III	-6.53	0.001
2.	Group II	Group I	1.36	0.07
		Group III	-5.11	0.001
3.	Group III	Group I	6.53	0.001
		Group II	5.11	0.001

The average microhardness values for restorative materials on staining solutions are shown in Figure 4. The soldex group recorded the lowest value, and the results are contrasted with those of other materials.

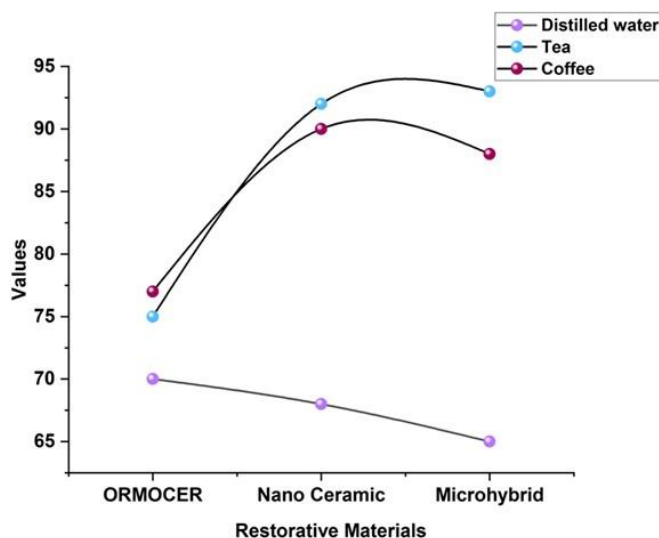


Figure 4 Average values of microhardness for restoration materials on staining solutions.

4. Discussion

The present in-vitro study included 120 samples which were divided into 40 samples each. Group I had organically modified ceramics (ORMOCER), Group II had nanoceramics, and Group III had microhybrid composite restorations. On assessing the mean surface hardness of the three study groups at baseline, before placing them in the acidic beverage, it was seen that the mean hardness was 58.12 ± 1.74 , 60.06 ± 0.36 , and 63.22 ± 0.44 respectively, for ormocer, nanoceramics, and microhybrid composite. It was seen that the microhardness was higher for the microhybrid composite. However, the difference was statistically non-significant between the three groups with $p=0.864$. These outcomes were in line with the previous findings of Poggio et al (2018) and Wang et al (2023), where no discernible difference was seen in the microhardness of the assessed esthetic restorative resources using the Vickers intender.

Concerning the assessment of the microhardness at 10th days after immersion in the acidic beverage, it was seen that the microhardness was 49.82 ± 0.81 , 51.16 ± 0.67 , and 56.33 ± 0.04 for ormocer, nanoceramics, and microhybrid composite respectively. The microhardness on the 10th day was highest for the microhybrid composite, followed by nanoceramics and ormocer. The statistical difference between the three groups was substantial, and the p-value was 0.001. These results were in agreement with the studies of Hamdy et al (2023) and Abdallah et al (2021), where authors in their findings reported that pH largely affects the solubility and hardness of different esthetic restorative materials with different filler sizes.

The study results showed that after 20-day immersion of the study samples in the acidic beverage, it was seen that surface microhardness with the Vickers hardness intender was higher for Microhybrid composite and was 53.16 ± 0.21 followed by Group II (nanoceramics), where it was 50.34 ± 0.26 , and the least surface microhardness was seen for Group I, ORMOCER where microhardness was 48.12 ± 0.44 . However, the difference between the three study groups was statistically non-significant, with $p=0.6$. These results can be explained by the studies by Nica et al (2022) and Wheeler et al (2019) after immersing samples in Coca-Cola for glass ionomer and compomers and other acidic agents, and no statistically significant difference was seen on microhardness of any restorative material following immersion in the acidic beverages.

For multiple comparisons of the three groups using Turkey's post hoc test, Group I and Group III, Group II and Group III, and Group III and Group II had microhardness differences that were significantly different from each other ($p=0.001$). However, a statistically non-significant difference was seen in Group I and Group II with $p=0.07$ and Group II to Group I with $p=0.07$. These outcomes were in line with the studies of Ahmed et al (2022), where similar results were reported by the authors in their respective studies.

5. Conclusions

The usage of Facebook news has been shown to have a complicated and multidimensional impact on political beliefs and engagement. While Facebook gives users a place to obtain a variety of news items and participate in political debates, its effect on people's political opinions and actions is impacted by a number of different elements. Examining the factors that most clearly separate Facebook users from nonusers revealed some information on a potential second-level digital divide. Given that these people tend to be early adopters of new technology, it may not come as a huge surprise that Facebook users are often richer, younger, and more knowledgeable. This research has a number of shortcomings that should be noted.

First, more Facebook features could possibly contribute to the OSROR model. In future research, increased network heterogeneity, for instance, might add another variable to the first O and provide a wider variety of information and debate. Second, this study's focus is just on Facebook use. Although it is one of the most widely used social networking sites in HK, users also communicate via WeChat and WhatsApp. Despite these drawbacks, this research adds significantly by employing the OSROR model to explain the processes behind various Facebook usages for political involvement and protest. Future studies should take into account and review the system's key characteristics, then evaluate its benefits and consequences using algorithms instead of seeing one platform having significant influence as Facebook or similar online social connections, which might potentially influence decisions regarding utilization with generic measures.

Ethical considerations

Not applicable.

Declaration of interest

The authors declare no conflicts of interest.

Funding

This research did not receive any financial support.

References

- Abdallah RM, Aref NS (2021) Development of newly formulated nanoalumina-/alkasite-based restorative material. *International Journal of Dentistry* 2021.
- Ahmed MA, Jouhar R, Vohra F (2022) Effect of different pH beverages on the color stability of smart monochromatic composite. *Applied Sciences* 12:4163.
- Alauddin MS, Mohammad N, Jaafar A, Abdul Fatah F, Ahmad AA (2021) A contemporary evaluation on posterior direct restoration teaching among undergraduates in dental schools in Malaysia. *Dentistry Journal* 9:123.
- Alshali RZ, Alqahtani MA (2022) The Effect of Home and In-Office Bleaching on Microhardness and Color of Different CAD/CAM Ceramic Materials. *Materials* 15:5948.
- Azmy E, Al-Kholy MRZ, Fattouh M, Kenawi LMM, Helal MA (2022) Impact of nanoparticles additions on the strength of dental composite resin. *International Journal of Biomaterials* 2022.
- Barve D, Dave P, Gulve M, Saquib S, Das G, Sibghatullah M, Chaturvedi S (2021) Assessment of microhardness and color stability of micro-hybrid and nano-filled composite resins. *Nigerian journal of clinical practice* 24:1499-1505.
- Bharathwaj VV, Dhamodhar D, Sathiyapriya S, Prabu D, Rajmohan M, Sindhu R (2023) The effect of coffee on color stability and surface characteristics of a nanofilled composite resin—A Systematic Review. *Journal of Advanced Medical and Dental Sciences Research* 11:23-27.
- Bhatia CM, Chandak M, Rahul A, Sedani S, Chandak R, Adwani N, Dass A, Bhatiya P (2016) Comparative evaluation of effect of different beverages on surface hardness of nanohybrid resin composite: An in vitro study. *Journal of Interdisciplinary Dentistry* 6:60.
- Cangul S, Erpocal B, Adiguzel O, Unal M, Gunay A (2022) Effect of Surface Wetting Resin on the Color Stability and Microhardness of Esthetic Composites. *Odotos-International Journal of Dental Sciences* 23:82-89.
- Conti GB, de Lima Oliveira RF, Amorim AA, de Oliveira HF, Pires-de-Souza FDCP, de Queiroz AM (2022) Color stability and microhardness alteration of irradiated dental enamel treated with a high fluoride concentration toothpaste. *Clinical Oral Investigations* 26:5885-5892.
- Elnour M, Krejci I, Bortolotto T (2021) Surface degradation of composite resins for direct restorations: effects on wear and gloss retention. *General dentistry* 69:34-39.
- Espíndola-Castro LF (2020) Evaluation of microhardness, sorption, solubility, and color stability of bulk fill resins: A comparative study. *Journal of Clinical and Experimental Dentistry* 12:e1033.
- Hamdy TM, Abdelnabi A, Othman MS, Bayoumi RE, Abdelraouf RM (2023) Effect of Different Mouthwashes on the Surface Microhardness and Color Stability of Dental Nanohybrid Resin Composite. *Polymers* 15:815.
- Mahrous AA, Alhammad A, Alqahtani F, Aljar Y, Alkadi A, Taymour N, Alotaibi A, Akhtar S, Gad MM (2023) The Toothbrushing Effects on Surface Properties and Color Stability of CAD/CAM and Pressable Ceramic Fixed Restorations An In Vitro Study. *Materials* 16:2950.
- Muralidasan K, Prasad S, Sruthipriya M, Balachandran J, Pavankumar O (2023) Influence of home bleaching regimen on microhardness and flexural strength of two contemporary composite resins—an in vitro evaluation. *European Oral Research* 57:90-95.
- Nica I, Stoleriu S, Iovan A, Tărăboanță I, Pancu G, Tofan N, Brânzan R, Andrian S (2022) Conventional and Resin-Modified Glass Ionomer Cement Surface Characteristics after Acidic Challenges. *Biomedicines* 10:1755.
- Poggio C, Viola M, Mirando M, Chiesa M, Beltrami R, Colombo M. Microhardness of different esthetic restorative materials: Evaluation and comparison after exposure to acidic drink. *Dent Res J (Isfahan)* 2018:166-72.
- Sato T, Fukuzawa Y, Kawakami S, Suzuki M, Tanaka Y, Terayama H, Sakabe K (2021) The onset of dental erosion caused by food and drinks and the preventive effect of alkaline ionized water. *Nutrients* 13:3440.
- Tseng CC, Lin PY, Kirankumar R, Chuang ZW, Wu IH, Hsieh S(2021) Surface degradation effects of carbonated soft drink on a resin based dental compound. *Heliyon* 7:e06400.
- Unsal KA, Karaman E (2022) Effect of additional light curing on colour stability of composite resins. *International dental journal* 72:346-352.
- Veena Kumari R, Pradeep PR, Aswathi S, Evaluation of surface roughness of composite resins with three different polishing systems and the erosive potential

with apple cider vinegar using atomic force microscopy-an in vitro study. *Acta Sci Dent Sci* 2019:08–16.

Wang X, Li J, Zhang S, Zhou W, Zhang L, Huang X (2023) pH-activated antibiofilm strategies for controlling dental caries. *Frontiers in Cellular and Infection Microbiology* 13:223.

Wheeler J, Deb S, Millar BJ (2020) Evaluation of the effects of polishing systems on surface roughness and morphology of dental composite resin. *British Dental Journal* 228:527-532.

Wu H, Dave F, Mokhtari M, Ali MM, Sherlock R, McIlhagger A, Tormey D, McFadden S (2022) On the application of Vickers micro hardness testing to isotactic polypropylene. *Polymers* 14:1804.

Correlation of pulp stones to hyperlipidemia and hypertension: a clinico pathological hospital-based study



K. Asha^a | Shikhar Verma^b | Garima Yeluri^c

^aJain (Deemed-to-be University), Bangalore, India, Assistant Professor, Department of Life Sciences.

^bMaharishi University of Information Technology, Lucknow, Uttar Pradesh, India, Associate Professor, School of Science and Humanities.

^cTeerthanker Mahaveer University, Moradabad, Uttar Pradesh, India, Professor, Department of Oral Medicine & Radiology.

Abstract Pulp stones signify the calcification of the discrete origin seen in the pulp tissues and are seen either embedded or attached to the dentin. Pulp stones can be a pathological or physiological entity. The pathogenesis of the pulp stone formation is idiopathic. However, various theories have been proposed. Pulp stone frequency is in the range of 8% to 90%. They are more identified on the histopathologic examination than radiographic assessment. The present study aimed to assess and correlate the histopathologic analysis and clinical parameters of the pulp stones to hyperlipidemia and systemic hypertension. The study assessed 140 subjects for the correlation of histopathologic analysis and clinical parameters of the pulp stones to hyperlipidemia and systemic hypertension. After inclusion, detailed case history was recorded for all the participants. This was followed by the radiographic assessment, and the pulp tissue after extirpation was sent for processing. The data gathered was statistically assessed with the Chi-square test and SPSS software. The study showed that on radiographic assessment, pulp stones were seen in 28 subjects and histopathologic assessment in 60 subjects among the total studied 140 subjects. Hyperlipidemia and hypertension were significantly associated with using nonlaminated and uneven varieties of pulp stone. The study concludes that subjects having irregularly shaped and nonlaminated pulp stones on histopathologic analysis should undergo assessment for systemic hypertension and hyperlipidemia.

Keywords: hyperlipidemia, hypertension, lipid profile, pulp stones

1. Introduction

The pulp in the human teeth signifies a highly vascular and fibrous tissue present in the rigid chamber of teeth comprising of the cementum, dentin, and enamel protecting from the microorganisms present in the oral cavity and lending strong mechanical support to the pulpal tissue (Silva et al 2017). Pulp stones represent a discrete calcification noted in the pulpal tissue, which can be seen in both the radicular and the coronal portion of the pulpal tissue of teeth. Pulp stones can be seen in erupted as well as unerupted teeth, deciduous as well as permanent teeth, and maxillary as well as mandibular teeth (Zaeneldin et al 2022).

The pulp stones are usually identified accidentally during root canal procedures or radiographic assessment. Pulp stones present no symptoms unless placed on a nerve causing the impingement. The pulp stones are classified based on their location as embedded, adherent and free pulp stones signifying the stones are surrounded by dentin, partially fused to dentin, and fully surrounded by the pulpal tissues (Gabardo et al 2019). The stones are also classified depending on their structure into true pulp stones and false pulp stones, where true pulp stones are formed of odontoblasts from the dentin and false pulp stones from degenerated pulp cells (KanthJaju et al 2021).

The exact mechanism of pulp stone formation is not well-understood. However, they are attributed to be formed of various factors, including idiopathic factors, genetic predisposition, remnants of epithelial rests, periodontal diseases, wasting diseases, alteration in the pulpal circulation, fibrosis, hypervitaminosis, increasing age, systemic diseases, orthodontic tooth movement, caries, trauma, long-standing local irritants, etc. Hence, it can be considered that non-mineralized pulp tissue on irritation can lead to inflammation which, if left unmanaged, can gradually result in calcification and necrosis of the dental pulp (Queiroz et al 2019).

Previous literature studies have reported that pulp stones on histopathologic analysis can be seen as stones with or without distinct concentric laminations. The previous literature data also revealed that pulp stones could either be ovoid or spherical with a rough surface, no lamination, and no form to the ones with concentric lamination and smooth surfaces. The



association between cardiovascular diseases and the presence of pulp stones has also been identified in the previous literature data (Patro et al 2022).

One of the major risk factors for cardiovascular disease is hypercholesterolemia which is also a modifiable factor. Lipid has a vital role in initiating the formation of hydroxyapatite and can affect the development of cardiovascular diseases, hypertension, and arterial calcifications. However, pulp stones' presence in the teeth and their role in cardiovascular diseases, hyperlipidemia, and hypertension are scarce and inconclusive (Sezgin et al 2021). Thus, the current research aimed to assess the stones made of pulp histopathologically in subjects undergoing root canal treatment and to assess the total serum cholesterol and hypertension in those subjects. The study aimed to evaluate parameters such as trauma, age, dental caries, gender, and tooth involved with the histologic and radiographic features of the pulp stones and evaluated the correlation of pulp stones to hyperlipidemia and hypertension.

Both independent risk factors for ischemic stroke are hyperlipidemia (HLP) and hypertension (HTN). The study examined the possibility that HTN and HLP may reduce the risk of ischemic stroke in a synergistic manner (Wang et al 2022). Alexandru et al (2019) sought to determine the impact of EPC transplantation on the miRNA expression patterns seen in plasma, platelets, and platelet-derived microvesicles (PMVs) produced from experimentally induced atherosclerotic animal models. Kaira et al (2022) discussed the function of hypertension and hyperlipidemia in the etiology of dementia and the effects of antihypertensive and antihyperlipidemic medications on dementia therapy. They provide a high-throughput method for locating and vetting potential medication repurposing candidates. This method combines clinical data from freely accessible sources with information on pharmacological perturbations and human gene expression. This method is used to identify potential medication repurposing candidates for hyperlipidemia and hypertension (Wu et al 2022). Yilmaz et al (2019) was to ascertain the association between pulp stone (PS) and carotid artery calcification (CAC). The study included 60 chronic hemodialysis (HD) patients, of whom 30 had CAC positivity, and 30 had CAC negativity. Geography is one of several variables that might influence the human gut flora. Li et al (2019) aimed to assess the associations of certain gut microbiota with clinical indices for hypertension and hyperlipidemia as well as to clarify the area-specific features of the gut microbiota in rural people of Xinxiang County, Henan province. Young individuals display inadequate treatment and management of hypertension compared to older adults. The variables influencing the management of hypertension in young people are, however, poorly understood. Ji-Soo and Chul-Gyu, (2020) was to determine the gender-specific characteristics influencing early adult hypertension therapy and management in South Korea. They provide a high-throughput method for locating and vetting potential medication repurposing candidates. This method combines clinical data from freely accessible sources with information on pharmacological perturbations and human gene expression. This method is used to identify potential medication repurposing candidates for hyperlipidemia and hypertension (Jarell et al 2022).

2. Materials and Methods

The current study intended to assess and correlate the histopathologic analysis and clinical parameters of the pulp stones to hyperlipidemia and systemic hypertension. The study participants were from the Department of Conservative and Endodontics of the Institute. After explaining the detailed study design to all the participants, all participants gave their informed permission in both written and spoken form.

The research had 140 participants of both genders, ranging in age from 8 to 65 years, who were involved in having permanent dentition and undergoing endodontic treatment (root canal). The exclusion criteria for the study were subjects having periodontally weakened teeth, teeth having any developmental anomaly, and subjects who were not willing to participate in the study or refused to give consent.

A thorough history was kept for each participant when the research subjects were all finally included the demographic details as gender, age, trauma history, dental caries, and systemic disease as hypertension was noted following the 2017 criteria by AHA (American Heart Association) (Gerhard-Herman et al 2016). After the assessment, for the subjects having Stage II hypertension, the blood samples were collected following strict aseptic and sterile conditions to assess the total serum cholesterol levels. Hyperlipidemia was considered for the subjects having blood pressure values of more than 190 mg/dl.

This was followed by taking the IOPAR (intra-oral periapical radiographs) to assess the absence or presence of the pulp stones. The pulp tissue was then extirpated during the root canal procedure and fixed in the 10% formalin. The tissues were then processed, and the sections were made of 4 μ thickness. The prepared sections were then stained using hematoxylin and eosin stains and were examined under a microscope.

The information collected was statistically analyzed using the SPSS version 16 and the Chi-square test. The data were expressed in mean and standard deviation and frequency and percentages. The student's t-test was also used for the statistical analysis of the collected data. The significance level was depicted by the p-value of <0.05.

3. Results

The present study aimed to assess and correlate the histopathologic analysis and clinical parameters of the pulp stones to hyperlipidemia and systemic hypertension. 140 participants of both genders, aged 8 to 65, were enrolled in the research having permanent dentition and undergoing endodontic treatment (root canal). The demographic and pulp stone-related data are summarized in Table 1. The mean age of the study participants was 33.16 ± 10.2 years. The age was <40 years in 54% (n=68) subjects and was 41-60 years in 46% (n=72) participants. There were 48.5% (n=76) males and 51.4% (n=64) females in the current research. The stones for pulp were present in 43% (n=60) of study subjects, where 20 pulp stones were in the mandible, and 40 pulp stones were in the maxilla. History of dental trauma was positive in 67% (n=32) study subjects, and dental caries was present in 30% (n=28) study subjects. Radiographic evidence of pulp stones was observed in 20% (n=28) of research topics. Inflammation was seen histopathologically in 20% (n=28) of study subjects, and pulp stones were seen histopathologically in 60% (n=43) of study subjects (Table 1).

Table 1 Demographic data and pulp stone distribution in study participants.

S. No	Characteristics	Percentage (%)	Number (n=140)
1.	Gender		
a)	Males	48.5	76
b)	Females	51.4	64
2.	Age (years)		
a)	<40	54	68
b)	41-60	46	72
3.	Pulp stones		
a)	Present	43	60
b)	Absent	57	80
4.	Mandible	29	40
a)	Present	50	20
b)	Absent	50	20
5.	Maxilla	71	100
a)	Present	40	40
b)	Absent	60	60
6.	Dental trauma	35	48
a)	Present	67	32
b)	Absent	33	16
7.	Dental caries	65	92
a)	Present	30	28
b)	Absent	70	64
8.	Radiographic pulp stones	20	28
9.	Histologic inflammation	20	28
10.	Histologic pulp stone	60	43

Pulp stones were seen in 32 males out of 72 and in 28 females among 68 study females. The gender difference for pulp stones was statistically non-significant, with $p=0.86$. In subjects aged 40 years, pulp stones were seen in 4 subjects, and from 41-60 years were seen in 56 study subjects. No correlation was seen between pulp stones and the age of the study subjects with $p=0.07$. Laminated pulp stones were seen in 16 subjects compared to non-laminated pulp stones in 44 study subjects. Non-laminated pulp stones had a significantly higher prevalence than laminated stones, with $p=0.000$. The shape of the pulp stones was ovoid in 28 subjects and irregular in 32 study subjects which were statistically significant with $p=0.000$. Single pulp stones were seen in 36 subjects and multiple in 24 study subjects ($p=0.000$). Hypertension was seen in 44 study subjects, whereas pulp stones were seen in 36 subjects 44. This was a statistically significant correlation with $p=0.000$. In subjects having inflammatory cells, pulp stones were present in 28 subjects ($p=0.000$). In subjects where Endodontic treatment was intentional, pulp stones were present in 4 study subjects. With routine endodontic treatment, pulp stones were present in 56 study subjects which were non-significant with $p=0.85$. On radiographic assessment, pulp stones were seen in 28 subjects which were non-significant with $p=0.17$. In 92 subjects having caries, pulp stones were present in 26 subjects, and in 48 subjects with trauma, pulp stones were present in 34 study subjects. This difference was statistically significant, with $p=0.03$. Among 100 maxillary sites, pulp stones were seen in 40 sites, and in 40 mandibular sites, 20 sites pulp stones were seen. This was statistically non-significant with $p=0.56$. In 100 anterior sites, pulp stones were seen in 40 subjects, and in 40 posterior sites, pulp stones were seen in 20 sites ($p=0.56$), as depicted in Table 2. Figure 1 to 3 depicts the percentage of pulp stone pattern, shape, and number.

On histopathologic assessment, in a laminated pattern, pulp stones were seen in 20% (n=12) subjects and hypertension in 22% (n=8) study subjects. In the non-laminated pattern of the pulp stones, pulp stones were seen in 80% (n=48) subjects and hypertension in 78% (n=28) study subjects. In spherical-shaped pulp stones, pulp stones were seen in 47% (n=28) subjects and hypertension in 38% (n=14) study subjects. In irregularly shaped pulp stones in 53% (n=32) subjects, hypertension was seen in 62% (n=22) of study subjects. In single pulp stones, pulp stones were seen in 60% (n=36) study

subjects and hypertension in 445 (n=16) study subjects. In multiple pulp stones, the stones were seen in 40% (n=240 study subjects and hypertension in 54% (n=20) study subjects, as seen in Table 3. Figure 4 shows the Pulp stone histopathologic evaluation and its relationship to hypertension.

Table 2 Clinical variables in the study participants and their correlation with pulp stones.

S. No	Clinical variables	Number (n)	Pulp stones present (n)	Pulp stones absent (n)	p-value
1.	Gender				
a)	Males	72	32	40	0.86
b)	Females	68	28	40	
2.	Age (years)				
a)	<40	68	4	64	0.07
b)	41-60	72	56	16	
3.	Pulp stone pattern				
a)	Laminated		16/60	44/60	0.000
b)	Non-laminated		44/60	16/60	
4.	Pulp stone shape				
a)	Ovoid		28/60	32/60	0.000
b)	Irregular		32/60	28/60	
5.	Pulp stone number				
a)	Single		36/60	24/60	0.000
b)	Multiple		24/60	36/60	
6.	Hypertension	44	36	8	0.000
7.	Inflammatory cells				
a)	Present		28/60	32/60	0.000
b)	Absent		32/60	28/60	
8.	Endodontic treatment				
a)	Intentional		4/60	56/60	0.85
b)	Routine		56/60	4/60	
9.	Radiographic assessment				
a)	Present	28	28/60	0	0.17
b)	Absent	112	32/60	80	
10.	Clinical factors				
a)	Caries	92	26	66	0.03
b)	Trauma	48	34	14	
11.	Site				
a)	Maxilla	100	40	60	0.56
b)	Mandible	40	20	20	
12.	Location				
a)	Anterior	100	40	60	0.56
b)	Posterior	40	20	20	

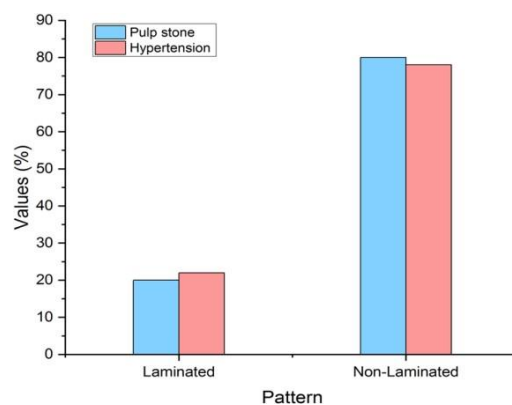


Figure 1 Percentage of pulp stone pattern.

The study showed a significant association of pulp stones to hypertension and hyperlipidemia with p=0.001. Also, a significant association was seen between nonlaminated pulp stones and hyperlipidemia and hypertension. Chi-square analysis showed a highly significant association with trauma and caries to the pulp stones. Hence, the pulp chamber narrowing is governed by various factors, including water, environment, food, and genetics. The histopathologic assessment showed a significant association of pulp stones and inflammatory cells with p<0.05. A similar significant association was seen in pulp stones and inflammatory cells' presence and pattern, shape, and several pulp stones with p<0.05.

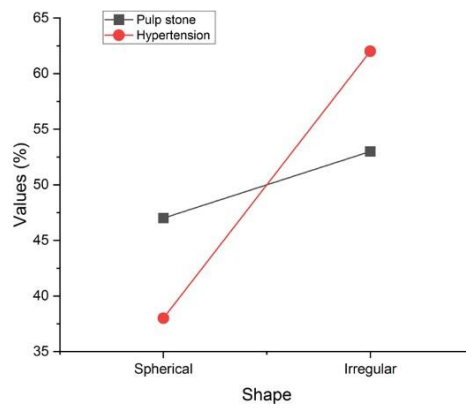


Figure 2 Percentage of pulp stone shape.

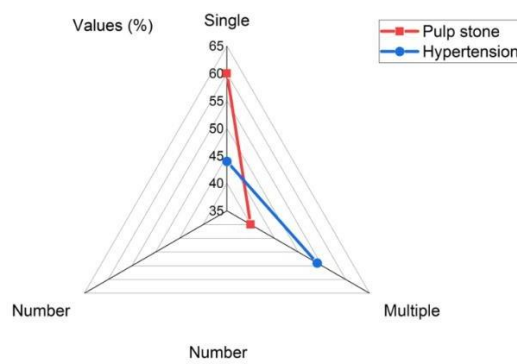


Figure 3 Percentage of pulp stone number.

Table 3 Histopathologic assessment of pulp stones and their correlation with hypertension.

S. No	Histopathology	Pulp stone number n=60 (%)	Hypertension n=36 (%)
1.	Pattern		
a)	Laminated	12 (20)	8 (22)
b)	Non-laminated	48 (80)	28 (78)
2.	Shape		
a)	Spherical	28 (47)	14 (38)
b)	Irregular	32 (53)	22 (62)
3.	Number		
a)	Single	36 (60)	16 (44)
b)	Multiple	24 (40)	20 (54)

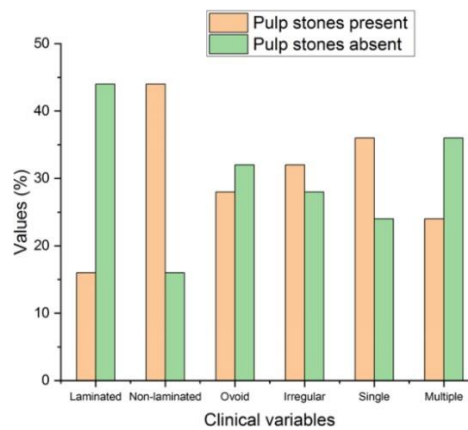


Figure 4 Pulp stone histopathologic evaluation and its relationship to hypertension.

4. Discussion

In the research 140 participants, aged 8 to 65, from both sexes were enrolled, having permanent dentition, and undergoing endodontic treatment (root canal). The study's participants' average age was 33.16 ± 10.2 years. The age was <40 years in 54% (n=68) subjects and was 41-60 years in 46% (n=72) participants. There were 48.5% (n=76) males and 51.4% (n=64) females in the current research. The stones for pulp were present in 43% (n=60) of study subjects, where 20 pulp stones were in the mandible, and 40 pulp stones were in the maxilla. History of dental trauma was positive in 67% (n=32) study subjects, and dental caries was present in 30% (n=28) study subjects. Radiographic evidence of pulp stones was seen in 20% (n=28) of study subjects. Inflammation was seen histopathologically in 20% (n=28) of study subjects, and pulp stones were seen histopathologically in 60% (n=43) of study subjects. These characteristics were similar to the previous studies of (Mathew et al (2019) and (Nachiappan et al (2021), where researchers evaluated patients using demographic information similar to that of the current study.

The study's findings revealed that pulp stones were seen in 32 males out of 72 and in 28 females among 68 study females. The gender difference for pulp stones was statistically non-significant, with $p=0.86$. In subjects with age 40 years, pulp stones were seen in 4 subjects, and from 41-60 years were seen in 56 study subjects. No correlation was seen between pulp stones and the age of the study subjects with $p=0.07$. Laminated pulp stones were seen in 16 subjects compared to non-laminated pulp stones in 44 study subjects. Non-laminated pulp stones had a significantly higher prevalence compared to laminated stones with $p=0.000$. The shape of the pulp stones was ovoid in 28 subjects and irregular in 32 study subjects which were statistically significant with $p=0.000$. Single pulp stones were seen in 36 subjects and multiple in 24 study subjects ($p=0.000$). Hypertension was seen in 44 study subjects, whereas pulp stones were seen in 36 subjects among 44 subjects. This was a statistically significant correlation with $p=0.000$. In subjects having inflammatory cells, pulp stones were present in 28 subjects ($p=0.000$). In subjects where Endodontic treatment was intentional, pulp stones were present in 4 study subjects, and with routine endodontic treatment, pulp stones were present in 56 study subjects which were non-significant with $p=0.85$. On radiographic assessment, pulp stones were seen in 28 subjects which were non-significant with $p=0.17$. In 92 subjects having caries, pulp stones were present in 26 subjects, and in 48 subjects with trauma, pulp stones were present in 34 study subjects. This difference was statistically significant, with $p=0.03$. Among 100 maxillary sites, pulp stones were seen in 40 sites, and in 40 mandibular sites, 20 sites pulp stones were seen. This was statistically non-significant with $p=0.56$. In 100 anterior sites, pulp stones were seen in 40 subjects, and in 40 posterior sites, pulp stones were seen in 20 sites ($p=0.56$). These outcomes agreed with the research of (Maikhuri et al (2023) and (Ravichandran et al 2022), where a similar association was noted between non-laminated pulp stones, caries, trauma, and hypertension.

Concerning histopathologic assessment, in a laminated pattern, pulp stones were seen in 20% (n=12) subjects and hypertension in 22% (n=8) study subjects. In the non-laminated pattern of the pulp stones, pulp stones were seen in 80% (n=48) subjects and hypertension in 78% (n=28) study subjects. In spherical-shaped pulp stones, pulp stones were seen in 47% (n=28) subjects and hypertension in 38% (n=14) study subjects. In irregularly shaped pulp stones in 53% (n=32) subjects, hypertension was seen in 62% (n=22) of study subjects. In single pulp stones, pulp stones were seen in 60% (n=36) study subjects and hypertension in 44% (n=16) study subjects. In multiple pulp stones, the stones were seen in 40% (n=24) study subjects and hypertension in 54% (n=20) research topics. These findings were in agreement with the previous studies of Hoshyari et al (2022) and Parashar et al (2022), where authors reported a significant association of hyperlipidemia and hypertension in irregularly shaped and non-laminated pulp stones as of the current research.

The study outcomes showed a significant association of pulp stones to hypertension and hyperlipidemia with $p=0.001$. Also, a substantial correlation between nonlaminated pulp stones and hyperlipidemia and hypertension. Chi-square analysis showed a highly significant association with trauma and caries to the pulp stones. Hence, the pulp chamber narrowing is governed by various factors, including water, environment, food, and genetics. The histopathologic assessment showed a significant association of pulp stones and inflammatory cells with $p<0.05$. A similar significant association was seen in pulp stones and inflammatory cells' presence and pattern, shape, and several pulp stones with $p<0.05$. These findings were in line with the studies of Kritikou et al (2023) and Chen et al (2022), where authors reported a significant association of hyperlipidemia and hypertension to inflammatory cells and pulp stones.

4. Conclusions

Considering its limitations, the present study concludes that subjects having irregularly shaped and nonlaminated pulp stones on histopathologic analysis should undergo assessment for systemic hypertension and hyperlipidemia. The pulp stones, which are distinct lesions important in the long-term prognosis of the tooth and the systemic illness, are often disregarded by clinicians. Because there is a significant association between hypertension, hyperlipidemia, and the presence of pulp stones with a nonlaminated pattern in our research, we require that every extruded piece of pulp tissue be given a histological analysis to determine the pattern of pulp stones. The existence of pulp stones with a nonlaminated pattern may be a predictor of hypertension and hyperlipidemia, which should be proven in the future by further research.

Ethical considerations

Not applicable.

Declaration of interest

The authors declare no conflicts of interest.

Funding

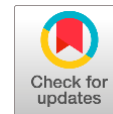
This research did not receive any financial support.

References

- Alexandru N, Constantin A, Nemezc M, Comarița IK, Vilcu A, Procopciuc A, Tanko G, Georgescu A (2019) Hypertension associated with hyperlipidemia induced different microRNA expression profiles in plasma, platelets, and platelet-derived microvesicles; effects of endothelial progenitor cell therapy. *Frontiers in Medicine* 6:280.
- Chen G, Huang LG, Yeh PC (2022) Detecting calcified pulp stones in patients with periodontal diseases using digital panoramic and periapical radiography. *Journal of Dental Sciences* 17:965-972.
- Gabardo MCL, Wambier LM, Rocha JS, Küchler EC, de Lara RM, Leonardi DP, Sousa-Neto MD, Baratto-Filho F, Michel-Crosato E (2019) Association between pulp stones and kidney stones: a systematic review and meta-analysis. *Journal of Endodontics* 45:1099-1105.
- Gerhard-Herman MD, Gornik HL, Barrett C, et al (2016) AHA/ACC guideline on the management of patients with lower extremity peripheral artery disease: a report of the American College of Cardiology/American Heart Association Task Force on Clinical Practice Guidelines. *Circulation* 2017:726-79.
- Hoshiyari N, Farahbod F, Nabati M, Haddadi A, Mousavi J, Shahsavari N (2022) Association between Coronary Artery Sclerosis and Dental Pulp Calcification in Patients Attending Sari Touba Clinic, 2019. *Journal of Mazandaran University of Medical Sciences* 31:157-164.
- Jarell A, Gastman BR, Dillon LD, Hsueh EC, Podlipnik S, Covington KR, Cook RW, Bailey CN, Quick AP, Martin BJ, Kurley SJ (2022) Optimizing treatment approaches for patients with cutaneous melanoma by integrating clinical and pathologic features with the 31-gene expression profile test. *Journal of the American Academy of Dermatology* 87:1312-1320.
- Ji-Soo KIM, Chul-Gyu KIM (2020) Gender differences in hypertension treatment and control in young adults. *Journal of Nursing Research* 28:e88.
- Kaira M, Walia V, Garg M (2022) Role of Hypertension and Hyperlipidemia in the Pathogenesis of Dementia. In *Current Thoughts on Dementia: From Risk Factors to Therapeutic Interventions* pp 251-272. Singapore: Springer Nature Singapore.
- KanthJaju K, Sandhya R, Datta K (2021) Prevalence Of Pulpal Calcification In Patients With Hypertension-A Retrospective Study. *Int J Dentistry Oral Sci* 8:3638-3642.
- Kritikou K, Imre M, Tanase M, Vinereanu A, Ripszky Totan A, Spinu TC, Miricescu D, Stanescu-Spinu II, Bordea M, Greabu M (2022) Assessment of Mineralization, Oxidative Stress, and Inflammation Mechanisms in the Pulp of Primary Teeth. *Applied Sciences* 12:1554.
- Li H, Liu B, Song J, An Z, Zeng X, Li J, Jiang J, Xie L, Wu W (2019) Characteristics of gut microbiota in patients with hypertension and/or hyperlipidemia: a cross-sectional study on rural residents in Xinxiang County, Henan Province. *Microorganisms* 7:399.
- Maikhuri B, Sahoo N, Jena S, Dash BP, Dash S (2023) Prevalence Of Pulp Stones After Orthodontic Treatment-A Review. *Journal of Pharmaceutical Negative Results* 71-77.
- Mathew ST, Al-Mutlaq MA, Al-Eidan RF, Al-Khuraishi DM, Adam H (2019) Prevalence of pulp stones and its relation with cardiovascular diseases and diabetes mellitus using digital radiographs: a retrospective study. *Ann Dent Spec* 7:18-23.
- Nachiappan S, Chandran A, Swathika B, Ganesan S, Mahaprasad A, Muddebihal F, Nayyar AS (2021) Pulp Stones: Diagnostic Significance in Early Diagnosis and Radiographic Correlation with Ischemic Heart Diseases. *Indian Journal of Radiology and Imaging* 31:277-283.
- Parashar SR, Kasabwala K, Ulaganathan S, Ashritha MCV, Khandelwal P, Arockiam S, Natanasabapathy V (2022) Association of pulp calcifications and cardiovascular disease: a systematic review and meta-analysis. *Journal of Evidence-Based Dental Practice* 22:101707.
- Patro S, Meto A, Mohanty A, Chopra V, Miglani S, Das A, Luke AM, Hadi DA, Meto A, Fiorillo L, Karobari MI (2022) Diagnostic Accuracy of Pulp Vitality Tests and Pulp Sensibility Tests for Assessing Pulpal Health in Permanent Teeth: A Systematic Review and Meta-Analysis. *International Journal of Environmental Research and Public Health* 19:9599.
- Queiroz AF, Hidalgo MM, Consolaro A, Panzarini SR, França AB, Pires WR, Poi WR (2019) Calcific metamorphosis of pulp after extrusive luxation. *Dental Traumatology* 35:87-94.
- Ravichandran S, Vadivel JK (2022) Prevalence of pulp stones in IOPA radiographs. *Journal of Advanced Pharmaceutical Technology & Research* 13:S63.
- Sezgin GP, Kaplan SS, Kaplan T (2021) Evaluation of the relation between the pulp stones and direct restorations using cone beam computed tomography in a Turkish subpopulation. *Restorative Dentistry & Endodontics* 46.
- Silva BSF, Bueno MR, Yamamoto-Silva FP, Gomez RS, Peters OA, Estrela C (2017) Differential diagnosis and clinical management of periapical radiopaque/hyperdense jaw lesions. *Brazilian oral research* 31.
- Wang C, Du Z, Ye N, Shi C, Liu S, Geng D, Sun Y (2022) Hyperlipidemia and hypertension have synergistic interaction on ischemic stroke: insights from a general population survey in China. *BMC cardiovascular disorders* 22:47.
- Wu P, Feng Q, Kerchberger VE, Nelson SD, Chen Q, Li B, Edwards TL, Cox NJ, Phillips EJ, Stein CM, Roden DM (2022) Integrating gene expression and clinical data to identify drug repurposing candidates for hyperlipidemia and hypertension. *Nature Communications* 13:46.
- Yilmaz SG, Yilmaz F, Bayrakdar IS, Harorli A (2019) The relationship between carotid artery calcification and pulp stone among hemodialysis patients: A retrospective study. *Saudi Journal of Kidney Diseases and Transplantation* 30:755-763.
- Zaeneldin A, Ollie YY, Chu CH (2022) Effect of silver diamine fluoride on vital dental pulp: A systematic review. *Journal of dentistry* 104066.



Depicting the levels of resistin and adiponectin in GCF (gingival crevicular fluid) in chronic periodontitis subjects before and following treatment



Nayana Borah^a | Nidhi Srivastava^b | Shalabh Mehrotra^c

^aJain (Deemed-to-be University), Bangalore, India, Assistant Professor, Department of Life Sciences.

^bMaharishi University of Information Technology, Lucknow, Uttar Pradesh, India, Associate Professor, School of Science and Humanities.

^cTeerthanker Mahaveer University, Moradabad, Uttar Pradesh, India, Professor, Department of Periodontology.

Abstract Adipokines including resistin and adiponectin are vital in periodontal inflammation along with host response and infection. Adiponectin also had anti-inflammatory action. Assessment of resistin and adiponectin in gingival crevicular fluid (GCF) of subjects with chronic periodontitis serves as a biomarker to predict the active phase of periodontitis. The purpose of this research was to determine the relationship between resistin and adiponectin levels in GCF of subjects in subjects with chronic periodontitis before and following treatment. 70 subjects were split into two groups where Group I had 35 healthy subjects and Group II had 35 subjects having periodontitis. Group III comprised subjects with periodontitis after the treatment. Samples of GCF were taken earlier to therapy 21 days after therapy. Stages of resistin and adiponectin were assessed with ELISA. The levels and clinical indicators were linked, and conclusions were drawn. The study results presented a reduction in mean stages of resistin and an increase was seen in the mean levels of adiponectin after the periodontal therapy in subjects with chronic periodontitis. The study concludes that adiponectin is an anti-inflammatory compound that increases in subjects following periodontal treatment, whereas resistin is an inflammatory component that shows a reduction after periodontal treatment.

Keywords: adiponectin, chronic periodontitis, periodontal therapy, periodontitis, resistin

1. Introduction

Chronic periodontitis is a chronic and contagious illness affecting some of the tissues that support teeth, and untreated dental problems are likely to lead to tooth loss. Periodontitis mainly has a multifactorial etiology caused by the interaction of causative factors, including inflammatory mediators, immune cells, bacteria, and their products (Guilherme et al 2019). Immune cells are activated by the immune-inflammatory process of the host, initiating the release of inflammatory mediators, including arachidonic acid metabolites, adipokines, and/or chemokines. These cytokines play a crucial role in the development of periodontal illness and tissue destruction (Hajishengallis et al 2021).

Adipokines constitute a set of molecules with biological activity constructed by adipose tissues. Among these adipokines, resistin plays a vital role in subjects with periodontal inflammation. These cytokines and adipokines also play a crucial role in the reaction of the host toward periodontal inflammation and infection (Mărginean et al 2020). Adiponectin imparts anti-inflammatory action by stimulating heme oxygenase-1 and IL-10 (interleukin-10), which are anti-inflammatory components that inhibit LPS (lipopolysaccharide) and stimulate NF- κ B (nuclear factor kappa beta) translocation. Adiponectin also hinders the generation of proteolytic and anti-inflammatory compounds in periodontal cells (Koka et al 2020). Figure 1 shows adiponectin's function in periodontitis.

Resistin causes an increase in monocyte chemoattractant protein-1, IL-12, TNF- α tumor necrosis factor, and proinflammatory cytokines (IL-1 and IL-6), which are all examples of proinflammatory cytokines. In the hepatic stellate cells, macrophages, and peripheral blood mononuclear cells of the humans by NF- κ B pathway. A protein hormone called resistin was first identified in mice and subsequently proven to exist in humans. Its levels are often higher in people who are obese and have insulin resistance since it is largely released by macrophages and adipocytes (fat cells). Resistin is considered to have a role in the etiology of several inflammatory illnesses, including periodontal disease, and has been linked to the emergence of persistent low-grade inflammation. This finding indicates that resistin has the main role in inflammation (Carrion et al 2019). Nonsurgical periodontal treatment particularly aims to restore gingival health after the complete removal of the causative and etiologic factors leading to gingival inflammation in the oral cavity, including endotoxins,



calculus, and plaque-causing periodontal inflammation and destruction (Nongrum et al 2022). Ultrasonic and hand-used periodontal instruments can drastically reduce the number of microorganisms seen subgingivally in periodontal diseases. Despite the different treatment modalities available for treating periodontal diseases, nonsurgical periodontal therapy, including scaling and root planing, is still the gold standard technique for treating periodontal diseases (Tsuchiya and Fujio, (2022).

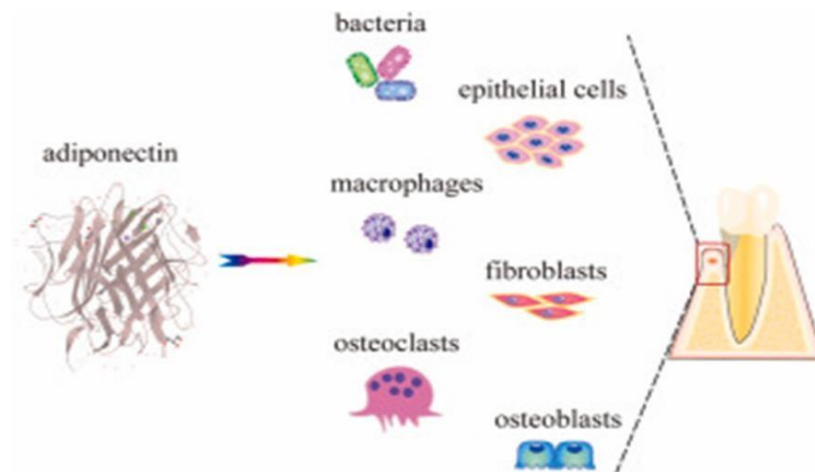


Figure 1 Adiponectin function in periodontitis.

Researchers have examined resistin and adiponectin as possible periodontal disease biomarkers in the GCF. According to research, resistin levels may be higher in the GCF of people who have periodontitis, suggesting a potential link between resistin and the inflammatory processes in periodontal tissues. The GCF of people with periodontitis has been discovered to have lower levels of adiponectin, indicating that this adipokine may have a protective function in maintaining periodontal health. The previous literature has limited data concerning the association of resistin and adiponectin with the clinical parameters in the GCF of subjects with periodontal disease. A biomarker for predicting periodontal damage and the active stage of periodontal disease is the measurement of adiponectin and resistin in the GCF of persons with chronic periodontitis. In previous studies, the association of resistin and adiponectin GCF levels and clinical indicators in periodontal disease has not been well established (Wielento et al 2023). Hence, the present biochemical-clinical study was performed to assess the stages of resistin and adiponectin in the GCF of individuals with persistent periodontitis and periodontal health before and following scaling and root planing (SRP).

Bremont et al (2019) assessed the levels of three adipokines in typical canine skin. Punch biopsy specimens were taken from the thinly hairy caudal ventral skin belly of a clinically sound dog without a history of skin problems. The samples were formalin-fixed and paraffin wax-embedded. Utilizing rabbit polyclonal primary antibodies that are specific for leptin, adiponectin, and resistin, immunohistochemistry was used. Insulin resistance, visceral adiposity, dyslipidemia, hyperglycemia, and hypertension are all associated with obesity. are just a few of the metabolic and cardiovascular complications that make up metabolic syndrome (MetS). These conditions all raise the risk of cardiovascular diseases (CVDs) and type 2 diabetes (DM2). An increased risk of CVD occurs in those who have rheumatic conditions such as rheumatoid arthritis and osteoarthritis. Since MetS discovered a potential relationship between arthritic conditions and cardiovascular disease, there have been recent improvements in treating arthritic conditions. The prevalence of CVD also remains high (Rezaee et al 2020). Cai et al (2020) investigated the connection between Kawasaki disease (KD) and the levels of circulating adipokines in the blood. Resistin may play a significant role in the pathogenesis of KD, and as a result, it may serve as a biomarker for the identification of KD. In contrast, adiponectin may only play a significant pathogenic role in coronary artery lesions (CALs), and as a result, it might serve as a biomarker to identify CALs from noncoronary artery lesions (NCALs).

Musovic et al (2021) examined the cellular and molecular level control of the secretion of resistin in primary and cultured adipocytes from mice. Adipose tissue hormone resistin is thought to have a role in metabolic illness. Resistin is produced by various cell types inside white adipose tissue in humans as opposed to rats, where it is released by white adipocytes. Asthma is a long-term inflammatory condition of the airways, with a wide range of overlapping pathologies and phenotypes that significantly alter how it manifests clinically. Obesity may alter the prognosis, phenotype, and risk of asthma. Systemic inflammation is one theory for the relationship between fat and asthma. It was proposed that a connection between overweight and asthma may be made via adipokines released by adipose tissue (Osman et al 2023). Adipocytokines have been intimately related in recent studies to the development of fibrosis and liver inflammation in people with nonalcoholic liver disease. According to the length of antiviral medication, the goal of this research was to ascertain how blood levels of adiponectin and resistin related to how severe the fibrous liver was in patients with chronic hepatitis B (CHB) (Custovic and Rasic,2022). Habib et al (2021) determined the relationship between body adiposity indices in healthy adult

men and the blood levels of resistin, adiponectin, and the adiponectin/resistin ratio (AR ratio). With respect, adiponectin serum levels were favorably associated, and resistin was adversely linked to physical condition assessments that used having an appropriate body composition, a smaller percentage of a greater percentage of fat-free mass, and increased body adiposity.

2. Materials and Methods

The present biochemical-clinical research was performed to assess the concentrations of adiponectin and resistin in the GCF of individuals with persistent periodontitis and prior periodontal health following SRP. The study population contributed subjects from the Institute's Department of Periodontology. After the detailed study design was explained to all the subjects, informed consent was obtained in both written and verbal formats.

The research involved 70 participants who were split into two groups: 35 periodontally healthy subjects and 35 subjects with periodontal disease. The subjects with periodontal diseases were included according to the following standards: subjects with at least 20 teeth present, periodontally and systemically using healthy volunteers and a probing depth of <3 mm for healthy subjects and >5 mm for the periodontal disease group (recorded with 15 mm periodontal probe), individuals who did not undergo any dental care, the period within the past 6 months, and subjects with 6 minimum sites with bleeding on probing in the periodontal disease group.

The 70 2 groups of subjects were formed of 35 subjects each, where Group I had healthy subjects with a probing depth of <3 mm, Group II had subjects with chronic periodontitis with a probing depth of >5 mm, and Group III comprised 35 subjects of Group II after completion of SRP.

The clinical indicators assessed were CAL (clinical attachment level), probing pocket depth, sulcus bleeding index (Klewin-Steinböck and Wyganowska 2023), GI (gingival index) (Seleem et al 2021) and plaque index (Masood et al 2019). All these parameters were assessed at baseline and after 21 days following SRP. The GCF was gathered from the test site after isolation with the cotton roll and air-drying the site, and without touching the marginal gingiva, a supragingival plaque was removed. The GCF sample was collected with a calibrated capillary pipette. Two microliters of GCF were collected from each test site by placing the pipette in the gingival sulcus for 30 seconds. The samples of GCF collected if there was blood or saliva contamination were discarded. All samples were collected at the 1st visit in both groups, and samples gathered on the 21st day contributed to Group III. After collection, the samples were labeled, stored, and processed after being sent to the laboratory.

SRP was performed in all subjects at the same appointment after the collection of GCF as a part of nonsurgical periodontal therapy. The whole mouth underwent ultrasonic scaling at the baseline initial visit. This was followed by root planing under local anesthesia with adrenaline at 1:80,000 with Hu-Friedy Gracey curettes. Twenty-one days later, GCF was gathered for Group III clinical parameters and was collected at the same spot and reassessed after 21 days. Resistin and adiponectin were evaluated biochemically with ELISA (enzyme-linked immunosorbent assay). Adiponectin levels were assessed first, followed by resistin levels.

The data gathered were statistically analyzed using a paired t test and Pearson correlation analysis with Version 19 of SPSS, which was released by IBM Company in Armonk, New York, USA. The significance levels were kept at $p < 0.05$.

3. Results

The 70 study subjects were split into two groups of 35 subjects each. Group I had wholesome themes with a probing depth of <3 mm, Group II had subjects with chronic periodontitis with a probing depth of >5 mm, and Group III comprised 35 subjects from Group II after the completion of SRP. For the assessment of clinical parameters in Groups II and III, it was seen that CAL was 4.81 ± 0.34 mm and 2.65 ± 0.43 mm for Groups II and III, respectively, which was expressively greater for Group II with $p < 0.001$. The probing depth was also significantly higher in Group II (5.35 ± 0.45 mm) than in Group III (3.22 ± 0.56 mm) ($p < 0.001$). The sulcus bleeding index, gingival index, and plaque index were significantly higher in Group II (3.45 ± 0.47 , 2.64 ± 0.61 , and 2.84 ± 0.59 , respectively) than in Group III (1.94 ± 0.54 , 1.75 ± 0.34 , and 1.74 ± 0.26 , respectively), and the p value was < 0.001 for all three parameters, as shown in Table 1. Figure 2 depicts the study parameter comparison between Group II and Group III participants.

Table 1 Comparison of study parameters in Group II and Group III subjects.

S. No	Parameters	Group II	Group III	p value
1.	CAL (mm)	4.81 ± 0.34	2.65 ± 0.43	< 0.001
2.	Probing depth (mm)	5.35 ± 0.45	3.22 ± 0.56	< 0.001
3.	Sulcus bleeding index	3.45 ± 0.47	1.94 ± 0.54	< 0.001
4.	Gingival index	2.64 ± 0.61	1.75 ± 0.34	< 0.001
5.	Plaque Index	2.84 ± 0.59	1.74 ± 0.26	< 0.001

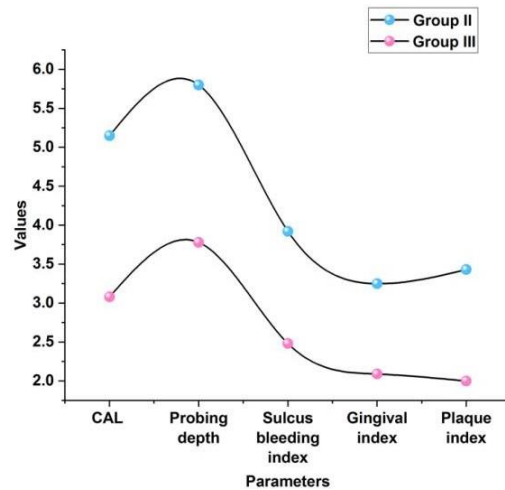


Figure 2 Comparison of study parameters in Group II and Group III subjects.

On comparing the resistance levels in the three research groups, it was observed that in the comparison of Group I and Group II, the resistin level was 7.17 ± 0.36 , which was quantitatively significant with $p < 0.05$. On comparing Groups II and III, the resistin levels were 18.14 ± 0.45 pg/ml, which exhibited statistical significance with $p < 0.05$, and for Groups I and III, it was 11.26 ± 0.37 pg/ml, which was statistically nonsignificant with $p > 0.05$, as depicted in Table 2. Figure 3 shows the subjects in Groups I, II, and III resistin.

Table 2 Comparison of levels of resistin in Group I, II, and III subjects.

S. No	Resistin (pg/ml)	Comparative groups	Mean \pm S. D	p value
1.	Group I	Groups I and II	7.17 ± 0.36	< 0.05
2.	Group II	Groups II and III	18.14 ± 0.45	< 0.05
3.	Group III	Groups I and III	11.26 ± 0.37	> 0.05

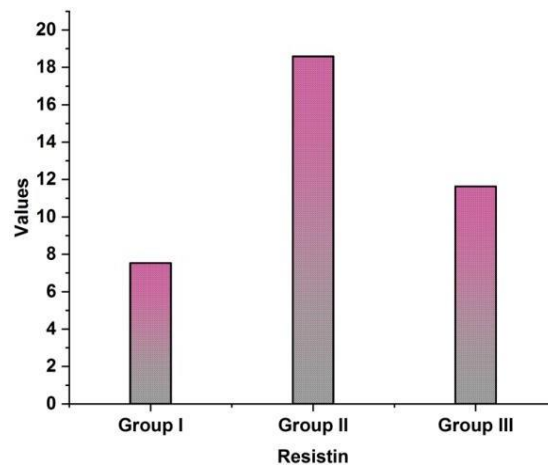


Figure 3 Resistin values in Group I, II, and III subjects.

Concerning the assessment of the adiponectin levels in the three study groups, it was observed that in Group I in comparison to Group II, the mean adiponectin levels were 20.16 ± 0.28 ng/ml, which was a difference that was quantitatively significant with $p < 0.05$. For Comparing Group II to Group III, the mean adiponectin levels were found to be 9.94 ± 0.29 ng/ml with a substantial difference in terms of statistics and $p < 0.05$. For the comparison of Group III to Group I, the mean value of adiponectin was 15.44 ± 0.34 ng/ml, which was statistically nonsignificant with $p > 0.05$, as shown in Table 3. Figure 4 denotes the adiponectin levels of the subjects in Groups I, II, and III.

Table 3 Comparison of levels of adiponectin in Group I, II, and III subjects.

S. No	Adiponectin (ng/ml)	Comparative groups	Mean \pm S. D	p value
1.	Group I	Groups I and II	20.16 ± 0.28	< 0.05
2.	Group II	Groups II and III	9.94 ± 0.29	< 0.05
3.	Group III	Groups I and III	15.44 ± 0.34	> 0.05

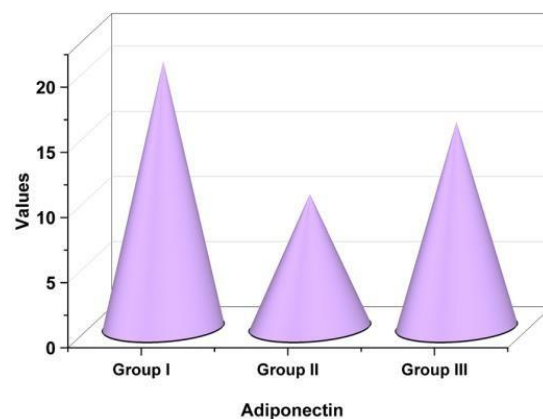


Figure 4 Adiponectin values in Group I, II, and III subjects.

4. Discussion

In the current biochemical-clinical study, patients with chronic periodontitis had their levels of resistin and adiponectin measured in GCF and prior periodontal health following SRP. In the 70 studies, 2 groups of subjects were formed of 35 subjects each, where Group I had healthy subjects with a probing depth of <3 mm, Group II had subjects with chronic periodontitis with a probing depth of >5 mm, and Group III comprised 35 subjects from Group II after the completion of SRP. For assessment of clinical standards in Groups II and III, it was seen that CAL was 4.81 ± 0.34 mm and 2.65 ± 0.43 mm for Groups II and III, respectively, which was much greater for Group II with $p < 0.001$. The probing depth was also substantially greater in Group II (5.35 ± 0.45 mm) than in Group III (3.22 ± 0.56 mm) ($p < 0.001$). The sulcus bleeding index, gingival index, and plaque index were significantly higher in Group II (3.45 ± 0.47 , 2.64 ± 0.61 , and 2.84 ± 0.59 , respectively) than in Group III (1.94 ± 0.54 , 1.75 ± 0.34 , and 1.74 ± 0.26 , respectively), and the p value was < 0.001 for all three parameters. These findings are consistent with the earlier research of (Rode et al 2019) and (Suresh et al 2018), where authors reported similar parameters in their study subjects as in the present study.

Concerning the comparison of the resistin levels in the three study groups, it was seen that in the comparison of Group I and Group II, the resistin level was 7.17 ± 0.36 , which was quantitatively significant with $p < 0.05$. Comparing Groups II and III, the resistin levels were 18.14 ± 0.45 pg/ml, which exhibited statistical significance with $p < 0.05$, and for Groups I and III, the resistin levels were 11.26 ± 0.37 pg/ml, which was not statistically significant with $p > 0.05$. These outcomes were in agreement with the previous studies of Alkan et al (2020) and Borilova Linhartova et al (2019), where similar levels to the present study were reported for leptin by authors in their respective studies.

For assessing the adiponectin levels in the three study groups, it was observed that in Group I in comparison to Group II, the mean adiponectin levels were 20.16 ± 0.28 ng/ml, which was a distinction with statistical significance at $p < 0.05$. For Comparing Group II to Group III, the mean adiponectin levels were found to be 9.94 ± 0.29 ng/ml with a substantial difference in terms of statistics and $p < 0.05$. For group comparison III to Group I, the mean value of adiponectin was 15.44 ± 0.34 ng/ml, which was statistically nonsignificant with $p > 0.05$. These results were in line with the previous outcomes of Nepomuceno et al (2019) and Pamuk and Kantarci (2022), where adiponectin levels reported by the authors were comparable to the results of the present study.

4. Conclusions

The current research derives conclusions despite its limitations that adiponectin is an anti-inflammatory compound that increases in subjects following periodontal treatment, whereas resistin is an inflammatory component that shows a reduction after periodontal treatment. Adiponectin can be considered a biomarker in periodontal diseases. Resistin is an adipokine that is largely released by adipose tissue and has been linked to insulin resistance and inflammation. Resistin levels have been discovered to be higher in people with periodontitis than in those with healthy periodontium in the GCF, which is related to periodontal disease. This shows that resistin could aggravate the development of periodontal disease by promoting inflammation in periodontal tissues. However, further investigation is required to completely comprehend the precise pathways via which resistin affects periodontal health. However, further long-term studies with more samples should be performed to reach a definitive conclusion.

Ethical considerations

Not applicable.

Declaration of interest

The authors declare no conflicts of interest.

Funding

This research did not receive any financial support.

References

- Alkan, B, Güzeldemir Akçakanat E, Odabaş Özgür B, Özgür T, Demirdizen Taşkıran A, Kır HM, Alpay N, Çaycı Akkan E (2020) Effects of exercise on periodontal parameters in obese women. *Nigerian Journal of Clinical Practice*.
- Borilova Linhartova P, Janos J, Poskerova H, Kavrikova D, Fassmann A, Dusek L, Izakovicova Holla L (2019) Adipokine gene variability and plasma levels in patients with chronic periodontitis—a case–control study. *Brazilian Oral Research*, 33.
- Brément T, Cossec C, Roux C, Knol AC, Dréno B, Khammari A, Bourdeau P, Bruet V (2019) Expression of three adipokines (Adiponectin, Leptin and Resistin) in normal canine skin: a pilot study. *Journal of comparative pathology* 167:82-90.
- Cai X, Zhu Q, Wu T, Zhu B, Liu S, Liu S, Aierken X, Ahmat A, Li N (2020) Association of circulating resistin and adiponectin levels with Kawasaki disease: A meta-analysis. *Experimental and Therapeutic Medicine* 19:1033-1041.
- Carrion M, Frommer KW, Pérez-García S, Müller-Ladner U, Gomariz RP, Neumann E (2019) The adipokine network in rheumatic joint diseases. *International journal of molecular sciences* 20:4091.
- Custović N, Rašić S (2022) Relationship of serum adiponectin and resistin levels with the severity of liver fibrosis in patients with chronic hepatitis B. *Journal of Medical Biochemistry* 41:176.
- Guilherme A, Henriques F, Bedard AH, Czech MP (2019) Molecular pathways linking adipose innervation to insulin action in obesity and diabetes mellitus. *Nature Reviews Endocrinology* 15:207-225.
- Habib SS, Sultan M, Khan A, Al-Khlaiwi T, Bashir S (2021) Circulating adiponectin and resistin levels are associated with adiposity indices and physical fitness in healthy adult males. *Medical Science Monitor Basic Research* 27:930322-1.
- Hajishengallis G, Hasturk H, Lambris JD, Apatzidou DA, Belibasakis GN, Bostanci N, Corby PM, Cutler CW, D'Aiuto F, Hajishengallis E, Huber-Lang M (2021) C3-targeted therapy in periodontal disease: moving closer to the clinic. *Trends in immunology* 42:856-864.
- Klewin-Steinböck S, Wyganowska M (2023) Reduction in Gingival Bleeding after Atelocollagen Injection in Patients with Hashimoto's Disease—A Pilot Study. *International Journal of Environmental Research and Public Health* 20:2954.
- Koka K, Verma A, Dwarakanath BS, Papineni RV (2022) Technological advancements in external beam radiation therapy (EBRT): An indispensable tool for cancer treatment. *Cancer Management and Research* 1421-1429.
- Marginean CO, Meliț LE, Huțanu A, Ghiga DV, Săsăran MO (2020) The adipokines and inflammatory status in the era of pediatric obesity. *Cytokine* 126:154925.
- Masood M, Younis LT, Masood Y Bakri NN, Christian B (2019) Relationship of periodontal disease and domains of oral health-related quality of life. *Journal of clinical periodontology* 46:170-180.
- Musovic S, Shrestha MM, Komai AM, Olofsson CS (2021) Resistin is cosecreted with adiponectin in white mouse adipocytes. *Biochemical and Biophysical Research Communications* 534:707-713.
- Nepomuceno R, Vallerini BDF, da Silva RL, Corbi SC, Bastos ADS, Dos Santos RA, Takahashi CS, Orrico SRP, Scarel-Caminaga RM (2019) Systemic expression of genes related to inflammation and lipid metabolism in patients with dyslipidemia, type 2 diabetes mellitus and chronic periodontitis. *Diabetes & Metabolic Syndrome: Clinical Research & Reviews* 13:2715-2722.
- Nongrum AD, Guru SR, Nisha KJ, Aghanashini S (2022) Analyzing adipokine Omentin-1 in periodontal disease and type-2 diabetes mellitus: An interventional comparative study. *Journal of Oral Biology and Craniofacial Research* 12:273-278.
- Osman AM, Motawie AA, Al-Aziz A, Amany M, Mostafa NA, Hasan NS, El-Baz MS (2023) Role of adiponectin, resistin and monocyte chemo-attractant protein-1 in overweight/obese asthma phenotype in children. *BMC pediatrics* 23:1-11.
- Pamuk F, Kantarci A (2022) Inflammation as a link between periodontal disease and obesity. *Periodontology 2000* 90:186-196.
- Rezaee M, Putrenko I, Takeh A, Ganna A, Ingelsson E (2020) Development and validation of risk prediction models for multiple cardiovascular diseases and Type 2 diabetes. *PLoS one* 15:e0235758.
- Rode PA, Kolte RA, Kolte AP, Purohit HJ, Ahuja CR (2019) Relevance of single-nucleotide polymorphism to the expression of resistin gene affecting serum and gingival crevicular fluid resistin levels in chronic periodontitis and type 2 diabetes mellitus: A randomized control clinical trial. *Journal of Indian Society of Periodontology* 23:131.
- Seleem D, Dadjoo S, Ha A, Santos C, Mirfarsi S, Matsumura-Lem K, Lazarchik D (2021) Effect of 10% carbamide peroxide on tooth shade, plaque index and gingival index during invisalign treatment. *Dentistry Journal* 9:48.
- Suresh S, Mahendra J, Singh G, Pradeep Kumar AR, Thilagar S, Rao N (2018) Effect of nonsurgical periodontal therapy on plasma-reactive oxygen metabolite and gingival crevicular fluid resistin and serum resistin levels in obese and normal weight individuals with chronic periodontitis. *J Indian Soc Periodontol* 22:310-6.
- Tsuchiya H, Fujio K (2022) Emerging role of leptin in joint inflammation and destruction. *Immunological Medicine* 45:27-34.
- Wielento A, Lagosz-Cwik KB, Potempa J, Grabiec AM (2023) The Role of Gingival Fibroblasts in the Pathogenesis of Periodontitis. *Journal of Dental Research* 1025:489-496.

Integrating evidence-based interventions in cardiac and pulmonary rehabilitation guidelines



Kavina Ganapathy^a | Vipin Kesharwani^b | Md Mazhar Alam^c | Sneha Verma^d

^aJain (Deemed-to-be University), Bangalore, India, Assistant Professor, Department of Biotechnology.

^bMaharishi University of Information Technology, Lucknow, Uttar Pradesh, India, Associate Professor, School of Science and Humanities.

^cTeerthanker Mahaveer University, Moradabad, Uttar Pradesh, India, Professor, Department of T.B. & Chest.

^dMaharishi University of Information Technology, Lucknow, Uttar Pradesh, India, Associate Professor, School of Science and Humanities.

Abstract Cardiac rehabilitation (CR) and pulmonary rehabilitation (PR) programs play a crucial role in optimizing the functional capacity and quality of life of individuals with cardiac and respiratory conditions. These programs are guided by evidence-based interventions that have shown effectiveness in improving clinical outcomes and reducing the burden of disease. Patients with chronic diseases like chronic obstructive pulmonary disease (COPD) and cardiovascular disease (CVD) suffer a disproportionate share of healthcare costs, and many see a decline in their physical and mental abilities as a result. Breathlessness is the first sign of both COPD and cardiovascular disease. Rehabilitation programs (RP) symptoms and improving overall health are two of rehabilitation's demonstrated benefits. Management recommendations for COPD and CVD include participation in a PR and CR program. This study looks at similar evidence-based strategies in rehabilitation guidelines that aim to help patients with COPD and CVD feel less short of breath and better able to function physically and mentally. The results of the show that there was agreement in terms of program structure, setting, healthcare provider teams, pre- and post-program patient assessments, and educational content (with some exceptions related to disease-specific content). Evidence-based recommendations for CR and PR differ from rehabilitation guidelines most noticeably in their emphasis on nutritional screening, inspiratory muscle exercise, and psychological evaluations.

Keywords: PR, CR, cardiovascular disease, rehabilitation programs

1. Introduction

Programs for improving the physical and mental health of people with heart and lung diseases are known as CR and PR treatments. To give all-encompassing care and support, these programs often use a multidisciplinary approach that includes medical experts, fitness specialists, physiotherapists, and psychologists (Yang & Yang 2020). Individuals go through a complete medical assessment before beginning an RP to determine their present health state, identify risk factors, and set baseline data. In CR and PR, education is essential. Patients are informed about their disease, risk factors, medication administration, and changes to a healthy lifestyle. This includes advice on proper eating, quitting smoking, managing stress, and methods to enhance general well-being (Tsutsui et al 2021). A crucial part of cardiac and PR is exercise training. The workout program is customized based on the person's ability and health. It often includes strength training activities to increase muscular strength and endurance as well as aerobic workouts to improve cardiovascular fitness, such as walking or cycling. Exercise sessions are monitored to guarantee their safety (Gordon et al 2019). Programs for PR concentrate on enhancing lung health and treating respiratory problems. Interventions such as breathing exercises, methods to increase lung capacity, and ways for dealing with shortness of breath are offered by respiratory therapists. Techniques including diaphragmatic breathing, pursed-lip breathing, and controlled coughing may be used in these therapies (Bourbeau et al 2020). Drug management is often a part of cardiac and PR programs to ensure proper drug administration and adherence to recommended schedules. The medical staff keeps track of pharmaceutical efficacy, modifies doses as necessary, and instructs patients on how to take their medications correctly (Rutkowski et al 2021). Programs for CR and PR may work with psychologists or counselors to assist, with coping mechanisms, and mental health therapies. They address problems including stress, worry, and depression as well as how to acclimatize to the diagnosis and alter one's lifestyle. The management of heart and pulmonary diseases heavily depends on nutrition. Registered dietitians provide recommendations for a heart- or lung-healthy diet, emphasizing nutrient-rich meals, portion management, and methods for controlling illnesses like hypertension or diabetes (Oates et al 2019). Heart disease risk factors are identified and addressed in CR programs. Dealing with conditions like high blood pressure, high cholesterol, managing diabetes, controlling weight, and giving up smoking might be part of this. Regular vital sign monitoring, exercise performance, symptom assessment, and progress evaluation are all parts of cardiopulmonary therapy. This makes it possible for the medical team to keep tabs on the patient's development,



alter the therapy as needed, and provide ongoing support (Vitacca et al 2020). Cardiac Rehabilitation: In RP, each person receives a long-term maintenance plan to continue their progress. This plan may involve maintaining your workout regimen, altering your lifestyle, getting regular checkups, and having access to support systems in your local area. A dietitian may assist patients in establishing better dietary practices that may minimize their risk of heart disease, such as consuming less saturated fats and cholesterol and more fruits, vegetables, and whole grains (Jiang et al 2020). Quitting smoking is a top goal for the patient. To assist them in quitting smoking, tools, treatments, and counseling may be made available. Living with heart disease might affect one's mental health. Depression, anxiety, and stress therapy may be provided by mental health specialists. Cardiac rehab programs may assist patients in comprehending and appropriately administering their medicines. This involves educating patients about their illness, risk factors, the importance of exercise and nutrition, and methods to stop the development of heart disease (Zhao et al 2020). Exercises that focus on increasing tolerance and stamina are included in this, as well as strength training. The improvement of lung function may also include breathing exercises. Patients get instructions on how to lead normal lives without experiencing breathlessness. To manage shortness of breath, breathing techniques including pursed-lip breathing and diaphragmatic breathing may be taught. Similar to cardiac rehab, assistance for mental health conditions including depression and anxiety is often provided. This can include teaching them about their disease, how to take their meds properly, how to spot and deal with flare-ups, and, if necessary, how to utilize oxygen treatment (Zhu et al 2020). It's crucial to remember that depending on each patient's unique demands, particular therapies may change. Furthermore, both cardiac and PR often adopt a comprehensive strategy that addresses other risk factors (such as high blood pressure, diabetes, and high cholesterol) as well. This study looks at similar evidence-based strategies in rehabilitation guidelines that aim to help patients with COPD and CVD feel less short of breath and better able to function physically and mentally.

2. Related Works

Thomas et al (2019) defined the fundamental elements, effectiveness, advantages, disadvantages, gaps in the evidence, and research required to guide the future delivery of HBCR in the United States. Low- to moderate-strength data from prior randomized studies suggests that center-based CR and HBCR may both enhance clinical outcomes for three to twelve months. They conclude that for certain clinically stable, low- to moderate-risk patients who are qualified for CR but are unable to participate in a conventional center-based CR program, HBCR may be a viable choice. Siddi et al (2020) emphasized PR in COVID-19 and is based on 40 recent articles. There is a dearth of excellent research on this subject. In addition, oxygen treatment, early mobility, airway clearing, cardiovascular activity, gradual-graded limb muscle resistance training, and nutritional, and psychological therapies should be taken into account in instances of mechanical ventilation and post-PICS COVID-19 patients. Holland et al (2021) held to establish prerequisites for the effective implementation of developing program models and to reach agreement on the key elements of PR. In a Delhi process, experts from all around the world came together to determine the 13 essential PR components that any program model must have. These components include patient assessment, program content, delivery strategy, and quality control. Only PR models that have completed clinical studies are now recognized as being suitable for usage.

Wang et al (2020) extrapolate data from earlier research and experience to provide a PR viewpoint & interference with the multi-corrective conduct of COVID-19. Patients with COVID-19 may benefit from PR by reducing their dyspnea symptoms, anxiety levels, complications, disability, loss of function, and overall quality of life. The selection of various training methods includes cardiopulmonary exercise testing, as discussed by Kumar. The addition of additional treatments such as noninvasive ventilator support, and oxygen, in certain individuals, is explored together with neuromuscular electrical stimulation, gait evaluation, and training. In individuals with underlying pulmonary hypertension, the possibility of pulsed inhaled nitric oxide is investigated, together with nutritional assistance. It reviewed how sleep quality affects PR results (Wouters et al 2020). Recommendations for rehabilitation procedures in each of the 5 phases of the COVID-19 scale ambulatory patients and epidemiological risk factors; ventilator-supported patients with obvious cognitive function; and patients with no cognitive impairment (Cheng et al 2019). Evidence also points to a potential decrease in post-COPD exacerbation healthcare use. Since its origin, PR has progressively developed into the organized, multi-component intervention that is provided by a multidisciplinary team today. This intervention addresses the unique health requirements of each respiratory patient and generally lasts for several weeks. To modify behaviors permanently, emphasis is put on boosting self-efficacy via group self-management training (Nici et al 2019).

Spencer & McKeough (2019) assessed the most recent research on maintenance exercise programs for COPD patients and identify the kinds of programs that can sustain the effects of PR for at least a year. The present research on maintenance exercise programs that included supervised maintenance exercise was insufficient, and the research on maintenance exercise programs that included unsupervised maintenance exercise was confusing and, in many cases, did not demonstrate any superiority above standard care. The writers of this paper, who are all members of the Canadian Thoracic Society (CTS), came to these conclusions based on the data available at the time this document was published. In the post-peak phase of the COVID-19 pandemic, this position statement intends to provide direction for the restart of PR programs Dechman et al (2020). Clinical procedures of "thinking differently" and "pushing the frontiers" are now underway, particularly in the United

Kingdom and Australia, where novel PR strategies are being piloted. The primary goals are to reach the COPD population and send them to rehabilitation services (McNamara et al 2019).

3. Methods

These methodical review objectives were to locate and assess existing countrywide and worldwide standards for CR and PR. The main goal of this evaluation was to locate within these rehabilitation recommendations evidence-based therapies and outcome measures that would reduce breathlessness.

3.1. Search strategy

The Preferred Reporting Items for Systematic Reviews and Meta-Analyses (PRISMA) statement's recommendations were followed while conducting the preceding procedure's ambitious and methodical investigation of gaze review journalism. For pertinent citations, the following electronic databases were searched: MEDLINE (OVID), EMBASE, and CINAHL (EBSCO). These databases include Epub Ahead-of-Print, In-Process, and Other Non-Indexed Citations. To make guarantee that the most current recommendations were found, search outcomes were restricted to English-language sources, and the search technique was applied to citations produced between January 2000 and July 2016. In the title and abstract fields, the search phrases CR and PR were combined with "guideline." Each database's relevant medical topic headings were used to shorten and modify the search phrases, and Table 1 shows the search method used for the MEDLINE database.

Table 1 Search Strategy for MEDLINE.

No.	Search Term(s) Utilised	Results
1	(guideline or practice guideline).pt.	(23091)
2	One or two	(6694)
4	3 and 7	(165)
5	Practice Guideline/	(18998)
6	4 or 5 or 6	(36468)
7	(pulmonary adj4 rehab*).ti,ab.	(2390)
8	Limit eight to (English Language and yr = "2000-current")	(122)
9	(Cardi* adj4 rehab*).ti, ab.	(4430)

3.2. Eligibility criteria

Practice guidelines that outlined the evidence foundation for interventions and were a main document supported or certified by a countrywide or worldwide group qualified for inclusion. The relevant criteria have to include either cardiac RP or PR programs. Practice or clinical recommendations that expressed broad opinions and descriptions without supporting data or that were not supported were disregarded. Integrating evidence-based therapies and outcomes measurements were the main results of interest for this evaluation. To guarantee that concordance could be established, these review results were assessed via the detailed description of rehabilitative therapies or outcome assessment.

3.3. Guideline and statement selection and data extraction

Duplicates were eliminated when the database and online searches were finished. The inclusion criteria were used to independently filter the title and abstract of the retrieved recommendations and statement. Guidelines in the full text were located and then reviewed for inclusion. Any differences of opinion over the inclusion of a guideline were addressed until an agreement was reached. Using a pre-made spreadsheet, data extraction was done and checked for completeness

3.4. Quality assessment

Utilizing the guidelines for "advancing guideline development, reporting, and evaluation in healthcare (AGREE II)", the quality of the contained recommendations was assessed. The AGREE instrument consists of 23 elements, which are divided into 6 areas. These domains include scope and goal, stakeholder engagement, applicability, clarity of presentation, rigor of development, and editorial independence. Grading of Recommendations Evaluation, Development, and Evaluation (GRADE) was used to evaluate guideline recommendations in addition to the excellent evaluation of the guidelines.

4. Results

The combined database searches turned up 410 documents in total, 165 of which were eliminated because they were duplicates of records in another database. The remaining 21 records, which may have directly treated breathlessness via RP and were supported by worldwide associations on respiratory or cardiac medicine, remained after the titles and abstracts were evaluated. An additional 9 articles were eliminated after reading the complete content of these articles. Two articles published in both the journals of the collaborating societies were deemed to be redundant, four guidelines that had been retired but were later updated, and two COPD management guidelines that did not rely on evidence were all deemed to be

ineligible for inclusion. Figure 1 shows the method for the selection of articles and lists all nine guidelines publications that were included.

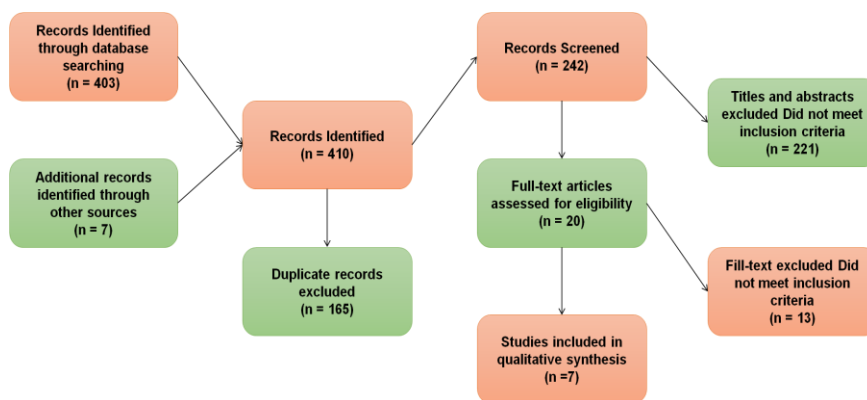


Figure 1 Flow diagram for guideline selection.

4.1. Overview of the Declarations and Guidelines

Of the listed clinical or practice guidelines, 3 pertained to PR and 6 to cardiac rehabilitation. There was one guideline from Australia with interdisciplinary authorship, and the recommendations were supported by societies in Europe and North America. The features of these published rules are outlined in Table 2.

Table 2 Summary of the Approved CR and PR Clinical Practice Guidelines.

Author	Country of Society	CR or PR	Endorsing civilization	Year of Publication	Graded technique
BACPR, 2012	United Kingdom	CR	British Heart Foundation and the British Association for Cardiovascular Prevention and Rehabilitation (BACPR)	2012	No
Ries et al 2007	United States	PR	American Association of Cardiovascular and PR and American College of Chest Physicians	2007	Yes
Bolton et al 2013	United Kingdom	PR	United Kingdom Thoracic Society	2013	Yes
JCS et al 2014	Japan	CR	JCS, the Japanese Circulation Society	2014	Yes
Achtstien et al 2015	Netherlands	CR	Physiotherapy Royal Society of the Netherlands	2015	No
Piepoli et al 2016	European Union	CR	American Association of Cardiovascular and PR and the American Heart Association	2016	No
Woodruffe et al 2015	Australia	CR	Association for Australian Cardiovascular Health	2015	No

Figure 2 shows that only a tiny percentage of people with COPD participate in annual rehabilitation activities. Additionally, a systematic study looked for reasons why people don't enroll in or finish cardiac RP and tried to find solutions to those reasons. The review found that between 10 and 30 percent of people who initially agreed to participate in a cardiopulmonary RP eventually dropped out due to issues.

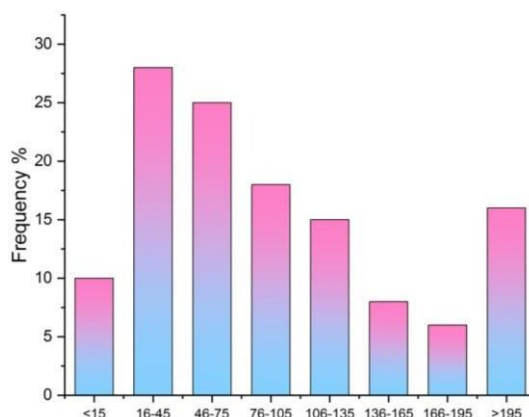


Figure 2 Quantity of potential participants for each PR initiative.



4.2. Characteristics of intervention design

Rehabilitation was defined in all regulations as an individualized plan that would involve both physical activity and learning opportunities, as well as an initial evaluation and periodic progress checks throughout the program. The locations of the RP varied, although most practice standards for important healthcare venues including hospitals, communities, and private homes included evidence to this effect. Another discrepancy between the pulmonary and cardiac recommendations was the program length. Guidelines identifying individuals from the fields of nursing, medicine, and allied health who lead and manage RP described a wide range of program facilitation.

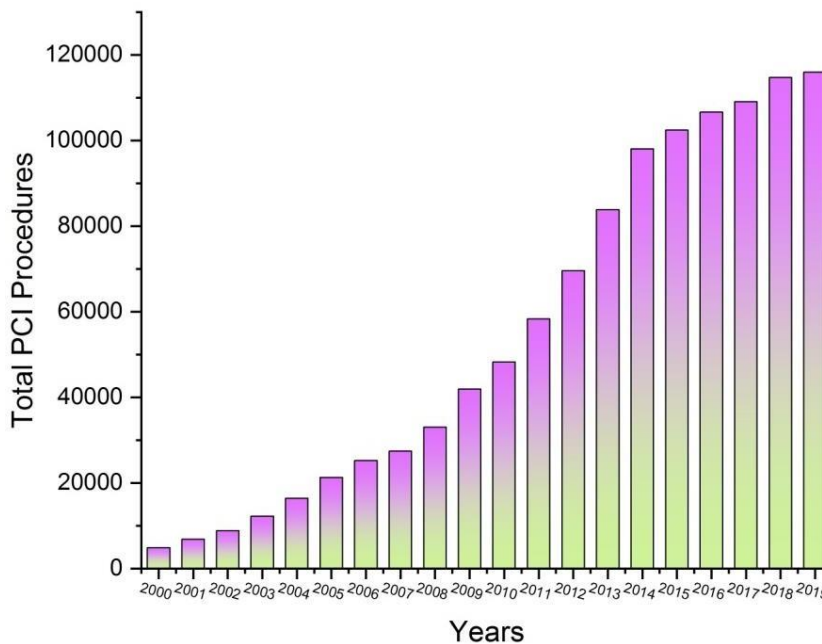


Figure 3 Comparison of years with PCI procedures.

Treatment of coronary heart disease using percutaneous coronary intervention (PCI) has been more prevalent during the last twenty years. The number of percutaneous coronary interventions (PCI) has surpassed that of coronary artery bypass grafts. Currently, there are over 1.2 million PCI operations done annually in the United States (Figure 3). The level of CR engagement varied significantly across institutions, ranging from 0% to 36% (Figure 4).

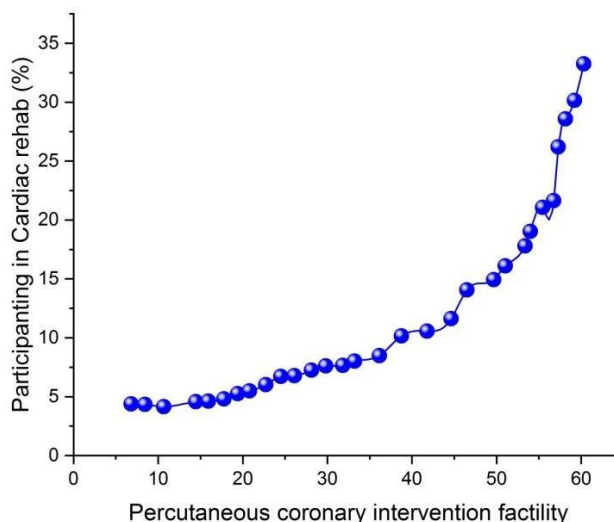


Figure 4 Participation in CR by facility among veterans undergoing PCI.

4.2.1. Location and Duration of Intervention

The cardiac RP had two practice guidelines that specifically mentioned that phase one was carried out in hospitals and phases two and three were conducted in community or home settings. The venue was recommended based on the



program phase, and all of the practice guidelines that discussed the topic mentioned either a hospital or a community setting for the RP, with all of them stating that the setting did not affect the outcomes.

4.2.2. *Personnel*

The individuals responsible for carrying out the RP were outlined in four recommendations. A multidisciplinary team was mentioned in every article as being necessary for the creation of the best RP. As part of the central rehabilitation team, physical therapists, physiotherapists, and exercise physiologists were specifically included. The participation of several other medical specialties varied amongst the recommendations and included psychologists, dieticians, pharmacists, occupational therapists, general practitioners, and specialists in social services.

4.2.3. *Assessment of Patients*

Two CR recommendations also included mid-program evaluations, while the majority of guidelines advised post-rehabilitation patient evaluations. Only one of three recommendation publications for PR recommended patient evaluation, which is an interesting difference from CR guidelines. All of the recommendations made in the guidelines about the evaluation of patients called for thorough, specific evaluations, including patient interviews to ascertain health conditions and/or measurements of exercise ability. The context of the guideline-based patient group and additional information beyond these characteristics differed between CR and PR. For instance, in CR after myocardial infarction, cardiac possibility factors and psychological state were thought to be essential outcomes to be assessed.

4.2.4. *Components of Interventions*

Exercise education and training were the main elements included in every practice or therapeutic recommendation. Depending on the standards, the specifics of the exercise instruction and training varied and were sometimes tailored to the patient group. The recommended fitness training treatments are included. Smoking cessation, stress management, risk factors, food, and exercise were pertinent instructional subjects.

4.2.5. *Additional Program Elements*

Numerous practice recommendations included the following rehabilitation components: noninvasive ventilation (NIV), inspiratory muscle exercise, psychosocial therapies, social support, and dietary assessment and nutritional interventions. Four CR practice recommendations advised dietary evaluation and nutritional management. In contrast, only one of the three recommendations for PR included a dietary component, and the other two said that there was insufficient data to support such a suggestion. There were few recommendations for nutritional components and sequence on how to check for nutritional status; the most often used method was self-reporting one's calorie intake and diet. Body mass index and waist circumference were among the objective measurements discussed, and just one recommendation included the use of a validated screening instrument to determine caffeine and alcohol use. Guidelines for CR included dietary therapies such as goal-setting for weight reduction, diet journals, education, and cholesterol control (pharmacological and dietary). All CR practice or clinical guidelines recommended psychological screening and/or interventions, but PR guidelines did not specifically mention psychological screening and/or interventions outside. Family members should mostly participate in small-group or individual activities that are based on guidelines. Only one practice guideline specified a set number of sessions for psychosocial intervention, with each session lasting between sixty and ninety minutes: eight to ten. Two CR practice recommendations included social support, however, they did so in terms of the program's ethos or how psychological therapies were incorporated into them rather than particular social support initiatives. There was little support for such behavior, and there were few suggestions. Five practice guidelines advocated smoking cessation; two of them included particular treatments in their direct recommendations, while the other two included them in the list of educational activities for rehabilitation. The particular guidelines-based therapies include behavior modification interventions, education, hypnotherapy, and acupuncture. Training the inspiratory muscles, oxygen treatment, and NIV were additional therapies included in the cardiac and pulmonary recommendations. A PR practice guideline did not support inspiratory muscle exercise although one CR practices guideline.

4.3. *Guidelines and statement quality evaluation*

Only 3 of the recommendations included in this assessment were determined to fulfill twenty-three criteria across the six domains of the AGREE II checklist when their quality was evaluated. The areas of rigor, guideline formulation, and application where the criteria were inadequately stated in CR and PR clinical recommendations were predominant. A straightforward connection between suggestions and evidence, as well as search techniques and evidence selection standards, were all absent in this field. Limited reporting was also included in the editorial independence area of the included rules. The GRADE criteria were used to evaluate the quality of the suggestions made by the guidelines, and it was discovered that 4 of them satisfied every criterion.

4. Discussion

The findings of this systematic analysis show that the clinical practice guidelines for CR and PR, which center on treating the symptom of breathlessness, have common design principles. The programs' design principles were in agreement in that they were described as individually tailored interventions, had durations of between six and twelve weeks, were conducted in similar settings by similar multidisciplinary staff, including patient assessments both before and after the agenda, and be built to consist of exercise instruction and learning. The finding of concordance is not unexpected since the goal of rehabilitation is to enhance health conclusion via learning, exercise preparation, and patient empowerment to treat the indication of dyspnea present in CR and PR disorders. Although the core ideas and underlying principles of CR and PR historically were identical, they were developed and assessed independently. The body of research supporting the efficacy of CR and PR programs with a focus on exercise instruction and behavior modification is constantly expanding. This might help with the possibility of creating RP in collaboration. The possibility of delivering some components of CR and PR programs jointly may be taken advantage of to benefit patients in the future, particularly those who have comorbid conditions of heart and lung disease, where breathlessness is a common symptom of both conditions. Despite the agreement, there are differences in the focus of the educational activities and other complementing parts of the RP. It is recommended that PR programs include things like NIV and oxygen therapy for particular patient groups, whereas CR programs should include things like therapy for the mind (psychotherapy). While nutritional treatment is highly recommended for lowering risk factors associated with CVD, its role in PR is less clear. These differences are to be anticipated since they help shape RP so that it meets the unique requirements of each participant. When concentrating on the psychological well-being of CR and PR patients, a divergence from concordance is seen. By combining the necessary evidence-based therapies, a program is tailored to fit the patient's requirements and personal objectives. Although the subjects covered in the CR and PR programs were similar, the way the instruction was delivered seemed to have little support from an educational framework. To provide a genuinely personalized learning experience, future studies should investigate the impact of RP's mandated sequence for delivering subjects. This research suggests that, rather than just classifying patients as completing PR or CR, there is potential to uncover synergies in establishing lifestyle modification programs to aid in the rehabilitation of patients with dyspnea. People with COPD had a significantly increased risk of developing cardiovascular disease (OR equal to 4.98; 95 percent CI equal to 4.85 to 5.81; P.001, n equal to 1 204 100). They have a 1.76 (95 percent CI, 1.64-1.89) increased risk of arrhythmias, a 1.61 (95 percent CI, 1.47-1.76) increased risk of angina pectoris, a 1.61 (95 percent CI, 1.43-1.81) increased risk of acute myocardial infarction, and a 3.84 (95 percent CI, 3.56-4.14) increased risk of congestive heart failure compared to the general population. People with COPD have a higher risk of being hospitalized owing to a cardiovascular event, and they have a 2.07-fold (95 percent CI, 1.82-2.36) higher risk of dying from cardiovascular diseases.

Lung function decline seems to be linked to cardiovascular events via traditional CVD risk factors. It's important to weigh the pros and cons of operating two distinct RP for people with persistent cardiopulmonary dysfunction, one labeled PR and the other CR. The low rates of patient completion seen in existing PR and CR models highlight the need of developing patient-centered, long-term solutions. About half of all referrals end up starting pulmonary rehabilitation, and of those who do start, thirty percent don't end up finishing. It has been suggested that difficulties in getting to and from PR sessions, as well as a general lack of interest in the treatment, contribute to its low uptake and completion rates. Non-attendees in CR are similar to those in other types of rehabilitation in terms of age, income, level of social deprivation, and denial of the seriousness that their doctor does not recommend CR. The patient's experience of benefit may be enhanced by tailoring a program to reduce breathlessness to the unique needs of the individual within a rehabilitation framework. Such novel approaches to rehabilitating patients who suffer dyspnea on the part of medical experts may increase participation and provide lasting benefits. It may be reasonable to pursue studies of a centralized rehabilitation paradigm that prioritizes the treatment of symptoms and the whole person by combining CR and PR therapies.

5. Conclusion

The findings of this systematic review, which focused on treating the symptom of breathlessness, show agreement in many design concepts across CR and PR clinical practice guidelines. These results point to the potential to develop synergies within RP so that they may focus on symptom management rather than aspects that are mandated based on disease processes. Future studies may concentrate on dissecting existing CR and PR programs and revamping them to be more comprehensive, individually personalized, and with a stronger emphasis on the symptoms and concerns of the patient.

6. Limitations

Furthermore, it's possible that recommendations that were released after the a priori specified search time wasn't found and weren't included in this study. In addition to searching databases, a thorough search of worldwide the general public websites about CR and PR disorders was carried out. Despite this, some important recommendations were probably missed. Overall, it was determined that several of the recommendations in the included guidelines had poor levels of

evidence, and many of them had not employed the GRADE method to evaluate the literature, which may have limited the applicability of the recommendations to clinical practice.

Ethical considerations

Not applicable.

Declaration of interest

The authors declare no conflicts of interest.

Funding

This research did not receive any financial support.

References

- Achtien RJ, Staal JB, Van der Voort S, Kemps HM, Koers H, Jongert MWA, Practice Recommendations Development Group (2015) Exercise-based cardiac rehabilitation in patients with chronic heart failure: a Dutch practice guideline. *Netherlands Heart Journal* 23:6-17.
- BACPR (2012) BACPR standards and core components for cardiovascular disease prevention and rehabilitation. Available in: www.bacpr.com/resources/46C_BACPR_Standards_and_Core_Components_2012.pdf. Published
- Bolton CE, Bevan-Smith EF, Blakey JD, Crowe P, Elkin SL, Garrod R, Walmsley S (2013) British Thoracic Society guideline on pulmonary rehabilitation in adults: accredited by NICE. *Thorax* 68:ii1-ii30.
- Bourbeau J, Gagnon S, Ross B (2020) Pulmonary rehabilitation. *Clinics in Chest Medicine* 41:513-528.
- Cheng YY, Chen CM, Huang WC, Chiang SL, Hsieh PC, Lin KL, Chou W (2021) RP for patients with COroNaVirus Disease 2019: consensus statements of Taiwan.
- Dechman G, Acheron R, Beauchamp M, Bhutani M, Bourbeau J, Brooks D, Stickland MK (2020) Delivering pulmonary rehabilitation during the COVID-19 pandemic: A Canadian Thoracic Society position statement. *Canadian Journal of Respiratory, Critical Care, and Sleep Medicine* 4:232-235. DOI: 10.1080/24745332.2020.1828683.
- Gordon CS, Waller JW, Cook RM, Cavallera SL, Lim WT, Osadnik CR (2019) Effect of pulmonary rehabilitation on symptoms of anxiety and depression in COPD: a systematic review and meta-analysis. *Chest*, 156(1), 80-91. DOI: 10.1016/j.chest.2019.04.009.
- Holland AE, Cox NS, Houchen-Wolloff L, Rochester CL, Garvey C, ZuWallack R, Singh SJ (2021) Defining modern pulmonary rehabilitation. An official American Thoracic Society workshop report. *Annals of the American Thoracic Society* 18:e12-e29. DOI: 10.1513/AnnalsATS.202102-146ST.
- JCS Joint Working Group (2014) Guidelines for Rehabilitation in Patients With Cardiovascular Disease (JCS 2012)—Digest Version—. *Circulation Journal* 78: 2022-2093.
- Jiang Y, Liu F, Guo J, Sun P, Chen Z, Li J, Wu X (2020) Evaluating an intervention program using WeChat for patients with chronic obstructive pulmonary disease: randomized controlled trial. *Journal of medical Internet research* 22:e17089. DOI: 10.2196/17089.
- McNamara RJ, Dale M, McKeough ZJ (2019) Innovative strategies to improve the reach and engagement in pulmonary rehabilitation. *Journal of thoracic disease* 11:S2192. DOI: 10.21037/jtd.2019.10.29.
- Members TF, Piepoli MF, Hoes AW, Agewall S, Albus C, Brotons C, Zamorano JL (2016) European Guidelines on cardiovascular disease prevention in clinical practice: The Sixth Joint Task Force of the European Society of Cardiology and Other Societies on Cardiovascular Disease Prevention in Clinical Practice (constituted by representatives of 10 societies and by invited experts): Developed with the special contribution of the European Association for Cardiovascular Prevention & Rehabilitation (EACPR). *European journal of preventive cardiology* 23:NP1-NP96.
- Nici L, Singh SJ, Holland AE, ZuWallack RL (2019) Opportunities and challenges in expanding pulmonary rehabilitation into the home and community. *American journal of respiratory and critical care medicine* 200:822-827. DOI: 10.1164/rccm.201903-0548PP.
- Oates G R, Niranjani SJ, Ott C, Scarinci I, Schumann C, Parekh T, Dransfield MT (2019) Adherence to pulmonary rehabilitation in COPD: a qualitative exploration of patient perspectives on barriers and facilitators. *Journal of cardio pulmonary rehabilitation and prevention* 39:344. DOI: 10.1097%2FHCR.0000000000000436.
- Ries AL, Bauldoff GS, Carlin B W, Casaburi R, Emery CF, Mahler DA, Herreras C (2007) Pulmonary rehabilitation: joint ACCP/AACVPR evidence-based clinical practice guidelines. *Chest* 131:4S-42S.
- Rutkowski S, Szczegielniak J, Szczepańska-Gieracha J (2021) Evaluation of the efficacy of immersive virtual reality therapy as a method supporting pulmonary rehabilitation: A randomized controlled trial. *Journal of Clinical Medicine* 10:352. DOI: 10.3390/jcm10020352.
- Siddi MAB, Rathore, FA, Clegg D, Rasker JJ (2020) pulmonary rehabilitation in COVID-19 patients: A scoping review of current practice and its application during the pandemic. *Turkish journal of physical medicine and rehabilitation* 66:480. DOI: 10.5606%2Ftjtrd.2020.6889.
- Spencer LM, McKeough ZJ (2019) Maintaining the benefits following pulmonary rehabilitation: achievable or not?. *Respirology* 24:909-915. DOI: 10.1111/resp.13518.
- Thomas RJ, Beatty AL, Beckie TM, Brewer LC, Brown TM, Forman DE, Whooley MA (2019) Home-based cardiac rehabilitation: a scientific statement from the American Association of Cardiovascular and Pulmonary Rehabilitation, the American Heart Association, and the American College of Cardiology. *Circulation*, 140:e69-e89. DOI: 10.1161/CIR.0000000000000663.
- Tsutsui M, Gerayeli F, Sin DD (2021) Pulmonary rehabilitation in a post-COVID-19 world: telerehabilitation as a new standard in patients with COPD. *International journal of chronic obstructive pulmonary disease* 379-391.
- Vitacca M, Lazzeri M, Guffanti E, Frigerio P, D'Ambrosia F, Gianola S, Clini E (2020) Italian suggestions for pulmonary rehabilitation in COVID-19 patients recovering from acute respiratory failure: results of a Delphi process. *Monaldi Archives for Chest Disease* 90:1-9. <https://dx.doi.org/10.4081/monaldi.2020.1444>.



Wang TJ, Chau B, Lui M, Lam GT, Lin N, Humbert S (2020) PM&R and pulmonary rehabilitation for COVID-19. *American journal of physical medicine & rehabilitation*. DOI: 10.1097%2FPHM.0000000000001505.

Woodruffe S, Neubeck L, Clark RA, Gray K, Ferry C, Finan J, Briffa TG (2015) Australian Cardiovascular Health and Rehabilitation Association (ACRA) core components of cardiovascular disease secondary prevention and cardiac rehabilitation 2014. *Heart, Lung and Circulation* 24:430-441.

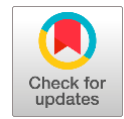
Wouters EF, Posthuma R, Koopman M, Liu WY, Sillen MJ, Hajian B, Franssen FM (2020) An update on pulmonary rehabilitation techniques for patients with chronic obstructive pulmonary disease. *Expert review of respiratory medicine* 14:149-161. DOI: 10.1080/17476348.2020.1700796.

Yang LL, Yang T (2020) Pulmonary rehabilitation for patients with coronavirus disease 2019 (COVID-19). *Chronic diseases and translational medicine* 6:79-86. DOI: 10.1016/j.cdtm.2020.05.002.

Zhao HM, Xie YX, Wang C, Chinese Association of Rehabilitation Medicine, Respiratory Rehabilitation Committee of Chinese Association of Rehabilitation Medicine, & Cardio pulmonary rehabilitation Group of Chinese Society of Physical Medicine and Rehabilitation. (2020). Recommendations for respiratory rehabilitation in adults with coronavirus disease 2019. *Chinese medical journal* 133:1595-1602.

Zhu Y, Wang Z, Zhou Y, Onoda K, Maruyama H, Hu C, Liu Z (2020) Summary of respiratory rehabilitation and physical therapy guidelines for patients with COVID-19 based on recommendations of World Confederation for Physical Therapy and National Association of Physical Therapy. *Journal of physical therapy science* 32:545-549. DOI: 10.1589/jpts.32.545.

Exploring sleep disorders in multiple sclerosis: a case-control study utilizing the São Paulo epidemiologic sleep study database



Renuka Jyothi S.^a | Shikhar Verma^b | Prerana Gupta^c | Ramakant^d

^aJain (Deemed-to-be University), Bangalore, India, Assistant Professor, Department of Life Sciences.

^bMaharishi University of Information Technology, Lucknow, Uttar Pradesh, India, Associate Professor, School of Science and Humanities.

^cTeerthanker Mahaveer University, Moradabad, Uttar Pradesh, India, Professor, Department of Psychiatry.

^dMaharishi University of Information Technology, Lucknow, Uttar Pradesh, India, Associate Professor, School of Science and Humanities.

Abstract Sleep disorders (SD), such as obstructive sleep apnea (OSA), restless legs syndrome (RLS), and others, may affect anybody, regardless of health or the presence of chronic problems like Multiple Sclerosis (MS). People with Multiple Sclerosis (PwMS) and a community population from So Paulo, Brazil, were compared for issues with sleep, depression, fatigue, and the chronotype. Participants in the PwMS trial were not the same as those in the So Paulo Epidemiologic Sleep (SPES) study. Analysis of variance (ANOVA) and multivariate analysis of variance (MANOVA) tests were used to investigate the sleep questionnaire responses to determine the impact of various factors. Covariates are factors that include age, sex, and activity. The results of the sleep surveys with the Expanded Disability Status Scale (EDSS) have been analyzed utilizing the Pearson correlation test (PCT). Propensity score matching additionally decreased predict bias for differences between the two groups. The tools for the analysis were Stata 14 with IBM SPSS Statistics for Windows, version 22.0. By comparing the PwMS, the Episono group (EG) slept less soundly and felt more sleepy when they woke up. In the Episono group, OSA and RLS were more common. The two groups' choices for the morning and the middle did not differ according to chronotype. The EDSS and sleep problems did not correlate. PwMS described being completely worn out. Sleep issues were less common, although disease-modifying drug-treated weariness was more common in PwMS than in a sample of So Paulo city residents. There was no difference in chronotype. The immunomodulatory medications often used for MS may have affected these results.

Keywords: sleep, restless legs syndrome, fatigue, multiple sclerosis, obstructive sleep apnea

1. Introduction

MS is a chronic, inflammatory, and neurodegenerative disease caused by autoimmune responses that eventually demyelinate the spinal cord and central nervous system (CNS) (Ordoñez et al 2023). Even in the early stages of this neurological illness, gait impairment is a typical symptom. Ataxia, hypertonic muscles, and musculoskeletal abnormalities are just a few of the things that can prevent the plantigrade foot from making proper contact with the ground, which will drastically diminish the patient's functional independence and well-being (Ruiz-Sánchez et al 2023). MS patients often have sleep issues connected to several problems that significantly affect daily functioning and quality of life. According to epidemiological research, sleep disturbances are more prevalent in MS patients than in healthy controls, particularly in females who have had the illness longer, are on immunotherapy, and are under higher stress (Comi et al 2023). Inflammatory plaques are a hallmark of MS, and depending on where they exist, they may result in various neurological symptoms. The four most common early syndromes are a double vision from a brain stem issue, ataxia from a cerebellar lesion, optic neuritis-induced monocular visual loss, and transverse myelitis-induced limb weakness or sensory loss (Pivovarova et al 2023). Treating their fatigue is a top goal for MS patients. Medication, non-pharmacological therapies like physical therapy, exercise therapy, and non-invasive brain stimulation are all possible treatments for MS-related fatigue (Qomi et al 2023). People with PwMS often suffer increased tiredness, intellectual challenges, prolonged stress, shifts in mood, and a lower quality of life, including adaptability or decreased well-being, physical disability, and pain (Novak and Lev-Ari 2023). Shift employment is prevalent throughout adolescence when sleep and circadian timing begin to phase delay. As a result, regular sleep-wake cycles and short sleep duration may be side effects of shift work. Poor sleeping habits and sleep deprivation affect immunological pathways that have elevated proinflammatory signaling, which may raise the chance of developing a chronic Inflammatory Disease (CID) (Pivovarova et al 2023). According to nearly three decades of scientific study, rehabilitation therapies should be incorporated into comprehensive MS care to minimize impairments, enhance activity, and



boost involvement for people with MS (Fakolade et al 2023). Despite its high prevalence, fatigue in MS patients only responds weakly to treatment. This is partly due to inaccurate biomarkers and poor mechanistic knowledge (Chang et al 2023).

2. Literature Review

Moussa et al (2023) revealed probable links between certain occupations and the development of MS. A healthy control group (HCP) was used to compare the effects of the COVID-19 pandemic on people with MS, Parkinson's disease (PD), and Alzheimer's disease (AD) in terms of neuropsychiatric problems (de Oliveira et al 2023). Rocchi et al (2023) outlined the actigraphic patterns in MS patients receiving dimethyl fumarate medication. Present a review of the most current studies on sleep disturbances (SD) in MS and suggest a practical method for identifying and treating the most prevalent CSD in this group. (Braley et al 2023) provided an overview of the most recent information on sleep disturbances in MS. They offered a practical method for identifying and treating this population's most prevalent sleep issues. Souissi et al (2023) determined how the first relapse of MS affected the progression of the illness and the onset of new disabilities. Genç et al (2023) measured the total volume of demyelinating lesions (TLV), the extended disability status scale (EDSS), and the hypothalamus' overall size in RRMS patients. Ghareghani et al (2023) demonstrated that MS prevalence rose with latitude from the equator to the poles. Zhang et al (2023) showed that MS patients can have polysomnographic abnormalities. Our findings further highlight the necessity of a thorough polysomnographic evaluation of sleep alterations in MS patients. Akerstedt et al (2023) compared the sleep habits of healthy control individuals and patients with MS. The endocannabinoid system's function in neuroinflammatory diseases will be briefly reviewed in (Abd-Nikfarjam et al 2023). Papiri et al (2023) emphasized the shared biological processes underlying MS, autoimmune illnesses, and neurodegenerative disorders. In reality, there is a gap in our knowledge regarding potential novel targets for master regulators of autoimmunity, inflammation, and nerve cell survival. Bader and Ellouz (2022) used a templated sheet to examine the patient's sociodemographic, clinical, and treatment data. Madhaw and Kumar (2022) focused on the frequency, etiology, and management of sleep problems in MS patients. Sparasci et al (2022) compared a group of MS patients with SRBD to healthy controls (HC) and considered the neuroimaging study's findings. Riccitelli et al (2022) examined the connection between CI and sleep problems in MS patients and the impact of anxiety and sadness on this association. Tarasiuk et al (2022) investigated the pathogenesis, approaches for assessing and discriminating fatigue and depression in MS, and potential therapies. In a more extensive study involving veterans with MS, Aljundi et al (2022) looked at the connections between daytime performances, sleep quality, insomnia symptoms, and sleep-disordered breathing (SDB).

3. Materials and Methods

The importance of obsessive-compulsive behaviour (OCB) and the extent to which point-of-service (POS) rewards are given for good work performance are examined. A structured questionnaire with the necessary levels of reliability and validity is utilized to gather information from a model of 380 respondents. The research goals are established using both univariate and bivariate statistical analytic methodologies.

3.1. Design

PwMS and a CG are compared in this case-control study. From March to December 2016, patients for the Neuroimmunology Clinic were sought out from the Neurological and Neurosurgery Department at the Escola Paulista de Medicina, a tertiary centre for treating persons with MS and other demyelinating disorders. Participants in the Episono experiment made up the CG.

3.2. Patients

They were invited to participate in the research and complete sleep surveys after being randomly selected from among the day's planned visits. The exclusion criteria included severe cognitive impairment, recent relapse history, and corticosteroid usage over the previous four weeks, and untreated coexisting illnesses such as diabetes, hypothyroidism, or urinary tract infection. All the interviews were done, and the questionnaires were actively filled out during the patients' medical appointments by a researcher with training in sleep problems but not an expert.

3.3. Episono study's control group

The SPES investigation database has the findings of the most significant and most comprehensive epidemiologic investigation on problems with sleep ever conducted in Brazil. The Instituto Datafolha hired and trained the team to conduct house interviews with experts from the Instituto do Sono. When the technician reached the selected person's home, sleep questionnaires were given out. Seven hundred fifteen people participated in the trial's second wave, which lasted from July 2015 to April 2016. They responded to surveys and interviews on their sleep.

3.4. Ethics approval

All participants completed the informed consent form after the Universidad Federal de So Paulo study ethics committee accepted the research protocol.

3.5. Questionnaires

Our team employed these questionnaires and assessment tools in the Episono study: the Epworth sleepiness scale (ESS), the Berlin Questionnaire, the Beck depression inventory (BDI), and the Pittsburgh sleep quality index (PSQI). The fatigue severity scale questionnaire was used to evaluate the patients, whereas the Chalder Fatigue Scale was used to assess the CG. Only those who insisted they had physically powerful advice for traveling their legs during the past 12 months were diagnosed with International Restless Legs Syndrome (IRLS). Each group's response was contrasted only once. Every member of the EG completed the entire questionnaire.

3.6. Clinical variables

We collected data on demographic factors, including race, age at onset of symptoms, length of follow-up, medical form, time since the most recent relapse, before and during MS treatments, medications for other comorbidities, drinking and smoking habits, medical histories, and neurological dysfunction as assessed by Kurtzke Expanded Disability Status Scale (KEDSS) scores.

3.7. Study's goal

The main goal was to identify the association between weariness and impairment by comparing the prevalence of snooze complaints involving PwMS with the Episono database.

3.8. Statistical analysis

Everyone concurred that the terms mean and standard deviation (SD) denote continuous variables, whereas absolute numbers (n), relative frequency (%), and percentage are used to indicate categorical data. Our team first used MANOVA to examine the effects of contrasting the two groups in the five distinct polls. We looked at each dependent variable, in turn, using univariate ANOVA and the variables sex, age, and physical activity until a statistically significant MANOVA was achieved. The sleep survey and EDSS results were linked using the Pearson correlation test. Each ANOVA was adjusted for Type I error rates for multiple comparisons using the Bonferroni technique with a significance level of 0.0088. The MS and Episono databases were developed due to numerous observational research. Using the propensity score matching (PSM) approach, we appropriately matched patients and controls to remove bias when evaluating treatment results and consider imbalances between the two groups. The patients and the rules had the same race, years of age, and amounts of physical activity. Editions 14 of Stata Statistical Software as well as 22.0 of IBM SPSS Statistics for Windows were utilized in the inquiry.

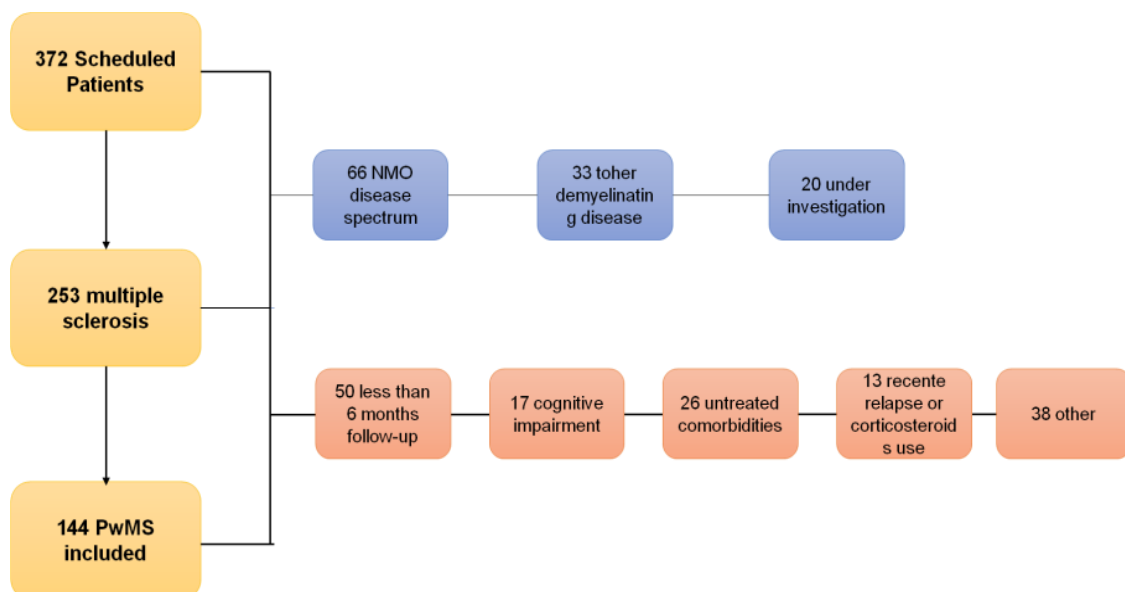


Figure 1 Recruitment details.

Table 1 MS clinical information group.



MS Information		Min-Max (%)	Mean (n)
Disease duration		0.5–27	9.3
Follow-up duration		0.5–25	6.02
Age at onset		7–58	28.7
EDSS		0.0–8.0	2.5
MS treatment	MS treatment	21.9	25
	Fingolimod	21.9	25
	Glatiramer acetate	13.1	15
	Natalizumab	6.1	7
	Dimethyl fumarate	5.2	6
Concomitant diseases	Hypertension	11	11
	Hypothyroidism	7.0	8
	Depression and anxiety	21.0	24
	Fatigue (FSS)		
Fatigue (FSS)	None	42.9	49
	Mild	12.2	14
	Moderate	15.7	18
	Intense	28.9	33
Dimethyl fumarate	Drugs for pain and spasticity	17.5	20
	Antidepressants	28.0	32
	Benzodiazepines and sleep inducers	7.0	8
	Anticonvulsants	147.9	17
Clinical forms	RRMS	88%	101
	SPMS	7%	7
	PPMS	5%	6

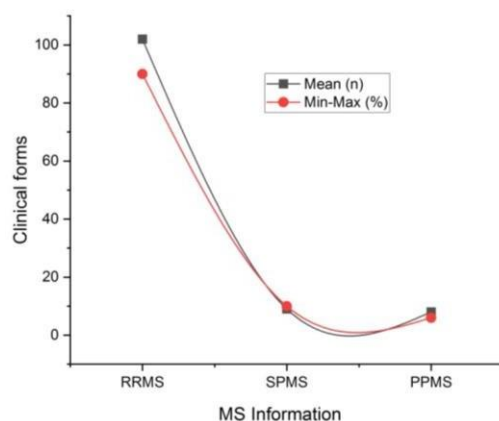


Figure 2 Clinical forms.

In MS, the body's immune response erroneously attacks the myelin protective coating of nerve fibers (Figure 2). This immunological assault causes inflammation, damages the myelin, and interferes with the regular flow of nerve messages. Figure 3 displays different clinical types of MS that can appear and are used to explain disease development and symptom presentation patterns.

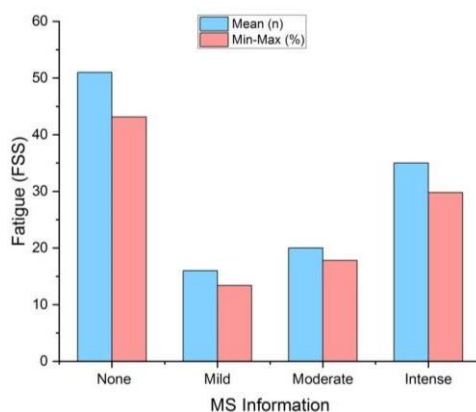


Figure 3 Fatigue (FSS).



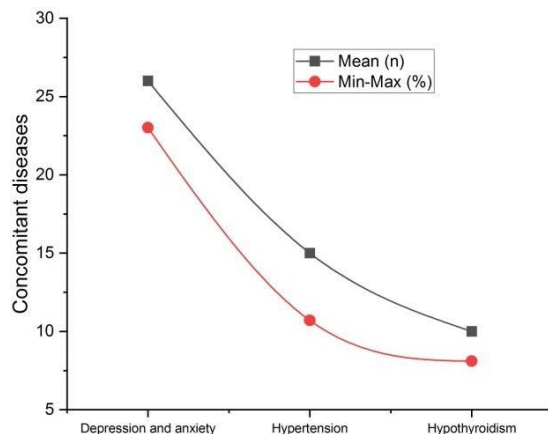


Figure 4 Concomitant diseases.

Figure 4 displays Concomitant diseases, usually called comorbidities when two or more illnesses exist in a person at once. The person's general health (GH) and course of therapy may be affected by the coexistence and interaction of certain disorders. Figure 5 shows the chronic autoimmune illness MS affects the central nervous system. Even though there is currently no treatment for MS, many therapy alternatives may assist patients in managing their symptoms, slowing the progression of the condition, and overall living a better life.

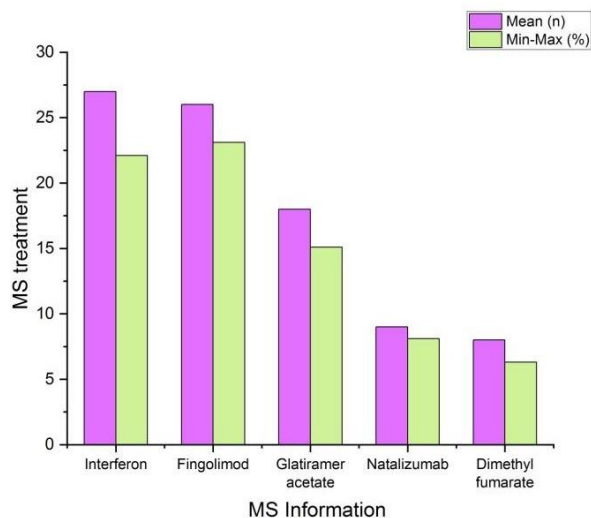


Figure 5 MS treatment.

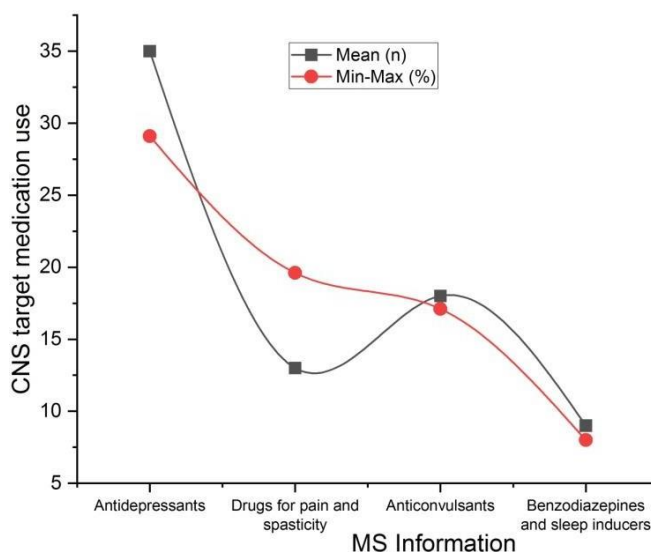


Figure 6 CNS target medication use.



The drug use with a CNS target is shown in Figure 6. Anxiety, panic attacks, seizures, and other conditions are all treated with CNS depressants. They could be used before surgery to ease stress and anxiety. At the MS clinic, the average follow-up time was 6.02 years, while the average length of the disease was 9.3 years. The range of the EDSS was 0 to 8, and the usual patient had an EDSS of 2.5 and a minor neurological impairment. Twenty-six individuals had EDSS values of more than 6.0, indicating a need for assistance with walking. On 32 people, a typical neurological examination was conducted. The most impacted functional systems are shown in table 2.

Table 2 Main functional systems impacted by the MS group on the expanded disability score scale.

Frequency (%)	Symptoms
Mental impairment (MI)	0
Cerebellar symptoms (CS)	29
Bladder and anal sphincter (BAS)	9
Sensitivity symptoms (SS)	22
Visual symptoms (VS)	34
Brain stem (BS)	16
Pyramidal tract (PT)	55

Interferon, or fingolimod, was the most often prescribed MS disease-modifying drug (DMDs), while they were followed by a drug called glatiramer acetate, or the solution of dimethyl fumarate. Only 15 patients were refused treatment because of a severe illness or a recent diagnosis. Sixty-five persons were reported to be fatigued to any degree. Anxiety and depression frequently coexist as mental disorders. There were 62 patients taking medications known to affect sleep habits. Patients in this group were taking antidepressants, painkillers, spasticity medications, anticonvulsants, benzodiazepines, and sleep aids. The primary categories of non-DMD treatments are listed in Table 3.

Table 3 The total dosage of the non-disease modifying medication used by MS patients.

Drug	Number of patients (%)
Benzodiazepines/sleep inducers	8
SSNRI antidepressants	4
Baclofen	7
Amantadine	13
Tricyclic antidepressants	4
Anticonvulsants	17
SSRI antidepressants	32

Only 7 of the 114 MS patients had a clinically validated diagnosis of RLS. The findings are summarized in table 6. Regarding patients and controls that were matched for gender, age, and level of physical activity, table 7 shows the usual therapeutic impact of PSM. The PSQI and ESS scores were 3 and 4.5 points lower for the MS group, respectively. Additionally, MS patients had a 33.3% reduced chance (p 0.001) of developing OSA compared to the general population.

Table 4 Number and proportion of people in response to the question.

	Positive answer	Interviewed
Multiple sclerosis	7	114
Episono	138	715

Table 5 The results from the MS and Episono groups were compared using Propensity Score Matching.

Outcome	Z	p-value	CI	Robust std. error	Coefficient ATE
Berlin	-0.759	<0.001	-0.308 -0.181	0.030	-0.244
BDI	-2.080	0.038	-6.143 -0.183	1.520	-3.163
MEQ-SA	-1.970	0.049	-8.252 -0.022	2.099	-4.137
PSQI	-7.600	<0.001	-3.785 -2.234	0.395	-3.000
ESS	-6.100	<0.001	-6.067 -3.116	0.753	-4.591

4. Discussion

Patients with MS are more likely to have sleep problems, and they could even discover that these problems worsen their MS symptoms, such as exhaustion. In contrast, PwMS receiving continuous DMD treatment in the current study reported decreased excessive daytime sleepiness and enhanced sleep quality as compared to a CG of city residents. The Episono database contains information on numerous neurological diseases, medical conditions, other procedures, and information on sleep from people who may or may not have sleep issues. Various diseases and unexplained health issues could have impacted our results since the So Paulo residents who made up the CG were selected from a database. Due to its older demographic and a more significant number of men, the EG may be more susceptible to OSA and experience lower-quality sleep. Even though gender, age, and physical activity were the same between the patients and controls, the disparity



in sleep quality was maintained. But in MS patients, EDS was lower, and sleep quality was higher. It's essential to remember that MS patients receive regular follow-up care in the outpatient clinic. They receive therapy for the pain, exhaustion, and sadness they experience due to their MS, which improves their sleep and lowers their risk of developing EDS. The prevalence of sleep disruptions in PwMS may have been exaggerated in older studies, especially those published more than ten years ago. For instance, it's likely that participants in this research mistakenly included people with NMOSD, one of the numerous demyelinating illnesses. A contemporary MS-modifying medication may also help to lessen the disease's effects on patients' sleep patterns, even though certain DMDs hurt sleep. There weren't a lot of folks who had persistent, progressive MS, either. Due to the small number of patients with advanced disease, we cannot do more studies on this subgroup. Thus, we cannot determine whether or not these individuals are more likely to have sleep problems. In addition to MS treatment, we assessed a sample of patients who had previously had therapy for depression, stiffness, and pain. This conclusion could add bias to the current study. Various outcomes are possible for patients with long-term, progressing diseases, those who have just been diagnosed, and those who have never had treatment.

5. Conclusion and Implications

MS is a neurological disorder that impacts the central nervous system. Even while myelin, the protective covering of nerve fibres, is the fundamental feature of MS, it can also cause other symptoms and problems, such as sleep disturbances. People with MS frequently experience sleep problems, which can negatively affect their GH and Quality of Life (QL). Our findings imply that, in contrast to a control population, a competently managed MS patient population only sometimes exhibits sleep difficulties. Consequently, compared to So Paulo residents, the prevalence of complaints about sleep difficulties were reduced in PwMS receiving treatment. The chronotype profile was the same for both groups, with shapes primarily morning or intermediate. Even though PwMS reported having trouble sleeping, fatigue was still very much present. Despite the current study's limitations, our findings regarding PwMS sleep complaints may be related to current MS treatments.

Ethical considerations

All participants completed the informed consent form after the Universidad Federal de So Paulo study ethics committee accepted the research protocol.

Declaration of interest

The authors declare no conflicts of interest.

Funding

This research did not receive any financial support.

References

- Abd-Nikfarjam B, Dolati-Somarin A, Baradaran Rahimi V, Askari VR (2023) Cannabinoids in neuroinflammatory disorders: Focusing on multiple sclerosis, Parkinson's, and Alzheimer's diseases. *BioFactors*.
- Akerstedt T, Olsson T, Alfredsson L, Hedström AK (2023) Insufficient sleep during adolescence and risk of multiple sclerosis: results from a Swedish case-control study. *Journal of Neurology, Neurosurgery & Psychiatry* 94:331-336.
- Aljundi NA, Kelly M, Zeineddine S, Salloum A, Pandya N, Shamim-Uzzaman QA., Martin JL (2022) Sleep disorders, daytime symptoms, and quality of life in veterans with multiple sclerosis: preliminary findings. *Sleep Advances*, 3(1), zpac012.
- Bader S, Ellouz E (2022) Sleep Disorders in Multiple Sclerosis Patients. *Multiple Sclerosis and Related Disorders*, 59.
- Bralely TJ, Shieu MM, Zaheed AB, Dunietz GL (2023) Pathways between multiple sclerosis, sleep disorders, and cognitive function: Longitudinal findings from The Nurses' Health Study. *Multiple Sclerosis Journal* 13524585221144215.
- Chang YT, Kearns PK, Carson A, Gillespie DC, Meijboom R, Kampaite A, Foley P (2023) Network analysis characterizes key associations between subjective fatigue and specific depressive symptoms in early relapsing-remitting multiple sclerosis: *Multiple Sclerosis and Related Disorders* 69:104429.
- Comi G, Leocani L, Ferini-Strambi L, Radaelli M, Costa GD, Lanzillo R, Hi-Tec Italian Multicentre Study Group (2023) Impact of treatment with dimethyl fumarate on sleep quality in patients with relapsing-remitting multiple sclerosis: A multicentre Italian wearable tracker study. *Multiple Sclerosis Journal—Experimental, Translational and Clinical* 9:20552173221144229.
- de Oliveira, Marcos Paulo Braz, Ana Emilia Fonseca de Castro, Andressa Leticia Miri, Carla Rigo Lima, Brendon David Truax, Vanessa Suziane Probst, Suhaila Mahmoud Smaili (2023) The impact of the COVID-19 pandemic on neuropsychiatric and sleep disorders, and quality of life in individuals with neurodegenerative and demyelinating diseases: a systematic review and meta-analysis of observational studies. *BMC neurology* 23:150.
- Fakolade A, Akbar N, Mehelay S, Phadke S, Tang M, Alqahtani A, Busse M (2023) Mapping two decades of multiple sclerosis rehabilitation trials: A systematic scoping review and call to action to advance the study of race and ethnicity in rehabilitation research. *Multiple Sclerosis and Related Disorders* 104606.
- Genç B, Şen S, Aslan K, İncesu L (2023) Volumetric changes in hypothalamic subunits in patients with relapsing-remitting multiple sclerosis. *Neuroradiology* 65:899-905.
- Ghareghani M, Zibara K, Rivest S (2023) Melatonin and vitamin D are two sides of the same coin; better to land on its edge to improve multiple sclerosis—



proceedings of the National Academy of Sciences 120:e2219334120.

Madhaw G, Kumar N (2022) Sleep Disorders in Multiple Sclerosis. In *Sleep and Neuropsychiatric Disorders*, pp 707-720. Singapore: Springer Nature Singapore.

Moussa A, Kacem I, Moussa A, Abiadh R, Hassine A, Nakhli R, Chouchane A, Bouhoula M, Aloui A, Maoua M, Brahem A (2023) O-293 Work-related risk factor for multiple sclerosis: a case-control study in Tunisia.

Novak AM, Lev-Ari S (2023) Resilience, Stress, Well-Being, and Sleep Quality in Multiple Sclerosis. *Journal of Clinical Medicine* 12:716.

Ordoñez-Rodríguez A, Roman P, Rueda-Ruzafa L, Campos-Rios A, Cardona D (2023) Changes in Gut Microbiota and Multiple Sclerosis: A Systematic Review. *International Journal of Environmental Research and Public Health* 20:4624.

Papiri G, D'Andreamatteo G, Cacchiò G, Alia S, Silvestrini M, Paci, C, Vignini A (2023) Multiple sclerosis: inflammatory and neuroglial aspects. *Current Issues in Molecular Biology* 45:1443-1470.

Pivovarova-Ramich O, Zimmermann HG, Paul F (2023) Multiple sclerosis and circadian rhythms: Can diet act as a treatment? *Acta Physiologica* e13939.

Qomi M, Rakhshan M, Ebrahimi Monfared M, Khademian Z (2023) The effect of distance nurse-led fatigue management on fatigue, sleep quality, and self-efficacy in patients with multiple sclerosis: a quasi-experimental study. *BMC neurology* 23:1-9.

Riccitelli GC, Pacifico D, Manconi M, Sparasci D, Sacco R, Gobbi C, Zecca C (2022) Relationship between cognitive disturbances and sleep disorders in multiple sclerosis is modulated by psychiatric symptoms: *multiple Sclerosis and Related Disorders* 64:103936.

Rocchi C, Lombardi L, Broggi S, Danni MC, Lattanzi S, Viticchi G, Buratti L (2023) Impact of dimethyl fumarate on sleep in multiple sclerosis patients: an actigraphic study. *CNS & Neurological Disorders-Drug Targets (Formerly Current Drug Targets-CNS & Neurological Disorders)* 22:1102-1108.

Ruiz-Sánchez FJ, Martins MDR, Losa-Iglesias ME, Becerro-de-Bengoa-Vallejo R, Gómez-Salgado J, Romero-Morales C, López-López D (2023) Impact of Multiple Sclerosis on Foot Health and Quality of Life: A Prospective Case-Control Investigation. *International Journal of Public Health* 38.

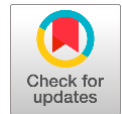
Souissi Amira, Saloua Mrabet, Amal Atrous, Youssef Abida, Alya Gharbi, Amina Nasri, Amina Gargouri, Imen Kacem, Riadh Gouider (2023) Impact of Multiple Sclerosis First Relapse on Disease History: Reports of a Tunisian Cohort. *Multiple Sclerosis and Related Disorders* 71:104304.

Sparasci D, Fanfulla F, Ferri R, Aricò D, Distefano D, Pravatà E, Manconi M (2022) Sleep-Related Breathing Disorders in Multiple Sclerosis: Prevalence, Features and Associated Factors. *Nature and Science of Sleep* 14:741.

Tarasiuk J, Kapica-Topczewska K, Czarnowska A, Chorąży M, Kochanowicz J, Kułakowska A (2022) Co-occurrence of fatigue and depression in people with multiple sclerosis: a mini-review. *Frontiers in Neurology* 12:2546.

Zhang Y, Ren R, Yang L, Zhang H, Shi Y, Vitiello MV, Tang X (2023) Sleep in multiple sclerosis: a systematic review and meta-analysis of polysomnographic findings. *Journal of Clinical Sleep Medicine* 19:253-265.

Addictive digital media use and psychiatric symptoms: a cross-sectional study



Saubhagya Mishra^a | H. Malathi^b | Prakash Deep^c

^aTeerthanker Mahaveer University, Moradabad, Uttar Pradesh, India, Professor, Department of Medicine.

^bJain (Deemed-to-be University), Bangalore, India, Assistant Professor, Department of Life Sciences.

^cMaharishi University of Information Technology, Lucknow, Uttar Pradesh, India, Associate Professor, School of Science and Humanities.

Abstract The past 10 years have seen a substantial change and increase in the research of "addictive technological behaviors." Additionally, studies have found a strong association between concomitant psychiatric issues and technological dependency. In the present study, 23,533 Participants in a cross-sectional online study of adults survey to investigate potential role of demographic variables, attention deficit/hyperactivity disorder (ADHD), obsessive-compulsive disorder (OCD), in the a range of addictive use, which is defined as compulsive and excessive use linked to undesirable effects, there are two forms online technologies of the present: YouTube and social media. We made use of instruments with robust psychometric capabilities. Every substantial and positive correlation the interaction between the two addictive technological behaviors when contrasting the signs of various mental problems and those of addicted technology use. The compulsive utilization of these technologies and age seems to be unrelated. Being a man was substantially correlated with a video game addiction, but being a woman was strongly correlated with a social media addiction. Addiction to online gaming and social networking was positively correlated with being single. According to hierarchical regression research, demographic traits approximately 11% to 12% of the difference in the use of addictive technologies was explained by this. Mental health-related variables accounted for 7% to 5% of the difference. The study significantly expands our knowledge of the signs of mental illness and how they relate to technological addiction. Discussions of the clinical relevance, limitations, and strengths are included.

Keywords: ADHD, anxiety, depression, internet gaming disorder, online social networking addiction

1. Introduction

The majority of nations experienced an increase in Internet users over the past ten years. According to the Iranian Internet Network Information Center, 32 million people used the internet in 2009 (Chegeni et al 2022). The Internet has become a crucial aspect of our lives because of improved access. Experts in social pathology, psychology, and education are aware of the psychological and physical problems associated with excessive Internet use as well as the potential negative consequences that could emerge from it. Internet addicts are those who become uncontrollable in their daily lives and, on average, log on for more than 38 hours per week (Kuss, and Pontes 2018). The typical description of internet addiction is that of a disorder of impulse control that shares many symptoms with pathological gambling but entails the use of any intoxicating substances. Modern civilizations are plagued by addiction to digital media, and this problem has been the focus of many studies (Niedermoser et al 2021). Currently, an increasing number of people are using the internet. The internet has many benefits, but there are also growing problems related to excessive internet use. Internet dependence interdisciplinary phenomena are problems that have been studied from numerous angles by various sciences, including health, technology, sociology, law, morality, and psychology (Melonashi 2019). Problematic Internet use has been linked to psychiatric diseases of Axis I, functional impairment, and subjective distress. Additionally, a number of studies have shown links between teenage internet concerns and addiction and mental health issues, such as depression, fear and loneliness, and self-efficacy. The most common psychiatric symptom is depression connected to excessive Internet use. A high score on sorrow did not, however, appear to be correlated with a high score on Internet addiction. According to a study conducted in Iran, people who spend too much time online feel less social and environmental responsibility and are more likely to experience social isolation (Dubey et al 2019). They typically experience low self-esteem, reduced social support, and a sense of failure in both their educational and professional endeavors (Taylor 2020). Although many researchers have examined the connection between Internet addiction and mental health issues such as sadness, there are very few studies that have concentrated on the link between psychiatric disorders such as summarization and psychosis and Internet addiction (Siste et al 2020). The results of earlier studies were inconsistent and rather scant. The pattern of Internet use must be determined, the relationship between

mental health conditions and Internet addiction must be investigated, and the psychological aspects of Internet addiction must be explored (D'Arienzo et al 2019). The study sought to ascertain the association between psychiatric signs of Internet addiction and education level in a population. Cham et al (2019). There may be a connection between mental health issues and the frequency of Internet addiction, especially signs of obsessive-compulsive disorder (OCD). Poor sleep and online harassment both have a small role in regulating social media use, and depressive symptoms, poor self-esteem, and body image are connected. ii) Poorer sleep, a negative body image, and low self-esteem might somewhat moderate the link between online harassment and depressive symptoms. iii) Self-esteem issues could play a role in mediating the link between negative body image and depressive symptoms. Figure 1 depicts social media use and depressive symptoms.

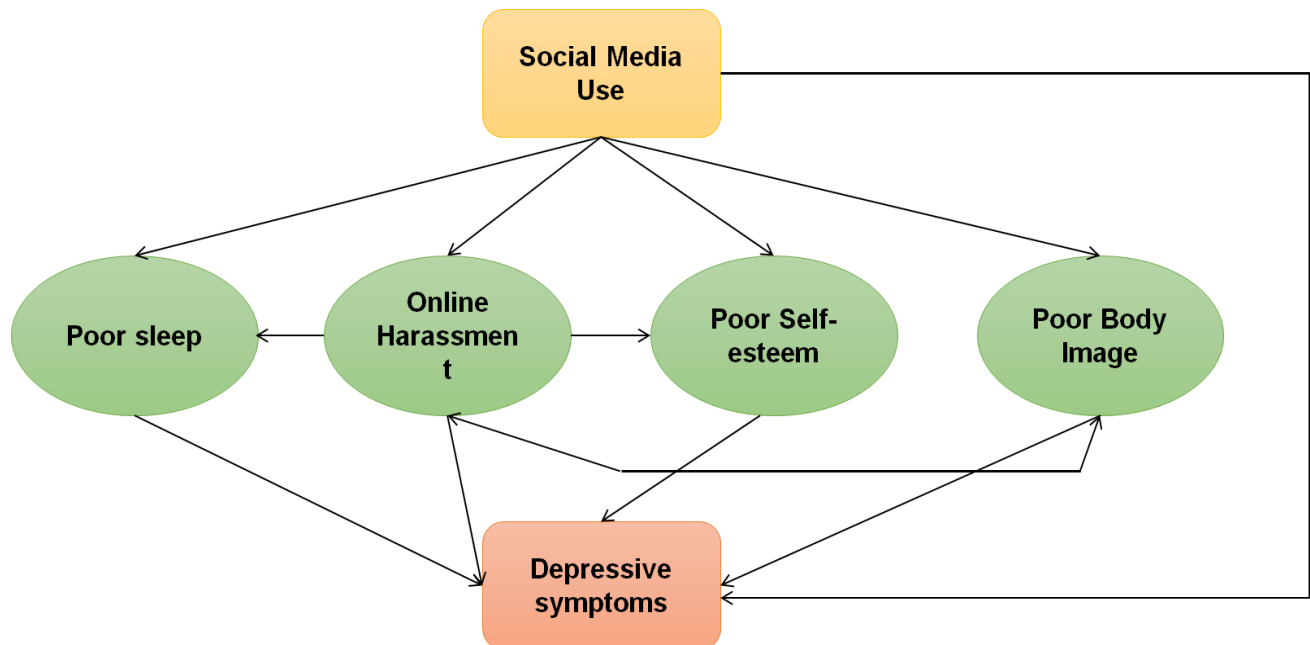


Figure 1 Hypothesized social media and depression.

2. Literature Review

Cataldo et al (2021) examined findings relating to genetics and neuroscience difficulties, clinical treatment repercussions, and multidisciplinary perspectives on future directions, focusing on eating, eating disorders, disorders of neurodevelopment, depression, anxiety, and anxiety disorders. Haand and Shuwang (2020) investigated melancholy, and in Afghanistan's Khost province, college students are addicted to social media. Ahmad Shah Abdali and were given a 46-item self-administered survey, and Pamir University made use of random stratification. The use of social media was evaluated utilizing the Internet Addiction Test (IAT) developed by Kimberly Young, while the Center for Epidemiologic Research was used to measure the Depression Depressive Index (CES-D). Malaeb et al (2021) showed a connection between improper mental illnesses and social media use. There are several mental health disorders that are correlated with using social media.

Wong et al (2020) examined relationships between young adults' intensity of psychological distress, sleep quality, and internet gaming disorder (IGD) and unreliability using social media. Shensa et al (2018) showed various use trends on social media (SMU) and evaluated the connections between these trends and indicators of anxiety and sadness. Methods: A nationwide representative sample of 1730 US people between the ages of 19 and 32 took an online survey in October 2014. SMU patterns were found using cluster analysis, and anxiousness and depression were measured. Firat et al (2018) sought to ascertain that teens who were referred to clinics frequently used problematic smartphones, as well as the association between these factors and psychiatric symptoms, emotional regulation issues, and sociodemographic traits. A total of 150 teenagers with smartphones between the ages of 12 and 18 were included.

Kolhar et al (2021) reported uses via social media outlets and how it affects sleep, learning, and social interaction. The chi-squared test was used to evaluate the data. Masthi et al (2018) evaluated health issues relating to how the study subjects used social media. Different elements that contribute to social media addiction. Chen (2020) determined the relative importance of social and psychological variables in determining various levels of usage of the widely used social mobile app (app) LINE in Asia. The findings showed that for those in the cluster of addictive behavior, positive predictions were made by subjective standards and social identity, whereas self-worth and social abilities were predicted unfavorably. Mazhar et al (2020) contributed to the provision of trustworthy data needed to comprehend the severity of the current issue. Should look into the following behavioral addiction symptoms, modifying mood, relapsing, salience, both retreat and toleration.

3. Methodology

In the present study, 23,533 participants participated in a cross-sectional online study of adults to investigate the potential role of demographic variables and attention deficit/hyperactivity disorder (ADHD).

3.1. Procedure

A free link to a cross-sectional online database study concentrating on a number of addictive behaviors was published between March and May 2014 in addition to articles in five different national Norwegian publications' online editions. Accessing the survey here, participants were instructed to click on the link. The research team considered this to be an incentive to participate based on earlier studies; therefore, details of the study were included on page one, along with respondents receiving rapid comments about their likelihood of "addiction" ratings of the survey's conclusion. Responses from participants included kept on a server run by a business with specialized knowledge for this use (SurveyXact). The research team (N=41,970) received all collected data one week after the start of the study. A total of 23,533 people answered the questions in the poll. Respondents (n=18,437) who merely clicked the link or responded with couple questions were removed from the data file. The research was performed in keeping with the Norwegian Health Research Act and the Helsinki Convention, and all information was collected in an unbiased, anonymous manner. Beyond the previously specified input, no material or monetary reward was offered.

3.2. Sample

The sample included 23,533 individuals, having a 35.8-year-old median age and ages ranging from 16 to 88 (SD=13.3). A total of 40.7%, 35.0%, 19.8%, and 4.5% of the sample, according to the specified age groups, were between the ages of 16 and 30, 31 to 45, 46 to 60, and 61 to 88, respectively. In 2014. The sample's gender distribution was 15,299 females (65%) and 8,234 males (35%), and it substantially pared to the equivalent percentages. Regarding spouse identity, 15,373 (65.3%) of the participants were dating each other at the time of the survey (married, common-law partners, boyfriends or girlfriends, compared to 8,160 (34.7%) who were not (married, divorced, or separated), widows or widowers). In terms of education, 2,350 had finished compulsory education (10.0%), and 5,949 had finished 3,989 had graduated from high school (25.3%), finished a vocational program (17.0%), 7,630 the majority (32.4%) 3,343 had a bachelor's (14.2%), and 272 had a PhD (1.2%). Comparing the data obtained from the current sample with full statistics on education levels and marital status at the population level was not possible.

3.3. Instruments

The Bergen Social Networking Addiction Scale (BSNAS), which is a modification of the Bergen Face book Addiction Scale (BFAS) (Andreassen, Torsheim, Brunborg, & Pallesen 2012), has six items that reflect the core components of addiction as described by Griffith's (2005). On a Likert scale of very seldom (1) to very often (5), each question regarding experiences from the preceding year receives a response, generating a composite score between 6 and 30 (for example, "How often during the last year have you tried to cut down on the use of social media with no success?"). For the BFAS, a single-factor answer was discovered. In the instructions to participants, the word "Face book" was changed to "social media" alone, with the internet characterized as "Face book, Twitter, Instagram, and the like." In numerous studies, the BFAS has demonstrated adequate psychometric qualities. In the current investigation, internal consistency with the BSNAS was good. Appendix B contains a complete list of the scale's components.

The Game Addiction Scale (GAS), created by Peter, Lemmens, and Valkenburg (2009), consists of seven items that evaluate the signs of addicted video gaming. The GAS was initially created and evaluated in two separate Dutch teenage populations, where it was discovered that there was evidence for a one-factor answer. The GAS is appropriate for and has been administered to persons between the ages of 14 and 90, although it was initially created to evaluate the signs of adolescent gaming addiction. An overall score between 7 and 35 is produced by rating each item on a scale of 1 to 5 that ranges from never (1) to very often (5). For example, "How often during the last 6 months did you play games to forget about real life?" is a question about experiences from the previous six months. The scale was initially tested against indicators of constructs that gaming was anticipated to link with. A study of scales designed to evaluate compulsive video gaming revealed that the GAS has strong validity based on the correlation pattern in the original and follow-up research. The objects and instructions utilized in the current investigation are listed in Appendix C.

According to Foa et al. (2002), the Obsession-Compulsive Inventory-Revised (OCI-R) consists of 18 items that evaluate six typical OCD symptoms. That includes obsessing (e.g., "I have trouble controlling my own thoughts," "I check things more than necessary," "I get upset if objects are not arranged properly," "I feel compelled to count while I am doing things," "I find it difficult to touch an object when I know it has been touched by strangers or certain people," "I check things more than necessary," "I order things," "I get frustrated if things are not properly arranged," "I wash," and "I each item is answered. High scores show that the person's OCD symptoms are bothersome. According to recent psychometric analyses of the OCI-R, it is trustworthy. All items were combined to create a composite score, and the Cronbach's alpha of the OCI-R in this study

was .87, which indicates strong internal consistency. Measures of anxiety include seven items, and seven elements are used to measure depression indications.

3.4 . Data analytic strategy

To evaluate the relationships between each pair of research variables, the correlation indices between products and moments of Pearson calculations were made. Next, we carried out two linear hierarchical regression analyses using the corresponding addictive technological behaviors as the dependent variables. Education level was dummy coded, with the reference category consisting of the largest group. The second phase involved entering symptoms for ADHD, OCD, anxiety, and sadness. Preliminary investigations supported the suppositions of normality, linearity, multicollinearity, and homoscedasticity.

4. Results and discussion

Table 1 lists the average ratings and standard deviations, correlation coefficients, and mean scores for each of the study factors. The two compulsive technological activities were highly and favorably related, and important and positive negative correlations were also seen for all the other variables in the current investigation.

Table 1 Descriptive information and coefficients of correlation between the studied variables (N=23,533).

Variables	1	2	3	4	5	6
1 Addictive Social Networking	--					
2 Addictive video Gaming	.12**	--				
3 ADHD	.21**	.26**	--			
4 OCD	.31**	.23**	.42**	--		
5 Anxiety	.33**	.17**	.54**	.45**	--	
6 Depression	.18**	.23**	.38**	.34**	.54**	--
M	11.31	9.49	43.95	29.23	6.63	4.11
SD	4.73	4.26	9.72	9.16	3.93	3.21
Range	6-30	7-36	18-91	18-91	0-22	0-22
Alpha	.89	.88	.85	.83	.81	.74
Items	6	7	16	17	7	7

It is noteworthy that social media addiction exhibited fairly strong correlations with tests for OCD (r=.33), ADHD (r=.41), and anxiety (r=.34). Overall, enslaving video games displayed the same pattern of correlation with the various symptom rating scales, although the coefficients, with the exception of depression, were slightly inferior to addicting video game use than for addictive social media use. Table 2 displays the findings for social media addiction. Step 1 involved entering information on age, gender, marital status, and educational attainment. These variables explained 11.6% of the variation in harmful social networking.

Table 2 Results of the hierarchical regression analysis.

	Addictive Social Networking					Addictive Video Gaming				
	B	SE	β	t	ΔR^2	B	SE	β	t	ΔR^2
Step 1					.116***					.112***
Age	-0.085	.001	-.242	-37.021***		-0.064	.002	-.205	-31.246***	
Gender	1.973	.061	.195	31.791***		-1.653	.054	-.186	-30.081***	
Marital Status	0.607	.063	.062	9.554***		1.416	.095	.101	14.631***	
Education										
Primary School	0.743	.108	.048	6.782***		1.415	.096	.101	14.630***	
High School	0.081	.078	.008	1.025		0.0630	.071	.066	8.972***	
Vocational school	-0.033	0.088	-.003	-4.346***		-0.338	.083	-.027	-4.108***	
Master’s Degree	-0.402	.093	-.030	-4.345		-0.338	.082	-	-4.109***	
PhD degree	-0.714	.276	-.016	-2.582***		-0.160	.245	-.003	-0.653	
Step 2					.149***					.065***
Age	-0.053	.002	-.153	-25.011***		-0.052	.001	-.165	-25.503***	
Gender	1.8021	.059	.181	30.970***		-1.513	.053	-.171	-27.843***	
Marital Status	0.532	.059	.181	30.970***		0.117	.053	.013	2.172*	

An additional 14.9% in Step 2 provided an explanation for the variance in ADHD, OCD, anxiety, and depression. A total of 26.4% of the variation was fully explained by the model, F12, 23520=705.99, p.001. Age (β =-.154), master's and PhD degrees (β =-.023, β =-.016, and depression were found to be negatively associated with addictive social networking, whereas gender (β =.180), marital status (β =.055), ADHD (β =.268), OCD (β =.147), and anxiety (β =.074) were all found to be positively correlated with social media addiction. The regression results for video game addiction are also shown in Table 2. According



to the analysis, Step 1's independent variables accounted for 11.4% of the variation ($F_{8, 23524}=376.66, p.001$). Step 2 entries for ADHD, OCD, anxiety and sadness contributed an extra 6.6% to the variance's explanation.

Table 2 displays the outcomes of the studies using hierarchical regression, where factors such as age, female sex, marital status, level of education, ADHD, and OCD and the scores for addicted technology behavior were regressed on anxiety and depression ($N=23,533$). Overall, the independent factors contributed to a variance explanation rate of 17.9% ($F_{12,23520}=427.71, p.001$).

4.1. Depressive symptoms by social media usage

Regarding the correlation between using face books and depression, more girls than boys had symptoms. A stepwise rise in depressive symptoms and the percentage of girls reporting clinically significant symptoms was correlated with longer daily social media use. The use of social media by boys three or more hours per day scored higher for depressive symptoms.

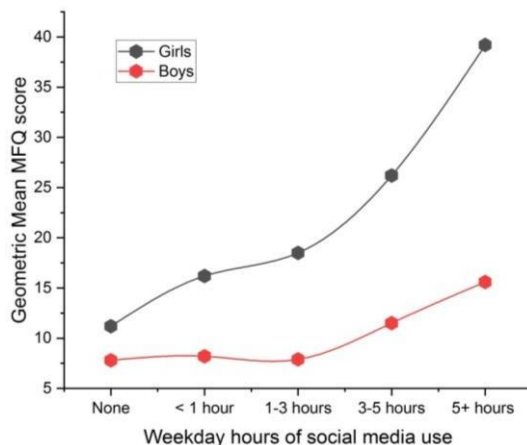


Figure 2 Depressive symptoms by social media usage.

Table 3 Computation analysis of depressive symptoms.

	High depression symptoms	Low depression symptoms
0-8	19	36
9-30	27	24
31-57	26	23
58+	29	16

4.2. Social Media and Depression

People with social media and mental diseases used social media more frequently when they had more depressive symptoms. Twenty-nine percent of those who used social media for at least 58 sessions reported having severe depression symptoms, compared to 19% of those who used it no more than eight times each week. Similarly, compared to 36% of those who used social media 8 times a week or less, only 16% of those who used it 58 times or more each week showed mild depressive symptoms.

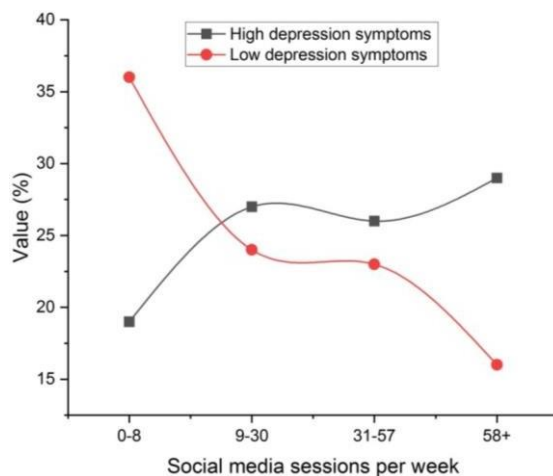


Figure 3 Social Media and Depression.



Table 4 Computation analysis of social media and depression.

Weekday hours of social media use	Geometric Mean MFQ score	
	Girls	Boys
None	11.2	7.8
< 1 hour	16.2	8.2
1-3 hours	18.5	7.9
3-5 hours	26.2	11.5
5+ hours	39.2	15.6

5. Conclusions

The findings of the current research imply that compulsive use of technology, such as addicted video games and social networking, is linked to the symptoms of underlying psychiatric problems. Although there was a favorable correlation between addictive internet habits, there was little overlap. Social media addiction was favorably correlated with being a woman, being single, being younger, having ADHD, OCD, anxiety, and having decreased depression levels. Video game addiction was favorably correlated, and having depression, OCD, ADHD, and being unmarried at a younger age were all negatively connected with anxiety symptoms. According to this study, teenagers and young adults who exhibit some of these traits may be given special attention to prevent the emergence of addictive online behavior. To further understand the similarities and differences between addictive technology usages, as well as their nature (such as fluctuation, stability, or natural recovery), more research is needed. In this under researched area, these studies must be carried out using representative samples and longitudinal approaches.

Ethical considerations

Not applicable.

Declaration of interest

The authors declare no conflicts of interest.

Funding

This research did not receive any financial support.

References

- Ali H, Gueyie JP, Chrysostome EV (2022) Gender, credit risk and performance in sub-Saharan African microfinance institutions. *Journal of African Business* 1-25.
- Balamal A, Madhumathi R, Ganesh MP (2019) Performance evaluation frameworks in the context of Indian microfinance institutions. *Foundations of Management* 11:209-228.
- Cham S, Algashami A, Aldhayan M, McAlaney J, Phalp K, Almourad MB, Ali R (2019) Digital addiction: Negative life experiences and potential for technology-assisted solutions. In *New Knowledge in Information Systems and Technologies 2*, pp 921-931. Springer International Publishing.
- Chegeni M, Nakhaee N, Shahrababaki ME, Mangolian Shahrababaki P, Javadi S, Haghdoost A (2022) Prevalence and motives of social media use among the Iranian population. *Journal of Environmental and Public Health*
- Chen CY (2020) Smartphone addiction: psychological and social factors predict the use and abuse of a social mobile application. *Information, Communication & Society* 23:454-467.
- D'Arienzo MC, Boursier V, Griffiths MD (2019) Addiction to social media and attachment styles: A systematic literature review. *International Journal of Mental Health and Addiction* 17:1094-1118.
- Dai X, Gu N (2021) The impact of social capital on mental health: evidence from the China Family Panel Survey. *International journal of environmental research and public health* 19:190.
- Dubey R, Gunasekaran A, Childe SJ, Papadopoulos T, Luo Z, Wamba SF, Roubaud D (2019) Can big data and predictive analytics improve social and environmental sustainability?. *Technological Forecasting and Social Change* 144:534-545.
- Firat S, Gül H, Sertçelik M, Gül A, Gürel Y, Kılıç BG (2018) The relationship between problematic smartphone use and psychiatric symptoms among adolescents who applied to psychiatry clinics. *Psychiatry Research* 270:97-103.
- Haand R, Shuwang Z (2020) The relationship between social media addiction and depression: A quantitative study among university students in Khost, Afghanistan. *International Journal of Adolescence and Youth* 25:780-786.
- Hameed WU, Mohammad HB, Shahar HBK (2020) Determinants of microenterprise success through microfinance institutions: a capital mix and previous work experience. *International Journal of Business and Society* 21:803-823.
- Kolhar M, Kazi RNA, Alameen A (2021) Effect of social media use on learning, social interactions, and sleep duration among university students. *Saudi Journal of Biological Sciences* 28:2216-2222.
- Kuss DJ, Pontes HM (2018) *Internet addiction*. Hogrefe Publishing GmbH.
- Lebenbaum M, Laporte A, de Oliveira C (2021) The effect of mental health on social capital: An instrumental variable analysis. *Social Science & Medicine* 272:113693.

- Malaeb D, Salameh P, Barbar S, Awad E, Haddad C, Hallit R, Sacre H, Akel M, Obeid S, Hallit S (2021) Problematic social media use and mental health (depression, anxiety, and insomnia) among Lebanese adults: Any mediating effect of stress?. *Perspectives in psychiatric care* 57:539-549.
- Masthi NR, Pruthvi S, Phaneendra MS (2018) A comparative study on social media usage and health status among students studying in preuniversity colleges of urban Bengaluru. *Indian journal of community medicine: official publication of Indian Association of Preventive & Social Medicine* 43:180.
- Mazhar N, Khan TB, Zafar K, Warris SH, Nikhet S, Tahir A (2020) A study of components of behavioral addiction to social media use in current generation of Pakistani youth. *The Professional Medical Journal* 27:1680-1685.
- Niedermoser DW, Hadjar A, Ankli V, Schweinfurth N, Zueger C, Poespodihardjo R, Petitjean S, Wiesbeck G, Walter M (2021) A typical case report: Internet gaming disorder psychotherapy treatment in private practice. *International Journal of Environmental Research and Public Health* 18:2083.
- Ojong N, Simba A (2019) Fostering microentrepreneurs' structural and relational social capital through microfinance. *Journal of Small Business & Entrepreneurship* 31:1-20.
- Shensa A, Sidani JE, Dew MA, Escobar-Viera CG, Primack BA (2018) Social media use and depression and anxiety symptoms: A cluster analysis. *American journal of health behavior* 42:116-128.
- Siste K, Hanafi E, Sen LT, Christian H, Adrian, Siswidiani LP, Limawan AP, Murtani BJ, Suwartono C (2020) The impact of physical distancing and associated factors toward internet addiction among adults in Indonesia during COVID-19 pandemic: a nationwide web-based study. *Frontiers in psychiatry* 11:580977.
- Tahmasebi A, Askaribezayeh F (2021) Microfinance and social capital formation-a social network analysis approach. *Socio-Economic Planning Sciences* 76:100978.
- Taylor KN (2020) How does a social medium use impact students' addiction, interpersonal skills, and well-being? Doctoral dissertation, Northcentral University.
- Vilvanathan L (2021) Efficiency assessment of microfinance institutions: using DEA with weighted Russell directional distance model. *Benchmarking: An International Journal* 28:769-791.
- Wong HY, Mo HY, Potenza MN, Chan MNM, Lau WM, Chui TK, Pakpour AH, Lin CY (2020) Relationships between severity of internet gaming disorder, severity of problematic social media use, sleep quality and psychological distress. *International journal of environmental research and public health* 17:1879.

Understanding socialization in interprofessional practice: health science perspectives



Vinod Singh K.^a | Upendra Sharma US^b | Ramakant^c | Nishant Kumar^c

^aTeerthanker Mahaveer University, Moradabad, Uttar Pradesh, India, Professor, Department of Medicine.

^bJain (Deemed-to-be University), Bangalore, India, Assistant Professor, Department of Life Sciences.

^cMaharishi University of Information Technology, Lucknow, Uttar Pradesh, India, Assistant Professor, School of Science and Humanities.

Abstract According to a study of the research, there is a lack of understanding about how students see the professional obligations and functions of other professions. This research aimed to investigate how health professional students (HPS) perceived Inter professional socialization (IPS). Participants came from eight different health-related academic fields, including nursing, radiological science, occupational therapy, clinical lab science, social work, nutritional science, and physical therapy. In all, 300 undergraduate (UG) and 114 graduate students participated. The Interprofessional socialization and Valuing Scale (ISVS-21) was used to gather the data. On a Likert scale with 1 being not at all and 7 being to a very large amount, the participants were asked to score 21 questions concerning their beliefs, practices, and perspectives towards IPS. To examine variations across the health fields, descriptive statistics and analysis of variance were used to analyze the information. According to a descriptive study, 95.2% of students believed IPS was happening to a rather considerable level, with a mean of 5.12 or higher on a scale from 1 to 7. The health fields didn't vary all that much from one another. The results indicate that pupils are prepared to comprehend one another's professional duties and obligations. There are several things to keep in mind for future Interprofessional collaborative activities even if there are no standardized educational methodologies to encourage student cooperation across disciplines.

Keywords: interprofessional socialization, health profession students, health science, interprofessional practice

1. Introduction

Interprofessional Practice (IPP) is the term for the collaborative and coordinated method of delivering healthcare in which experts from many fields collaborate to give patients or customers comprehensive and holistic treatment. It stresses the value of collaboration, communication, and respect amongst healthcare professionals to improve patient outcomes and raise the standard of care. Healthcare professionals from multiple specialties, including doctors, nurses, pharmacists, social workers, psychologists, and other allied health professionals, collaborate in an IPP environment to share their specialized knowledge and viewpoints. To meet the multifaceted demands of patients, they collaborate by exchanging information, deciding together, and coordinating their efforts (Arnold et al 2020). Socialization is a method using which people get the information, abilities, attitudes, and behaviors required to contribute to society. It requires adapting to the norms, values, and expectations of one's culture and community as well as lifelong learning. Socialization takes place through a variety of social encounters, relationships, and institutions including family, school, peers, religious institutions, and the press. Building trust, establishing good communication, and encouraging group decision-making within the team all depend on socialization in IPP. It entails fostering a welcoming and accepting atmosphere where experts may freely impart their knowledge, benefit from one another, and work together to improve patient care (Mahler et al 2022).

A multidisciplinary area called Health Science Perspectives (HSP) looks at numerous facets of healthcare and wellness. It spans a broad variety of fields and viewpoints, spanning biological sciences, social sciences, public health, epidemiology, psychology, healthcare administration, and more. In fusing information and ideas from several fields, HSP seeks to create a thorough understanding of health and wellbeing. The ethical, legal, and policy ramifications of matters about health are also taken into account in Health Science Perspectives. It examines issues including healthcare inequities, health promotion, illness prevention, healthcare systems and policies, patient-centered care, global health, bioethics, and the social determinants of health. To encourage and improve health outcomes, HSP attempts to provide a comprehensive knowledge of health. To solve complicated health concerns and improve evidence-based healthcare practices, it promotes cooperation across many disciplines, experts, and consumers (Karnish et al 2019).

In the professional practice information, socializing continues beyond the school environment. Professionals in the health sciences collaborate across disciplines and continue their professional development to improve their Interprofessional



abilities. They take part in case conferences, quality improvement projects, and team meetings, all of which help them become more proficient at working as an organized Interprofessional team. Students learning health sciences may have little experience working with other professionals at this point in their education and training. Their past experiences, educational background, and exposure to collaborative healthcare environments may have an impact on how they perceive socializing in this situation (Powers and Kulkarni 2023). IPP socialization starts throughout the health science professionals' education and training. Interprofessional education events, collaborative practice opportunities, and peer-to-peer learning are all promoted for students from many academic fields. Health science workers get an appreciation for the distinctive contributions that each field makes to the team throughout the socialization process. They learn about the range of their colleagues' knowledge and abilities as well as their own. This knowledge encourages a collaborative approach to patient care and aids in tearing down professional silos (Khalili and Orchard 2020). It is acknowledged in the Institute of Medicine (IOM) study that there needs to be better coordination among academic IPP initiatives and incorporation into practice. They contend that interactions between practice and education groups often focus on only one health profession. Even though most health professions education programs now include IPP as a necessary academic requirement for approval and that IPP outcomes indicate a positive trend toward suitable professional socialization, there is little research on the experience of transferring skills learned during IPP operations into clinical practice environments (Shustack et al 2021). The process through which students from multiple health-related disciplines learn to communicate, cooperate, and perform well as a team is referred to as IPS among HPS. It entails the growth of respect, understanding, and information sharing amongst students from various professional backgrounds, including occupational therapy, nursing, medicine, and more. IPS is crucial because complicated patient requirements call for a team effort in contemporary healthcare. To provide complete and patient-centered care, healthcare professionals from many disciplines must collaborate, communicate effectively, and share their special knowledge (Kneck et al 2019). According to a study of the investigation, there is insufficient knowledge about how the profession is viewed by students' requirements and functions of additional professions. This study intended to establish how HPS perceived IPS. Figure 1 shows the IPP information flow for Health care. In the context of healthcare, the notion of IPP information flow captures the dynamic and iterative nature of information sharing, cooperation, and decision-making. It emphasizes the connections and ongoing information flow among diverse stakeholders, including healthcare professionals, patients, researchers, and administrators.

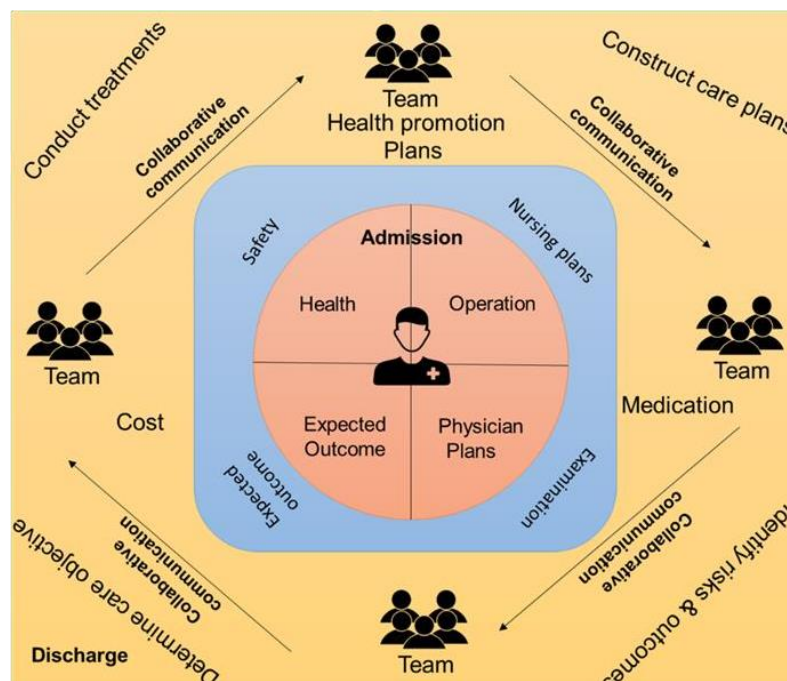


Figure 1 IPP information flow for Health care.

2. Literature Review

Ribeiro et al (2019) looked into the obstacles that currently exist to creating and executing One Health (OH) efforts, as well as their causes and possible remedies. Additionally, the study will point out strategic solutions that can overcome practical issues. In the course of carrying out OH efforts, a methodical study of the relevant literature was carried out to look for newly developing difficulties and potential answers to those challenges. Haugland et al (2019) delivered a reader's understanding of how IPE may support both professional and Interprofessional identities. In IPE, group cooperation helped students connect with their profession and provided a secure atmosphere they could acquire the skills of additional

professions. Langlois et al (2020) presented a singular chance for researchers, educators, and practitioners to build on what has previously benefited IPE and preparation, abandon what hasn't worked as effectively, and start to envision the future. The study examined how different parties felt about a potential IPE effort at the University of Malta's Faculty of Health Sciences. 59 people, including academics and senior policymakers, participated in the study using a purposive sample technique.

Bonello and Morris (2020) established that the Medical Faculty at TU Dresden created an optional course on Interprofessional Palliative Medicine that has been taught in conjunction with trainees in other health professions since the summer term of 2017. Interprofessional thinking and decision-making will be more and more necessary in the delivery of healthcare, hence these skills should be taught throughout medical school and professional development. The IPE movement is helping to advance the advantages of a creative workforce that is prepared for patient-centered care on a global scale. Coordinated healthcare staff is emphasized and supported in policy papers in Malta, an isolated nation. Gawrisch et al (2020) provided a theoretical framework based on occupational socialization theory to assist preservice teachers of physical education in developing technical pedagogical topic knowledge. The structure for incorporating computers into programs for training teachers is provided by an understanding of technological pedagogical material. Roopnarine and Boeren (2020) investigated the variations in Interprofessional learning preparedness between medical students and students of other allied human health professions, such as veterinary medicine students seeking education dual degrees with a Master of Public Health.

Haley et al (2019) discussed encouraging learners to learn through and learn through other professions by bringing together learners and educators from other academic fields. The investigation that follows outlines a novel approach to include health professions readers and academics in the creation of an Interprofessional literature conversation and proposes tactics to deal with difficulties with implementation. Interprofessional book discussion groups for incoming health professions students were set up by university medical librarians in collaboration with the IPE Coordinating Committee. El-Awaisi et al (2021) investigated the attitudes of healthcare professionals (HCP) at primary healthcare (PHC) centers regarding Interprofessional collaboration and pinpoint the enablers and impediments to collaborative practice. Given that it often serves as the patients' initial point of interaction, PHC settings are recognized as a key component of the system of healthcare. The region of the Middle East has never completely investigated Interprofessional cooperation amongst HCP in PHC settings. Boshoff et al (2020) offered a summary of the characteristics, results, and lessons learned about IPE Placements in Allied Health professional-entry programs. One of the strategies that may be used to get students ready for IPP is the availability of these placements. Olenick et al (2019) investigated the elements, both good and negative, that impact the application of IPE in healthcare education programs in the United States. The researchers asked 439 healthcare faculty members from 7 changed healthcare professions about the factors, both positive and negative, that influence their decisions to participate in IPE. The study sample consisted of healthcare faculty members.

Holmes et al (2020) examined the psychological, sociological, and neuroscientific impacts of COVID-19 and outline both short-term goals and long-term research plans for the field of mental health science. Public opinion polls and an expert group assembled by the UK Academy of Medical Sciences and the mental health research charity, MQ, served as the basis for these goals. The coronavirus illness epidemic in 2019 has made a significant impact on many facets of society, involving both physical and mental health. Shadmi et al 2020 examined COVID-19 disproportionately affects low-income people, people of color, and a wide range of other vulnerable groups because it spreads unevenly in densely populated areas and has a limited ability to be mitigated due to the high prevalence of chronic diseases or limited access to high-quality public health and medical care. Furthermore, people in the lowest power strata of civilizations are being disproportionately affected by the pandemic's side effects brought on by the global economic collapse, as well as social isolation and restrictions on travel measures.

3. Methodology

A qualitative study using a cross-sectional design was carried out. Students in various health professions were given a survey that examined their views, attitudes, and actions in addition to their perspectives on IPS. The results were tabulated and analysed. Face-to-face administration of the IPS and Valuing Scale (ISVS-21) was performed with each student to boost the percentage of students who responded to the survey. This survey has already been conducted, authorization was secured from the survey's original creators by way of the Flint box repository, which is copyright owned by Wellspring Global, LLC. This survey is a shortened version of a psychometrically verified instrument, which was used as the basis for its development. The internal uniformity of the 21-item IVIS was very high, demonstrated by its Cronbach alpha value of 0.988.19. The structure of the subjects consists of 21 different questions that are assessed using a Likert-type scale with 7 points and 7 indicates. The demographic details concerning college significance, conventional or unconventional learners, graduate student or undergraduate (UG), sex, and racial/ethnic profession served as the independent factors in this study.

3.1. Selection of Participants

The research sample consisted of 414 HPS students (both UG and graduate levels) from an individual university of health professions. There were students from 8 different fields, the greatest number of which was nursing with 149 UG students, subsequently monitored by communication disorders with 76 UG students, physical therapy with 52 graduate learners, social work with 43 UG students, radiologic science with 35 UG students, occupational therapy with 28 graduate students, medical laboratory science with 16 undergraduate students, and nutritional science with 15 UG students.

3.2. Sampling Procedure

The investigators made connections to professors in the College of health professions' 8 health disciplines after acquiring permission from the term institutional review board, clinical lab science, physical therapy, nursing, radiological science, nutritional science, communication disorders, and social work. The instructor from every specific subject committed on a mutually agreeable day and time for the investigators to be present at the beginning of their lesson and personally administer the questionnaire. During each of the courses that preceded the survey, there have been any IPE incidents. The investigators presented themselves and obtained knowledge from the survey participants before delivering the questionnaires. A lack of identifiable data was gathered and research participants were told not to enter their names on the questionnaires to maintain their anonymity. To enhance the uniformity of data collection by several researchers, a series of identical written instructions were given to each team of students learning for a health profession. The investigators surveyed over two months to gather information regarding the many courses provided by several faculty members. The students who were present on campus were polled by the investigators. However, several student organizations were unable to be polled because they were off-campus participating in clinical educational activities.

4. Results

In the context of IPP, socialization describes the process through which members of several health science professions come together to cooperate and function as a team. Since it improves communication, coordination, and shared decision-making among experts from many disciplines, this cooperation is essential for providing good health care.

4.1. Participant Characteristics

The initial section of the survey included information on the demographics of higher education significant, conventional or non-traditional students, female or male, UG or graduate students, and racial/ethnic education. 29% of the 414 HPS students in the sample were non-traditional, compared to 71% of conventional students. The researchers identified college students as conventional if they were under 24 and non-traditional students if they were 24 or over. 72 percent of UG and 27 percent of graduate students responded to the poll. 82% of those participating were female students, while 18.1% were male students. Only around 1.7% of pupils identified as being of Pacific Islander, Native American, Caucasian-Asian, Hispanic ethnicity, or White. Students were mostly of European descent, with smaller numbers of African-American, Hispanic, and Asian students. It indicated the majority of the study's participants were generic college-aged Caucasian students (Table 1).

Table 1 Features of Sample.

Features	type	Percentage (%)	Number (n=414)
Type of Student	Non-traditional	28.7	117
	Traditional	71.3	297
Level of Student	Graduate	27.5	116
	UG	72.5	298
Sex	Female	81.9	341
	Male	18.1	77
Ethnic or Racial Background	African American	5.3	20
	Asian	1.7	9
	Caucasian	89.1	371
	Hispanic	2.2	11
	Other	1.7	9
Health Profession	Communication Disorder	18.4	74
	Nursing	36	151
	Physical Therapy	12.6	50
	Social Work	10	41
	Nutritional Science	17	3.6
	Clinical Lab Science	14	3.9
	Occupational Therapy	26	6.8
	Radiologic Science	35	8.5

4.2. Data Analysis

The Statistical Package for the Social Sciences (SPSS) the measurable reactions to the IVIS-21 survey's 21 questions were analyzed with the use of special software. The standard deviation and mean information were utilized to conduct the descriptive analysis. Based on the Likert scale on the IVIS-21 questionnaires, participants' beliefs, attitudes, and behaviors regarding IPS received ratings in the following order; Not Applicable= zero, not the least bit = one, to a very limited amount = two, to a lesser amount = Three, to an adequate amount = four, to an average great amount = five, to a great amount = six, and an unlimited amount = seven. This information was utilized to calculate the mean for each question. Following data analysis, it was discovered that 95% of students believed that 20 out of the 21 questionnaire queries occurred to a reasonably big amount to a considerable amount, with M=5.12 or above the 1to7 to Likert scale. I have a greater understanding of the value of a collaborative approach, according to the review question with the highest mean. For the statement (I feel comfortable leading a team situation), the lowest mean was found. The review items' mean and standard deviation are shown in Table 2 and Table 3. Survey on the scales of IPS and value for mean and standard deviation are shown in Figure 2 and Figure 3. This section A, B, C, D, and E mentioned Participating in team conversations, being aware of one's assumptions, an improved sense of one's involvement in IPP, Capability of speaking out in a group, Enhanced understanding of team roles, Ability to accept delegation of responsibilities within a team.

Table 2 Results of an IPS and valuation scale survey for Mean.

Survey Item	Mean
The capability of speaking out in a group	5.35
Enhanced understanding of team role	5.57
Improved impression of one's involvement in IPP	5.29
Improved comprehension of the team approach	5.96
Ability to accept delegation of responsibilities within a team	5.91
Participating in team conversations, being aware of one's assumptions	5.12

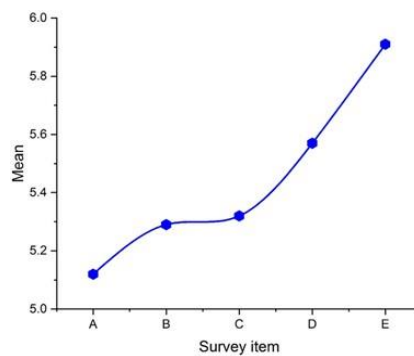


Figure 2 Survey on the scales of IPS and value for Mean.

Table 3 Results of an IPS and valuation scale survey for standard deviation.

Survey Item	standard deviation
The capability of speaking out in a group	1.17
Enhanced understanding of team roles	1.23
Improved impression of one's involvement in IPP	1.25
Improved comprehension of the team approach	1.19
Ability to accept delegation of responsibilities within a team	0.99
Participating in team conversations, being aware of one's assumptions	1.17

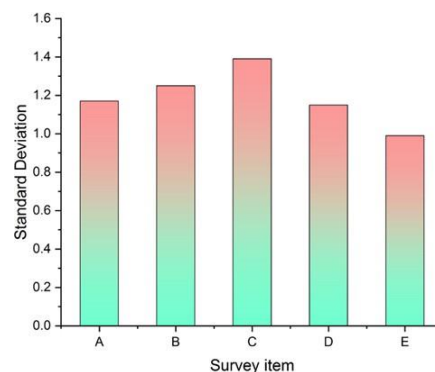


Figure 3 Survey on the scales of IPS and value for Standard deviation.



5. Discussion

5.1. Constructs of Perceptions

The purpose of this research was to investigate how HPS felt about IPS and its principles. The IVIS-21 scale's data on IPS and values were analyzed to search for variations in the students' perspectives on working as a collaborative care team. According to our research, 95.2% of students believed IPS was happening to a rather significant or considerable level. It highlights that students' participation in Interprofessional education activities and clinical practice has increased their knowledge of each of the basic concepts of action, belief, and attitude. The first theory supports their optimistic beliefs regarding becoming effective group members, learning to work together effectively, and recognizing the benefits of a team-based strategy. The second section reveals how health professions graduates feel about their own biases and how much they value working as part of a group. The results additionally offer support for cooperative actions including speaking out for what you believe in, clearing up any confusion others may have about your job, and generally being yourself in a group setting. Those who took part in the study had the same set of behaviors, beliefs, and attitudes when it came to working together. Since they suggest that learners are well-equipped to understand sharing each other's professional responsibilities and expectations.

5.2. Challenge for Educators

The difficulty for health care instructors is to improve students' understanding of each other's duties, even though maximum students show a propensity to study the characters and duties of additional corrections. Although the students may possess the ideas, attitudes, and actions, they lack the support necessary to understand the roles played by other health professionals. The duty of fostering more inclusive collaboration partnerships across disciplines falls to the teacher. The National League for Nursing (NLN) asserts that instructors have to view ourselves as Interprofessional professors with the responsibility of motivating students to support an Interprofessional team-based healthcare system rather than as profession-centric practitioners. In educational contexts, Woodworth discovered that the educator must expand these possibilities for Interprofessional encounters. Buhler recommends that students use an integrated approach to collaborate as a team. Members of the team may work together to provide the patient with their finest work as a whole. To strengthen these team ties, Interprofessional education must be included in the curriculum while students are still at such a formative period of their careers. The difficulty is in how to successfully include Interprofessional collaboration activities into educational programs even though considerations for such operations have been specified.

6. Conclusions

The findings of this research further demonstrate the significance of including IPP in student curriculum to teach them about the functions of various health professionals. To collaborate across disciplinary boundaries, HPS must comprehend different fields. To provide safe, high-quality patient care, there is a growing dependence on inclusive teamwork and open communication. The long-term objective is to implement academic approaches to team-based, cross-disciplinary cooperation in healthcare. In conclusion, socialization in IPP is an important process for health science professionals to learn how to collaborate effectively and provide high-quality, patient-centered care. It involves developing shared values, effective communication skills, and a deep understanding and appreciation for the roles and expertise of different disciplines. By fostering collaboration and teamwork, socialization in IPP recovers patient outcomes and improves the general distribution of healthcare services.

Ethical considerations

Not applicable.

Declaration of interest

The authors declare no conflicts of interest.

Funding

This research did not receive any financial support.

References

Arnold C, Berger S, Gronewold N, Schwabe D, Götsch B, Mahler C, Schultz JH (2020) Exploring early IPS: a pilot study of student's experiences in medical history taking. *Journal of Interprofessional Care* 1-8.

Bonello M, Morris J (2020) Institutionalizing interprofessional education in small states: perspectives from faculty and key stakeholders in Malta. *Journal of interprofessional care* 34:36-43.

- Boshoff K, Murray C, Worley A, Berndt A (2020) Interprofessional education placements in allied health: A scoping review. *Scandinavian Journal of Occupational Therapy* 27:80-97.
- El-Awaisi A, Awaisu A, Aboelbaha S, Abedini Z, Johnson J, Al-Abdulla SA (2021) Perspectives of healthcare professionals toward interprofessional collaboration in primary care settings in a Middle Eastern Country. *Journal of multidisciplinary healthcare* 363-379.
- Gawrisch DP, Richards KAR, Killian CM (2020) Integrating technology in physical education teacher education: A socialization perspective. *Quest* 72:260-277.
- Haley J, McCall RC, Zomorodi M, de Saxe Zerdan L, Moreton B, Richardson L (2019) Interprofessional collaboration between health sciences librarians and health professions faculty to implement a book club discussion for incoming students. *Journal of the Medical Library Association: JMLA* 107:403.
- Haugland M, Brenna SJ, Aanes MM (2019) Interprofessional education as a contributor to professional and interprofessional identities. *Journal of interprofessional care* 1-7.
- Holmes EA, O'Connor RC, Perry VH, Tracey I, Wessely S, Arseneault L, Ballard C, Christensen H, Silver RC, Everall I, Ford T (2020) Multidisciplinary research priorities for the COVID-19 pandemic: a call for action for mental health science. *The Lancet Psychiatry* 7:547-560.
- Karnish K, Shustack L, Brogan L, Capitano G, Cunfer A (2019) IPS through acute-care simulation. *Radiologic Technology* 90:552-562.
- Khalili H, Orchard C (2020) The effects of an IPS-based IPE program on IPS and dual identity development. *Journal of interprofessional care* 1-11.
- Kneck Å, Flink M, Frykholm O, Kirsebom M, Ekstedt M (2019) The information flow in a healthcare organisation with integrated units. *International journal of integrated care* 19.
- Langlois S, Xyrichis A, Daulton BJ, Gilbert J, Lackie K, Lising D, MacMillan KM, Najjar G, Pfeifle AL, Khalili H (2020) The COVID-19 crisis silver lining: interprofessional education to guide future innovation. *Journal of interprofessional care* 34:587-592.
- Mahler C, Orchard C, Berger S, Krisam J, Mink J, Krug K, King G (2022) Translation and psychometric properties of the German version of the "IPS and Valuing Scale" (ISVS-21-D). *Journal of Interprofessional Care* 1-7.
- Olenick M, Flowers M, Muñecas T, Maltseva T (2019) Positive and negative factors that influence health care faculty intent to engage in interprofessional education (IPE). In *Healthcare* 7:29.
- Powers K, Kulkarni S (2023) Examination of Online Interprofessional Education to Develop Graduate Students' IPS and Collaborative Competencies. *Journal of Social Work Education* 59:506-519.
- Ribeiro CDS, van de Burgwal LH, Regeer BJ (2019) Overcoming challenges for designing and implementing the One Health approach: A systematic review of the literature. *One Health* 7:100085.
- Roopnarine R, Boeren E (2020) Applying the Readiness for Interprofessional Learning Scale (RIPLS) to medical, veterinary and dual degree Master of Public Health (MPH) students at a private medical institution. *PLoS One* 15:e0234462.
- Shadmi E, Chen Y, Dourado I, Faran-Perach I, Furler J, Hangoma P, Hanvoravongchai P, Obando C, Petrosyan V, Rao KD, Ruano AL (2020) Health equity and COVID-19: global perspectives. *International journal for equity in health* 19:1-16.
- Shustack L, Karnish K, Brogan L (2021) Perceptions of socialization in interprofessional practice among health science students and first-year practicing professionals. *Journal of Interprofessional Education & Practice* 23:100420.

Psychological skills in athletic rehabilitation (AR): trainers and therapists perceptions



Prerana Gupta^a | Suhas Balla^b | Sneha Verma^c

^aTeerthanker Mahaveer University, Moradabad, Uttar Pradesh, India, Professor, Department of Psychiatry.

^bJain (Deemed-to-be University), Bangalore, India, Assistant Professor, Department of Chemistry.

^cMaharishi University of Information Technology, Lucknow, Uttar Pradesh, India, Assistant Professor, School of Science and Humanities.

Abstract: Sport-injury recovery is said to benefit from psychological abilities, yet there is little use of mental imaging in treatment protocols. To determine if the opinions of Physical Therapists (PTs) and Athletic Trainers (ATs) on the healing process for harmed sportsmen may be sped up by the use of positive language, setting targets, and mental imagery in treatment. To participate in an experiment that was only administered once and asked participants about the efficiency of psychological techniques, the ATs and PTs were approached for increasing adherence and speeding up the healing of wounded sportsmen enduring treatment. A total number of 309 ATs and 356 PTs responded out of the one thousand ATs and PTs that were randomly selected. The Attitudes about Imagery (AAI) study gauges opinions on psychological techniques for improving injured athletes' commitment and recovery speed. The AAI asks questions on demographics and measures attitudes regarding the influence of pain management on injured athletes' compliance with therapy and utilizes fifteen inquiries and a Likert scale with seven points to measure recovery speed. To ascertain if variations in views occurred due to the professionals' educational background, training experience, and interest, we performed 1-way analyses of variances. The usefulness of psychological skills to support the recovery process was generally viewed favourably by ATs and PTs. The utilization of mental abilities is considered in terms of clinical ramifications.

Keywords: athletic trainers, physical therapists, injured athletes, mental imagery, recovery speed

1. Introduction

The powerful impact that coaches have on their players is well documented in the sport psychology field. A sportsperson's ability to play well does not just depend on their physical condition or technical proficiency. The purpose and character of the sport determine how much demand there is from outside causes. The relationship between psychological abilities and performance seems to be acknowledged by coaches and players. The advantages of improving an athlete's psychological capabilities are acknowledged. Consequently, professional sports organizations have sought the participation of sports psychologists more often (Feddersen et al 2021). The phrase "psychological skills" is wide and encompasses a variety of psychological aptitudes that assist athletes in maximizing their performance. These abilities include visualization, goal-setting, relaxation, self-talk, emotional restraint, and self-assurance. Although they are used differently in practice and competition, psychological skills are connected to performance. There are numerous different tests available to evaluate psychological aptitude. One of them is the Test of Performance Strategies (TOPS) (Blumenstein and Orbach 2020). This uses many subscales to evaluate psychological abilities and tactics in competition and practice.

Olympic medalists and non-medal winners exhibit different images, emotional control, and automaticity during competition. Additionally, there is evidence that practicing psychological skills may be helpful in the recovery from sports injuries (Trotter et al 2021). A dedication to recommended treatment procedures is a further part of sports injury recovery that might benefit from applying psychological skills. Athletic rehabilitation (AR) is a crucial stage on the road to recovery and peak performance for athletes. The importance of psychological skills cannot be understated, even while physical therapy and pharmacological interventions are crucial steps in the recovery process (Lim et al 2018).

During the recovery phase, an athlete's perspective, motivation, and general well-being may be significantly impacted by using psychological tactics and strategies. The perception of an athlete that he or she can affect the result of rehabilitation is likely reflected in the use of psychological treatments to recover more quickly and fully from injury. Both adherence to sport-injury rehabilitation plans and the perceived speed of recovery after knee surgery has been favorably connected with beliefs about control over rehabilitation outcomes (Mori et al 2020). As a result, athletes are more likely to take action to exercise this control and adhere to their injury-rehabilitation plans more closely when they feel like they have some influence over the recovery process.

Athletes may enhance their capacity to deal with setbacks, sustain enthusiasm, and hasten their physical recovery by concentrating on certain psychological abilities. The combination of these abilities not only improves an athlete's psychological fortitude but also helps them perform physically as best they can when they return to the field (Karpov et al 2019). There are distinctions between elite and non-elite athletes in individual sports as well. Goal planning, relaxation, activation, imagery, emotional regulation, and negative thinking were all psychological abilities that members of Greece's top national track and field team utilized more often than non-elite track and field athletes. Sports psychology abilities are often improved via psychological skills training (PST). It is described as the systematic and constant use of psychological or mental abilities to improve performance, heighten the fun, or raise self-satisfaction in sports and physical exercise (Einarsson et al 2020). In this research, we explored the psychological abilities involved in AR using the perspectives of both ATs and PTs.

2. Literature Review

Shaari et al 2019 investigated whether the psychological skills training program affected the accuracy of netball shots. Three groups of an 8-week intervention were subjected to the experimental method: group one received a combination of diaphragmatic breathing, imaging, and physical exercise; group two received a combination of DB and self-talk; and group three received physical practice alone. Pankow et al 2021 looked at the manner in which players in the National Hockey League (NHL) developed their Psychological Skills and Characteristics (PSCs). We conducted six individual semi-structured conversations with NHL players (4 active players and two retired players) using an interpretative description approach. Data were verbatim transcribed and then reflexively thematically analyzed. The necessity of understanding the psychological features of athletes, who compete in martial arts, as well as the distinction between the psychological characteristics of athletes who compete in categories of art and combat, was the driving force for the study (Dongoran et al 2020). Veskovc et al (2019) showed an increase in self-regulation, and because improved self-regulation leads to improved competitive performance, it is essential to assess psychological skill development programs. In contrast to routine training and competitive activities, it was expected that adding autogenic exercise and imagery guidance might improve anxiety and self-assurance.

Borsboom et al (2021) enhanced the process of creating explanatory theories in psychology by creating a helpful approach known as a theory-building methodology (TCM). The five stages of TCM are listed below. The area of empirical facts that will be the subject of explanation is first chosen by the theorist. The theorist then develops a prototheory, a theory that explains these events. In terms of treating knee osteoarthritis, it has been shown that both physical treatment and intraarticular glucocorticoid injections are clinically beneficial. In the primary care context of the U.S. Military Health System, Deyle et al (2020) performed a randomized experiment comparing physiotherapy with glucocorticoid administration. van Doormaal et al (2020) updated the Royal Dutch Society for Physical Therapy's (KNGF) Dutch guideline for physical therapy (PT) in patients with hip or knee osteoarthritis (OA). Clinical questions were developed by an integrated advisory panel according to alleged obstacles to current therapy. Physical therapists must be aware of the difficulties they may face while caring for COVID-19 patients since they play a crucial role in their support. Felten-Barentsz et al (2020) attempted to give direction and specific suggestions for hospital-based physical therapists treating patients hospitalized with COVID-19 via a national strategy in the Netherlands, keeping with worldwide approaches.

3. Methodology

In this section, we explain that ATs had formal training in the use of psychological techniques for injured athletes and how they had views that were notably more favorable regarding the came to the 15 AAI inquiries.

3.1. Participants

Due to their importance in the healing of sports injuries, physical therapists and athletic trainers were chosen. Every participant in our research had a professional national certification and was at least 21 years old. The ATs worked in the following American settings: medical, clinical/college, college, professional athletics, and secondary school; participants were selected at random from typical, licensed members of the National Athletic Trainers Association (NATA). The PTs were working in orthopedic outpatient rehabilitation facilities in the United States and were chosen at random from American Physical Therapy Association (APTA) participants.

3.2. Procedures

The NATA investigation representative chose the ATs (n = 1000) at random and sent them an inquiry link along with a cover note from NATA. The AAI assessment was preceded by a section requesting informed consent. Another message was issued as a reminder after two months for the participants who had been allowed three months to reply to the original email. The individual who responded was acknowledged for completing the inquiry.

The principal study received postal addresses online, and the APTA research representative also randomly chose the PTs ($n = 1000$). Each 1000 PT received a mailing that included the AAI, an informed consent form, a cover letter, and a pre-paid return envelope. The APTA prohibited sending a second letter to nonrespondents as a follow-up notification.

3.3. Psychological Skills in Athletic Rehabilitation (AR)

The recovery from injuries and restoration of an athlete's physical and mental talents are facilitated by psychological skills, which are essential to Athletic Rehabilitation (AR). The following are some crucial psychological abilities that are useful in the context of sports rehabilitation:

Goal Setting: During their recovery, athletes should set SMART (specific, measurable, achievable, relevant, and time-bound) objectives. Setting goals gives one direction, inspiration, and a feeling of accomplishment. They may be used to concentrate on certain psychological and physical milestones during the healing process.

Positive Self-Talk: During recovery, an athlete's confidence and drive may be increased by using encouraging and motivating self-talk. Athletes may enhance their mental state, lessen anxiety, and improve well-being by substituting positive ideas for negative ones.

Visualization and Mental Imagery: Visualization entails building imaginal representations of effectively executing certain abilities or motions. Athletes may improve their attention, confidence, and motor abilities by picturing themselves doing exercises precisely and receiving positive results. When physical practice is restricted due to an injury, mental images may be very helpful.

Relaxation Techniques: Athletes may manage stress, decrease muscular tension, and increase general relaxation by learning and using relaxation methods, including progressive muscle relaxation, deep breathing, and meditation. These methods help with both physical and emotional healing.

Understanding and Managing Pain and Anger: Athletes may struggle psychologically as a result of their injuries and related suffering. Athletes undergoing rehabilitation may find it easier to deal with pain and frustration if they learn effective pain management strategies, including distraction, mindfulness, and cognitive reframing.

Resilience and Adaptability: Setbacks and difficulties are common throughout rehabilitation. Athletes who want to recover quickly from losses, adapt to changing conditions, and have a good attitude while recovering must develop resilience and adaptability.

Social Support and Communication: An athlete's recovery process may be greatly influenced by having a strong support network that includes medical experts, coaches, teammates, and family. Emotional support, motivation, and a feeling of belonging may be obtained via effective communication and the search for social support.

Time Management and Patience: Rehabilitation takes time and perseverance. To match their rehabilitation schedules with other obligations, athletes must learn good time management techniques. In order to avoid irritation and have a good outlook during the rehabilitation process, patience, and reasonable expectations are crucial.

It's crucial to remember that depending on the person and the kind of injury, athletes may have different psychological demands throughout recovery. Athletes' recovery processes might benefit from individualized direction and assistance from a certified sports psychologist or mental skills trainer.

3.4. Assessment

The 15 inquiries in the AAI assessment seek comments on the importance of encouraging self-talk, goal-setting, pain tolerance, and mental imagery in promoting faster and more compliant recovery in athletes. To reduce anxiety before and after surgery, using mental imagery as a kind of relaxation is very useful, according to a sample question from the AAI assessment. Seven points are assigned to the answer on a Likert scale, with the marks firmly agreeing and strongly rejecting. For this investigation, the AAI was created using elements from the integrative theory of response, and its material reliability was evaluated by four specialists from sport psychology, athletic training, and physical therapy.

The measure's item phrasing, relevance, and suitability for gauging attitudes about psychological talents were all criticized by experts. If half of the experts made the same modification recommendations, the original instruments' specifications were changed. The metric was subsequently changed, and the same four specialists were given a second chance to evaluate it. Based on feedback, three things about the final measurement diverged from the initial AAI: (1) Due to duplication, the number of elements was decreased from 17 to 15; (2) the Likert scale's value ranges increased from five to seven degrees; and (3) item wording was altered for simplicity.

The AAI was also assessed using reliability coefficients such as test-retest scores and Cronbach's alpha. In a trial group of students focusing on kinesiology, the two-week test-retest accuracy coefficients ranged from .60 to .73 on all 15 measures; every association was significant at the .01 level. Four groups were found when the AAI items were categorized by their emphasis. Cronbach's alpha was employed as an extra reliability indicator for seven mental imagery measures (.80), four self-talk measures (.64), three setting goals measures (.66), and two pain tolerance measures (.74). The experts' recommendations about content validity were validated by the metrics of internal consistency and interitem consistency.

3.5. Statistical evaluation

The significance threshold for our statistical analysis was fixed at .05. We used Statistical Package for the Social Sciences (SPSS) statistics. Several one-way Analysis of Variance (ANOVA) techniques were used to examine how ATs and PTs felt about their work. Using statistical techniques, we looked at participant variables which include age, sex, and years of work experience. The association between professional experience and the use of psychological abilities was investigated using Pearson correlations. The setting of (1) education in a program that is authorized, (2) formal instruction in the use of mental imagery to injured players, and (3) an interest in pursuing formal instruction in the use of mental visualization with injured players.

4. Results

The polling received 665 responses, including 309 ATs and 356 PTs, for a response rate of 33.3% (n = 665). Of these individuals, 42.8% were male and 53.2% were female. It is significant to note that the assessment distribution method had no impact on response rates: 34.5% of PTs who completed the physical postal assessment and returned the AAI, compared to 30.9% of ATs who were questioned through email. Table 1 displays the sample's statistics, such as age, sex, and years of field experience.

Table 1 Demographics of Participants by Professional Group.

	Physical Therapists	Athletic trainers
N	356	309
Experience, and		
Mean \pm Sd	15.19 \pm 7.18	11.68 \pm 8.35
Range	1-39	1-35
Age, and		
Mean \pm Sd	24.65	22-69
Range	40.55 \pm 8.52	34.19 \pm 9.35
Sex, No. (%)		
Men	149 (42.8)	151 (49.3)
Women	210 (59.5)	162 (52.9)

The value of psychological skills in accelerating the healing process was not found to be influenced by education inside an approved athletic training program, according to the results of a 1-way ANOVA. In addition, none of the 15 AAI constituents showed any mean variations. We performed two further 1-way ANOVA calculations using the variable "years of experience in the profession" to reduce the subject population to 10 years or less and then to 5 years or fewer to conduct a more in-depth analysis.

No significant variations were seen between individuals who did not graduate from an accredited school and those who did so in the last ten or previous five years on any of the AAI measures, which is compatible with our whole-group analysis. Additionally, on 14 of the 15 questions on the AAI, ATs, and PTs who indicated that they had received formal instruction in using mental imaging responded more favorably than those who weren't, as shown in Table 2 below.

Table 2 Programs for the Rehabilitation of Sports Injuries Utilize Psychological Skills.

	Yes Mean \pm SD	No Mean \pm SD	P	F	Effect size
Interest in formal training	N=326	N=149			
Mental imagery	6.58 \pm 0.95	5.15 \pm 1.01	.001	60.68	0.68
Goal setting	7.31 \pm 0.88	5.98 \pm 2.06	.000	21.05	0.41
Positive self-talk	7.09 \pm 0.98	5.81 \pm 0.93	.000	19.61	0.38
Pain control	7.31 \pm 0.89	7.05 \pm 1.00	.002	12.17	0.29
Formal training	N=113	N=451			
Mental imagery	6.65 \pm 0.83	6.28 \pm 0.99	.001	16.33	0.47
Goal setting	7.51 \pm 0.64	6.11 \pm 1.98	.004	11.69	0.45
Positive self-talk	7.21 \pm 1.65	6.95 \pm 0.96	.274	1.20	0.15
Pain control	6.29 \pm 0.895	6.19 \pm 1.94	.288	1.18	0.17
Accredited program	N=209	N=134			
Mental imagery	5.35 \pm 1.08	6.35 \pm 0.96	.965	0.004	0.02
Goal setting	6.41 \pm 1.95	6.35 \pm 0.85	.457	0.575	0.11
Positive self-talk	6.05 \pm 0.88	6.08 \pm 0.82	.835	0.047	0.04
Pain control	7.35 \pm 0.92	7.25 \pm 0.92	.241	1.41	0.15

Additionally, we discovered that ATs and PTs who said that they had received formal training or that they intended to do so had more favorable opinions about using psychological techniques on injured athletes. The ability to think positively is

probably a result of educational preparation and practical use of the strategies with wounded sportsmen. In the future, ATs and wounded athletes may benefit from simultaneous treatment of the psychological stress brought on by physical injury due to continuous research into the efficacy of such approaches and education for therapists. Figures 1 and 2 depict the effective size of an accredited program and formal training in psychological techniques for programs to treat sports injuries.

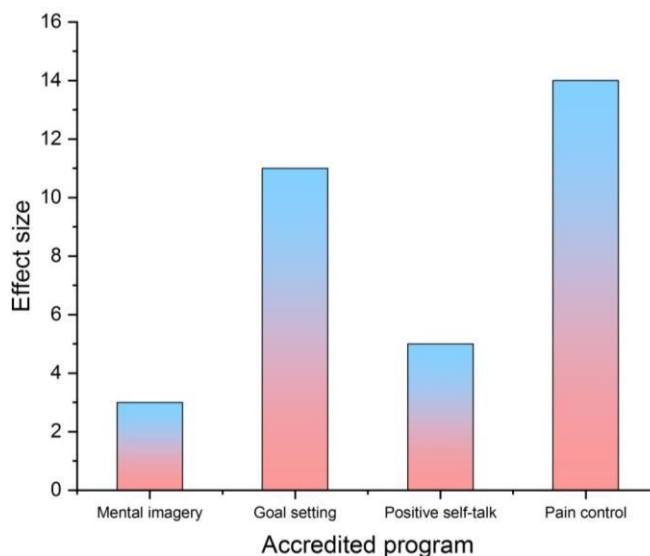


Figure 1 Effective size of an accredited program.

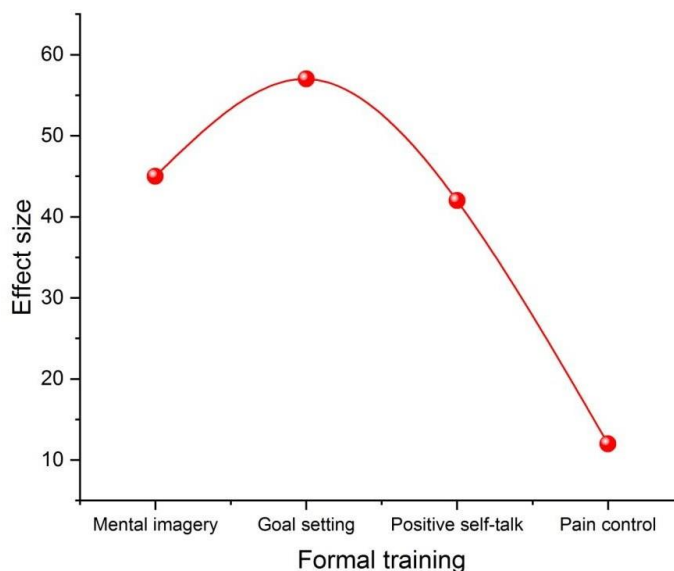


Figure 2 Effective size of formal training.

On a scale of from one to seven, with four denoting a neutral viewpoint, both parties agreed that the ability to tolerate discomfort was crucial, regardless of prior formal training. Additionally, those ATs and PTs who requested formal training on using mental imagery expressed greater favorable sentiments on all 15 AAI inquiries compared to those who did not ($P < .001$).

Further analysis of the subscale means responses and the results of mental imagery are given in Table 3, with ATs displaying more favorable attitudes than PTs on the efficacy of self-talk, goal setting, and pain tolerance. The AAI's eight imagery items received good overall mean scores from both groups, ranging from 4.73 to 5.95 for the eight imagery items, which represents the usefulness of mental imagery overall.

We discovered good reactions generally to the effect of psychological skills inside the rehabilitation program, in contrast to earlier studies' findings. Different metrics and how the devices were calibrated may have impacted the findings. Figure 3 illustrates the difference in the efficacy of mental imaging used by PTs and ATs.



Table 3 Findings from the mental imagery sub-scale.

Attitudes about imagery subscale and items	Physical therapists	Athletic trainers	Analysis of variance		
	Mean ± SD	Mean ± SD	P	F	Effect size
Mental imagery	5.31 ± 0.98	5.41 ± 1.00	.21	2.71	0.11
A. Increased attention to certain rehabilitation activities may be achieved via mental imagery.	6.66 ± 1.28	5.48 ± 1.25	.15	3.65	0.15
B. It is beneficial to boost concentration on certain therapeutic objectives by using mental images.	6.45 ± 1.29	6.55 ± 2.20	.15	2.18	0.15
C. Mental images might help you feel less discomfort when doing rehabilitation activities.	5.92 ± 1.34	5.71 ± 2.47	.11	2.66	0.15
D. A protracted period of recovery following a sports injury may be successfully managed by using mental images.	5.71 ± 1.18	6.95 ± 1.11	.005	10.1	0.25
E. By imagining the body recovering, mental imagery used during rehabilitation helps speed up recovery.	4.88 ± 1.45	5.95 ± 1.51	.25	1.45	0.11

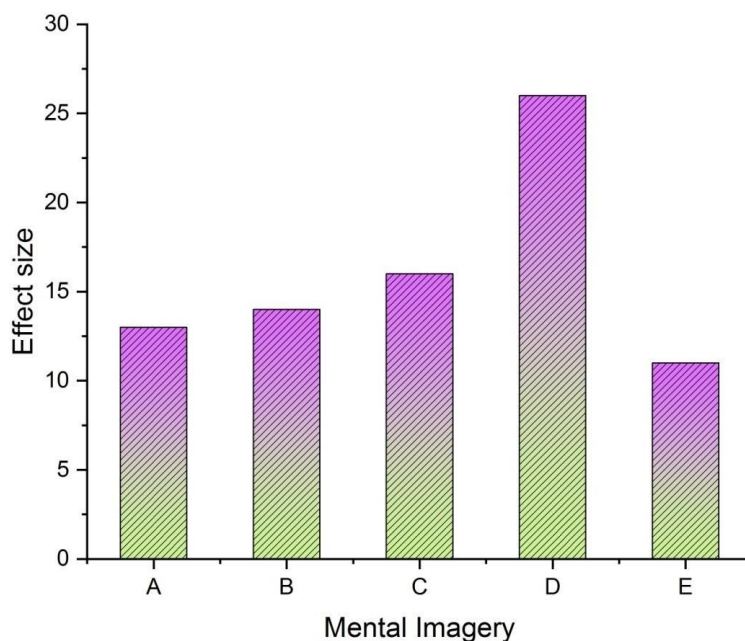


Figure 3 Effectiveness of mental imagery employed by PTs and ATs.

In other words, address scores of 3.0 on a scale of 1 to 5, with points denoting replies stated differently, changing the interpretation of the data. In addition, the differing outcomes might be a function of the study's period or location. Figure 4 and Table 4 illustrate the difference in the efficacy of positive self-talk used by PTs and ATs.

Table 4 Findings from the positive self-talk sub-scale.

Attitudes about imagery subscale and items	Physical therapists	Athletic trainers	Analysis of variance		
	Mean ± SD	Mean ± SD	P	F	Effect size
Positive Self-Talk	5.90 ± 1.91	7.11 ± 1.74	.002	11.67	0.35
A. To lessen discomfort during recovery, one helpful strategy is to utilize positive self-talk.	5.35 ± 1.28	6.29 ± 1.41	.89	0.027	0.07
B. The participant's compliance rate will rise when they maintain a good attitude throughout recovery.	7.18 ± 2.05	7.55 ± 0.91	<.002	0.027	0.39
C. The athlete's possibility of adhering to the program will rise with a good outlook throughout recovery.	7.15 ± 2.00	7.47 ± 0.85	<.002	18.55	0.38

In the United States, changes have undoubtedly occurred since the early 1990s, leading to an increase in readiness and openness to employ psychological skills; however, in other countries, public acceptability of utilizing psychological abilities for use in treating sports injuries facilities may not be as high. Figure 5 and Table 5 illustrate the difference in the efficacy of controlling pain and goal setting used by PTs and ATs.



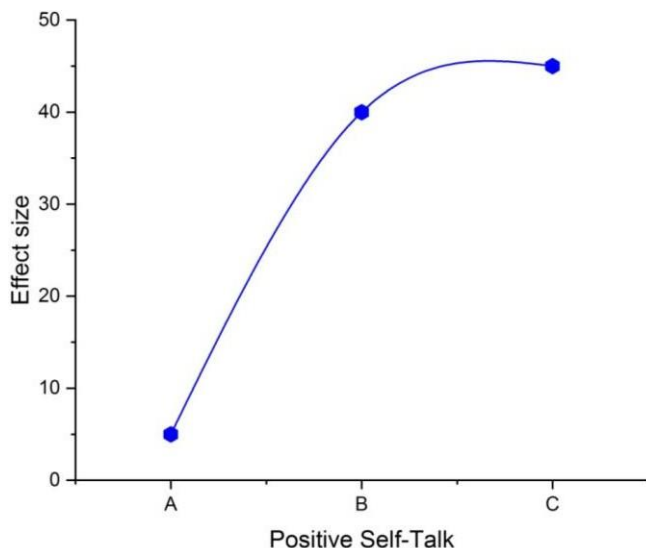


Figure 4 Effectiveness of positive self-talk employed by PTs and ATs.

Table 5 Findings from the controlling pain and goal setting sub-scale.

Attitudes about imagery subscale and items	Physical therapists	Athletic trainers	Analysis of variance		
	Mean ± SD	Mean ± SD	P	F	Effect size
Controlling pain	7.05 ± 1.05	7.37 ± 0.78	<.002	18.00	0.39
A. Decreasing the degree of discomfort brought on by rehabilitation activities can hasten the healing process. Process.	7.11 ± 1.21	7.38 ± 0.95	.001	15.61	0.35
B. The athlete's compliance rate will rise if the amount of discomfort associated with rehabilitation activities can be managed.	7.05 ± 1.06	7.35 ± 0.79	.000	17.45	0.37
Goal setting	5.95 ± 1.01	6.48 ± 1.77	<.001	50.32	0.63
C. Setting realistic rehabilitation objectives can hasten the healing process.	6.97 ± 2.11	7.42 ± 1.02	<.002	31.81	0.45
D. The athlete's compliance ratio might be increased by setting realistic objectives for their recovery.	6.95 ± 2.08	7.48 ± 0.82	<.002	52.75	0.68

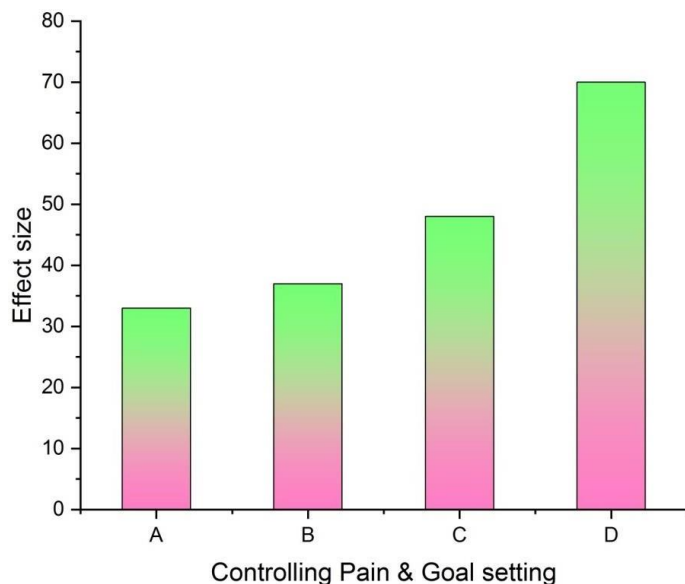


Figure 5 Effectiveness of controlling pain and goal setting employed by PTs and ATs.

Consequently, professionals' attention to their educational background and to athletes who enhance their performance through psychological techniques may be to blame for the generally good sentiments regarding psychological skills discovered in this research. This exposure could spark a desire to learn more about methods used in the rehabilitation program.



5. Discussion

Our research sought to ascertain whether favorable opinions and using mental images and other psychological techniques while undergoing rehabilitation were associated with the educational requirements of recognized initiatives, formal training, and interest in obtaining such training, as well as to ascertain whether ATs and PTs who manage injured athletes have similar or dissimilar attitudes toward these methods.

We assessed the perceptions of ATs and PTs on the efficacy of several psychological approaches that prior research had shown to be beneficial in rehabilitating injured athletes. According to our research, in inquiries that asked about both a psychological ability and a behavioral result, ATs had higher favorable opinions than PTs. This may be seen by the statements "Setting appropriate rehabilitation goals will help speed up the recovery process" and "Setting appropriate rehabilitation goals will help improve the athlete's adherence rate." To elaborate, ATs in college and university settings may deal with injured athletes' incapacity to adhere to therapy more often and experience more pressure to hasten the healing process than PTs do in outpatient clinical settings.

It's also possible that in their therapeutic work, the two specialists take a distinct approach to the psychological effects of injuries. The nine factors mostly dealt with managing discomfort and pain tolerance, having an optimistic outlook, and creating inspiring goals. ATs and PTs performed similarly on item 6 of 8 on mental imagery might be explained by a lack of familiarity with the method and its widespread use in both professions. Initially, we believed that because of their formal education, ATs would have more favorable opinions regarding psychological abilities; nevertheless, this wasn't the case. Goal-setting is recommended to increase rehabilitation compliance and hasten recovery, consistent with earlier studies.

The PT's clinical and educational background may help to explain the findings above regarding opinions concerning the effectiveness of mental imagery during recuperation for athletics. For instance, Commission on Accreditation in Physical Therapy Education (CAPTE) excludes specialized clinical psychology courses from the list of requirements for the PT's professional education. Although the behavioral sciences constitute an essential didactic element of the practical training framework under CAPTE, there is no need for advanced training in mental exercises and visualization as direct therapies. Additionally, the Guide to Physical Therapist Practice excludes mental exercises or images from the list of possible main interventions PTs may provide to their clients. PTs have, however, shown that using mental imagery methods is a successful strategy for treating patients with neurologic impairments. Despite the research's focus on neurologic problems, the authors demonstrated the potential advantages of using mental images with a group of athletes that needed physical treatment support.

6. Conclusions

In this regard, psychological techniques have been demonstrated to help wounded athletes by encouraging and keeping a positive outlook, emphasizing the recovery of the damaged bodily part, and lowering tension and anxiety via positive self-talk and imagery. The aforementioned cognitive effects of imaging are associated with two crucial behavioral elements: increased adherence rates and accelerated healing from sports injuries. These behavioral effects remain troublesome for those who deal with wounded athletes; thus, further research is necessary to find effective rehabilitation strategies. Regarding the efficacy of psychological aids for rehabilitation, ATs and PTs appear to have modified their views. The encouraging attitudes shown by both ATs and PTs in our research have implications for enhancing the athlete's recovery process. We advise that professionals who oversee wounded athletes' rehabilitation programs and educators who train the next generation of ATs continue to learn the most recent techniques and equipment needed for a full recovery.

Ethical considerations

Not applicable.

Declaration of interest

The authors declare no conflicts of interest.

Funding

This research did not receive any financial support.

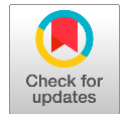
References

- Blumenstein B, Orbach I (2020) Periodization of psychological preparation within the training process. *International Journal of Sport and Exercise Psychology* 18:13-23.
- Borsboom D, van der Maas HL, Dalege J, Kievit RA, Haig BD (2021) Theory construction methodology: A practical framework for building theories in psychology. *Perspectives on Psychological Science* 16:756-766.
- Deyle GD, Allen CS, Allison SC, Gill NW, Hando BR, Petersen EJ, Dusenberry DI, Rhon DI (2020) Physical therapy versus glucocorticoid injection for osteoarthritis of the knee. *New England Journal of Medicine* 382:1420-1429.



- Dongoran MF, Fadlih AM, Riyanto P (2020) Psychological characteristics of martial sports Indonesian athletes based on categories of art and fight. *Enfermeria Clinica* 30:500-503.
- Einarsson EI, Kristjánsson H, Saavedra JM (2020) Relationship between elite athletes' psychological skills and their training in those skills. *Nordic Psychology* 72:23-32.
- Feddersen NB, Keis MAB, Elbe AM (2021) Coaches' perceived pitfalls in delivering psychological skills training to high-level youth athletes in fencing and football. *International Journal of Sports Science & Coaching* 16:249-261.
- Felten-Barentsz KM, van Oorsouw R, Klooster E, Koenders N, Driehuis F, Hulzebos EH, van der Schaaf M, Hooijboom TJ, van der Wees PJ (2020). Recommendations for hospital-based physical therapists managing patients with COVID-19. *Physical therapy* 100:1444-1457.
- Karpov VY, Zavalishina SY, Dorontsev AV, Skorosov KK, Ivanov DA (2019) Physiological Basis of Physical Rehabilitation of Athletes after Ankle Injuries. *Indian Journal of Public Health Research & Development* 10.
- Lim TH, Jang CY, O'Sullivan D, Oh H (2018) Applications of psychological skills training for Paralympic table tennis athletes. *Journal of Exercise Rehabilitation* 14:367.
- Mori T, Mataka K, Shimizu Y, Matsuba K, Miura K, Takahashi H, Koda M, Kamada H, Yamazaki M (2020) Dropped Head Syndrome Treated with Physical Therapy Based on the Concept of Athletic Rehabilitation. *Case Reports in Orthopedics* 2020.
- Pankow K, Fraser SN, Holt NL (2021) A retrospective analysis of the development of psychological skills and characteristics among National Hockey League players. *International Journal of Sport and Exercise Psychology* 19:988-1004.
- Shaari JS, Hooi LB, Siswantoyo S (2019) The effectiveness of psychological skills training program on netball shooting performance. *Cakrawala Pendidikan* 38:174-187.
- Trotter MG, Coulter TJ, Davis PA, Poulus DR, Polman R (2021) Social support, self-regulation, and psychological skill use in e-athletes. *Frontiers in psychology* 12:722030.
- van Doormaal MC, Meerhoff GA, Vliet Vlieland TP, Peter WF (2020) A clinical practice guideline for physical therapy in patients with hip or knee osteoarthritis. *Musculoskeletal Care* 18:575-595.
- Vesković A, Koropanovski N, Dopsaj M, Jovanović S (2019) Effects of a psychological skill training program on anxiety levels in top karate athletes. *Revista Brasileira de Medicina do Esporte* 25:418-422.

Effect of music therapy on diabetes distress among patients with diabetic foot ulcer in a selected tertiary care hospital, Mangalore, India - A pilot study



Anju Ullas^a  | Prabha Adhikari MR^b  | Vijayalakshmi Subramaniam^c 

^aYenepoya Nursing College, Mangalore, Karnataka, India, PhD Scholar, Department of Medical Surgical Nursing.

^bYenepoya Medical College Hospital, Mangalore, Karnataka, India, Professor, Department of Geriatric Medicine.

^cYenepoya Medical College Hospital, Mangalore, Karnataka, India, Professor, Department of Otorhinolaryngology.

Abstract Diabetic distress (DD), which is unnoticed in diabetes, may lead to depression. The study's objectives are to identify DD in patients with diabetic foot ulcer (DFU) and to use music therapy to help them cope with their stressful circumstances and improve their overall wellness' non-probability purposive sampling technique was used to assign 30 DFU patients, 15 each to the intervention group and the control group respectively. With the 17 items Diabetic Distress Scale (DDS), diabetes distress is assessed. Pretest is done on day one and post-test on day 21 for both the groups. During a period of 21 days, the intervention group received both routine treatment and music therapy for 20 minutes in the morning and the evening, while the control group received only routine treatment. The majority (53.3%) of the participants in control and intervention group was over 60 years old and was men. 93.3% participants of intervention and control group had moderate DD during pretest. Post test shows that the only 6.7% participants had moderate DD and 93.3% had no DD in the intervention group whereas the control group had no changes in distress level. The mean \pm SD of overall DD scores was reduced in the intervention group from pretest to post-test (3.7 ± 0.6 to 2.4 ± 0.2) and increased in the control group from 3.4 ± 0.5 to 3.8 ± 0.5 . The distress associated with diabetes appears to be significantly reduced by music therapy. As a result, music therapy might be recommended as a complementary therapy for people with diabetes foot ulcers in order to preserve good physical and mental health and to improve quality of life.

Keywords: music therapy, diabetes distress, diabetic foot ulcer

1. Introduction

The One of the most prevalent chronic diseases worldwide is diabetes mellitus (DM). Adults (20-79 years) with diabetes mellitus account for 537 million of the world's population. In 2030 and 2045, respectively, this figure is expected to increase to 643 million and 783 million (International Diabetes Federation 2023) Diabetic foot ulcer (DFU) is one of the most serious complications of DM (Oliver and Mutluoglu 2022). According to earlier estimates, people with diabetes mellitus have a 15 to 25% lifetime risk of developing foot ulcers, but when more information is taken into account, the risk rises to between 19% and 34% (Ahmad et al 2018).

Patients with Type 2 DM frequently experience diabetes distress (DD). The risk variables for DD were younger age at diabetes diagnosis, living in a rural area, using insulin and having any diabetic complications (Kamrul-Hasan et al 2023). DFU patients are more likely to experience anxiety, depression and diabetes distress (Ahmad et al 2018).

Patients with physical, mental, and emotional issues have found music therapy to be helpful. It improves the depression, anxiety, and stress levels of those who suffer from depression and lessens the severity of their condition. These discoveries have made it easier to comprehend the real-world uses of Indian music in the diverse psychological, emotional, and physical states of people (Singh 2021).

Diabetes distress in DFU patients may lead to slow healing process and poor quality of life. The aim of the study is to identify diabetes distress among patients with diabetic foot ulcer and to find the effect of music therapy on diabetes distress and can be used as a complementary therapy.

2. Materials and Methods

Using a quasi-experimental pretest posttest control group research design, a pilot study was carried out on DFU patients admitted in a tertiary care hospital to examine the effects of music therapy on diabetic distress. Using a non-probability purposive sampling technique, 30 participants were selected (Intervention group-15, Control group-15). Diabetes Distress Scale (DDS)-17 item, which has four subscales measuring emotional burden (EB), physician-related distress (PRD), regimen-related distress (RRD) and interpersonal distress (ID) was the instrument used to detect diabetes distress. The test-retest approach was used to determine the tool's dependability in our setting; the R-value was 0.88.

The participants were chosen based on a number of criteria, including their interest in listening to music, their admission with a foot ulcer ranging in severity from grade 2 to 4 according to Wagner's classification of DFU, and their ability to maintain stable insulin therapy for three days in a row (with an insulin dosage variation of no more than 12 units/day). Those who were severely ill and had profound hearing loss were not included in the study.

The pretest for DD was conducted in the control group and intervention group on Day 1, and in the intervention group, music therapy is administered in addition to usual treatment for 21 days, whereas control group received routine care. On day 21, both groups took a post-test in the evening.

2.1. Music therapy intervention

The participants in the intervention group were instructed to listen their favorite music with headphone while lying or sitting on the bed for duration of 20 minutes in the morning between 7am to 8am and evening 7pm to 8pm, for 21 days and the control group received typical routine care.

2.2. Statistical analysis

Descriptive and inferential statistics using SPSS Statistical software 22nd version

3. Results

3.1. Description of demographic and clinical characteristics of study participants

The demographic and clinical details of the study participants are provided in Tables 1 and 2. The majority (53.3%) of the participants in both groups was over 60 years old and was men, 80% and 73.3% respectively. Most of the participants in both the group have primary education. All the participants were married in both the groups, but in control group one was widow. 80% of control group and 86.7% of intervention groups belong to rural population. Majority of the participants in both groups were self-employed and had less than Rs. 25000/- as family monthly income. The majority of patients in both groups had diabetes for longer than six years and had a history of type 2 diabetes in their families. 73.3% of control group and 80% of intervention group had grade 3 of foot ulcer. Co morbidities were more in control group (53%) compared to intervention group (40%) and majority had hypertension in both the groups.

3.2. Distribution of frequency and percentage of study participants based on diabetes distress score

The frequency and percentage of participants' area wise and overall distress scores between the pretest and posttest in the control group and intervention group are shown in Figure 1. At the pretest, Emotional Burden (EB) was moderately experienced by 14 participants (93.3%) in the intervention group and 13 participants (86.7%) in the control group. After the posttest, it was reduced in the intervention group to 5 participants (33.3%) and increased in the control group to 14 participants (93.3%). 2 participants (13.3%) in the intervention group and no participants in the control group reported moderate Physician Related Distress (PRD) during pretest. Following the posttest, the intervention group had no participants with physician-related distress, while the control group had 2 (13.3%). In the intervention group 13 participants (86.7%) and 14 (93.3%) in the control group reported moderate Regimen Related Distress (RRD). After the posttest, in the intervention group no participants had regimen related distress, whereas the control group had no changes. In the intervention group, 10 participants (66.7%) and 09 participants (60%) in the control group reported moderate Interpersonal Distress (ID). After the posttest, the number of participants in the intervention group was decreased to 1 (6.7%), and the number of participants in the control group was increased to 10 (66.7%). In total, 14 participants (93.3%) in the intervention group and 14 (93.3%) in the control group reported moderate overall DD. After the posttest, the intervention group had just one participant (6.7%), whereas the control group had the same number of participants with overall DD.

3.3. Effectiveness of music therapy on diabetes distress in intervention group as compared to control group

The data in table 3 shows a statistically significant difference ($p < 0.05$) in EB, PRD, RRD and overall DD score within control group and intervention group. For ID, the difference ($p < 0.05$) was observed only within intervention group. The mean \pm SD of area wise and over all DD scores was reduced in the intervention group from pretest to posttest related to EB (4.5 ± 0.6 to 3.0 ± 0.5), PRD (2.1 ± 0.7 to 1.6 ± 0.4), RRD (4.2 ± 0.9 to 2.5 ± 0.3), ID (3.7 ± 1.1 to 2.4 ± 0.5) and overall DD (3.7 ± 0.6 to 2.4 ± 0.2). However, in the control group, there was an increase in scores from pretest to posttest related to EB (4.0 ± 0.7 to

4.4 ± 0.7), PRD (1.6 ± 0.4 to 2.2 ± 0.7), RRD (4.5 ± 0.8 to 4.7 ± 0.7), ID (3.0 ± 1.0 to 3.0 ± 1.0), and overall DD (3.4 ± 0.5 to 3.8 ± 0.5). This shows the effectiveness of music therapy.

The data in table 4 depicts the comparison of area wise and over all diabetes distress post test score between the groups showed a very highly found in statistically significant difference in ED, RRD and overall DD whereas, ID was highly significant and PRD was significant.

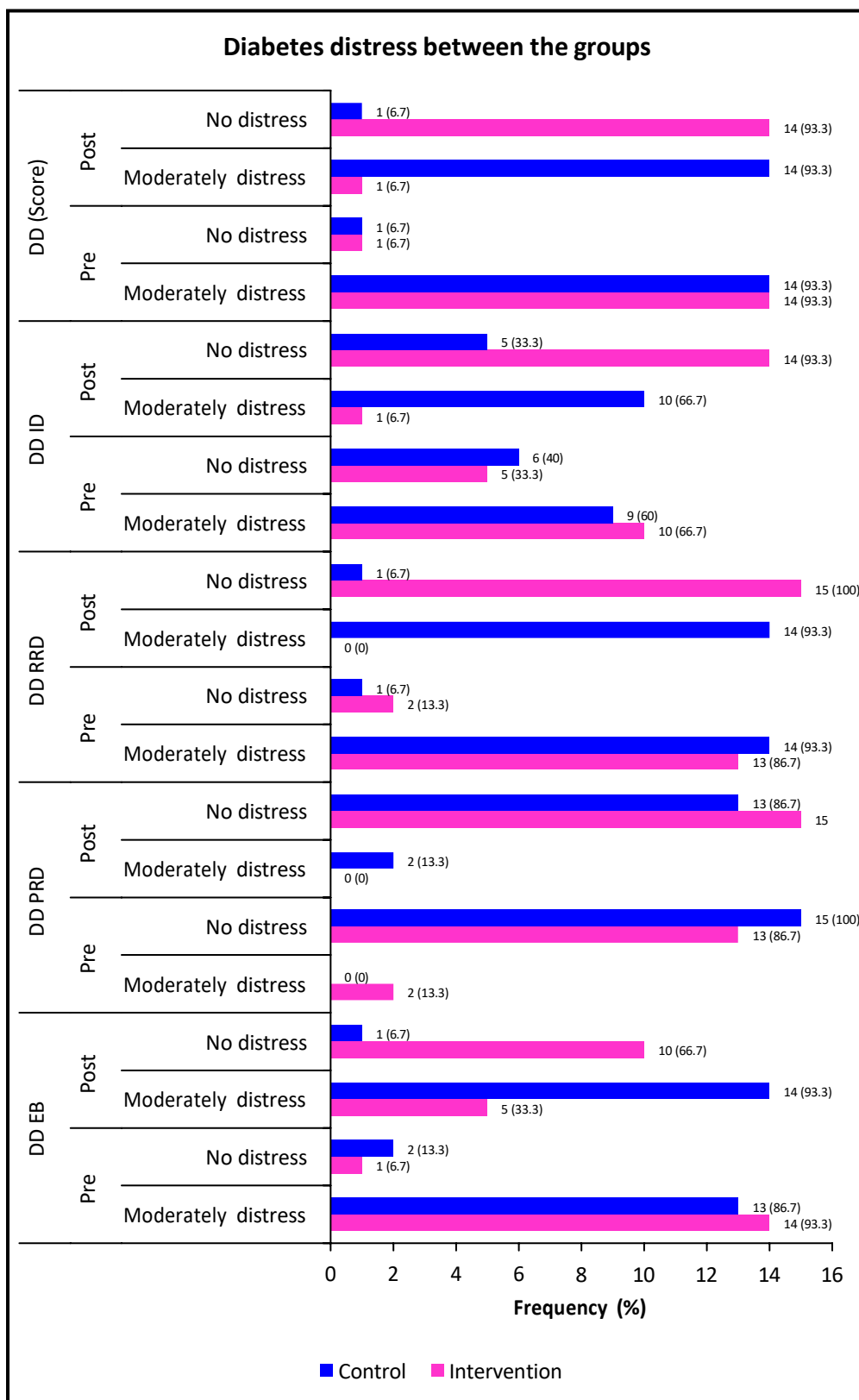


Figure 1 Bar graph on frequency diabetes distress pretest posttest score between the groups.

Table 1 Distribution of participants based on demographic characteristics.

Variables	Frequency (%) n=15+15		Likelihood ratio	p value	
	Control group	Intervention group			
Age in years	41 – 50	4 (26.7)	3 (20.0)	0.287	0.866
	51 -60	3 (20.0)	4 (26.7)		
	> 60	8 (53.3)	8 (53.3)		
Gender	Male	12(80.0)	11 (73.3)	0.187	0.666
	Female	3 (20.0)	4 (26.7)		
Educational status	No formal education	2 (13.3)	3 (20.0)	1.752	0.416
	Primary education	8 (53.3)	10 (66.7)		
	Secondary education	5 (33.3)	2 (13.3)		
Marital status	Married	14 (93.3)	15 (100)	1.421	0.233
	Widow	1 (6.7)	0 (0)		
Area of residence	Urban	3 (20.0)	2 (13.3)	0.241	0.623
	Rural	12 (80.0)	13 (86.7)		
Occupational status	Private employee	1 (6.7)	1 (6.7)	0.268	0.966
	Self employed	7 (46.7)	8 (53.3)		
	Agriculture	4 (26.7)	4 (26.7)		
	Home maker	3 (20.0)	2 (13.3)		
Family monthly income	≤ 25000	14 (93.3)	13 (86.7)	0.377	0.539
	25001 - 50000	1 (6.7)	2 (13.3)		

Table 2 Distribution of participants based on clinical characteristics.

Clinical characteristics	Frequency (%) n = 15+15		
		Control group	Intervention group
Years since diagnosed with diabetes	3 to 6	1 (6.7)	0 (0)
	More than 6	14 (93.3)	15 (100)
Family history of diabetes mellitus	Yes	14 (93.3)	14 (93.3)
	No	1 (6.7)	1 (6.7)
Grade of foot ulcer	2	3 (20.0)	2 (13.3)
	3	11 (73.3)	12 (80.0)
	4	1 (6.7)	1 (6.7)
Co morbidities	Yes	8 (53.3)	6 (40)
	No	7 (46.7)	9 (60)
Types of Co morbidities	Arthritis	1 (11.1)	2 (28.6)
	Hypertension	6 (66.7)	4 (57.1)
	Low Back Pain	2 (22.2)	1 (14.3)

Table 3 Comparison of area wise and over all diabetes distress score within the groups.

DDS		Pre test n= 15+15	Post test	"t"	p value
		Mean ± SD			
EB	Control group	4.0 ± 0.7	4.4 ± 0.7	-4.896	< 0.001***
	Intervention group	4.5 ±0.6	3.0 ± 0.5	8.542	< 0.001***
PRD	Control group	1.6 ±0.4	2.2 ± 0.7	-4.230	0.001**
	Intervention group	2.1 ±0.7	1.6 ± 0.4	3.325	0.005**
RRD	Control group	4.5 ±0.8	4.7 ± 0.7	-4.219	0.001**
	Intervention group	4.2 ±0.9	2.5 ± 0.7	8.290	< 0.001***
ID	Control group	3.0 ±1.0	3.0 ± 1.0	-2.110	0.053
	Intervention group	3.7 ±1.1	2.4 ± 0.5	5.410	< 0.001***
Overall Diabetes Distress	Control group	3.4 ±0.5	3.8 ± 0.5	-6.070	< 0.001***
	Intervention group	3.7 ±0.6	2.4 ± 0.2	8.753	< 0.001***

Paired "t" test. *Significant p<0.05 **highly significant<0.01, ***very highly significant p<0.001



Table 4 Area wise and over all diabetes distress post test score between the groups.

Diabetes Distress Score (Post test)	Control group n=15 +15 Mean ± SD	Intervention group	"t"	p value
EB	4.4 ± 0.7	3.0 ± 0.5	-6.515	< 0.001***
PRD	2.2 ± 0.7	1.6 ± 0.4	-2.681	0.012*
RRD	4.7 ± 0.7	2.5 ± 0.3	-11.007	< 0.001***
ID	3.4 ± 1.2	2.4 ± 0.5	-3.233	0.003**
Overall Diabetes Distress	3.8 ± 0.5	2.4 ± 0.2	-10.393	< 0.001***

Independent sample "t" test, *significant p<0.05 **highly significant<0.01, ***very highly significant p<0.001,

4. Discussion

The effectiveness of music therapy on diabetes foot ulcer patients admitted to the hospital was investigated in this study. Patients who have foot ulcers will experience diabetes-related distress and will find it difficult to get out of bed. Since majority of the patients are old age group, physical exercise is a challenge. Music therapy does not necessitate physical exertion. Patients can listen while sitting comfortably. The majority of people enjoys listening to music but is unaware of its therapeutic benefits.

The current study revealed that majority (53.3%) of the participants in both the group belongs to the age group above 60 years and were male. Similar findings are supported by 52.00% of participants are above the age of 65 years, and males were more affected than females, with 68.57% and 31.43%, respectively (Al-Rubeaan et al 2023).

According to the present study, 93% had moderate diabetes distress, while 7% experienced no distress. Emotional burden- and regimen-related was the most frequently reported diabetes distress. Another study confirms that 90.82% of subjects experienced diabetes distress. The most frequently reported severe distress was regimen-related, emotional burden-related and interpersonal-related (Hu et al 2020). 52.5% of the study subjects exhibited diabetes distress, according to a supportive study. A prevalence of 68.7, 28.6, 66, and 37.7%, respectively, was found for interpersonal distress, physician-related distress, regimen-related discomfort, and emotional burden (Kamrul-Hasan et al 2023).

In this study, the music therapy reduces overall and area wise diabetes distress in intervention group, while the diabetes distress increases in the control group. A comparable trial with self-management education programs is done among diabetes patients and the result revealed a decrease in diabetes distress (Ahmad et al 2018). The management of diabetic wounds has been proven to benefit greatly by the addition of music therapy. It helps to reduce the tension and worry related to treating and debriding wounds. When debridement and dressings were applied, there was a little drop in blood pressure and heart rate (Shijina et al 2019). In chemotherapy patients, music therapy significantly reduced patients' anxiety, blood pressure, and respiration rate (Imran 2017). Another study on the benefits of music therapy for cancer patients found that it maintains good effects on anxiety, pain, quality of life, heart rate, breathing rate, and blood pressure (Bradt et al 2016).

Every single person's life depends on music in some way. Human emotions, including melancholy, happiness, rage, stress, and depression, are unavoidably influenced by music. The sounds of animals and birds served as the inspiration for early Indian classical music. These notes are combined and permuted to produce the melodic "Raga." These Ragas elicit various mental emotions, which in turn have beneficial physiological impacts. Different Ragas are sung or played at specific times of the day during the full 24-hour period for their incredibly beneficial effects on the mind and body. Because of this, it is utilized in a therapy modality called "music therapy" to treat a variety of ailments (Gandhe and Tare 2020).

5. Conclusion

Patients with diabetic foot ulcers finds difficult with physical movements and required long term hospitalization which may leads to distress. Providing support and comfort to patients when they are ill can be with music therapy, a new and successful complementary therapy. This study concluded that the majority of the patients reported diabetes distress and following intervention, it was evident that the majority of patient's diabetes distress level is reduced, but in control group it remains same.

6. Recommendations

Recommendation for future research is,

1. Present study can be replicated with a large sample size'
2. Prevalence of diabetes distress among diabetes foot ulcer patients
3. Comparison of different interventions to prevent or reduce diabetes distress.

Ethical considerations



Not applicable.

Declaration of interest

The authors declare no conflicts of interest.

Funding

This research did not receive any financial support.

References

- Ahmad A, Abujbara M, Jaddou H, Younes NA, Ajlouni K (2018) Anxiety and Depression Among Adult Patients With Diabetic Foot: Prevalence and Associated Factors. *J Clin Med Res*. 10:411-8. DOI: 10.14740/jocmr3352w
- Al-Rubeaan K, Al Derwish M, Ouizi S, Youssef AM, Subhani SN, Ibrahim HM (2023) Diabetic foot complications and their risk factors from a large retrospective cohort study. *PLoS One*. 10:e0124446: DOI: 10.1371/journal.pone.0124446.
- Bradt J, Dileo C, Magill L, Teague A (2016) Music interventions for improving psychological and physical outcomes in cancerpatients. *Cochrane Database Syst Rev*. 8:CD006911. DOI: 10.1002/14651858.CD006911.pub3
- Gandhe V, Tare M (2020) Therapeutic effects of ancient Indian classical music. *IJAR* 10:41-3
- Hu Y, Li L, Zhang J (2020) Diabetes distress in young adults with type 2 diabetes: A cross-sectional survey in China. *J Diabetes Res [Internet]*. 2020; 2020:4814378. Available from: DOI: 10.1155/2020/4814378
- Imran S (2017) Effects of music therapy on anxiety, blood pressure and respiratory rate in patients undergoing chemotherapy. *Nurs Care Open Access J* 2. Available in: DOI: 10.15406/ncoaj.2017.02.00053.
- International Diabetes Federation (2023) *Diabetes Atlas, Facts and Figure*. 10th ed. International Diabetes Federation. Available in: <https://www.diabetesatlas.org>.
- Kamrul-Hasan ABM, Hannan MA, Asaduzzaman M, Rahman MM, Alam MS, Amin MN (2023) Prevalence and predictors of diabetes distress among adults with type 2 diabetes mellitus: a facility-based cross-sectional study of Bangladesh. *BMC Endocr Disord* 22:28. Available in: <https://bmcendocrdisord.biomedcentral.com/articles/10.1186/s12902-022-00938-3>
- Oliver TI, Mutluoglu M (2022) *Diabetic Foot Ulcer*. In: *Stat Pearls*. Treasure Island (FL): Stat Pearls Publishing. Available in: <https://www.ncbi.nlm.nih.gov/books/NBK537328/>
- Shijina K, Chittoria RK, Chavan V, Aggarwal A, Gupta S, Reddy C, Mohan PB, Pathan I (2019) Effect of music therapy as an adjunct in management of diabetic foot ulcer. *Diabetes Res*. 5:23–5. Available in: DOI: 10.17140/droj-5-142.
- Singh P (2021) Exploring current Music Therapy practices in India. *Voices*. 21. Available in: <https://voices.no/index.php/voices/article/view/3246/3319>

Clinical and radiological characteristics of Covid-19 patients with acute cerebrovascular vents: A meta-analysis



Sumit Raghav^a | Renuka Jyothi R.^b | Sayantan Mukhopadhyay^c

^aIIMT University, Meerut, Uttar Pradesh, India, Associate Professor, Department of Physiotherapy.

^bJAIN (Deemed-to-be University), Karnataka, India, Assistant Professor, Department of Life Sciences.

^cDev Bhoomi Uttarakhand University, Dehradun, Uttarakhand, India, Associate Professor, School of Pharmacy and Research.

Abstract The Information on the 2019 coronavirus illness (COVID-19) in Egypt's severe cerebrovascular consequences is scant. In cases of acute cerebrovascular disease (CVD), this study aimed to examine the radiological and clinical characteristics of patients with and without COVID-19. Prospective research evaluated CVD patients with and without COVID-19 who were hospitalized at Qena University Hospital (QUH) before the global epidemic. Patients diagnosed with COVID-19 and able to be treated at either assist or Aswan University Hospitals (AAUH) for cardiovascular disease were compared. The data included patient demographics, medical history, risk factors, clinical presentation, comorbidities, and imaging results from CT and MRI scans of the chest and brain. In overall 439 individuals with COVID-19, 55 (12.5%) experienced acute CVD. Of these, 13 patients (2.9%) experienced hemorrhagic CVD, whereas 42 (9.6%) suffered an ischemic stroke. 180 of the 250 non-COVID-19 individuals suffered from ischemic stroke, and 70 from hemorrhagic stroke. Many COVID-19 patients had large vascular occlusions (LVO), which is a significant portion of individuals who had ischemic stroke symptoms (40 vs. 7.2%, $P < 0.001$) and was considerably more reciprocal than in CVD patients who were not COVID-19. Comorbidities were noted in 44 instances (80% of the total). Sufferers of ischemic stroke who had COVID-19 were much more likely to have dangerous elements such as hypertension and Ischemic Heart Disease (IHD) as well as concomitant conditions like hepatitis and kidney disease. Additionally, 6.5% of individuals with LVO had a hemorrhagic transition, and 23.5% had hemorrhagic CVD. In our research, individuals with COVID-19 often had severe CVD. The most typical LVO was. The most frequent risk factors, such as hypertension, IHD, and anemia, may make the clinical presentation worse. Patients with CVD often had comorbid conditions, but many also had high liver enzymes and creatinine levels that were partly brought on by the COVID-19 disease itself. The new findings start to describe the range of CVD linked to COVID-19 in patients from Upper Egypt.

Keywords: systematic assessment, cannabinoids, evidence, chronic non-cancer pain

1. Introduction

Acute cerebrovascular events (ACVE), which are among the most significant due to their associated mortality and deterioration of living quality, are among the neurological manifestations that people who have coronavirus two infection and have severe acute respiratory syndrome (SARS-CoV-2) have displayed since the start of the pandemic. Cerebrovascular problems among COVID-19 patients were found to occur in a small number of observational and secondary investigations (1.1-9.8%). Uncertainty exists about the intensity of COVID-19's effects on the likelihood of presenting ACVE. The disclosure of this could clarify the part COVID-19 plays in the emergence of ACVE (Rothstein et al 2020). A higher incidence of thrombotic events, especially serious cerebrovascular events in young individuals, has been linked to COVID-19. However, during the pandemic, certain institutions saw a decrease in acute cardiovascular and cerebrovascular cases and low rates of such events among hospitalized COVID-19 patients. We aimed to provide an overview of the characteristics and immediate results of patients hospitalized with acute cerebrovascular illness during the COVID-19 pandemic (Dhamoon et al 2021).

The term ACVE refers to incidents like ischemic stroke, transient ischemic attack (TIA), and hemorrhagic stroke. These occurrences take place when blood flow to the brain is interrupted, with potentially harmful results. For proper clinical therapy and resource allocation, it is essential to comprehend the features of COVID-19 patients who suffer from CVD (Dakovic et al 2022).

When a blood artery in the brain bursts or leaks, it may result in hemorrhagic stroke, which causes bleeding within the brain or in the areas around it. The brain tissue may be harmed by this bleeding, which might also impair regular neurological



function. There are two basic forms of hemorrhagic stroke: subarachnoid hemorrhage and intracerebral hemorrhage, which both entail bleeding into the area of the brain and the thin layers that protect it (Toyoda et al 2022). It is essential to seek urgent medical assistance if a person exhibits any of these signs since early action may greatly enhance results. Medical imaging methods, such as computed tomography (CT) scans or magnetic resonance imaging (MRI), are often used in the diagnosis of acute cerebrovascular events in order to pinpoint the kind and site of the stroke (Cantone et al 2021). The chance of COVID-19 individuals developing ACVE seems to depend on a number of demographic and clinical parameters. These patients often exhibit advanced age and pre-existing comorbidities, including hypertension, diabetes, and cardiovascular disease. The progression of cerebrovascular complications and the overall severity of the disease may be affected by these risk factors (Mo et al 2019; Maida et al 2022). ACVE linked to COVID-19 often has thrombotic and ischemic characteristics. Ischemic strokes in these individuals have been documented often as the consequence of blood vessel obstructions. The thrombotic tendencies linked to COVID-19 are further accentuated by the existence of coagulation abnormalities and an increased frequency of major vessel occlusions (Burkert and Patil 2020). The purpose of the article is to provide information on the distinctive traits seen in COVID-19 individuals who have ACVE. Due to their potentially fatal effects, worldwide burden, influence on the quality of life, economic ramifications, and the possibility of preventive and public health treatments, ACVE is of great concern. Healthcare systems may lessen the devastation caused by these occurrences and enhance outcomes for those impacted by them by putting a priority on early detection, efficient management, and preventative actions.

Prior to the onset of symptoms, he had been healthy and employed full-time, save from a tiny left-sided ischemic stroke that had left him with very little residual impairment. He had left-sided paralysis and hemi neglect shortly after starting non-invasive ventilation (NIV) in the emergency department. The relevance of the prothrombotic side effects linked to COVID-19 infection is shown in this instance. It also begs the issue of whether pressure changes after the start of NIV may cause clot migration (Takagi et al 2020). (Larson et al 2020) cerebral vascular events (CVEs) are a typical side effect of trans catheter aortic valve replacement (TAVR). They conducted the research to identify the risk factors for subacute and peri-procedural CVEs after TAVR. Numerous hospitalizations, fatalities, and financial problems have been caused by the severe acute respiratory syndrome coronavirus two pandemics that swept the globe in 2019 and 2020. The possible cardiovascular and cerebrovascular symptoms of individuals regarding the 2019 coronavirus disease COVID-19 are poorly studied, despite the fact that respiratory involvement in these patients is widely established. According to earlier studies, having a serious infection increases the likelihood of cardiovascular and cerebrovascular illness (Sojka et al 2022).

(Wadowski et al 2022) intended to assess cerebral circulation as a result of the direct viral invasion and hypoxemia caused by COVID, paying particular attention to the proposed path mechanism, sensitive patient subgroups, clinical course, and outcomes. The damage and malfunction of the endothelium shown in COVID-positive individuals in histological investigations may be explained by such an affinity and the resultant dysregulation of the cerebral circulation that results in temporary or acute cerebrovascular accidents (Ramamoorthy et al 2023). Chronic hypo perfusion and cerebral small vessel disease are influenced by capillary density rarefaction and endothelial dysfunction. Spatiotemporal microvascular remodeling is controlling post-stroke brain rearrangement, according to earlier animal investigations. They proposed that sublingual imaging may be used to reflect systemically the microcirculatory alterations that occur during acute cerebrovascular episodes (Schwarz et al 2020). (Ramamoorthy et al 2023) pursued to identify national patterns in the various subtypes of perioperative MACCE, as well as disease types related to high rates of perioperative MACCE following major cancer procedures. Patients 40 years of age and older who had surgery on their prostate, bladder, esophagus, lung, liver, colon, or breast were hospitalized. This idea is especially appealing since it may be used to treat individuals who are suffering from different types of acute stroke and can be implemented in areas with limited resources. A prospective study is necessary to comprehend the causes of BPV in various clinical groups as well as the connection between BPV and subsequent brain injury (Hawkes et al 2022). Acute myocardial infarction (AMI) and ACVE were the subjects of anonymized data collected from three tertiary care facilities in a single significant metropolitan region. Averaging observations from many city measuring sites run by the responsible regional environmental protection agency and the Meteorological Center of Italian Military Aviation, weather, and pollution data were collected (Testa et al 2022).

2. Materials and Methods

The meta-analysis of the clinical and radiological characteristics of COVID-19 patients with ACVE is included in this part. Recognizing the impact of the virus on multiple organ systems, particularly the central nervous system has been made difficult because of the COVID-19 epidemic. The aim of the meta-analysis is to thoroughly examine the radiological and clinical characteristics seen in COVID-19 individuals who have ACVE.

2.1. Data collection

Two academic medical centers in Upper Egypt that operated as quarantine sites received patients with probable from June 1 to August 10, 2020, COVID-19. "The Intensive Care Units (ICUs) of the Assiut Neurology and Neurosurgery Hospitals

and Aswan University Hospital were subsequently utilized to treat all COVID-19 infected patients who had acute CVD at that point". In the present research, according to the World Health Organization (WHO), a stroke is a sudden onset of clinical symptoms that create a focused impairment in brain function that lasts more than 24 hours or causes death and has a vascular origin thought to be the only possible cause. Using either CT or MRI, we provided further information on the latter's demographics, risk factors, and complications. "The National Institutes of Health Stroke Scale (NIHSS), the chest CT, and the Glasgow Coma Scale (GCS)" were used for clinical evaluation. Renal, Blood gases, hepatic function, and coagulation profile were all examined in the laboratory. When available, the levels of ferritin and D-dimer were examined for a few patients.

2.2. Statistical Evaluation

The Statistical Program for the Social Sciences was used to examine the data. Data were represented as numbers and percentages or means standard deviation (SD). The 2 test was used to evaluate demographic, risk, comorbidity, and other characteristics among patients with COVID-19 CVD and those without it. The significance level was set at $P < 0.05$.

3. Results

Acute CVD was seen in 55 instances (12.5%) out of 439 individuals with confirmed or probable COVID-19. Data from neuroimaging was used to categorize the cases. In this instance, 11 (2.5%) patients had hemorrhagic strokes, 42 patients had ischemic strokes, one case had simultaneous intracerebral and subdural hematomas, and the last case (.2%) had a subarachnoid hemorrhage. Figure 1 displays the CVD flow chart.

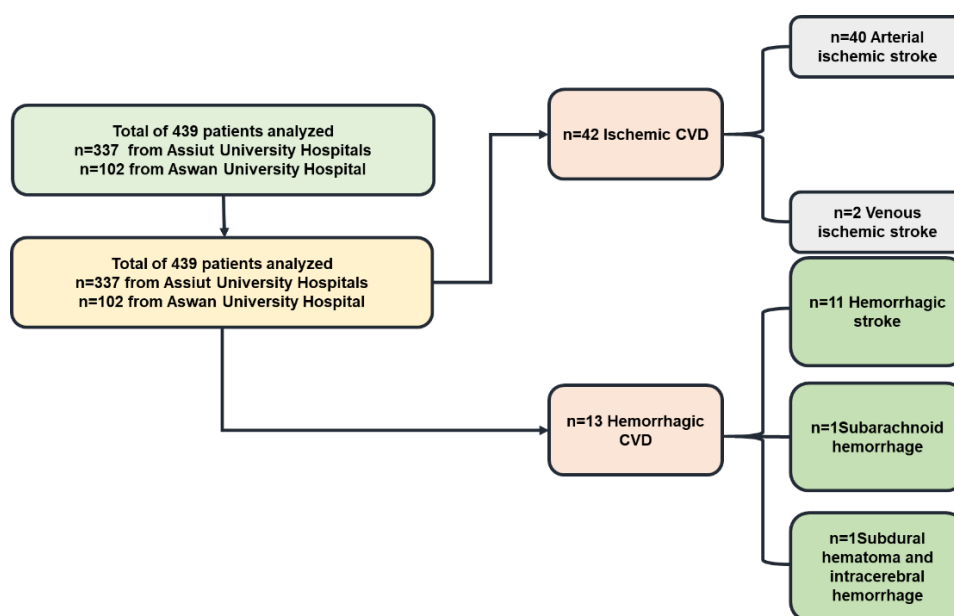


Figure 1 Flow chart for CVD.

The patients with COVID-19-CVD ranged in age from 35 to 90, including 30 men and 25 women. The other 43 cases were classified as believed COVID-19 as a result of their fever and respiratory symptoms as well as opacities with consolidation on both sides of the ground glass on a chest CT as well as lymphopenia or an increased ferritin or D-dimer levels. Twelve patients had PCR results that were considered to be COVID-19 positive.

3.1. Clinical Data

51 of the 55 people with COVID-19 showed bilateral ground-glass appearances with chest reorganization on the CT scan. Fever and respiratory symptoms were the most prevalent indications of COVID-19's constitutional symptoms in the CVD group, preceded by headache and gastrointestinal (GIT) issues. The least prevalent symptoms were malaise, fatigue, and vertigo. 44 individual risk factors were seen in the COVID-19 group for CVD or coexisting conditions. The comparison of demographic, clinical, risk element, and comorbidity information among CVD patients who have COVID-19 (55 instances) and those non-CVD revealed that the average age of CVD patients with COVID-19 was considerably older than that of people without a CVD. Headache, fever, and altered level of awareness were substantially more common compared to COVID-19 without CVD, although tiredness, malaise, myalgia, vertigo, and dizziness were substantially less common. Table 1 display the characteristics and clinical information of COVID patients and reveals that the comorbidities and risk factors were generally considerably greater compared to COVID-19 without CVD.



Table 1 Clinical and demographic information on COVID patients with and without cardiovascular disease.

Characteristics	People with CVD (n = 55)	People without CVD (n = 384)	P-value
Age (years)			
≤50 n (%)	13	184	<0.002
Range	35-90	18-86	
>50 n (%)	44	202	
Mean ± SD	63.9±15.2	50.6±17.9	<0.002
Sex n (%)			
Female	26	191	
Male	31	195	0.578
Presenting Symptoms n (%)			
GIT symptoms	13	82	0.903
Respiratory symptoms	46	284	0.196
Disturbed consciousness	28	18	<0.002
Dizziness and vertigo	3	62	0.016
Fatigue, myalgia, and malaise	6	171	<0.002
Headache	18	68	0.019
Fever	50	279	0.009
Comorbid risk factor and comorbidities n (%)			
Hypertension	33	141	0.003
Rheumatic heart disease	3	2	0.006
Ischemic heart disease	15	43	0.004
Diabetes mellitus	18	13	0.666
Atrial fibrillation	2	3	0.276
Renal disease	9	17	0.002
Liver disease	6	11	0.014
No risk factor or comorbidities	12	160	0.003
Chronic pulmonary disease	2	30	0.116

Table 2 contrasts individuals with COVID-19 ischemic stroke (42 patients) with those without (180 patients) according to demographics, clinical traits, risk factors, and consequences. While there was virtually no variation in terms of gender, Patients with COVID-19 were an average age substantially greater than that of patients without COVID-19. Patients with COVID-19 had significantly higher rates of hypertension and IHD than non-COVID-19 individuals, two conditions that raise the risk of stroke. Additionally, COVID-19 patients had much more comorbidities (such as renal and hepatic illness) than patients without COVID-19. With a greater proportion of people who arrive with a disordered state of awareness, Figure 2 displays a significant difference between the NIHSS and GCS scores of patients with COVID-19 ischemic stroke and those with other types of ischemic stroke.

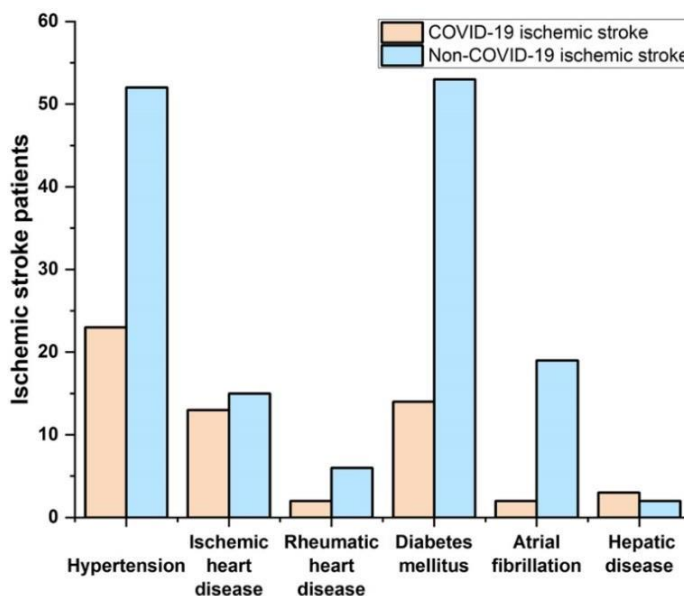


Figure 2 Comorbidities and stroke risk factors for ischemic stroke patients.

Table 2 Comparison of the demographics, with and without Covid-19 patients for ischemic stroke were compared for risk variables and comorbidities.

Characteristics, clinical manifestations, risk factors, and comorbidities	ischemic stroke with COVID-19 (n = 42)	ischemic stroke without COVID-19 (n = 180)	P-value*
Age (years)			
Age ≤ 50 n (%)	9	57	0.121
Age >50 n (%)	35	125	
Range	37–90	33–86	
Mean ± SD	64.9 ± 13.7	56.2 ± 1.5	<0.002
Sex n (%)			
Female	21	97	
Male	23	85	0.563
Stroke risk factors and comorbidities n (%)			
Hepatic disease	4	3	0.018
Rheumatic heart disease	3	7	0.655
Diabetes mellitus	15	54	0.622
Renal diseases	9	6	0.002
Hypertension	24	53	0.002
Heart fibrillation	3	20	0.248
An ischemic heart condition	14	16	0.002
No risk factor or comorbidities	11	36	0.527
Clinical presentation			
DCL n (%)	16	4	<0.002
GCS Mean ± SD (range)	9.6 ± 4.5 (0–15)	14.3 ± 1.9	<0.002
NIHSS Mean ± SD (range)	13.9 ± 5.6 (4–24)	9.3 ± 5.4	<0.002

Table 3 compares the hemorrhagic stroke rates for patients with COVID-19 and those without. Clinical presentations, risk factors, and comorbidities did not differ significantly across the groups. However, the COVID-19 group scored significantly higher on the NIHSS and lower on the GCS than the group without COVID-19, and they were more likely to be aware of something being wrong than those who did not have COVID-19. Figure 3 compares hemorrhagic stroke patients with individuals with COVID-19 and those without COVID-19.

Table 3 Comparison of the demographics, patients with and without Covid-19 who had hemorrhagic strokes had different associated conditions and risk factors.

Characteristics, concomitant conditions, and clinical presentation that increase the risk of stroke	The hemorrhagic CVD COVID-19 (n = 13)	Hemorrhagic CVD without COVID-19 (n = 70)	P-value*
Age			
Age ≤ 50 n (%)	6	39	0.295
Age >50 n (%)	9	33	
Range	35–80	19–99	
Mean ± SD	58.5 ± 14.6	51.4 ± 14.4	0.205
Sex n (%)			
Female	6	39	
Male	9	33	0.296
Stroke risk factors and comorbidities n (%)			
Hepatic disease	3	5	0.217
Rheumatic heart disease	3	7	0.655
Diabetes mellitus	4	24	0.486
Renal diseases	1	2	-
Hypertension	9	47	0.772
Atrial fibrillation	2	2	0.177
Ischemic heart disease	2	2	0.772
Chronic pulmonary disease	2	2	0.177
No risk factor or comorbidities	2	6	0.892
Clinical presentation			
DCL n (%)	7.2±4.3 10-23	10.7± 7.3	<0.002
GCS Mean ± SD (range)	9.6 ± 4.6 (6–160)	13.3 ± 2.7	<0.002
NIHSS Mean ± SD (range)	17.9 ± 4.3 (8–24)	11.7 ± 6.4	<0.002



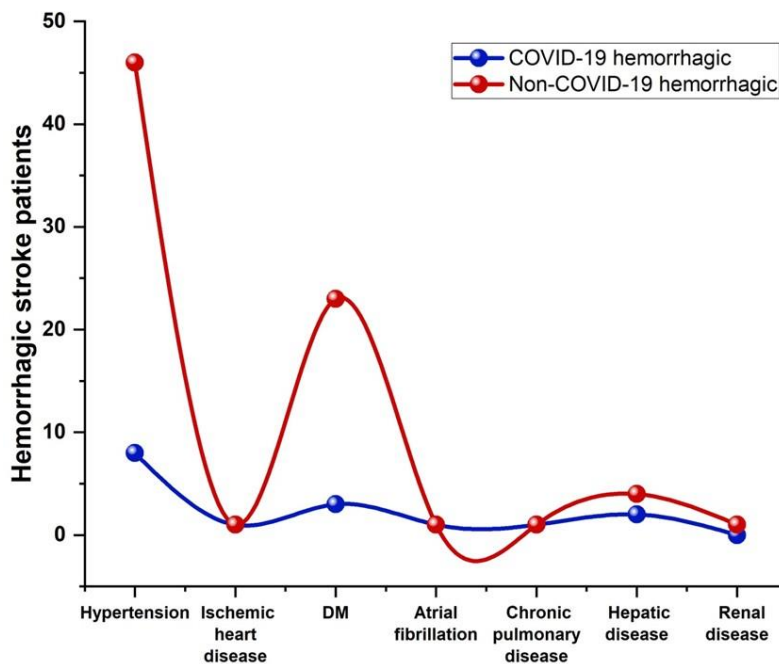


Figure 3 Comorbidities and stroke risk factors for hemorrhagic stroke patients.

3.2. Brain Imaging

According to radiological results, both the incidence of hemorrhagic and ischemic CVD were similarly low in COVID-19 patients compared to those who did not have the virus. The information is given in Table 4. But when compared to individuals who did not have COVID-19, COVID-19 patients had a considerably greater risk of major vascular blockage (40% vs. 7.2%, P 0.001). Additionally, COVID-19 patients (14.3%) had a considerably greater hemorrhagic disease risk transition than patients without COVID-19 (1.6%), with a P value of 0.001.

Table 4 Radiological results for 55 COVID-19 CVD patients.

Radiological results	CVD with COVID-19 (n = 55)	CVD without COVID-19 (n = 250)	P-value
I-*Venous/arterial ischemic stroke	43	181	0.511
1-Anterior circulation	32	126	0.394
Small vessel occlusion type B (MCA territory)	10	108	<0.002
A-Large artery occlusion	23	19	<0.002
2-Posterior circulation	10	48	0.674
B-Small vessels occlusion	8	46	0.348
A-large vessel occlusion	3	3	0.095
3-Mixed anterior and posterior circulation	1	7	-
4-Venous stroke:	3	3	0.095
II-Hemorrhagic CVD	14	71	0.511
1-Intra-parenchymal	7	50	0.130
Infra-tentorial	3	8	0.741
Lobar and deep	1	3	-
Lobar	3	13	0.998
Deep	5	31	0.092

42 COVID-Ischemic CVD affected 19 individuals in total, of whom 40 had the arterial disease, and two had CSVT. There were issues with the anterior circulation in 31 patients, and there were significant vascular occlusions in 22 cases. Out of the latter, 13 patients had blocked right middle cerebral arteries (MCAs), 8 patients had obstructed left internal carotid arteries, and 1 patient had blocked both. The hemorrhagic change occurred in six patients (10.9%). Four young people have significant vascular blockages. Small vessel occlusion occurred nine times. Two of the nine patients had LVO, and the posterior movement was impaired. Figure 4 denotes the 45-year-old man's non-contrast CT brain scan reveals a subacute infarct in the left middle cerebral artery (MCA) area, along with midline shift and significant edema that has a mass impact on the lateral ventricle.



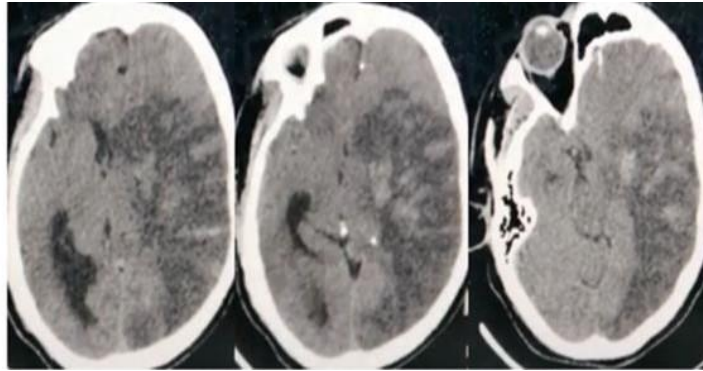


Figure 4 Sub-acute left middle cerebral artery (MCA) is shown on a 45-year-old man's brain non-contrast CT scan.

4. Discussion

The increased prevalence of CVD was the primary finding compared to earlier research. 55 patients (12.5%) among 439 COVID-19 participants had CVD. This is probably an exaggeration of the overall incidence. However, the fact that people with minor symptoms were advised to stay alone at home, with just those with symptoms ranging from mild to severe or those who had issues or comorbidities hospitalized. Although Cerebral Sinus Venous Thrombosis (CSVT) and hemorrhagic strokes were also reported, ischemic strokes accounted for the majority of instances. The majority of COVID-19 patients who have CVD are older, and being older is a persistent risk factor. Elderly people may already have comorbid conditions such as hypertension, diabetes, and cardiovascular disease, which makes them more vulnerable to cerebrovascular problems. These co-morbid conditions increase the prothrombotic state brought on by COVID-19 and add to the overall severity of the virus. The diagnosis of ACVE in COVID-19 patients depends heavily on imaging tests. One distinguishing feature of COVID-19 individuals with ACVE is the presence of neurological symptoms.

Typical symptoms include altered mental state, verbal difficulty, muscular weakness, sensory issues, and visual impairments. The interruption of blood flow to certain regions of the brain causes these symptoms, which result in neurological impairments. In certain circumstances, seizures and acute encephalopathy may also happen. On CT scans and MRIs, ischemic strokes are often characterized by massive vascular obstructions and multi-territorial infarction. Intraparenchymal hemorrhage, subarachnoid hemorrhage, and intraventricular hemorrhage are three types of hemorrhagic strokes that may occur. These imaging results aid in determining the best course of therapy.

5. Conclusion

To identify patients at increased risk and to improve the treatment of ACVE in COVID-19 patients, healthcare professionals must fully comprehend these features. These consequences are more susceptible as people become older and have comorbid conditions, including hypertension and cardiovascular disease. The presence of neurological symptoms such as altered mental state, speech impediments, and motor weakness is a critical warning sign that should prompt treatment. In the study we performed, LVO was the most frequent kind of stroke, and COVID-19-associated CVD was widespread. The most frequent risk variables were hypertension, IHD, and anemia, all of which had the potential to aggravate clinical presentation. Patients with CVD often have comorbid conditions, although, in many instances, high liver enzymes and creatinine levels may also be a result of COVID-19 infection.

Ethical considerations

Not applicable

Conflict of Interest

The authors declare no conflicts of interest.

Funding

This research did not receive any financial support.

Reference

- Burkert J, Patil S (2020) Acute cerebrovascular event in a COVID-19 positive patient immediately after commencing non-invasive ventilation. *BMJ Case Reports CP*, 13(9), p.e237737. DOI: 10.1136/bcr-2020-237737
- Cantone M, Lanza G, Puglisi V, Vinciguerra L, Mandelli J, Fiscaro F, Pennisi M, Bella R, Ciurleo R, Bramanti A (2021) Hypertensive crisis in acute cerebrovascular diseases presenting at the emergency department: a narrative review. *Brain Sciences* 11:70. DOI: 10.3390/brainsci11010070
- Dakovic I, Göttler J, Mpotsaris A (2022) Acute cerebrovascular events-fundamentals. *Radiologie (Heidelberg, Germany)*. DOI:10.1007/s00117-022-01084-6

- Dhamoon MS, Thaler A, Gururangan K, Kohli A, Sisniega D, Wheelwright D, Mensching C, Fifi JT, Fara MG, Jette N, Cohen E (2021) Acute cerebrovascular events with COVID-19 infection. *Stroke* 52:48-56. DOI: 10.1161/STROKEAHA.120.031668
- Hawkes MA, Anderson CS, Rabinstein AA (2022) Blood pressure variability after cerebrovascular events: a possible new therapeutic target: a narrative review. *Neurology* 99:150-160. DOI: 10.1212/WNL.0000000000200856
- Larson AS, Savastano L, Kadirvel R, Kallmes DF, Hassan AE, Brinjikji W (2020) Coronavirus disease 2019 and the cerebrovascular-cardiovascular systems: what Do We Know So Far?. *Journal of the American Heart Association* 9:e016793. DOI:10.1161/JAHA.120.016793
- Maida CD, Daidone M, Pacinella G, Norrito RL, Pinto A, Tuttolomondo A (2022) Diabetes and ischemic stroke: An old and new relationship an overview of the close interaction between these diseases. *International Journal of Molecular Sciences* 23:2397. DOI: 10.3390/ijms23042397
- Mo J, Huang L, Peng J, Ocak U, Zhang J, Zhang JH (2019) Autonomic disturbances in acute cerebrovascular disease. *Neuroscience Bulletin* 35:133-144. DOI: 10.1155/2022/3363672
- Ramamoorthy V, Chan K, Appunni S, Zhang Z, Ahmed MA, McGranaghan P, Saxena A, Rubens M (2023) Prevalence and trends of perioperative major adverse cardiovascular and cerebrovascular events during cancer surgeries. *Scientific Reports*, 13(1), p.2410. DOI: 10.1038/s41598-023-29632-7
- Rothstein A, Oldridge O, Schwennesen H, Do D, Cucchiara BL (2020) Acute cerebrovascular events in hospitalized COVID-19 patients. *Stroke* 51:e219-e222. DOI: 10.1161/STROKEAHA.120.030995
- Schwarz V, Mahfoud F, Lauder L, Reith W, Behnke S, Smola S, Rissland J, Pfuhl T, Scheller B, Böhm M, Ewen S (2020) Decline of emergency admissions for cardiovascular and cerebrovascular events after the outbreak of COVID-19. *Clinical Research in Cardiology* 109:1500-1506. DOI: 10.1007/s00392-020-01688-9
- Sojka M, Drelich-Zbroja A, Kuczyńska M, Cheda M, Dąbrowska I, Kopyto E, Halczuk I, Zbroja M, Cyranka W, Jargiełło T (2022) Ischemic and Hemorrhagic Cerebrovascular Events Related to COVID-19 Coagulopathy and Hypoxemia. *International Journal of Environmental Research and Public Health*, 19:11823. DOI: 10.3390/ijerph191811823
- Takagi K, Naganuma T, Tada N, Yamanaka F, Araki M, Shira S, Higashimori A, Watanabe Y, Yamamoto M, Hayashida K (2020) The predictors of peri-procedural and sub-acute cerebrovascular events following TAVR from OCEAN-TAVI registry. *Cardiovascular Revascularization Medicine* 21:732-738. DOI: 10.1016/j.carrev.2019.10.013
- Testa A, Biondi-Zoccai G, Anticoli S, Pezzella FR, Mangiardi M, Marchegiani G, Frati G, Sciarretta S, Perrotta A, Peruzzi M, Cavarretta E (2022) Cluster analysis of weather and pollution features and its role in predicting acute cardiac or cerebrovascular events. *Minerva Medica*. DOI: 10.23736/s0026-4806.22.08036-3
- Toyoda K, Yoshimura S, Nakai M, Koga M, Sasahara Y, Sonoda K, Kamiyama K, Yazawa Y, Kawada S, Sasaki M, Terasaki T (2022) Twenty-year change in severity and outcome of ischemic and hemorrhagic strokes. *JAMA neurology* 79:61-69. DOI: 10.1001/jamaneurol.2021.4346
- Wadowski PP, Schörghofer C, Rieder T, Ertl S, Pultar J, Serles W, Sycha T, Mayer F, Koppensteiner R, Gremmel T, Jilma B (2022) Microvascular rarefaction in patients with cerebrovascular events. *Microvascular Research* 140:104300. DOI:10.1016/j.mvr.2021.104300

Investigation on laparoscopic sleeve gastrectomy for the management of type II diabetes mellitus



Yogesh Tiwari^a | Samaniya Baig^b | H. Malathi^c

^aDev Bhoomi Uttarakhand University, Dehradun, Uttarakhand, India, Assistant Professor, School of Pharmacy and Research.

^bIIMT University, Meerut, Uttar Pradesh, India, Assistant Professor, Department of Medical Laboratory Technology.

^cJAIN (Deemed-to-be University), Karnataka, India, Assistant Professor, Department of Life Sciences.

Abstract In order to treat obesity and other disorders associated with it, laparoscopic sleeve gastrectomy (LSG) is increasingly being applied. This study examines a grading system's effectiveness in categorizing and forecasting TII-DM remission and the results of LSG aftereffects of TII-DM remission. The study included 160 TII-DM patients (80 men and 80 women) with a Body Mass Index (BMI) that is morbidly obese who had LSG between 2020 and 2023. The patient's BMI, Level of C-peptide, age, and TII-DM duration (years) comprise the ABCD score. Using this score, the absence of TII-DM following LSG was assessed. Ninety treated patients had complete follow-up information at 12 months following surgery. Both the mean HbA_{1c} and weight loss were lowered. Significantly more patients saw progress in their blood sugar control, including nine patients who improved, 18 who experienced partial remission, and 50 who underwent complete remission. The ABCD score was greater in those with TII-DM resolution following surgery than in those without. The success rate for TII-DM remission was better for patients with higher ABCD scores (100% at score 5, which increased from 0% at point 0). LSG is a safe and efficient technique for remission of TII-DM and weight loss. The ABCD score, a straightforward multifaceted grading system, can forecast how well TII-DM will respond to LSG therapy. Surgery ObesRelat Dis: American Society for Diabetic and Weight Loss Reserved rights.

Keywords: chronic metabolic, LSG, TII-DM, remission rate

1. Introduction

Insulin Resistance (IR) indicates TII-DM, a chronic metabolic condition, and elevated blood sugar levels. It greatly influences people's quality of life and general healthcare systems, making it a serious global health concern. Traditional methods for treating T2-DM include dietary changes, oral medicines, insulin injections, and bariatric surgery (Rao et al 2019). In the past few decades, weight-loss surgery has gained acceptance as a possible therapy for T2-DM patients who are obese. One of the various ways to lose weight is laparoscopic sleeve gastrectomy (LSG) (Fernández-Ananín et al 2022) has drawn a lot of interest as a potential alternative treatment method for people with T2-DM who want to lose weight and regulate their blood sugar levels (Wada et al 2020). LSG removes a significant stomach section, leaving a little gastric pouch as a sleeve. By reducing stomach capacity, this treatment causes early satiety and weight loss. LSG has been proven to have amazing effects on enhancing glycemic control and even inducing remission of T2-DM, so its advantages go beyond weight loss (Codina et al 2022). The underlying processes for LSG's metabolic actions are complex. A smaller stomach causes changes in gut hormone release, including a rise in the GLP-1 (glucagon-like peptide-1) and PYY (peptide YY), encouraging satiety and improving insulin secretion. Additionally, LSG has been demonstrated to improve insulin sensitivity, lower hepatic glucose production, and change the composition of the gut flora, all of which aid in better glycemic management (Shehata et al 2021). The effectiveness of LSG in treating T2-DM has been proven in numerous clinical investigations. According to these trials, many patients who underwent LSG experienced significant drops in HbA_{1c} levels, a decline in the requirement for diabetes medication, and even diabetes remission. Additionally, people with T2-DM who are not obese and have varied degrees of obesity have both experienced the advantages of LSG on glycemic control (Lukaszewicz et al 2022). According to the study, people with maximum Levels of C-peptides had a higher RR for TII-DM, which was revealed to be 50%. Nevertheless, data collected over time and a therapeutically practical forecasting method still need to be included. The article summarizes the findings of a prospective examination of the overtime impact of LSG on TII-DM patients to address these difficulties. It assesses the potential use of a specific diabetic surgery. This article is structured as follows for the remainder of it. While Part 3 focuses on the suggested methods, Part 2 introduces the linked work of this study. The experiments are laid out in Part 4, along with a focus on the LSG's performance assessment, and the process is eventually brought to a close in Part 5. This section discusses the pertinent work and the key techniques the previous researcher employed to manage Type II diabetes mellitus by laparoscopic sleeve gastrectomy. The study Murshid et al (2021) aimed to evaluate the effectiveness of LSG in



slimming down and assess how it affects T2-DM management. Results indicate a substantial difference between BMI and HbA_{1c} before surgery and between less than one month and one year later. The level of weight increase was low. Their study had limitations: sample size and data were only gathered from one location. The long-term results of LSG regarding the remission and recurrence of T2-D are presented in the study Lee et al (2020). The ABCD rating system assessed the T2-D remission in stratified groups. LSG is a successful T2D treatment method, although many patients have experienced a long-term T2D recurrence. The Authors of the study Saber et al (2022) evaluate the effect of SG on T2-D patients who are obese and have trouble controlling their blood sugar levels. After a sleeve gastrectomy (Kheirvari et al 2020) type II diabetic obese people can exhibit remission of diabetes without medication or at least significantly improved glycemic control. In article Wang et al (2019) was to determine how LSG affects TII-DM in patients with a BMI under 30 kg/m². Using SPSS 22.0, all of the clinical data were examined. LSG immediately impacts patients with T2DM whose BMI is less than 30 kg/m², but further research is required to determine its long-term efficacy. An article Guetta et al (2019) determines the LSG's safety in Type II diabetes mellitus. A complication was defined as any departure from the typical postoperative course. Data indicate that LSG is generally safe for TII -DM patients. A prospective study is required to determine whether lowering the hemoglobin A_{1c} level before surgery will reduce the likelihood of problems. The study Mizera et al (2021) aimed to pinpoint the variables influencing T2-DM resolution for a brief period in LSG patients. They conducted a multicenter trial to evaluate LSG's effects on T2-DM recuperation. The study design of this article resulted in some retrospective data analysis, which is a restriction. The aim of the study Chowbey et al (2021) served to retrospectively analyze diabetic morbidly obese individuals who underwent RYGB and assess the preoperative accuracy of the Dia Rem grade for estimating Type 2 diabetes resolution at one year of follow-up. Dia Rem score is a straightforward measure based on fundamental clinical indicators that could help identify T2DM patients who would benefit most from remission following bariatric surgery. The goal of article Attia R (2019) was to ascertain the effectiveness of weight-reducing procedures on DM control, particularly LSG, and to investigate the relationship between a high preoperative HbA_{1c} level, preoperative morbidity, and postoperative results following LSG. It is regarded as the Type II diabetes therapy option for obese patients that is the most effective over the long run. Study Zayed et al (2020) examine how LSG affects obese T2DM patients, its impact on diabetes remission, and the function of gastrointestinal GLP-1 and PYY hormones. In younger individuals with lower periods of diabetes, greater pre-conception post-MMT peptides tyrosine, smaller amounts of preoperative serum LDL-Ch, and lower levels of thyroid stimulating hormone, LSG may result in partial remission of the disease. The objective of the study Khaivari et al (2020) was to analyze and assess the recent data on the benefits and drawbacks of sleeve gastrectomy (SG). The research reviewed indicates that SG is a safe and effective procedure with no mortality, comorbidities resolved, and fewer complications.

2. Materials and Methods

These are the methods to manage type II diabetes mellitus used in laparoscopic gastrectomy.

Recruitment involved 160 individuals who received LSG for inadequately treated TII-DM. The hospital's human-research review board approved the study, and each individual signed a written informed permission form. Patients with TII-DM were considered eligible for the trial if they had an acceptable surgical risk, an appropriate BMI, and poorly managed TII-DM after six months of medication therapy. Patients ranged in age from eighteen to sixty-seven. End-organ damage, pregnancy, and prior weight loss surgery were the exclusion criteria. If a participant's C-peptide was less than nine percent, they were disqualified.

2.1. Surgical Technique

Laparoscopic surgery was used for every procedure. The following is the procedure for

Surgical techniques:

- Incisions: On the abdomen, three skin incisions were performed. The third incision was made on the left lateral abdominal wall, while the other two were done along the umbilicus (belly button) fold.
- Liver retractor: To access the angle of His, a subxiphoid puncture (an incision slightly below the sternum) was made. The liver retractor, a surgical tool used to retain and move the liver, was then inserted. The point where the esophagus and stomach converge is known as the angle of His.
- Devascularization: The minimum gastric arteries (arteries supplying blood to the stomach) and larger omentum (a fatty tissue connected to the stomach and covering the intestines) were de vascularized. This required ligating or searing them to cut off their blood supply. From 4 cm away from the pylorus (the stomach's opening) to the angle of His, the vessels were DE vascularized.
- Fat pad dissection: At the angle of His, there are big fat pads called Belsey. This was done to clear the surgical field so the stomach fundus could be removed.
- Vertical transection: A linear stapler was used to cut the stomach vertically. A surgical stapler with a length of 60 mm was employed. To check that the stapled segment was the proper size, a calibrator with an or gastric tube with a height of 36 Fr (French) was inserted through the mouth into the stomach.

- After gastric resection: The lengthy gastric remnant (remaining portion of the stomach) was stapled and then sutured shut with a 3-0 Vicryl suture. To stop bleeding and leakage, this was done. To prevent gastric volvulus (twisting of the stomach), the gastric tube was made from the remaining portion of the stomach and fixed to the posterior peritoneal tissue.
- Drainage and intraoperative leak test: An intraoperative leak test was not carried out, which looks for leaks at the surgical site. A drainage tube was not installed in the surgical site, as evidenced by the fact that using a drain was not routine.
- Abdominal resection: The abdominal resection was removed through the umbilical incision following dilation. According to this, the incision had to be made larger to empty the stomach. This instance did not include an endo bag, a specialized bag used to hold and remove organs or tissues.
- Closure: Vicryl suture, absorbable suture material or gauze, was used to seal the fascial defect, the opening in the fascia (the connective tissue layer under the skin). This procedure guarantees the healing and closure of the surgical incisions.

2.2. ABCD Score

The four independent indicators of TII-DM remission (BMI, Level of C-peptide, age, and length of diabetes) comprised the scoring system. According to analysis, C-peptide, BMI, age, and duration of diabetes were each assigned a four-point score, with the minimum value beings 0 and the maximum value beings 3. Only one point was awarded for age. After more analysis, the threshold value for each issue was slightly changed from its initial value.

Table 1 defines the adjusted score cut-off values. The BMI cut-off point was decreased from 30 to 29 kg/m2. C-peptide was increased to 4 ng/mL, and the Type II Diabetes Mellitus, threshold value length, was reduced to 1 year. The score of ABCD ranged from 0 to 5 points when the Scores for every factor were summed together.

Table 1 Results of ABCD Score.

The score of ABCD ranged from	C-peptide (mmol/L)	BMI (kg/m ²)	Duration of DM (yr)	Age range
0		<42		≥42
1	35-41.1	29-34.9	≥44	<29
2	3-5.1	2-2.9	≤6	<4
3	1-4.1	4-8	<1	>9

2.3. Study protocols

After enrolling in the cohort, the multidisciplinary team evaluated the TII-DM patients before surgery. They were then seen every three to six months for at least a year, then annually. If someone did not attend the appointment, their relatives were contacted to request medical records. A glyated hemoglobin value without utilizing the oral hypoglycemic or glucose was considered complete remission of TII-DM, whereas an HbA_{1c} value of 6.5% was supposed to be partial remission. Patients were deemed to have improved if their HbA_{1c} was less than 7% following surgery. The ABCD score was used to assess the RR.

2.4. Statistical Analysis

SPSS version 12.01 was used for all statistical analyses, and baseline comparisons were undertaken using two tests and two sample t-tests. The mean (SD) for continuous variables was used. The t-test for independent samples was used to determine the differences in relevant parameters between remission and non-remission. The RR was assessed using a distinct ABCD index score to gauge how well the score of ABCD can predict success. Statistical significance was defined as a 2-sided P value of 0.05.

3. Result and Discussions of Findings

Laparoscopic surgery enabled the effective completion of all procedures. Three patients experienced major complications, although none of them passed away. Eighty-five patients had a one-year follow-up with full data out of all the patients. One year after LSG, both the weight and BMI had significantly lowered. The 50 individuals experienced complete TII DM remission; another 20 saw partial remission, and 10 showed improvement. After LSG, there were notable changes in the blood lipid profile, IR, and BP in Table 2 (a) and 2(b). Tables 3(a) and 3(b) compare clinical metrics between people with full remissions of TII-DM and those without. Patients in total recovery had substantially older age, greater BMI, higher waist, greater C-peptide, a smaller time frame of TII-DM, greater hepatic enzyme, bigger IR, better WBC count, and faster weight loss. After surgery, those with complete TII-DM cured had higher ABCD scores than those without. Table 3 indicates 90 clients' profiles depended on the degree to which their diabetes completely disappeared after surgery. The ABCD score is shown in Table 5 as a bariatric surgery remission predictor. For comparison, Table 5 was updated to include the gastric bypass RR. The success rate for TII-DM remission was better for patients with higher ABCD scores (from 0% at score 0 to 100% at Score 5). Individuals getting LSG with an ABCD score of less than 4 had no full TII-DM remissions. Nearly all of the patients with ABCD scores of 4-5 experienced remissions. Patients who underwent gastric bypass had a higher rate of total



remission. The gastric bypass group's RR was likewise greater at each different score. This investigation shows that LSG is a safe and efficient slimming-down technique. In this study, the main LSG caused weight reduction that averaged one year and remained maintained for a maximum of five years.

Table 2 (a) Computation of medical data (Before LSG).

Factor	Before (n = 90) RYG	
	Mean (SD)	P
BMI (kg/m ²)	40.3 (8.6)	<.001*
C-peptide (ng/mL)	6.8 (3.4)	<.001*
WL (%)		
Systolic Blood Pressure (mm Hg)	138.9 (16.3)	<.001*
Diastolic Blood Pressure (mm Hg)	88.7 (12.6)	<.001*
Low-density lipoprotein cholesterol (mg/dL)	127.8 (34.9)	.396
TC (mg/dL)	200.2 (45.5)	<.001*
Triglyceride (mg/dL)	214.9 (116.3)	<.001*
HbA _{1c} %	8.3 (1.3)	<.001*
Iron, ug/dL	89.4 (47.6)	.499
Homeostasis Model Assessment	8.8 (10.2)	<.001*
Alanine Aminotransferase, U/L	57.6 (42.3)	<.001*
Hemoglobin, g/dL	14.7 (1.9)	.004*
Glucose (mg/dL)	154.8 (76.4)	<.001*
Calcium, mg/dL	9.3 (.8)	.374
Serum albumin, g/dL	4.6 (.5)	.005*
Waist (cm)	117.6 (16.8)	<.001*

Table 2 (b) Computation of medical data (after LSG).

Factor	After (n = 90)	
	Mean (SD)	P
BMI (kg/m ²)	28.7 (5.6)	<.001*
C-peptide (ng/ mL)	2.4 (1.4)	<.001*
WL (%)	26.8%	
Systolic Blood Pressure (mm Hg)	122.8 (18.1)	<.001*
Diastolic Blood Pressure (mm Hg)	77.7 (13.2)	<.001*
Low-density lipoprotein cholesterol (mg /dL)	127.7 (34.8)	.396
TC (mg/dL)	102.6 (36)	<.001*
Triglyceride (mg/dL)	103.3 (39.4)	<.001*
HbA _{1c} %	6.3 (1.3)	<.001*
Iron, ug/dL	86.9 (40.4)	.499
Homeostasis Model Assessment	1.7 (1.5)	<.001*
Alanine Aminotransferase, U/L	19.6 (2.4)	<.001*
Hemoglobin, g/dL	13.8 (2.4)	.004*
Glucose (mg/dL)	102.4 (34)	<.001*
Calcium, mg/dL	9.3 (.6)	.374
SA, g/dL	4.5 (.7)	.005*
Waist (cm)	90.6 (11.2)	<.001*

The post-LSG nutritional shift is similarly healthy. This outcome is consistent with recent papers detailing the long-term consequences of weight decrease. TII-DM remission following LSG, however, differed. Although it is less than eighty percent of the RR after gastric bypass, the complete TII-DM resolution percentage at one year following LSG is consistent with some earlier data. This study discovered that patients could be chosen using the ABCD score when contemplating LSG as a surgical treatment for those with TII-DM. We created the score of ABCD or Diabetes surgery. They validated its usage by demonstrating that it accurately indicates the success following surgery to remove the stomach for TII-DM treatment. The ABCD score is helpful as it involves a category that measures the level of weight gain (BMI) that measures the ability to secrete glucose (C-peptide), reflects the extent of the progress and decline of digestive WBC operation (duration), that is a broader capacity for age. Each variable in Tables 3(a) and 3(b), and Table 4 demonstrated good predictive power for TII-DM remission. Combined, the ABCD value can be an incredibly helpful weapon for patient selection. Patients with an ABCD greater than 4 are the only ones for whom the writers suggest the LSG for TII-DM.



Table 3 (a) The remission of after LSG.

Factors	Remission (n=50)	
	Mean (SD)	P
Age	38.7 (9.2)	.001*
Female, n (%)	22 (41.9)	.187
BMI (kg/m ²)	41.2 (7.8)	<.001*
Waist (cm)	122.8 (15.8)	<.001*
C-peptide (ng/mL)	7.8 (3.5)	<.001*
Duration of T2 DM (yr)	2.8 (3.7)	<.001*
Homeostasis Model Assessment–Insulin Resistance	12.8 (14.5)	.028*
SBP (mm Hg)	142.4 (16.4)	.025*
DBP (mm Hg)	89.6 (13.9)	.062
Glucose (mg/dL)	160.6 (92.3)	.312
TC (mg/dL)	206.9 (51.3)	.143
Triglyceride (mg/dL)	226.3 (124.3)	.262
Uric acid (mg/dL)	7.7 (1.9)	.020*
Aspartate Aminotransferase (IU/L)	42.3 (24.3)	.004*
ALT (IU/L)	69.4 (49.9)	.001*
Albumin (gm/dL)	4.5 (.6)	.132
Hb (gm/dL)	14.8 (1.6)	.064
Insulin (uIU/mL)	28.7 (24.9)	.004*
High-Density Lipoprotein Cholesterol (mg/dL)	43.9 (8.9)	.224
HbA _{1c} %	7.9 (1.4)	.009*
LDL (mg/dL)	133.6 (33.8)	.208
High-Sensitive C-Reactive Protein	1.6 (.34)	.005*
White Blood Cell (/μL)	8.8 (2.5)	.006*
ABCD score	7.3 (1.9)	<.001*
WL, %	31.8 (7.4)	<.001*

Table 3 (b) the Non-remission of after LSG.

Factor	Non-remission (n= 40)	
	Mean (SD)	P
Age	45.4 (10.1)	.001*
Female, n (%)	23 (56.9)	.187
BMI (kg/m ²)	34.8 (5.6)	<.001*
Waist (cm)	106.9 (14.7)	<.001*
C-peptide (ng/mL)	3.9 (1.8)	<.001*
Duration of T2 DM (yr)	3.8 (3.8)	<.001*
HOMA-IR	6.9 (6.8)	.028*
SBP (mm Hg)	135.6 (14.9)	.025*
DBP (mm Hg)	85.6 (8.8)	.062
Glucose (mg/dL)	169.7 (76.0)	.312
Total cholesterol (mg/dL)	195.6 (45.6)	.143
Triglyceride (mg/dL)	209.9 (107.2)	.262
UA (mg/dL)	6.5 (1.9)	.020*
AST (IU/L)	29.9 (15.9)	.004*
ALT (IU/L)	44 (23.4)	.001*
Albumin (gm/dL)	4.5 (.6)	.133
Hb (gm/dL)	15.5 (1.7)	.064
Insulin (uIU/mL)	16.5 (11.6)	.004*
HDL-C (mg/dL)	42.3 (7.7)	.224
HbA _{1c} , %	8.7 (1.7)	.009*
LDL (mg/dL)	126.8 (38.6)	.208
hs-CRP	.9 (.8)	.005*
WBC (/μL)	7.7 (2.4)	.006*
ABCD score	5.2 (2.2)	<.001*
WL, %	20.2 (7.8)	<.001*

In clinical practice, the score of ABCD can assist in selecting the procedure for surgery for TII-DM treatment. How TII-DM remission occurs after LSG is mysterious and difficult. Despite not avoiding the foregut with active enzymes, LSG was still considered a metabolic operation due to its food-stimulating effects on the hind intestine, which included a quick rise in the hormones glucagon-like peptide-1 (GLP-1) and peptide YY (PYY) following meals. Durable weight loss with a corresponding



decline in IR remains the key to TII-DM remission following surgery. In the current study, a significant weight loss after LSG was linked to a marked improvement in IR, as evaluated by HOMA. The current study had a few drawbacks. First, the study's relatively small case count disallowed a more detailed statistical analysis. When utilizing this rating for patients with lessened BMI, one must examine tiny quantities in a specific category carefully. According to this student's findings, the ABCD score is still useful for determining whether TII-DM reliefs follow LSG. Second, this study's follow-up period needs to be longer. The ABCD score's ability to predict persistent TII-DM remission following LSG surgery for obesity is unknown without follow-ups over time. The predictive power of this scoring system needs to be confirmed with data spanning up to 10 years.

Table 4 Rate of TII DM remission according to various clinical variables.

Factor	Amount of visitors	RR (HbA _{1c} o6%)	P
BMI (kg/m ²)	3	<27	0%
	29	27-34.9	29.8%
	34	35-42	64.9%
	24	≥42	81.9%
Gender	43	Female	48.9%
	46	Male	70.0%
C-peptide (ng/ mL)	7	<2	0%
	14	2-2.9	61.7%
	33	3-4.9	45.7%
	36	≥5	94.3%
Age (yr)	42	<40	75.2%
	47	≥40	42.6%
Waist/hip ratio	15	<.9	46.4%
	47	.9-1.0	52.4%
	27	>1.0	69.3%
Duration (yr)	23	<1	85.9%
	44	1-3.9	47.8%
	15	4-8	53.8%
	9	>8	25.2%

Table 5 TII-DM RR for each ABCD score.

TII-DM RR	ABCD score						Overall
	0	1	2	3	4	5	
Patient no.	0	3	2	4	12	9	87
Complete remission (HbA _{1c} o6.0%)	0	0	0	0	3 (30%)	7 (71.4%)	45 (52.9%)
Partial remission (HbA _{1c} o6.5%)	0	0	0	1 (33.3%)	5 (50%)	6 (85.7%)	63 (74.1%)
Improved (HbA _{1c} o7%)	0	0	0	1 (33.3%)	9 (90%)	6 (85.7%)	72 (84.7%)
Complete remission (HbA _{1c} o6.0%) in gastric bypass (n ¼ 63)	33%	33%	43%	46%	41%	57%	65.5%

4. Conclusion

A major stomach section, sometimes called an SG, is surgically removed during an LSG, leaving behind a smaller, sleeve-shaped stomach. Limiting the amount of food that can be consumed, this method causes weight loss. Furthermore, it has been noted that LSG can have a major impact on metabolic disorders like T2DM. The use of LSG is considered safe and successful; however, it's vital to remember that any surgical operation has hazards. Infection, bleeding, leakage, and vitamin deficiency are possible LSG side effects. Investigating the possible synergistic effects of LSG in the management of T2DM in comparison to other interventions, including as medication, lifestyle changes, or new therapies. Investigating integrated methods could provide patients with treatment plans that are more thorough and individualized.

Ethical considerations

Not applicable

Conflict of Interest

The authors declare no conflicts of interest.

Funding

This research did not receive any financial support.

References



- Attia R (2019) Role of sleeve gastrectomy in control of type 2 diabetes– a prospective clinical study. *The Egyptian Journal of Surgery*, 38(2):267-271. [https://DOI: 10.4103/ejs.ejs_195_18](https://doi.org/10.4103/ejs.ejs_195_18)
- Chowbey P, Kelkar R, Soni V, Khullar R, Sharma A, Baijal M (2021) Role of DiaRem score in preoperative prediction of type 2 diabetes mellitus remission after laparoscopic Roux-en-Y gastric bypass: Indian perspective. *Obesity Surgery* 31:1265-1270. DOI: 10.1007/s11695-020-05129-4
- Fernández-Ananín S, Ballester E, Gonzalo B, Codina C, Miñambres I, Pérez A, Gich IJ, González S, Serrano C, Balagué C (2022) Is sleeve gastrectomy as effective in older patients as in younger patients? A comparative analysis of weight loss, related comorbidities, and medication requirements. *Obesity Surgery* 32:1909-1917. DOI: 10.1007/s11695-022-05940-1
- Guetta O, Vakhrushev A, Dukhno O, Ovnat A, Sebbag G (2019) New results on the safety of laparoscopic sleeve gastrectomy bariatric procedure for type 2 diabetes patients. *World Journal of Diabetes* 10:78. DOI: 10.4239%2Fwjv.v10.i2.78
- Kheirvari M, Nikroo ND, Jaafarnejad H, Farsimadan M, Eshghjoo S, Hosseini S, Anbara T (2020) The advantages and disadvantages of sleeve gastrectomy; clinical laboratory to bedside review. *Heliyon* 6:e03496. DOI: 10.1016/j.heliyon.2020.e03496
- Lee MH, Almalki OM, Lee WJ, Chen SC, Chen JC, Wu CC (2020) Laparoscopic sleeve gastrectomy for type 2 diabetes mellitus: long-term result and recurrence of diabetes. *Obesity Surgery* 30:3669-3674. DOI: 10.1007/s11695-020-04737-4
- Łukaszewicz A, Gołaszewski P, Nadolny K, Łukaszewicz J, Ładny JR, Hady HR (2022) Effectiveness of laparoscopic sleeve gastrectomy and one anastomosis gastric bypass on the resolution of metabolic syndrome—a review. *Medical Research Journal*. DOI: 10.5603/MRJ.a2022.0055
- Mizera M, Wysocki M, Bartosiak K, Franczak P, Hady HR, Kalinowski P, Myśliwiec P, Ortowski M, Paluszkiewicz R, Piecuch J, Szeliga J (2021) Type 2 diabetes remission five years after laparoscopic sleeve gastrectomy: multicenter cohort study. *Obesity Surgery* 31:980-986. DOI: 10.1007/s11695-020-05088-w
- Murshid KR, Alsisi GH, Almansouri FA, Zahid MM, Boghdadi AA, Mahmoud EH (2021) Laparoscopic sleeve gastrectomy for weight loss and treatment of type 2 diabetes mellitus. *Journal of Taibah University Medical Sciences* 16:387-394. DOI: 10.1016/j.jtumed.2020.12.018
- Rao M, Gao C, Xu L, Jiang L, Zhu J, Chen G, Law BYK, Xu Y (2019) Effect of inulin-type carbohydrates on IR in patients with type 2 diabetes and obesity: a systematic review and meta-analysis. *Journal of diabetes research* 2019. DOI: 10.1155/2019/5101423
- Saber SA, Eissa MA, Mousa G, Abdraboh OH (2022) Role of laparoscopic sleeve gastrectomy in managing type II diabetes mellitus in morbidly obese patients. *The Egyptian Journal of Surgery* 41:1716-1721. DOI :10.1109/SNPD54884.2022.10051567864534
- Wada E, Onoue T, Kobayashi T, Handa T, Hayase A, Ito M, Furukawa M, Okuji T, Okada N, Iwama S, Sugiyama M (2020) Flash glucose monitoring helps achieve better glycemic control than conventional self-monitoring of blood glucose in non-insulin-treated type 2 diabetes: a randomized controlled trial. *BMJ Open Diabetes Research and Care* 8:e001115. DOI: 10.1136/bmjdr-2019-001115
- Wang L, Wang J, Jiang T (2019) Effect of laparoscopic sleeve gastrectomy on type 2 diabetes mellitus in patients with BMI less than 30 kg/m². *Obesity Surgery* 29:835-842. DOI: 10.1007/s11695-018-3602-4
- Zayed HH, Sabry K, Abdelraouf YM, Salah WM, Wahab IA, Sheikh MRE (2020) Impact of Laparoscopic Sleeve Gastrectomy on Obese Type 2 Diabetic Patients and Role of Gut Hormones Peptide Tyrosine Tyrosine and Glucagon-Like Peptide 1on Remission of Diabetes. *Journal of Advances in Medicine and Medical Research* 32:80-91. DOI: 10.1078/j.trc.2018.07.452